

PDF hosted at the Radboud Repository of the Radboud University Nijmegen

The following full text is a publisher's version.

For additional information about this publication click this link.

<http://hdl.handle.net/2066/53738>

Please be advised that this information was generated on 2018-07-08 and may be subject to change.

Changing Rivers:
Analysing fluvial landscape dynamics using
remote sensing

Gertjan Geerling

Changing Rivers: Analysing fluvial landscape dynamics using remote sensing

Een wetenschappelijke proeve op het gebied van de Natuurwetenschappen,
Wiskunde en Informatica

Proefschrift

ter verkrijging van de graad van doctor
aan de Radboud Universiteit Nijmegen
op gezag van de rector magnificus prof. mr. S.C.J.J. Kortmann,
volgens besluit van het College van Decanen
in het openbaar te verdedigen op donderdag 11 september 2008

om 10.30 uur precies

door

Gertjan Willem Geerling

geboren op 5 september 1972
te Laren (NH)

Promotor: prof. dr. A.J.M. Smits

Copromotor: dr. A.M.J. Ragas

Manuscriptcommissie: prof. dr. A.J. Hendriks (vz)
prof. dr. S.M. de Jong (Universiteit Utrecht)
prof. dr. J.C.J.M. de Kroon

Geerling GW (2008). *Changing Rivers: Analysing fluvial landscape dynamics using remote sensing*. PhD thesis, Centre for Sustainable Management of Resources, Radboud University of Nijmegen, The Netherlands.
ISBN/EAN: 978-90-810586-3-6

This thesis was commissioned by the Directorate for Public Works and Water Management (Rijkswaterstaat) and the project was coordinated by the Centre for Data and ICT of this directorate.

Cover: false colour aerial image of the Allier River (F).
Back cover: false colour aerial image of floodplain "Ewijkse Plaat", Waal River (NL).
Cover design: Lidwien van der Horst, Radboud University Nijmegen.

Printed by Printpartners Ipskamp B.V., Nijmegen, The Netherlands.

Contents

	Page	
Chapter 1	General Introduction	7
Chapter 2	Succession and rejuvenation in floodplains along the River Allier (France)	25
Chapter 3	Nature rehabilitation by floodplain excavation: The hydraulic effect of 16 years of sedimentation and vegetation succession along the Waal River, NL	47
Chapter 4	Classification of floodplain vegetation by data fusion of spectral (CASI) and LiDAR data	71
Chapter 5	Mapping floodplain plant communities: clustering and ordination techniques adopted in remote sensing	97
Chapter 6	Mapping river floodplain ecotopes by segmentation of spectral (CASI) and structural (LiDAR) remote sensing data	121
Chapter 7	Synthesis	145
	Summary	167
	Samenvatting	171
	Dankwoord	175
	Curriculum vitae	179
	Publications	181
	Full colour figures	185

1 General introduction

1.1 Rivers

Rivers are a vital part of the global water cycle in which they transport fresh water from land to ocean. They help sustain a high number of plant and animal species and provide fundamental resources to most societies varying from water, power, navigation, and food to recreation (Petts and Amoros 1996). Rivers convey water that precipitated in its drainage basin or catchment. Water that falls inside a catchment is transported through small tributaries merging into larger rivers and is finally released into the sea. Primary variables influencing form and functioning of rivers are discharge, sediment, and water quality regimes that relate to climate, vegetation, and landuse (Petts and Amoros 1996). The ever-varying water levels cause the river to expand and contract using the surrounding lands, i.e. floodplains, as a buffer (Tockner et al. 2000). The intensity of the water table variations decreases when moving away from the river, i.e. the influence of the hydrodynamics lessens, resulting in a gradual environmental change for plants and animals (Nilsson and Svedmark 2002). This typifies a fluvial landscape; a landscape with spatially and temporally distributed dynamics varying gradually (in ecotones) or sudden. In addition to dynamics caused by water table changes, the existing landform is reworked as water erodes soil and the eroded matter, i.e. sediment, is carried downstream. In a given river stretch, the influx of sediment will change the river bed and causes changes in channel form, leading to additional lateral erosion of adjacent



Figure 1.1 Lateral erosion (left) and sedimentation (right) along the Allier River (France). The sediment was deposited during one flood event in May 2003 (Photos G.W. Geerling).

floodplains (Knighton 1998). Large discharges can lead to erosion and sedimentation as shown in Figure 1.1 for the floodplains of the Allier River (F).

Rivers show different flow patterns like braided, anastomosing and meandering that depend on the type of sediment, hydrodynamic forces, and floodplain soils. Figure 1.2 summarises the different flow patterns and their main steering parameters. The floodplains of meandering rivers are the focus of this study.

Viewed from the floodplain perspective, the changes in water level and sedimentation are disturbances determining the shape and functioning of that floodplain. This is illustrated in Figure 1.1 for the Allier River in France. The left photo shows the erosion of high levees. As the erosion process proceeds, the vegetation on the levee, i.e. grass, herbs and trees, will be absorbed and carried off by the stream. In the right photo (Figure 1.1) sediment covers a pioneer black poplar settlement on newly formed banks, setting back succession. These disturbances revitalise the landscape, often by setting back ecological succession stages to a pioneer stage. This is called rejuvenation. Rejuvenation occurs continuously and is therefore regarded as a vital processes for the functioning of the river system (Sparks et al. 1990, Ward et al. 2001). Both, plant and animal species, have adapted to the rapid hydrological and morphological changes that occur in the fluvial environment. Many species rely on the periodical expansion and contraction of water on extended floodplains (Tockner et al. 2000). Input of water brings fresh sediment and nutrients to semi-connected or isolated water bodies and so determines local nutrient concentrations that regulate the distribution of algae and aquatic plants. Terrestrial vegetation species are distributed along elevation differences that influence soil separation from the groundwater aquifer, intensity of disturbance by flooding, and texture of the soil (Large et al. 1996, Nilsson and Svedmark 2002). Macroinvertebrates can be sensitive to environmental changes and quickly recolonise habitats when discharge diminishes or even establish new populations between two disturbances (Greenwood and Richardot-Coulet 1996). Other species, like the mayfly (*Leptophlebia cupida*), have adapted their lifecycle to the seasonal patterns of flow and the subsequent changes in habitats. During summer, it lays its eggs in the warm main channel, but in the cold winter months the hatched nymphs migrate to deeper pools for shelter. The spring floods flush out the nymphs and they migrate upstream to sheltered side arms (still connected to the main channel) and further into wetlands where the life cycle is

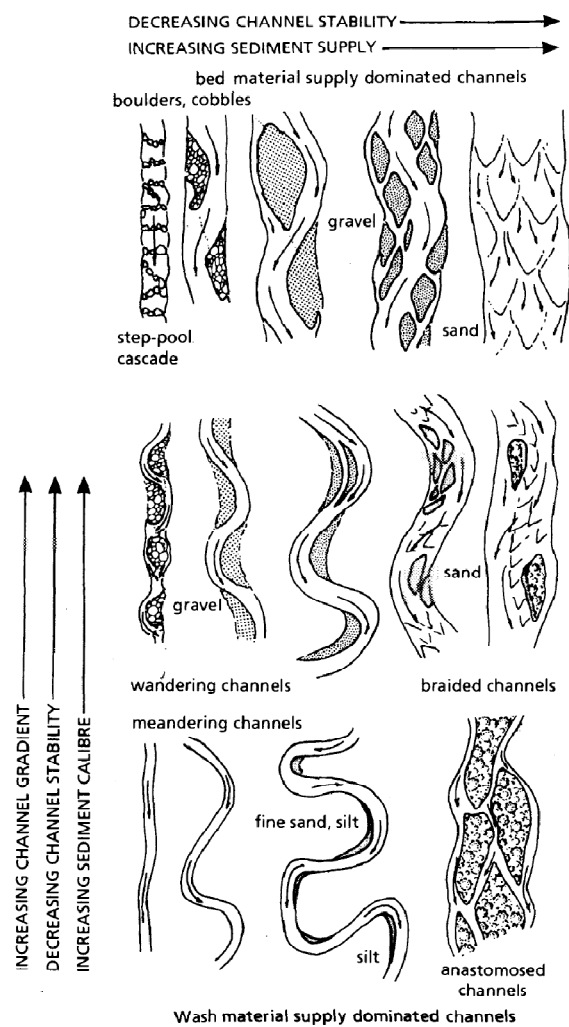


Figure 1.2 Morphological types of large river channels (adapted from Gurnell 1997).

completed (Greenwood and Richardot-Coulet 1996). Extended floodplains are also important for fish species and invertebrates; their biomass is greater in floodplain habitats than in the flowing channels of rivers (Greenwood and Richardot-Coulet 1996).

Although abiotic processes seem dominant in shaping the floodplain, the influence of biota on floodplain evolution has recently been recognised. These interactions between hydromorphological and ecological processes are studied in the field of biogeomorphology (Brown 1997, Hughes 1997, Hughes et al. 2001, Gurnell and Petts 2002, Stallins 2006, Corenblit et al. 2007). Examples of biogeomorphological interactions are the influence of vegetation on sedimentation pattern and the impact of small mammal species on floodplain topsoils by turbation (Steiger and Gurnell 2002, Wijnhoven 2007). One particular species that not only adapted to but also altered the fluvial environment is the human. Humans changed the riverine environment with increasing speed leading to substantial impacts on the river ecosystem (Tockner and Stanford 2002).

1.2 Man and the river

As river floodplains become more densely populated, the urge for control increases because firstly, the river provides more services and these services are used more intensively. Secondly, natural hazards such as floods or droughts affect society (Petts and Amoros 1996, Leuven et al. 2000, Lenders 2003, Van de Ven 2004). There is a strong relationship between population density and landuse change in floodplains worldwide; higher population density correlates to a surface area increase of intensive agriculture and urban areas in river corridors. The correlation is linear in



Figure 1.3 The Rhine River between Basel (S) and Karlsruhe (D) was regulated in the 19th century by the German engineer J.G. Tulla. An island dominated river of 5 km wide (left) was canalised, leaving a single small navigable channel in the present Restrhein (right; photo G.W. Geerling).

less developed countries, but logarithmic in Western countries (Tockner and Stanford 2002).

River regulation, also referred to as river training, is a step-by-step process, at least in present day regulated rivers such as the river Rhine. Along the Rhine, the first settlements appeared on natural levees, obviously to prevent disturbance by seasonal flooding. Until about 1200 AD, river training started locally with the construction of artificial levees (dykes) close to settlements to prevent flooding of arable land.

Especially in lowland rivers, the dyke system eventually encompassed whole branches and connected to natural elevations in the landscape. The gradual increase of shipping activities and the

extending spatial scale of river management (from local to national) further accelerated river regulation.

Groins were built to promote and stabilise the formation of arable floodplains locally. During the industrial revolution (1800-1900 AD), the complete course of the river was fixed by groins to prevent avulsions, braiding or meandering, and to stabilise the navigation channel (Havinga and Smits 2000).

Furthermore, the original river channel was altered and bends were cut off (Figures 1.3 and 1.4). Like the Rhine, many rivers in industrialised countries have been altered (Petts 1989, Gregory 2006).

The consequences of river training activities were numerous. The aquatic environment deteriorated due to increased shipping and manufacturing activities along the riverbanks (Admiraal et al. 1993). The terrestrial environment changed because most natural elements, such as softwood forests and swamps, were removed from the system, altering floodplain ecology (Bravard et al. 1986, De Bruin et al. 1987, Buijse et al. 2002, Tockner and Stanford 2002, Thoms 2003). The artificial levees (dykes) cut off the

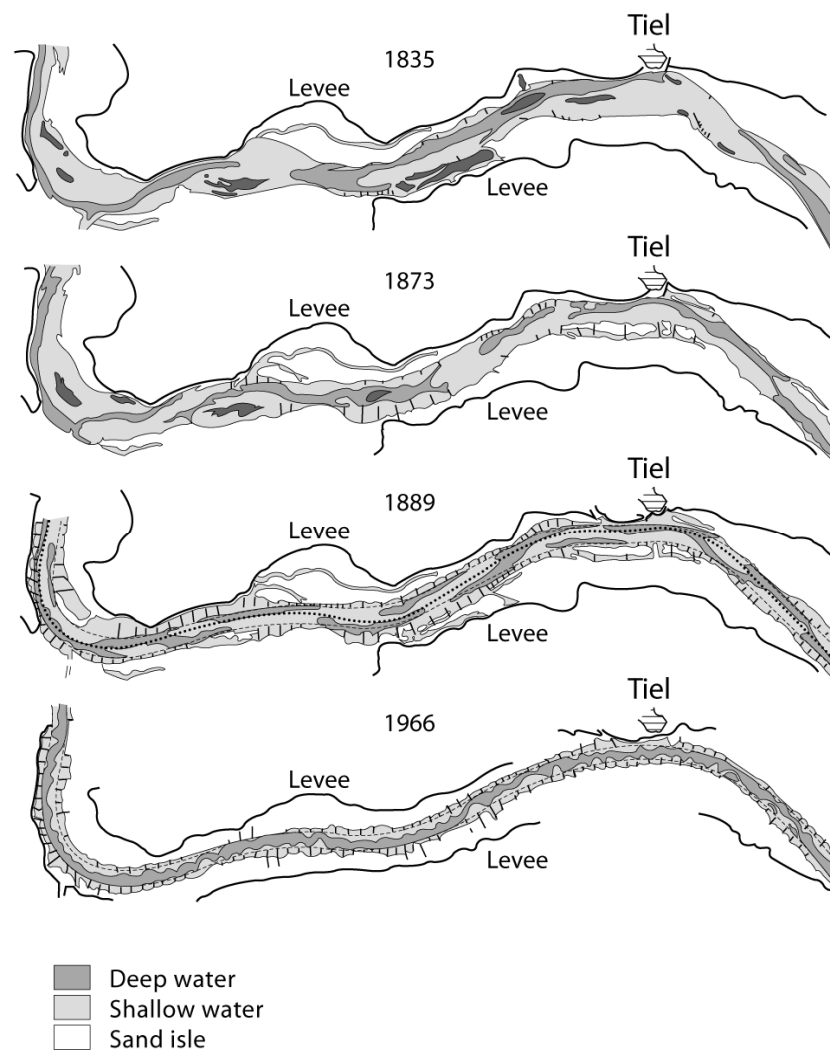


Figure 1.4 Regulation of the western part of the Dutch Waal river (one of the Rhine branches) between 1835 and 1966. Many river management measures were introduced to prevent ice dam formation and to improve the fairway for shipping. A system of small dykes and groins reduced the lateral movement of the river. Sandbanks and shoals were removed from the main channel. Nowadays, the floodplains are generally used as grassland for cattle (Smits et al. 2000).

largest part of the lowland floodplain, called the hinterland, and blocked the lateral connectivity to former floodplains (Gergel et al. 2002, Van der Velde et al. 2006). The floodplain area became smaller; depending on definitions, more than 50% of the original expanse has been cut-off (Buijse et al. 2002, Tockner and Stanford 2002). The river channel was confined to a single thread using regularly spaced groins, see Figure 1.4. So, lateral movement and sediment deposition (aggradation) that would otherwise produce downstream migrating meanders, point bars, and sand islands, were hampered (Middelkoop et al. 2005). Ward et al. (2002) says “In highly regulated river segments, landscape patterns may be ‘frozen in time’ by dams and artificial levees. For example, although floodplain segments of the French Rhone may contain highly diverse aquatic and riparian habitats, in many cases these are relicts of the formerly dynamic river system.”

Dutch floodplains and the hinterland have been in agricultural or urban use for centuries, which effectively halted ecological succession or confined it to relic habitats. Reasoning from a near-natural river perspective, hardly anything resembles the landscape pattern associated with an unconfined dynamic river (Ward et al. 2001).

After a few major floods and the prospect of more and greater floods in the future due to climate change effects, another consequence of the regulation became clear.

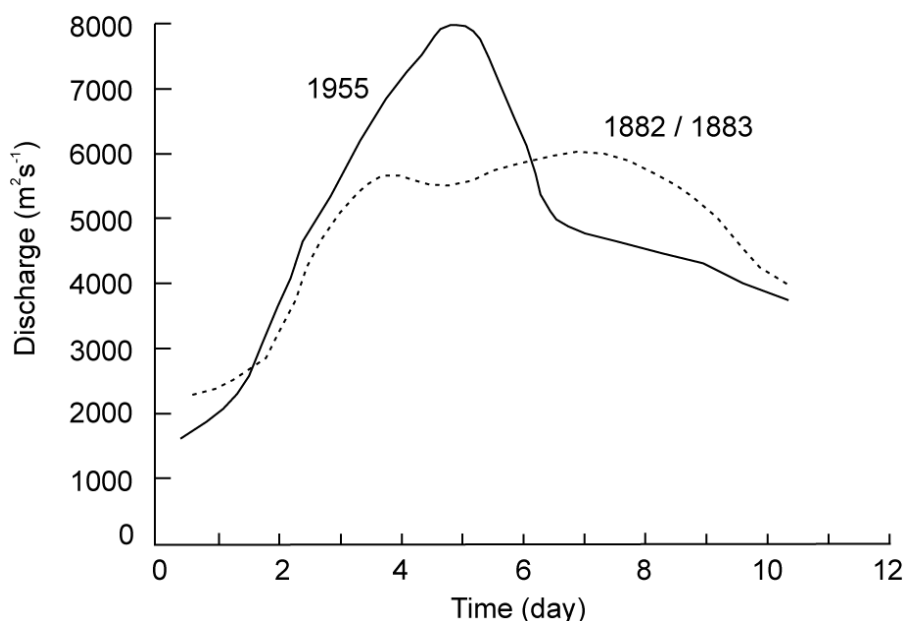


Figure 1.5 The discharge curves of a flood wave in 1882/1883 and 1955. The cumulative discharge is the same in both events (Havinga and Smits 2000).

The sum of local river training efforts in the Rhine catchment over the last centuries increased the flood intensity as shown in Figure 1.5. Deforestation, increased drainage of uplands by canalisation of small tributaries, and additional shortening of the main river course diminished the water retention capacity. This caused spiked flood peaks, and threatens the present level of flood safety (Smits et al. 2000).

1.3 Rehabilitation and Management

As almost all rivers in Europe and many in North America have undergone regulation to some extent; the cumulative ecological impact of river regulation is large. This recognition prompted a number of restoration projects of which the most successful are based on knowledge on the functioning of the system (Ward et al. 2001). For riverine nature restoration, the re-introduction of hydro-geomorphological dynamics is a prerequisite (Décamps et al. 1988, Amoros and Wade 1996, Gautier et al. 2000). Visions and plans were presented that promoted floodplain rehabilitation by introducing riverine nature reserves and improving river-floodplain interaction by lowering summer levees and by digging side channels (De Bruin et al. 1987, Schropp 1995, Schiemer et al. 1999, Amoros 2001, Buijse et al. 2002). However, restoring dynamics in highly regulated systems as the Rhine or Oder can downgrade safety measures against flooding, at least in existing circumstances. Besides, society often utilises floodplains for extraction of building materials and agriculture; activities that are seemingly in conflict with restoring hydrological and geomorphologic processes. Ward et al. (2002) recognise that the altered systems cannot always be restored to their pristine state. Nevertheless, the present regulated systems like the rivers Rhine or Oder have to change to accommodate the larger floods as consequence of climate change and the cumulative effect of catchment-wide regulations mentioned in the paragraph above. Can river restoration complement flood protection (Nienhuis and Leuven 2001)? Creation of side-channels, lowering levees or restoring the river to pre-regulated dimensions has a positive impact on flood levels and creates niches for species (Simons et al. 2001, Acreman et al. 2003). Flood protection can act as an incentive for nature restoration by the transformation of agricultural land into nature areas to create more space to accommodate floods (Helmer 1999, Smits et al. 2000). However, as ecological succession continues in these “new” nature areas, a river system lacking rejuvenation will end up “frozen in time” as indicated above.

Reasoning from the regulated Dutch Rhine system, Helmer (1999) and Smits et al. (2000) proposed a new approach for floodplain river restoration and management: (1) transformation of agricultural land into nature areas to create more room for water and nature, and (2) periodic artificial disturbance of those areas, e.g. by the removal of climax vegetation and other mechanical interventions, resulting in the creation of pioneer stages and the re-introduction of ecological succession. This management strategy is called Cyclic Floodplain Rejuvenation (CFR; Duel et al. 2001). CFR raises many questions about the functioning of medium to large regulated rivers and their natural references which need to be answered in order to underpin its validity and the planning of periodic rejuvenation actions.

1.4 GIS and Remote Sensing in river management

To successfully restore and manage regulated rivers, process examples are needed of natural functioning systems and evaluation of past restoration efforts is important (Ward et al. 2001, Van der Velde et al. 2006). Furthermore, the Cyclic Floodplain Rejuvenation strategy calls for continuous system monitoring and evaluation, to guide management actions. One way to gather this type of information is by the application of Geographic Information Systems (GIS) and Remote Sensing (RS) techniques. The definition, principles and some applications of GIS and RS are described below.

Spatial data is the basis of a GIS and is data that can be pinpointed to a location, such as "the bus stop in front of the Huygens building at the Heyendaalseweg in Nijmegen". Spatial data is stored in aerial images, satellite images, maps, GPS devices, people, etc. The computer environment that is used to work with these data is called a Geographical Information System, or abbreviated GIS. Burrough and McDonnell (1998) defined GIS as, "a set of tools for collecting, storing, retrieving at will, transforming and displaying spatial data from the real world for a particular set of purposes". GIS definitions are often extended to organisational aspects connected to the gathering, use and management of large spatial databases. Examples of GIS

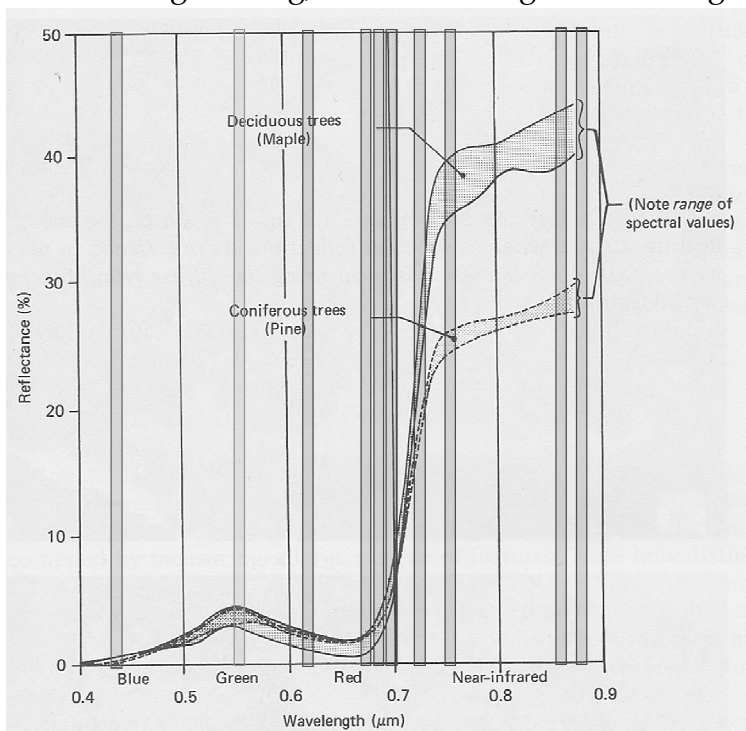


Figure 1.6 The spectral bands of the Compact Airborne Spectral Imager (CASI) as applied in this thesis. The band set used is optimised for vegetation mapping. Especially Red and Near-infrared are useful in discerning different vegetation types. The image below shows reflection of tree types (adapted from Lillesand and Kiefer 2000).

applications in the river environment can be found in Leuven et al. (2002). An important aspect of GIS, and the basis for its analysing capabilities, is the input of spatial data or as Burrough and McDonnell (1998) put it, collecting and storing spatial data. Spatial data can be collected manually in the field by human observations, connected to a known location and transferred to a GIS. Although many maps, like vegetation maps, are based on this procedure, it is a rather laborious process. Since the development of photographic film, spatial data can be gathered from a distance. The most logical distance with respect to analysing landscapes is vertical; vertical aerial photographs provide a view of the landscape that can be readily stored in a GIS. Gathering

spatial data, while not being in contact with the observed object, is called Remote Sensing (RS). Lillesand and Kiefer (2000) define remote sensing as “the science and art of obtaining information about an object, area, or phenomenon through the analysis of data acquired by a device that is not in contact with the object, area, or phenomenon under investigation.” In RS, sensors are applied to sense the object, and the type of sensor determines what can be detected. Mostly two kinds of sensors are distinguished, i.e. passive and active. Passive sensors, like a (digital) photo camera, record sunlight reflected by the examined object. Distinguishing features between sensors of this type are the type of data storage (analogue or digital), the resolution (or grain in case of film), and which part of the electromagnetic spectrum is recorded. The recorded parts in the electromagnetic spectrum are called the spectral bands of the sensor. Figure 1.6 shows the bands for an airborne scanner as used in this thesis. Digital sensors either are in orbit around the earth or mounted inside an aircraft. In contrast to passive sensors, active sensors emit signals directed at the object of interest and record reflectance of these signals. Examples are radar, often used in aviation and shipping, and sonar, which emits and records sound waves to gather information about an object. An active sensor that was developed in the 1990s is based on Light Detection and Ranging (LiDAR), called Airborne Laser Scanning (ALS) when implemented in an aircraft. It sends laser pulses towards the earth surface and records the return time in order to compute the surface elevation. When emitted and recorded in high densities, the sensor can be applied to generate elevation models and even data on vegetation height (Cobby et al. 2001, Straatsma and Middelkoop 2006). Wehr and Lohr (1999) give a good introduction to the functioning of ALS.

Both passive and active sensors are applied to investigate landscape properties. Aerial photographs (analogue RS) were the only source of RS data in 1950s and 1960s, and are nowadays still widely used to map vegetation and larger scale landscapes. Present day river map products are mostly derived by non-automated stereographic interpretation of aerial images using a standard interpretation key (Jansen and Backx 1998). Küchler and Zonneveld (1988) produced a standard work on vegetation mapping and photo-interpretation. Digital RS was boosted by the start of the American LANDSAT program in the 1970s with the launch of Landsat 1. Whereas analogue RS images were mostly interpreted by humans, the digital nature of LANDSAT images permitted analysis using computers. Furthermore, as the satellite in orbit repeatedly visits each site with a fixed time interval, it is possible to record and analyse time series. Already in 1971, Odum recognised the possibilities of digital RS in ecology, i.e. for mapping habitats and habitat changes in time (Johnson 1971). In the field of river studies, the use of remote sensing is recognised, especially now the range of available sensors keeps increasing (Leuven et al. 2002). Possible applications are the monitoring of floodplains for ecological evaluation or as input for flood models, risk assessment and analysis of river and floodplain functioning (Cobby et al. 2001, Leuven et al. 2002, Mertes 2002, Van der Sande et al. 2003,

Piettroniro and Leconte 2005).

In this study, GIS and RS are used as basic tools to track changes in floodplains using time series based on historical analogue aerial photographs. Additionally, images of two digital scanners are analysed, one based on imaging spectroscopy (IS) and the other on light detection and ranging (LiDAR) sensor technology. The IS sensor used is the Compact Airborne Spectrographic Imager (CASI). The sensor records spectral information in the visible and shortwave infrared (IR) range and has been used in vegetation mapping (Kurnatowska 1998, Shang et al. 1998, Protz et al. 1999, Von Hansen and Sties 2000, Leckie et al. 2005). The LiDAR technology's first promise was the ability to create accurate Digital Elevation Models (DEMs, (Ackermann 1999, Wehr and Lohr 1999, Charlton et al. 2003). However, some studies explored the use in vegetation mapping (Protz et al. 1999, Zimble et al. 2003, Suarez et al. 2005, Straatsma and Middelkoop 2006).

1.5 Aim

The aim of the present study is to utilise remote sensing data to support the implementation of the Cyclic Floodplain Rejuvenation strategy along regulated rivers, i.e. nature rehabilitation and safety measures. Remote Sensing can support the implementation of CFR in two major ways:

- By gathering landscape data on river dynamics in regulated and natural systems. This data can be used to support management questions such as “Where and how often to rejuvenate?” Basic questions on landscape dynamics relate to both temporal and spatial aspects of the riverine environment. One of the main aims of this thesis is to contribute new data and insights on floodplain and vegetation dynamics of natural and regulated river systems by applying remote sensing techniques and interpretation of the data.
- By developing and demonstrating new techniques to optimise the interpretation of RS data, allowing the river manager to take better informed decisions, e.g. about the impact of vegetation succession on flooding risks. Current RS applications are often limited to the use of data from a single sensor, e.g. spectral data only or LiDAR data only. The use of both data sets can be synergetic when applied together in classification (Leckie et al. 2005, Straatsma 2006). The principle of combining multiple sensors is called data fusion (Pohl and Van Genderen 1998). One of the main aims of this thesis is to develop and test new data fusion techniques and to demonstrate their value for monitoring floodplain and vegetation development along regulated rivers.

The river stretches studied in this thesis are part of moderate to large rivers and meander by nature. Therefore, the results and recommendations that follow should be regarded within that context.

1.6 Outline

Chapters 2 and 3 of this thesis focus on the application of remote sensing techniques to gather landscape data on river dynamics in natural and regulated systems. Chapters 4, 5 and 6 focus on the development and application of data fusion techniques to optimise the interpretation of RS data to describe floodplain and vegetation dynamics.

Chapter 2: Succession and rejuvenation in floodplains along the river Allier (France)

The aim of this chapter is to determine the dynamics of landscape units in a freely meandering stretch of the river Allier (France) and the consequences for the spatio-temporal constitution of its riparian landscape. A time series of aerial photographs spanning 46 years was analysed to answer the following questions:

- What are the transition rates of the different landscape units?
- What is the spatio-temporal distribution of rejuvenation?
- What is the surface area covered by the landscape units and how does it vary over time?
- Can a river stretch size be determined, on which the landscape unit distribution is stable in all years?

Chapter 3: Nature rehabilitation by floodplain excavation: The hydraulic effect of 16 years of sedimentation and vegetation succession along the Waal River, NL

In unregulated systems the higher discharges act upon the riparian landscape by removing or depositing sediment causing the river channel to shift and reshape its floodplain configuration (Gurnell 1997, Maekawa and Nakagoshi 1997, Steiger and Gurnell 2002, Uribe-larrea et al. 2003, Hooke 2004). Major man made alterations that inhibit acting processes cause changes in the floodplain configuration, mostly in favour of less dynamic habitats (Adamek and Sukop 1992, Large and Petts 1996, Piégay and Salvador 1997, Bryant and Gilvear 1999, Marston et al. 2001, Parsons and Gilvear 2002).

The aims of this chapter are to describe the geomorphological and vegetation evolution and to quantify the hydraulic effects of a floodplain after partial excavation down to 2 m below the previous floodplain surface level. After excavation, the existing agricultural use ceased and the site was left bare as an ecological pioneer situation, giving ecological and hydromorphological processes freedom to shape the topography. The topography and vegetation structure were monitored between 1986 and 2005. The questions addressed are:

- How and how fast did sedimentation and erosion processes shape the floodplain topography after excavation?
- What kind of vegetation structure evolved out of the pioneer situation under the acting hydromorphological regime?

- What was the impact of the intervention and subsequent evolution on water levels and flow velocities at high discharges?

Chapter 4: Classification of floodplain vegetation by data fusion of spectral (CASI) and LiDAR data

The combined use, or data fusion, of Spectral and LiDAR data can be synergetic (Leckie et al. 2005, Straatsma 2006) for mapping vegetation. Pohl and Van Genderen (1998) describe three types of data fusion: data fusion at the decision level, at the feature level, and at the pixel level. The aim of this paper is to combine spectral and LiDAR data by data fusion at the pixel level to improve the classification accuracy of an eight-class and five-class set of natural vegetation types. The eight-class set represents the vegetation classes relevant for nature and river management, while the five-class set serves as a minimum set to estimate hydraulic resistance for river-management purposes. Objectives of this study are:

- to devise a method for fusing spectral and LiDAR data at the pixel level, and
- to determine the classification advantage of the fused data set against the separate (non fused) spectral and LiDAR sets.

Chapter 5: Mapping floodplain plant communities: clustering and ordination techniques adopted in remote sensing

To be able to create a vegetation map classification set, plant community analysis can contribute to create classes that have ecological meaning and therefore are useful to detect processes operating in the landscape. However, classes aggregated on the basis of plant composition alone do not always give good classification results (Thomas et al. 2003). Building on the methodology from Chapter 4, we try to group plant communities into broader vegetation classes that can be discriminated through remotely sensed data and at the same time maintain ecological and syntaxonomical significance. Class composition is based on clustering and ordination techniques which are applied to data on plant species, vegetation abundance and environmental factors that can influence the spectral signature of the vegetation class. The remote sensing data set used is the CASI/LiDAR fused image as described in Chapter 4. The objectives of this study are:

- to explore the adequacy of field data using clustering techniques, and
- to optimise the class delineation procedure by incorporating ancillary abiotic variables and ordination techniques in the mapping process.

Chapter 6: Mapping river floodplain ecotopes by segmentation of spectral (CASI) and structural (LiDAR) remote sensing data

The studies of the previous chapters focused on the development of a simple and useful fusion approach of spectral and LiDAR data. The data set was tested against vegetation structure classes and different ecological vegetation classes on the pixel level, i.e. sub-ecotope level. However, maps produced at that scale level are not

suited to analyse or visualise landscape composition on the river stretch scale level. The aim of Chapter 6 is to test the CASI and LiDAR fusion approach from Chapter 4 for the classification of larger segments, i.e. floodplain ecotopes. The vegetation and land cover classes distinguished here are based on the Dutch riparian ecotope system (Rademakers and Wolfert 1994, Jansen and Backx 1998). The high-resolution spectral data (CASI) and elevation data (LiDAR) used are evaluated on their separate and combined segmentation and classification potential. To investigate the compatibility of automated segmentation and the current manual outlining method, the segmentation results are compared to an existing manually digitised ecotope map. The research questions are:

- How do manually drawn and automatically derived ecotope objects compare when using spectral data, LiDAR data and both?
- How does identification of ecotopes compare when using spectral data, LiDAR data and a combination of both?

Chapter 7: Synthesis

The synthesis of this thesis discusses relations between the results of the studies introduced above and their implications for floodplain restoration in temperate regulated rivers with special emphasis on the Cyclic Floodplain Rejuvenation strategy.

References

- Ackermann F (1999). Airborne laser scanning - present status and future expectations. *ISPRS Journal of Photogrammetry and Remote Sensing* **54**: 64-67.
- Acreman MC, Riddington R, Booker DJ (2003). Hydrological impacts of floodplain restoration: a case study of the River Cherwell, UK. *Hydrology and Earth System sciences* **7**: 75-85.
- Adamek Z, Sukop I (1992). Invertebrate communities of former southern Moravian floodplains (Czechoslovakia) and impact of regulation. *Regulated Rivers: Research & Management* **7**: 181-192.
- Admiraal W, Van der Velde G, Smit H, Cazemier WG (1993). The rivers Rhine and Meuse in the Netherlands: present state and signs of ecological recovery. *Hydrobiologia* **265**: 97-128.
- Amoros C (2001). The concept of habitat diversity between and within ecosystems applied to river side-arm restoration. *Environmental Management* **28**: 805-817.
- Amoros C, Wade PM (1996). Ecological successions. In: Petts GE, Amoros C (Eds.). *Fluvial Hydrosystems*. Chapman & Hall, London, pp. 211-241.
- Bravard J-P, Amoros C, Pautou G (1986). Impact of civil engineering works on the successions of communities in a fluvial system. *Oikos* **47**: 92-111.
- Brown AG (1997). Biogeomorphology and diversity in multiple-channel river systems. *Global Ecology and Biogeography letters* **6**: 179-185.

- Bryant RG, Gilvear, DJ (1999). Quantifying geomorphic and riparian land cover changes either side of a large flood event using airborne remote sensing: River Tay, Scotland. *Geomorphology* **29**: 307-321.
- Buijse AD, Coops H, Staras M, Jans LH, Van Geest GJ, Grifts RE, Ibelings BW, Oosterberg W, Roozen CJM (2002). Restoration strategies for river floodplains along large lowland rivers in Europe. *Freshwater Biology* **47**: 889-907.
- Burrough PA, McDonnell RA (1998). *Principles of Geographical Information Systems*. Oxford University Press, Oxford.
- Charlton ME, Large ARG, Fuller IC (2003). Application of airborne LiDAR in river environments: the River Coquet, Northumberland, UK. *Earth Surface Processes and Landforms* **28**: 299-306.
- Cobby DM, Mason DC, Davenport IJ (2001). Image processing of airborne scanning laser altimetry data for improved river flood modelling. *ISPRS Journal of Photogrammetry and Remote Sensing* **56**: 121-138.
- Corenblit D, Tabacchi E, Steiger J, Gurnell A (2007). Reciprocal interactions and adjustments between fluvial landforms and vegetation dynamics: a review of complementary approaches. *Earth Science Reviews* **84**: 56-86.
- De Bruin D, Hamhuis D, Van Nieuwenhuijze L, Overmars W, Vera F (1987). *Ooievaar, de toekomst van het rivierengebied*. Stichting Gelderse Milieufederatie, Arnhem (in Dutch).
- Décamps H, Fortun M, Gazelle F, Pautou G (1988). Historical influence of man on the riparian dynamics of a fluvial landscape. *Landscape Ecology* **1**: 163-173.
- Duel H, Baptist MJ, Penning WE (2001). *Cyclic Floodplain Rejuvenation. A new strategy based on floodplain measures for both flood risk management and enhancement of the biodiversity of the river Rhine*. Publication 14-2001. Netherlands Centre for River Studies, Delft.
- Gautier E, Piégay H, Bertaina P (2000). A methodological approach of fluvial dynamics oriented towards hydrosystem management: case study of the Loire and Allier rivers. *Geodinamica Acta* **1**: 29-43.
- Gergel SE, Dixon MD, Turner MG (2002). Consequences of human-altered floods: levees, floods, and floodplain forests along the Wisconsin River. *Ecological Applications* **12**: 1755-1770.
- Gregory KJ (2006). The human role in changing river channels. *Geomorphology* **79**: 172-191.
- Greenwood MT, Richardot-Coulet M (1996). Aquatic invertebrates. In: In: Petts GE, Amoros C (Eds.). *Fluvial Hydrosystems*. Chapman & Hall, London. 137-166.
- Gurnell AM (1997). Channel change on the river Dee meanders, 1946-1992, from the analysis of air photographs. *Regulated Rivers: Research & Management* **13**: 13-26.
- Gurnell AM, Petts GE (2002). Island-dominated landscapes of large floodplain rivers, a European perspective. *Freshwater Biology* **47**: 581-600.

- Havinga H, Smits AJM (2000). River management along the Rhine: A retrospective view. In: Smits AJM, Nienhuis PH, Leuven RSEW (Eds.). *New Approaches to River Management*. Backhuys Publishers, Leiden, pp. 15-32.
- Helmer W (1999). *Natuurlijke veiligheid; visie op de Rijntakken in het perspectief van stromende berging*. Staatsbosbeheer/Wereld Natuur Fonds, Arnhem (in Dutch).
- Hooke JM (2004). Cutoffs galore!: occurrence and causes of multiple cutoffs on a meandering river. *Geomorphology* **61**: 225-238.
- Hughes FMR (1997). Floodplain biogeomorphology. *Progress in Physical Geography* **21**: 501-529.
- Hughes FMR, Adams WM, Muller E, Nilsson C, Richards KS, Barsoum N, Decamps H, Foussadier R, Girel J, Guillooy H, Hayes A, Johansson M, Lambs L, Pautou G, Péiry J-L, Perrow M, Vautier F, Winfield M (2001). The importance of different scale processes for the restoration of floodplain woodlands. *Regulated Rivers: Research & Management* **17**: 325-345.
- Jansen BJM, Backx JJGM (1998). *Biologische monitoring zoete rijkswateren. Ecotopenkartering Rijntakken-Oost 1997*. Ministry of Transport, Public Works and Water Management. Institute for Inland Water Management and Waste Water Treatment (RIZA), Lelystad (in Dutch).
- Johnson PL (1971). Remote sensing as a tool for study and management of ecosystems. In: Odum EP (Ed.). *Fundamentals of ecology*. W.B. Saunders, Comp. Philadelphia - London - Toronto.
- Knighton D (1998). *Fluvial Forms & Processes*. Arnold Publishers, London.
- Küchler AW, Zonneveld IS (1988). *Vegetation mapping. Handbook of vegetation science. Volume 10*. Kluwer Academic Publishers, Dordrecht.
- Kurnatowska AM (1998). Large-scale vegetation mapping in mountain environments using remote sensing and plant physiology methods. In: Nieuwenhuis GJA, Vaughan RA, Molenaar M. (Eds.). *Operational Remote Sensing for Sustainable Development*. Balkema, Lisse. P:61-65.
- Large ARG, Petts GE (1996). Historical channel-floodplain dynamics along the River Trent. *Applied Geography* **16**: 191-209.
- Large ARG, Pautou G, Amoros C (1996). Primary production and primary producers. In: Petts GE, Amoros C (Eds.). *Fluvial Hydrosystems*. London, Chapman & Hall. pp. 117-136.
- Leckie DG, Gougeon FA, Tinis S, Nelson T, Burnett CN, Paradine D (2005). Automated tree recognition in old growth conifer stands with high resolution digital imagery. *Remote Sensing of Environment* **94**: 311-326.
- Lenders HJR (2003). *Environmental rehabilitation of the river landscape in the Netherlands. A blend of five dimensions*. PhD thesis, Department of Environmental Science, Faculty of Science, Radboud University, Nijmegen.
- Leuven RSEW, Smits AJM, Nienhuis PH (2000). From integrated approaches to sustainable river basin management. In: Smits AJM, Nienhuis PH, Leuven RSEW (Eds.). *New approaches to river management*. Backhuys Publishers, Leiden.

- Leuven RSEW, Pourdevigne I, Teeuw RM (2002). Remote sensing and Geographic Information Systems as emerging tools for riverine habitat and landscape evaluation: from concepts to models. In: Leuven, RSEW, Pourdevigne I, Teeuw RM (Eds.). *Application of Geographic Information Systems and Remote Sensing in River Studies*. Backhuys Publishers, Leiden.
- Lillesand TM, Kiefer RW (2000). *Remote sensing and image interpretation*. John Wiley & Sons, Inc. New York.
- Maekawa M-a, Nakagoshi N (1997). Riparian landscape changes over a period of 46 years, on the Azusa River in Central Japan. *Landscape and Urban Planning* **37**: 37-43.
- Marston RA, Girel J, Pautou G, Piegay H, Bravard J-P, Arneson C (2001). Channel metamorphosis, floodplain disturbance, and vegetation development: Ain river, France. *Geomorphology* **13**: 121-131.
- Mertes LAK (2002). Remote sensing of freshwater riverine landscapes: an update. *Freshwater biology* **47**: 799-816.
- Middelkoop H, Schoor MM, Wolfert HP, Maas GJ, Stouthamer E (2005). Targets for ecological rehabilitation of the lower Rhine and Meuse based on a historic geomorphologic reference. *Archiv für Hydrobiologie - Supplement* **155**: 63-88.
- Nienhuis PH, Leuven, RSEW (2001). River restoration and flood protection: controversy or synergism. *Hydrobiologia* **444**: 85-99.
- Nilsson C, Svedmark M (2002). Basic principles and ecological consequences of changing water regimes: riparian plant communities. *Environmental Management* **30**: 468-480.
- Parsons H, Gilvear D (2002). Valley floor landscape change following almost 100 years of flood embankment abandonment on a wandering gravel-bed river. *River research and applications* **18**: 461-479.
- Petts GE (1989). *Historical change of large alluvial rivers: Western Europe*. John Wiley & Sons, Chichester.
- Petts GE, Amoros C (1996). *Fluvial Hydrosystems*. Chapman & Hall, London.
- Piégay H, Salvador P-G (1997). Contemporary floodplain forest evolution along the middle Ubaye river, Southern Alps, France. *Global Ecology and Biogeography Letters* **6**: 397-406.
- Pietroniro A, Leconte R (2005). A review of Canadian remote sensing and hydrology 1999-2003. *Hydrological processes* **19**: 285-301.
- Pohl C, Van Genderen, JL (1998). Multisensor image fusion in remote sensing: concepts, methods and applications. *International Journal of Remote Sensing* **19**: 823-854.
- Protz R, van den Bygaart AJ, Wood MD, Hulthof BGA (1999). *Evaluation of high resolution airborne imagery and global positioning systems for monitoring changes in agro ecosystems*, COESA.

- Rademakers JGM, Wolfert HP (1994). *Het Rivier-Ecotopen-Stelsel; Een Indeling van Ecologisch Relevante Ruimtelijke Eenheden ten behoeve van Ontwerp- en Beleidsstudies in het Buitendijkse Rivierengebied (in Dutch with English summary)*. Ministry of Transport, Public Works and Water Management, Institute for Inland Water Management and Waste Water Treatment (RIZA), Lelystad.
- Schiemer F, Baumgartner C, Tockner K (1999). Restoration of floodplain rivers: the 'Danube Restoration Project'. *Regulated Rivers: Research & Management* **15**: 231-244.
- Schropp MHI (1995). Principles of designing secondary channels along the River Rhine for the benefit of ecological restoration. *Water Science and Technology* **31**: 379-382.
- Shang J, Jollineau MY, Howarth PJ, Wang J (1998). A comparison of spatial- and spectral-mode CASI imagery for coastal wetland mapping in the Lake St. Clair delta: preliminary results. *20th Canadian Symposium on Remote Sensing*. May 10-13, 1998. Calgary, Canada.
- Simons JHEJ, Bakker C, Schropp MHI, Jans LH, Kok FR, Grift RE (2001). Man-made secondary channels along the river Rhine (the Netherlands); results of post-project monitoring. *Regulated Rivers: Research & Management* **17**: 473-491.
- Smits AJM, Nienhuis PH, Leuven RSEW (2000). *New Approaches to River Management*. Backhuys Publishers, Leiden.
- Sparks RE, Bayley PB, Kohler SL, Osborne LL (1990). Disturbance and recovery of large floodplain rivers. *Environmental Management* **14**: 699-709.
- Stallins JA (2006). Geomorphology and ecology: unifying themes for complex systems in biogeomorphology. *Geomorphology* **77**: 207-216.
- Steiger J, Gurnell A (2002). Spatial hydrogeomorphological influences on sediment and nutrient deposition in riparian zones: observations from the Garonne River, France. *Geomorphology* **49**: 1-23.
- Straatsma M (2006). Floodplain roughness mapping synergy: LiDAR and spectral remote sensing. *ISPRS Commission VII Mid-term Symposium "Remote Sensing: From Pixels to Processes"*. ISPRS Commission VII, The Netherlands.
- Straatsma MW, Middelkoop H (2006). Airborne laser scanning as a tool for lowland floodplain vegetation monitoring. *Hydrobiologia* **565**: 87-103.
- Suarez JC, Ontiveros C, Smith S, Snape S (2005). Use of airborne LiDAR and aerial photography in the estimation of individual tree heights in forestry. *Computers & Geosciences* **31**: 253-262.
- Thomas V, Treitz P, Jelinski D, Miller J, Lafleur P, McCaughey JH (2003). Image classification of a northern peatland complex using spectral and plant community data. *Remote Sensing of Environment* **84**: 83-99.
- Thoms MC (2003). Floodplain – river ecosystems: lateral connections and the implications of human interference. *Geomorphology* **56**: 335-349.
- Tockner K, Malard F, Ward JV (2000). An extension of the flood pulse concept. *Hydrological Processes* **14**: 2861-2883.

- Tockner K, Stanford JA (2002). Riverine floodplains: present state and future trends. *Environmental Conservation* **29**: 308-330.
- UribeArrea D, Perez-Gonzalez A, Benito G (2003). Channel changes in the Jarama and Tagus rivers (central Spain) over the past 500 years. *Quaternary Science Reviews* **22**: 2209-2221.
- Van de Ven GP (2004). *Man-made lowlands. History of water management and land reclamation in the Netherlands*. Stichting Matrijs, Utrecht.
- Van der Sande CJ, de Jong SM, de Roo APJ (2003). A segmentation and classification approach of IKONOS-2 imagery for land cover mapping to assist flood risk and flood damage assessment. *International Journal of Applied Earth Observation and Geoinformation* **4**: 217-229.
- Van der Velde G, Leuven RSEW, Ragas AMJ, Smits AJM (2006). Living rivers: trends and challenges in science and management. *Hydrobiologia* **565**: 359-367.
- Von Hansen W, Sties M (2000). On the capabilities of digital high resolution multispectral remote sensing techniques to serve nature conservation requirements. *International archives of Photogrammetry and Remote Sensing XXXIII(Part B7)*.
- Ward JV, Tockner K, Uehlinger U, Malard F (2001). Understanding natural patterns and processes in river corridors as the basis for effective river restoration. *Regulated Rivers: Research & Management* **17**: 311-323.
- Ward JV, Malard F, Tockner K (2002). Landscape ecology: a framework for integrating pattern and process in river corridors. *Landscape Ecology* **17**: 35-45.
- Wehr A, Lohr U (1999). Airborne laser scanning - an introduction and overview. *ISPRS Journal of Photogrammetry and Remote Sensing* **54**: 68-82.
- Wijnhoven S (2007). *Small Mammal - heavy metal interactions in contaminated floodplains; bioturbation and accumulation in periodically flooded environments*. PhD Thesis, Radboud University, Nijmegen.
- Zimble DA, Evans DL, Carlson GC, Parker RC, Grado SC, Gerard PD (2003). Characterizing vertical forest structure using small-footprint airborne LiDAR. *Remote Sensing of the Environment* **87**: 171-182.

2 Succession and rejuvenation in floodplains along the River Allier (France)

G.W. Geerling, A.M.J. Ragas, R.S.E.W. Leuven, J.H. van den Berg, M. Breedveld, D. Liefhebber, A.J.M. Smits.

Hydrobiologia (2006) **565**:71–86.

2.1 Abstract

The spatio-temporal heterogeneity of a meandering part of the Allier river was studied by analysing ecotope composition and dynamics using a series of aerial images covering a period of 46 years (1954-2000). The ecotope dynamics was exemplified by two time series showing rejuvenating hydro-geomorphological processes, i.e. meander progression, meander cut-off and channel shift. The mean rejuvenation rate was 33.8 ha per 5 years for the 5.5 km long study area. The ecotope transition rates varied from 18% surface area change per 5 years to 58.7% surface area change per 5 years for pioneer vegetation. The combination of hydro-geomorphological processes and ecological succession resulted in a temporal diversity of the riparian area. In the year 2000 half of the total riparian landscape was 14 years or younger and 23% was not rejuvenated in 46 years. 80% of the pioneer vegetation was found on young soils (<14 years) while more than 50% of the surface area of low dynamic ecotopes like bush and side channels was located on parts which were stable for more than 46 years. Examining the relation between river stretch size and ecotope diversity showed that the ecotope diversity remained stable above a stretch size of 1.5 meander lengths for the years 1978, 1985 and 2000. The spatial and temporal analysis of the study area showed evidence supporting the steady state or meta-climax hypotheses, but influences of long term processes on landscape composition were also found. Some implications for floodplain management are discussed.

2.2 Introduction

Since the late eighties, floodplains of highly regulated rivers are being reconstructed to increase flood protection and to follow society's call for strengthening riverine nature (Nienhuis and Leuven 2001, Wolfert 2001, Nienhuis et al. 2002, Lenders 2003, Buijse et al. 2005, van Stokkom et al. 2005). Plans involve geo-morphological interventions to increase the discharge capacity and to create semi-natural floodplains by stimulating natural processes like spontaneous succession, sedimentation, and to a lesser extent, erosion (Amoros 2001, Prach and Pysek 2001, Vulink 2001, Wolfert 2001).

The landscape unit pattern in natural river systems is shaped by a combination of two main driving forces: succession and rejuvenation. Succession is the local transition of a landscape unit to another by changing species composition (Forman and Godron 1986), while erosion in outer river bends and sedimentation in inner bends rejuvenates the vegetation types to a previous stage. In natural systems, the continuous disturbance of succession by rejuvenation processes results in a diverse landscape pattern with a high biodiversity (Amoros and Wade 1996). However, semi-natural floodplains in regulated rivers generally lack natural rejuvenation mechanisms. This may result in a landscape pattern dominated by climax succession

stages which has a relatively low biodiversity and high hydraulic resistance (Bravard et al. 1986, Amoros and Wade 1996, Baptist et al. 2004). This explains why river managers want to incorporate artificial rejuvenation measures in their management strategies (Smits et al. 2000). It is anticipated that clever application of artificial rejuvenation measures may increase biodiversity and safeguard flood protection goals (Buijse et al. 2005). However, to sensibly embed rejuvenation measures in river management, knowledge of the dynamics and the spatio-temporal heterogeneity of natural river systems is required (Ward et al. 2001). The present paper analyses succession and rejuvenation processes in a freely meandering river stretch in order to obtain information relevant for river management.

In a meandering system, the hydro-geomorphological processes associated with river channel migration rejuvenate the units that comprise the riparian landscape. Existing landscape units are rejuvenated while pioneer landscape units arise and go into succession. Landscape units are continuously present but shift in space, creating a spatio-temporally heterogeneous landscape pattern. If the system is in process equilibrium, the overall landscape unit dynamics must be stable at a certain scale level. This concept is called the steady-state mosaic (Forman and Godron 1986) or meta-climax concept (Amoros and Wade 1996). The dynamics and scale of the steady state mosaic are largely controlled by flow and sediment regimes and the geological,

climatic and biogeographical character of the river sector. For example, process equilibrium of a braided alpine river could be manifest within years in contrast with decades or more for a low gradient meandering channel (Van der Nat et al. 2003).

The aim of this paper is to determine the dynamics of landscape units in a freely meandering stretch of the river Allier (France) and the consequences for the spatio-temporal constitution of its riparian landscape. A time series of aerial photographs spanning 46 years was analysed to answer the following questions: 1. what are the transition rates of the different landscape units? 2. What is the spatio-temporal distribution of rejuvenation? 3. What is the surface area covered by the landscape units and how does it vary over time? 4. Can a river stretch size be determined, on which the landscape unit distribution is stable in all years?

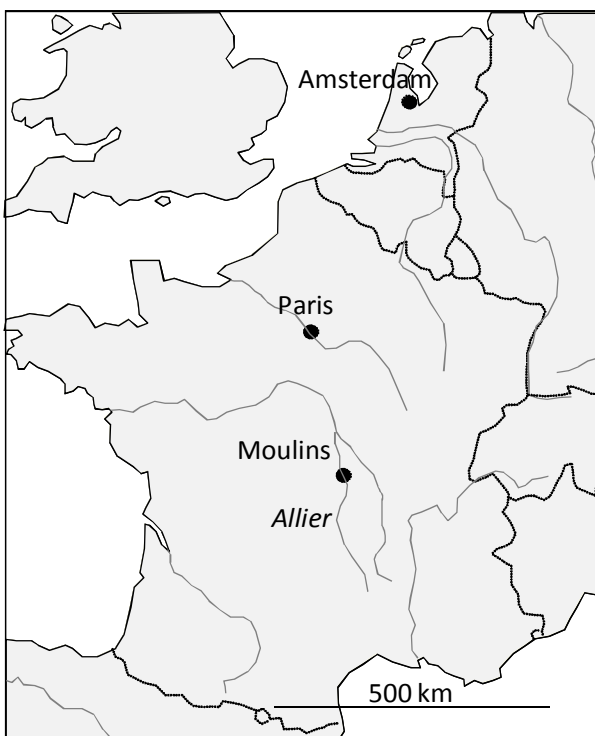


Figure 2.1 Location of the river Allier in Europe. The research area is located just south of Moulins. The north-west corner of the research area is (675330, 2170300) and the south-east corner is (678400, 2164550) in French national grid coordinates (Lambert zone II).

2.3 Material and methods

Study site

The study site is a 6 km stretch of the river Allier, south of Moulins (France, Figure 2.1). This is a meandering gravel river with lateral erosion in the outer bends and gravel point bars in the inner bends. Local sources state that before the transition to a nature area in the 1990s, the floodplains were subject to extensive grazing. It comprises about 500 ha of natural floodplain along a bit more than three meander lengths. The river is not used for navigation and the main channel in the research area is not regulated or excavated. These characteristics make it an interesting site to study meander processes in relation to riparian landscape composition and dynamics.

The Allier river's source is Lozère (1500 m altitude) located in the French 'Massif Centrale' (Wilbers 1997). After 410 km, the river converges with the Loire river at Bec-d'Allier (186 m altitude). The Allier is a rain fed river with an unpredictable discharge course. The mean annual discharge is $160 \text{ m}^3\text{s}^{-1}$ over the period 1850-1980 at Moulins (Gautier et al. 2000). Normally, peak discharges up to $1200 \text{ m}^3\text{s}^{-1}$ (occurrence once every 10 years at Moulins) occur in winter and spring while the discharges are generally low in the summer with a minimum of $12 \text{ m}^3\text{s}^{-1}$ (Gautier et al. 2000, Figure 2.2).

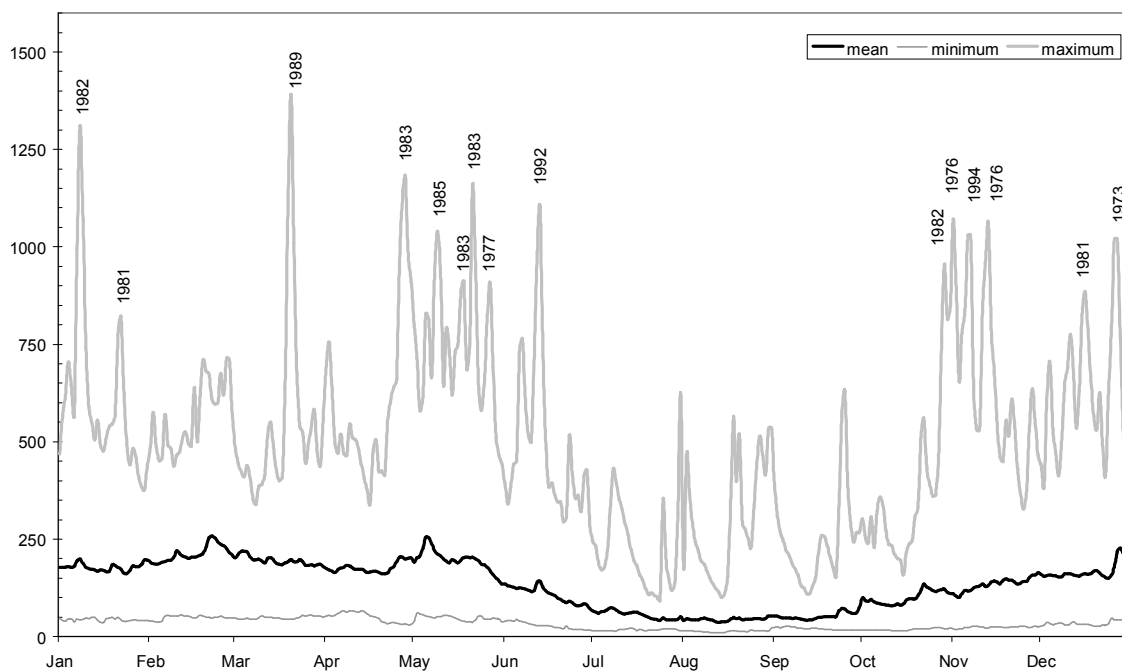


Figure 2.2 Minimum, mean and peak discharges of the river Allier at Moulins accumulated over the period 1968-2000. Peak discharges larger than $800 \text{ m}^3\text{s}^{-1}$ are labelled with the year of occurrence (data: l'Agence de l'Eau Loire Bretagne, France).

Preparing GIS Maps

Based on a set of aerial photographs, maps were produced to analyse the landscape changes in the research area using GIS (Miller et al. 1995, Muller 1997, Green and

Hartley 2000, Mendonca-Santos and Claramunt 2001). The photographic material consisted of stereographic coverage of aerial images of the years 1954, 1960, 1967, 1978, 1985, 2000 and a non stereographic set of 1992 (Photothèque-Nationale 2003). The photographic scale varied between 1:25,000 and 1:14,500 and all images were taken in the summer (July/August). For the years 1954 to 1992 black and white photographs were available; the photographs of the year 2000 were true-colour. The 1992 photograph set was not mapped and only used to determine a sinuosity value. Through a combination of field knowledge and expert knowledge on the interpretability of the available aerial image time series, a set of ecotope types was defined to classify landscape units (Table 2.1). A distinction is made between cultivated ecotopes (cultivated forest and agriculture) and natural ecotopes formed by river dynamics. An ecotope is a spatial unit of a certain extension (usually 0.25 to 1.5 ha) which is homogenous as to vegetation structure and the main abiotic factors on site (Forman and Godron 1986, Klijn and Udo de Haes 1994, Lenders et al. 2001). The aerial photographs were scanned and geo-referenced to a 1:25,000 topographical base map yielding rectified images of all years with a resolution between 2.1 and 2.5 m (IGN 1990, Erdas 1999, Mount et al. 2002). The maximum geo-reference error found relatively within the time series was about 10 m. In digitising ecotopes using aerial images two kinds of errors can be made: errors in outlining the ecotopes and errors in ecotope identification (Küchler and Zonneveld 1988, ESRI 2000).

Table 2.1 The mapped ecotopes (landscape units).

Ecotope (landscape unit)	Horizontal density	Human influence
Forest		C
Agriculture		C
Water, main channel		N
Bare soil (pointbar)		N
Pioneer vegetation		N
Grassland vegetation		N
Herbaceous vegetation		N
Bush (shrubs and trees < 5 m)	Open canopy (20% - 60% coverage)	N
	Closed canopy (>60% coverage)	N
Forest (> 5 m)	Open canopy (20% - 60% coverage)	N
	Closed canopy (>60% coverage)	N
Water, (closed) side channel		N

C: Cultivated landscape; N: Natural landscape.

First, the minimal mapping unit was defined as 40x40 m, i.e. 0.16 ha. The outline of the ecotopes was identified using colour, texture and vertical structure (explored using a stereoscope on the original images). ArcGIS 8.3 was used to manually digitise the outlines applying a fixed on-screen scale of 1:7500 (ESRI 2000). To minimise overlay errors in the analysis phase, the 2000 map was produced first and used as a basis for the older maps. Only borders of polygons that shifted more than the relative geo-reference error of 10m were considered ecotope outline changes and the

polygons were redrawn. For ecotope identification and evaluation of the digitised ecotope outlines, the stereoscope was used to exploit the original quality and vertical information of the aerial photos. For this, the arcGIS polyline maps were printed on transparencies and were placed on top of the original aerial images under a stereoscope (Topcon Model 3). This process resulted in ecotope maps for the years 1954 to 2000, which were subsequently used for the analysis.

GIS methods

All GIS analyses were performed using ArcGIS 8.3 and ArcGIS 9.0. For the raster calculations, the vector maps were rasterised to a 5x5 m grid.

To derive ecotope transition rates from the ecotope maps, transition matrices were produced of each map transition, e.g. 1954-1960, 1960-1967, and so on (Forman and Godron 1986, Miller et al. 1995, Van der Nat et al. 2003, Narumalani et al. 2004). Transition matrices show to which new ecotopes an ecotope is transformed during the time span between two successive photographs. To be able to compare transition rates between all the maps, the percentage change of each ecotope was computed and standardised to a 5-year period to compensate for the variety in years between maps. In this analysis, the main channel and the adjacent pointbars (bare soil) were grouped because fluctuations in water level influenced their relative surface areas.

To visualise ecotope dynamics, a general ecotope succession scheme was developed, based on the transition matrices and field expertise (Figure 2.3, Van den Berg and Balyuk 2004). The ecotope transition matrices were simplified by classifying every possible ecotope transition into three categories: succession, rejuvenation or stable. The classification was based on the direction of change in the succession scheme (Figure 2.3). Per ecotope the percentage area in succession, rejuvenation or remaining stability was computed for all transition periods. These percentages were visualised in triangular ternary plots. These plots are widely used in (soil) chemistry, to illustrate the composition of a three compound chemical mixture. In this paper, the axes show the area (as a percentage of the entire ecotope area) being stable, in succession, and in rejuvenation.

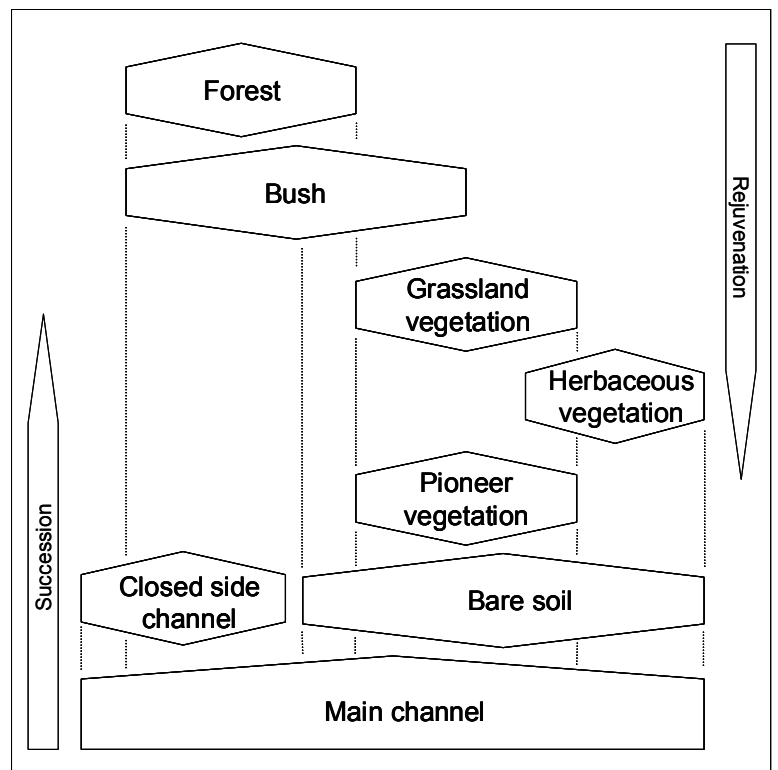


Figure 2.3 The succession scheme of the ecotopes along the river Allier.

To investigate the age distribution of the ecotopes in the year 2000, a map was constructed showing the year of last rejuvenation since 1954 by combining the ecotope types main channel and bare soil (pointbars) of the years 1954 to 2000. This floodplain age map was overlaid with the ecotope map of the year 2000 to determine the age distribution of each ecotope type in 2000. Parts of the floodplain, which were not rejuvenated within the time span of the photographic survey, were assumed to be in succession for more than 46 years.

To investigate scale in relation to ecotope diversity, a method was developed analogous to determining the minimum area size of vegetation quadrats in field vegetation surveys. Here, the quadrat size is increased until the species composition becomes constant; this is the minimum quadrat size (Kent and Coker 1994). To accomplish this with ecotope maps, the maps were cut into regular stretches perpendicular to the meandering direction of the river. The Shannon Index (SI) was used as landscape diversity measure, because it relates to the relative ecotope surface area distribution (McGarigal and Marks 1995). The SI is high when all ecotope types occupy a similar area and decreases when this ecotope area distribution becomes more uneven. Starting upstream, the SI was calculated for the first 600 m stretch of the mapped area. Subsequently, the area was stepwise enlarged in downstream direction and the SI was repeatedly calculated yielding SI values for a growing area until the area covered the complete map surface. Fragstats 3.3 was used to calculate the SI (McGarigal and Marks 1995).

Table 2.2 Total rejuvenation in the research area.

Time span (years 1900)	54-60	60-67	67-78	78-85	85-00	Mean
Rejuvenation (ha)	31.5	57.8	68.9	72.9	80.1	
Rejuvenation (ha / 5 yr)	26.3	41.3	31.3	52.1	26.7	33.8

2.4 Results

Ecotope maps

Figure 2.4 presents a time series demonstrating ecotope succession and rejuvenation caused by the hydro-geomorphological processes. The meander grew and moved northward in the years 1954, 1960, 1967.

Between 1967 and 1978 a bridge was constructed on the downstream border of the research area which probably caused or facilitated the cut-off shown in the 1978 excerpt, and so creating a side channel. The cut-off resulted in a peak in the rejuvenation activity (Table 2.2) and a drop in sinuosity (Table 2.3), but as the meandering process continued, sinuosity reached its former values again in 1992 to 2000. The mean rejuvenation rate within the 5.5 km straight (3 meanders long) research area is 33.8 ha every 5 years (Table 2.2).

Table 2.3 Sinuosity of the studied river stretch.

Year	Sinuosity
1954	1.35
1960	1.41
1967	1.45
1978	1.24
1985	1.27
1992	1.42
2000	1.47

Figure 2.4 (In full colour on page 185) Meander progression in a part of the research area over the period 1954 to 2000. The river flows from South to North. From 1954 to 1967 a meander progression is visible. In the period 1967 to 1978 the meander was cut-off. The meandering process is restored in 1985 and 2000.

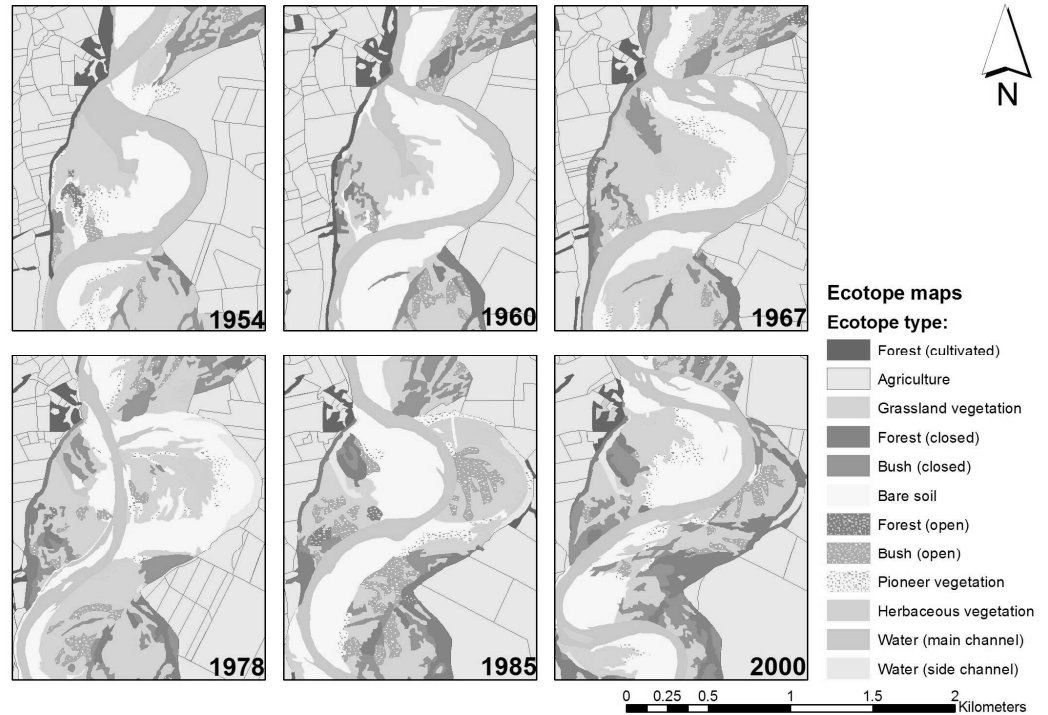


Figure 2.5 (In full colour on page 185) Meander shift rejuvenates ecotopes and creates niches for forest development over the period 1967-2000. The 1967-1978 shift rejuvenates ecotopes and creates niches for forest settlement in the former channels. In 1985 these channels are colonized by bush that grow to forest in the 1985-2000 period.

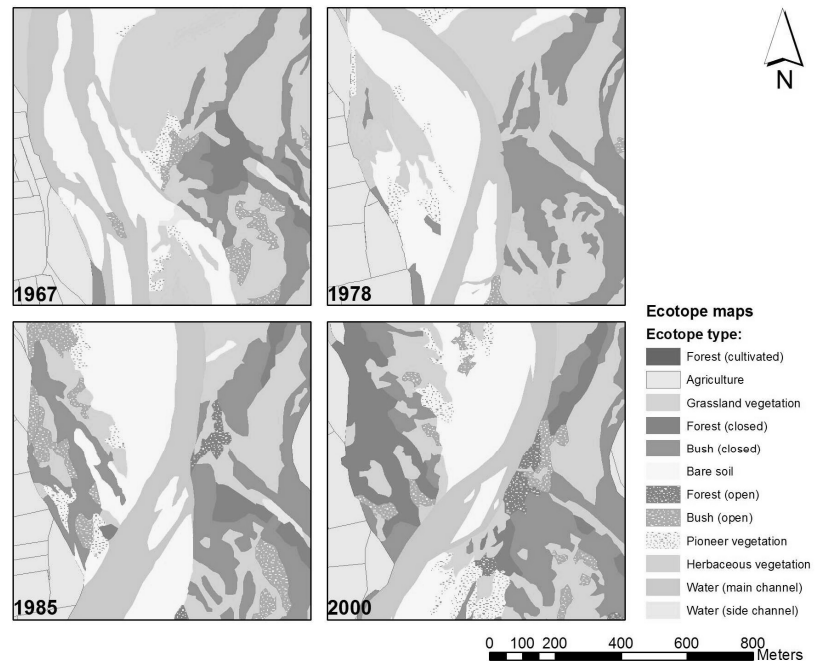


Figure 2.5 illustrates the influence of hydro-geomorphological processes on the spatial distribution of ecotopes, in this case the formation of a black poplar (*Populus nigra*) niche by a shift of the river channel in 1967 and 1978. The main channel shift left a depression in the landscape and simultaneously rejuvenated older succession stages across the stream. Subsequently, the depression (i.e. the former river channel) functioned as an environment for the settlement of black poplar. The small poplars grew from ecotope type bush to forest between the years 1985 and 2000.

Table 2.4 Example of change matrix for one transition between the years 1967 and 1978, expressed as the percentage surface area change per ecotope type and total area for 1967.

	Fcult	Ag	G	Fcl	Bcl	BS	Fo	Bo	P	H	MC	SC	Area (ha)
Fcult	36.98	47.11	0.53	1.43	6.90	0.00	0.00	0.00	0.05	6.99	0.00	0.00	51.59
Ag	1.18	97.28	0.86	0.18	0.27	0.02	0.02	0.00	0.02	0.12	0.04	0.01	954.96
G	0.00	1.39	62.20	0.88	2.17	19.99	0.44	2.92	3.50	0.85	5.30	0.36	148.72
Fcl	0.33	2.41	8.89	56.64	15.46	4.79	4.87	1.80	0.75	2.35	1.72	0.00	49.25
Bcl	0.00	0.60	18.30	10.63	45.79	1.41	0.10	13.20	0.56	2.16	7.20	0.05	59.56
BS	0.11	8.84	18.26	2.24	4.42	32.55	0.66	2.23	3.35	0.89	26.35	0.10	148.48
Fo	0.00	0.00	30.21	16.23	14.29	10.73	2.77	13.98	11.17	0.62	0.00	0.00	5.69
Bo	0.00	0.02	55.08	3.43	2.39	1.43	1.45	20.05	0.89	9.61	5.66	0.00	13.48
P	0.00	8.96	9.22	0.00	0.00	41.07	0.00	0.09	4.34	0.28	36.05	0.00	8.82
H	3.94	18.53	13.59	11.02	10.26	18.53	0.00	3.38	0.00	1.43	19.30	0.02	24.87
MC	0.08	8.43	23.64	2.04	6.86	21.65	0.49	1.91	3.53	0.05	31.10	0.21	57.45
SC	0.64	66.19	0.70	0.81	0.03	10.73	0.00	0.02	0.00	0.00	17.95	2.92	16.07

Fcult: Cultivated Forest; Ag: Agriculture; BS: Bare soil; P: Pioneer vegetation; G: Grassland; H: Herbaceous vegetation; Bo: Open Bush; Fo: Open Forest; Fcl: Closed forest; Bcl: Closed bush; MC: Main channel; SC: Side channel.

Ecotope dynamics

An example of the ecotope transition matrices that were produced is shown in Table 2.4. The rows show to what extent (percentage area) the 1967 ecotopes (row headers) developed into different ecotopes in 1978 (column headers). Table 2.5 shows the ecotope transition rates for all time steps and standardised to a 5 year period. The four most dynamic ecotopes with more than 50 percent change per 5 years were open forest, open bush, pioneer vegetation, and herbaceous vegetation. Next to the surrounding cultivated area, the main channel and point bar showed the lowest percentage of change and variability. Transition rates between the years 1954-1960 and 1978-1985 were higher than for other time spans.

Figure 2.6 Ternary plots of ecotope stability, rejuvenation and succession.

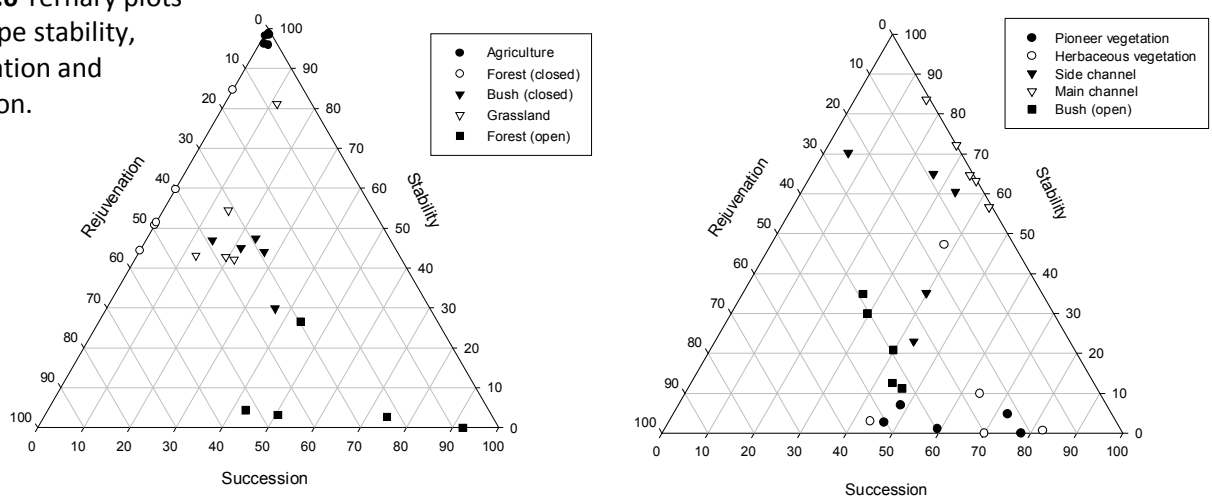


Table 2.5 Ecotope transition rates: percentage change to another ecotope for every map transition and standardised to a 5 year period. The data is numerically arranged based on the mean ecotope transition rate.

Ecotope	Time span (years)					Mean	SD
	54-60	60-67	67-78	78-85	85-00		
Agriculture and Cultivated forest	1.4	2.9	1.7	0.9	0.5	1.5	0.9
Main channel & Bare soil	13.8	19.9	16.7	25.3	14.5	18.0	4.7
Forest (closed)	12.8	35.1	18.3	39.7	16.2	24.4	12.2
Grassland vegetation	47.3	13.5	20.7	40.9	19.3	28.3	14.8
Side channel	64.2	21.2	29.5	25.1	13.2	30.6	19.7
Bush (closed)	58.4	37.5	24.1	39.2	18.6	35.6	15.5
Bush (open)	58.3	46.5	39.7	56.6	29.6	46.1	12.0
Herbaceous vegetation	82.8	37.6	44.1	71.4	30.0	53.2	22.7
Forest (open)	81.1	71.4	44.0	52.4	31.9	56.1	20.0
Pioneer vegetation	77.5	68.0	44.2	70.6	33.3	58.7	18.9

SD: standard deviation.

The results of the visualisation of ecotope dynamics in ternary plots are presented in Figure 2.6. Each data point represents the change of an ecotope in the period that lies between two successive maps. The most apparent example is the cultivated area, of which >95% of the surface area remained stable for each successive time span; all data of this ecotope type clearly show in the top corner of the ternary plot. The main channel and closed forest are opposites; their values lie respectively on the succession axis and on the rejuvenation axis. Grassland and closed bush had a relatively low tendency for succession (<30%). They remained stable (>40%) or rejuvenated (>30%). The open bush ecotope varied in stability and succession, but rejuvenation remained constant around 40%. The open forest type, the pioneer vegetation and herbaceous vegetation showed low stability (< 10%) and similar tendencies for succession and rejuvenation. The most diverse type in terms of succession, rejuvenation and stability was the side channel ecotope.

Table 2.6 The surface area of natural ecotopes and total natural floodplain (ha).

Ecotope	1954	1960	1967	1978	1985	2000
Forest (closed)	17.44	52.52	46.73	49.25	42.67	67.28
Bush (closed)	59.65	44.84	58.45	59.47	59.34	75.60
Forest (open)	12.20	3.63	4.91	5.67	9.12	10.62
Bush (open)	25.35	31.09	21.89	13.51	31.99	18.31
Herbaceous vegetation	11.91	1.94	11.50	24.89	18.08	24.56
Grassland vegetation	212.70	125.40	170.50	148.82	111.70	97.46
Pioneer vegetation	16.78	8.25	14.32	8.82	12.76	15.83
Side Channel	1.58	0.61	1.39	16.05	18.45	11.86
Main channel and Bare soil	191.80	208.25	186.50	205.91	184.27	158.78
Total	549.40	476.53	516.19	532.38	488.37	480.30

Floodplain and ecotope age

Figure 2.7 shows the year of last rejuvenation of the riparian area since 1954. Figure 2.8 shows the age distribution of the total floodplain area and of each ecotope in the year 2000. The age class >46 years consisted of the natural floodplain area that was not rejuvenated within the 46-year period of the map series. Half of the natural floodplain consists of ecotopes of 15 years and younger and about 24 percent of the surface area is older than 46 years. Viewed per ecotope type, the age distribution is different when compared to the age distribution of the entire area. The youngest ecotope type is pioneer vegetation; more than 80% of its area is younger than 15 years. Grassland, herbaceous vegetation and open bush form an intermediate group with 50 to 60 percent of their area younger than 22 years. Side channel and closed bush are the oldest ecotopes with about half their area older than 46 years.

Ecotope areas over time

The temporal variation in the surface area coverage of different ecotope types is shown in Figure 2.9 and Table 2.6. The surface area of natural ecotopes (Table 2.1) versus the surface area of cultivated ecotopes changes on the local scale (Figure 2.4 and 2.5) but fluctuates during the years at the river stretch scale only within a 10% range around a mean of 507 ha (see totals of Table 2.6). Grasslands and bare soil are the most variable, especially in the years 1954, 1960 and 1967, while for example the surface area of side channels is relatively stable. A decrease of open vegetation types like pioneer vegetation, grassland, herbaceous vegetation in favour of the closed types like bush and forest is visible. In 1954, 79% of the research area

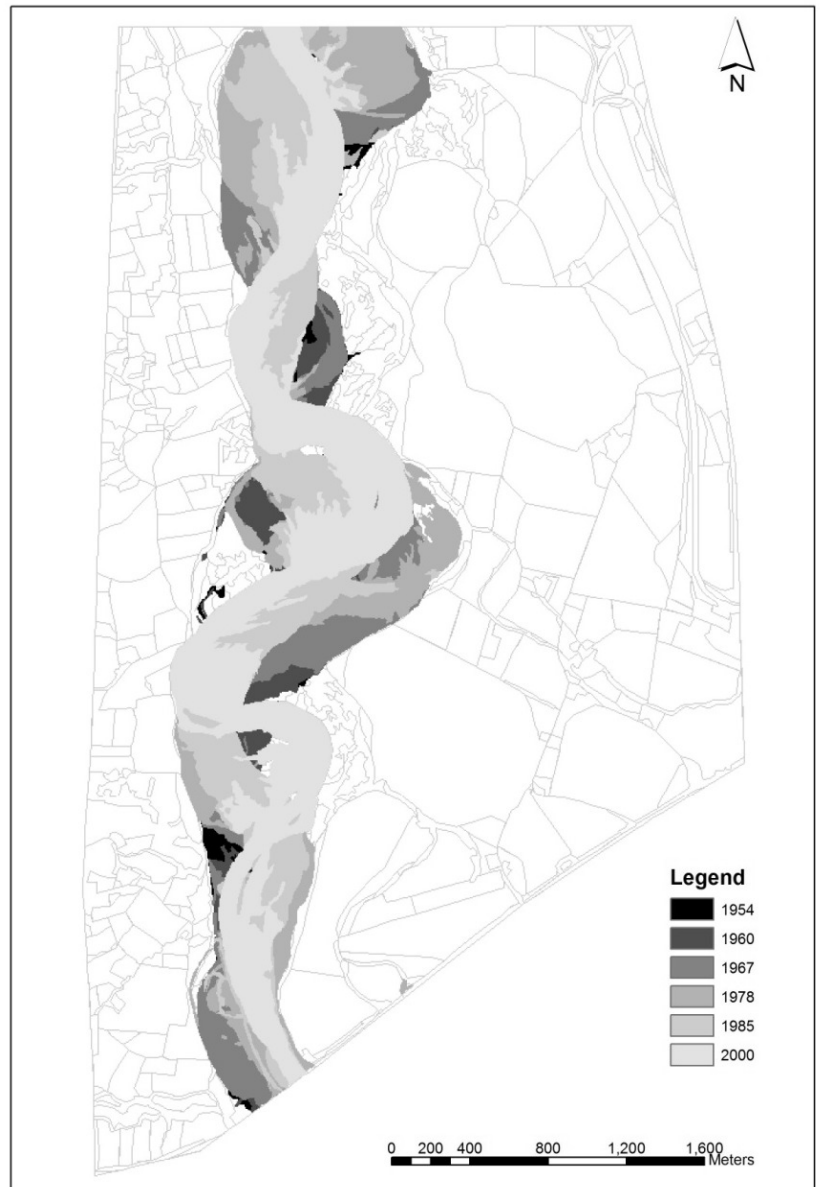


Figure 2.7 The floodplain age map illustrates the hydro-geomorphological activity of the research area by overlays of the ecotopes active main channel and bare soil (point bars) of 1954 to the year 2000. As background, the ecotope map of the year 2000 is used.

was open, in 1978 76% and 64% in 2000. The drop in area of grassland vegetation between 1954 and 1960 was caused mainly by transition to agricultural area (34.5%, data not shown, but see Table 2.2 for years 1954 and 1960).

Ecotope diversity and scale

Figure 2.10 shows the landscape diversity of the study area, expressed as Shannon Index (SI), as a function of scale. The variation in SI values decreases when sliding from ecotope to river stretch scale. For the year 2000, the ecotope diversity remained stable if the floodplain surface area was about 250 ha, i.e. about 1.5 meander lengths. This seems to hold for the 1985 and 1978 results, but the 1954, 1960 and 1967 show an upward trend of SI values within the research area and no real stabilisation. An overall temporal trend of the SI values is also clearly visible, in time the overall landscape diversity is increasing.

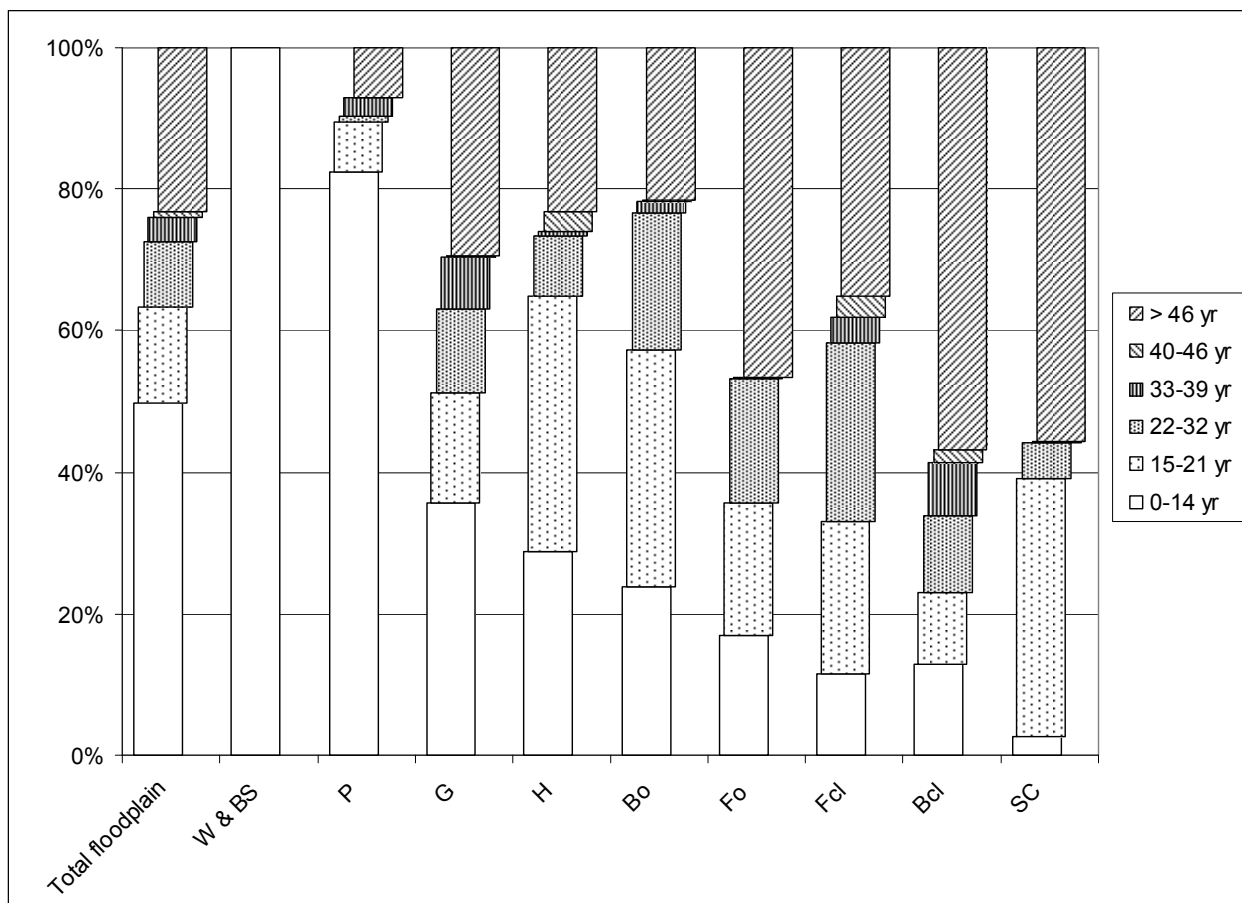


Figure 2.8 Floodplain and age distribution of natural ecotope types: W & BS: Water and Bare soil; P: Pioneer vegetation; G: Grassland; H: Herbaceous vegetation; Bo: Open bush; Fo: Open forest; Fcl: Closed forest; Bcl: Closed bush; SC: Side channel.

Figure 2.9 Total ecotope surface area (ha) over the period 1954 to 2000.

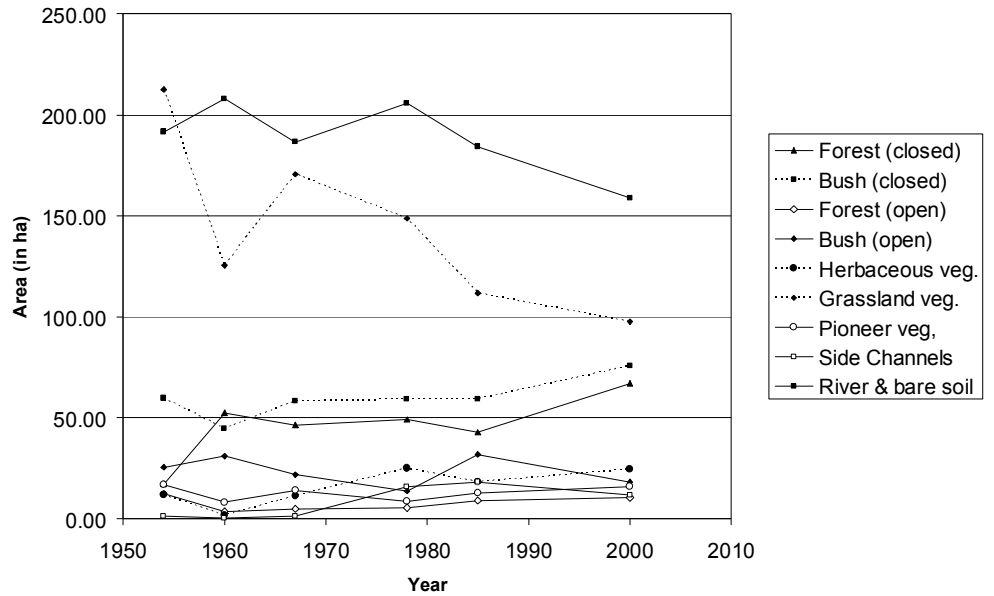
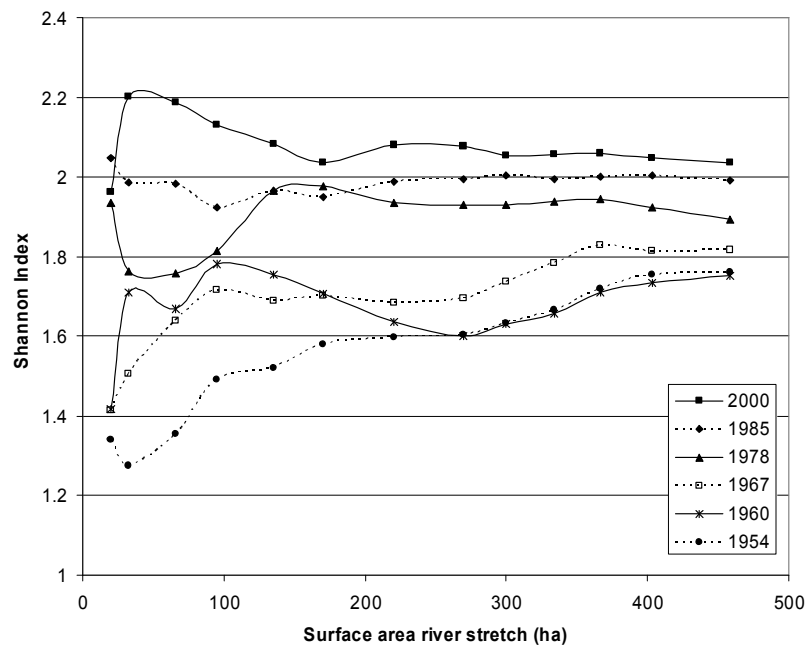


Figure 2.10 Landscape diversity in relation to the surface area of the river stretch that was used for calculation.



2.5 Discussion

Mapping and GIS-analyses

The spatio-temporal heterogeneity of a meandering part of the Allier river was studied by analysing ecotope composition and dynamics using a series of aerial images covering a period of 46 years. Ecotopes were mapped starting with the aerial photograph of 2000 and retracing the changes in ecotope borders through time. This procedure worked well to overcome small geo-rectification differences of the different aerial photograph years. The overall quality of the aerial images was good but the quality and interpretability of early photos (1954, 1960) determined to some

extent the resolution of the ecotope classification system.

The digitising process was optimised by a combination of digitising on screen and stereoscopic verification. In previous methods, the aerial images were viewed with a stereoscope and the ecotopes were traced on overlaid transparencies. Consequently, the minimal mapping unit depended on the trace-pen width. Subsequently the transparencies had to be scanned, geo-referenced and vectorised. Furthermore, before polygon vectorisation could start, the scan had to be checked and corrected manually for unclosed polygons using a drawing programme such as photoshop. This whole process was rather laborious and was shortened by digitising on screen. The verification and labelling of the on-screen digitising result was done by overlaying the digitised polygons (printed on transparencies) on top of the original aerial images under a stereoscope. In this way, the advantage of stereoscopic interpretation was kept.

Ecotope maps

The local dynamics are influenced by the succession speed of a particular ecotope and the local acting hydro-geomorphological processes. Figure 2.4 and 2.5 show the processes at work in the evolution of two small parts of the research area: rejuvenation of older succession stages by lateral erosion of outside bends, formation of new succession stages, formation of a side channel, and colonisation by vegetation of former channels. Figure 2.5 is a good example of the expansion and contraction events that steer riverine landscape heterogeneity (Tockner et al. 2000). The retracting water level followed the former channels in the point bar while seed dispersal took place and so steered the spatial distribution of vegetation settlement.

Ecotope dynamics

The mean ecotope transition rates (Table 2.5) follow the succession scheme illustrated in Figure 2.3 with dynamic ecotopes close to the main channel and less dynamic ecotopes to the climax stages, i.e. pioneer with the highest mean transition rate and closed forest with a relatively low mean transition rate. Two exceptions are grassland vegetation and open forest. Grassland is less dynamic than ecotope bush ecotope, probably because in the past the grasslands in the floodplains were used for grazing, so succession to open bush or open forest was inhibited. The open forest is relatively dynamic because in effect it is a mixed ecotope. Close to the river the ecotope type open forest consists of dynamic patches of young pioneer forest, so called softwood forest, and on well developed older stages it consists of low dynamic patches in succession to hardwood forest.

The ecotope transition rates in this study vary between 18% to 59% per 5 years. The mean rejuvenation rate is 33.8 ha per 5 years along the 5.5 km stretch of the study area. Studies presenting comparable values are scarce. As can be expected, the ecotope dynamics are lower when compared to dynamics in a braided alpine river where 80% of major landscape elements are rejuvenated within 3 years (Ward et al.

2001). A study on the river Ain (France) along a 40 km stretch of this river showed that rejuvenation rates decreased from about 100 ha per 10 years per 40 kms in the period 1945-1965 to 30 ha per 10 years per 40 kms in the period 1985 to 1991 (Marston et al. 1995). This river has a slightly lower mean annual discharge ($130 \text{ m}^3\text{s}^{-1}$) than the Allier. Between 1945 and 1991, the river dynamics decreased resulting in a single thread meandering river.

The transition rates of 1954-1960 and 1978-1985 transition are relatively high compared to the other years. In the period 1954-1960 the river channel was very active in the northern half of the research area. The limited availability of data on external pressures and influences that may explain this increase in activity, impede a satisfactory explanation. Possible explanations are listed below.

- 1) A peak flow could be the cause, but discharge data on this period is not available for this study, although in the Ubaye River in the Southern Alps about 400-500 km from the Allier catchment, a millennium flood is recorded in 1957 (Piégay and Salvador 1997).
- 2) An important factor is the sediment balance in the system; it can affect meander progression (Kondolf et al. 2002, Millar 2005).
- 3) The high activity could be a downstream geomorphological effect of the main channel running into a natural fixed bank and slowly passing this point in 1954 to 1967 (Figure 2.4).
- 4) The meander progression is increased when river banks consist of agricultural grounds (Micheli et al. 2004). The meander, shown in Figure 2.4, flows past agricultural area in the outer bend.

The increased dynamics in the 1978-1985 period can be attributed to the bridge effect (discussed later) and to the accumulation of major flood events in the early eighties (Figure 2.2: January and December 1981, January and October 1982, April and May 1983, May 1985).

Floodplain and ecotope age

As a consequence of the spatial distribution of rejuvenation in the floodplain as shown in Figure 2.7, the ecotopes present are spatio-temporally distributed (Figure 2.8). This spatio-temporal distribution is a characteristic of the steady state mosaic or meta-climax. Figure 2.7 also shows the separate and combined effect of rejuvenation and succession. The floodplain age shows the age distribution caused by hydro-geomorphological processes and without ecotope succession. Due to ecotope succession the ecotope-age distribution of separate ecotopes is different as compared to total floodplain age composition. For example, half of the total riparian area is younger than 15 years; the ecotope closed-forest is almost for 90% situated on parts older than 15 years.

In Figure 2.8 the order of the succession scheme (Figure 2.3 and Figure 2.6) can be identified. Generally, the ecotopes having lower transition rates are relatively abundant on the older floodplain parts. Interesting is the ecotope-age distribution of open forest, which was classified as a dynamic ecotope with low stability based on the transition rates. However, seemingly contradicting the dynamic nature of this ecotope, more than 40% of the ecotope is found on older grounds. But, on older parts, the ecotope is a recent development because the older areas are being colonised by trees, i.e. in succession to (hardwood) forest stages via the open forest stage. Unfortunately, photo interpretation did not permit recognition of different types of open forest.

Ecotope areas over time

As shown on the local scale, ecotopes are dynamic (Table 2.4, Figure 2.6), shifting in space through time (Figure 2.4, 2.5 and 2.7). Within the river stretch or functional sector the overall ecotope distribution is less dynamic (Figure 2.9), as assumed by the steady state mosaic or meta-climax hypotheses (Forman and Godron 1986, Amoros and Wade 1996).

A true (theoretical) steady state (or meta-climax) within a stretch homogeneous in processes and environment would show as a stable ecotope distribution time series. However, our study shows a general trend in decrease of the proportion of open, low structure ecotopes towards an increase of structure rich ecotopes, such as forest and bush (Figure 2.9). This trend in the ecotope distribution is caused by long term changes of acting processes. Most probably a decrease of the grazing intensities. The area became a nature reserve in the 1994 and all grazing was phased out.

Another bias is the construction of the bridge near Chemilly, just south to the research area. Although the meander pattern recovered (Figure 2.4, Table 2.3), the exact influence of the bridge near Chemilly is not known. It can be hypothesised that what the shift accomplished is similar to a major flood event, though now induced by human intervention of narrowing the channel downstream by building a bridge and short cutting the first meander (Wilbers personal communication) and simultaneously a flood occurrence in 1976 ($1,020 \text{ m}^3\text{s}^{-1}$). This channel shift created niches for various vegetation types, e.g. a poplar settlement. Together with lower grazing intensities, this can explain the increase in bush ecotope in 1985 and in 2000 the increase in forest ecotope (poplar becoming higher than 5 m) found in Figure 2.9. In general, over medium time scales (10-100 years) most river systems can be viewed as quasi-equilibrium states (Petts and Amoros 1996) but the (theoretical) steady state (or meta-climax) is in populated areas likely to be biased by either human interventions or land use change. Furthermore, the larger the time scale of the steady state dynamics of a particular system, like a continental scale river, the more influence can be expected of long term processes like climate change or geological change which affect discharge, sediment regimes and rates of succession.

Ecotope diversity and scale

When sliding from ecotope scale to river stretch scale; the surface area proportion of each ecotope will change. However, will it change indefinitely? Under similar hydro-geomorphological conditions along the stretch, i.e. a steady state situation, it should stabilise at a certain river stretch size. Therefore, the question is if this 'steady state unit' in which the relative ecotope diversity is at a constant level over time, can be determined in space.

Our results indicate that the steady state unit size has been decreasing over the years. It was smallest but stable for 1985 and 2000 at about one and a half meander length (Figure 2.10). However, a spatially consistent area containing a steady state or stable meta-climax 'unit' is not found because the area should be the same through all the years. Similar to the trend found in Figure 2.9, these results again point to an underlying long term process of change, like diminishing grazing intensities. This is also consistent with the rising SI values over the years (Figure 2.10), indicating a trend towards a more heterogeneous landscape.

In this study, the sliding scale approach is used to investigate the scale on which landscape diversity stabilises. When focussed on changes in the SI curve, the approach could facilitate locating transitions in landscapes, indicating a change in acting processes.

Implications for floodplain management

In regulated systems, the hydro-geomorphological processes are restricted because the main (navigation) channel is fixed. Therefore, rejuvenation processes such as lateral erosion are inhibited. As succession of ecotopes still proceeds, the imitation of rejuvenation processes in regulated river systems has two main advantages. First, the absence of rejuvenation mechanisms in regulated systems causes the gradual disappearance of ecotopes with high turnover, leading to a lower biological diversity (Bravard et al. 1986, Amoros and Wade 1996, Gilvear et al. 2000). The introduction of rejuvenation can increase biological diversity. Secondly, rejuvenating hydraulically rough vegetation, often the older climax stages, helps to maintain the discharge capacity, a major concern of the river manager (Smits et al. 2000, Baptist et al. 2004). The combined effect of succession and rejuvenation brings about unique spatio-temporal patterns for different streams and rivers. The ecological successions vary with the biogeographical region and rejuvenation is connected to the fluvial setting. A high dynamic braided alpine river, constrained geologically, will give rise to a landscape with young ecotopes with high turnover rates, and few older elements like trees (or forests) will survive. In rivers with moderate dynamics, like the Allier or ever larger rivers, turnover rates drop, ecotope succession may reach climax stages and consequently the temporal pattern changes (Marston et al. 1995, Petts and Amoros 1996, Ward et al. 2001, Van der Nat et al. 2003). It would be interesting to compare different rivers of various sizes on their landscape dynamics, but comparative material was hardly found in literature. The combined knowledge on

succession and rejuvenation processes of natural rivers and knowledge of the former river dynamics of the managed river gives the river manager insight in possible management options (Buijse et al. 2005).

Important in sound ecological management is the spatio-temporal context on which the riparian landscape has to be viewed (Bravard et al. 1986, Ward et al. 2001).

Therefore, the river and nature manager has to have knowledge on direction of change and information on the present day diversity in space and succession stage (time) before management options can be evaluated.

2.6 Conclusions

The results show that a freely meandering system generates a spatially and temporally diverse landscape. On the ecotope level, the dynamics are higher than on the river stretch. On the river stretch, the ecotope distribution was relatively stable, but showed long-term trends, generally changing towards a more closed and structure rich heterogeneous landscape.

The river Allier shows characteristics of a system in a steady state mosaic or meta-climax but this equilibrium is influenced by long-term changes in processes affecting landscape composition.

Riparian landscapes have to be viewed in their spatio-temporal context. Process knowledge is important to be able to anticipate on riverine landscape changes and to make ecologically sound management choices. Therefore, reference studies of non-regulated rivers can provide a guideline for ecological management of regulated systems.

Acknowledgements

This study was funded by the Ministry of Public Works and Transport, Survey Department, Delft. We would like to thank the project leaders M. Vreeken-Buijs and R. Brügelmann for their support. We would like to thank B. Peters for valuable field excursions along the river Allier. Furthermore, we thank all the people which we have met during the summers 'au bord d'Allier': M. Baptist, L. van den Bosch, A. Wilbers, J. de Kramer, and all the students from Delft University (TUD) and Utrecht University (UU). Finally yet importantly, we thank our colleagues E. Kater and A. Bos for their stimulating discussions. This is CWE publication 420.

References

- Amoros C (2001). The concept of habitat diversity between and within ecosystems applied to river side-arm restoration. *Environmental management* **28**: 805-817.
- Amoros C, Wade PM (1996). *Ecological successions*. In: Petts GE, Amoros C (Eds.). *Fluvial Hydrosystems*. Chapman & Hall, London. pp. 211-241.

- Baptist MJ, Penning WE, Duel H, Smits AJM, Geerling GW, van der Lee GEM, van Alphen JSL (2004). Assessment of the effects of cyclic floodplain rejuvenation on flood levels and biodiversity along the Rhine River. *River Research and Applications* **20**: 285-297.
- Bravard J-P, Amoros C, Pautou G (1986). Impact of civil engineering works on the successions of communities in a fluvial system. *Oikos* **47**: 92-111.
- Buijse AD, Klijn F, Leuven RSEW, Middelkoop H, Schiemer F, Thorp JH, Wolfert HP (2005). Rehabilitation of large rivers: references, achievements and integration. *Archiv für Hydrobiologie Supplement* **155**: 715-738.
- Erdas (1999). *Erdas Imagine 8.x. Tour Guide*. Erdas Inc., Atlanta, Georgia.
- ESR (2000). *ArcGIS 8.x and ArcInfo workstation*. Environmental Systems Research Institute, Redlands.
- Forman RTT, Godron M (1986). *Landscape Ecology*. John Wiley & Sons, New York.
- Gautier E, Piégay H, Bertainia P (2000). A methodological approach of fluvial dynamics oriented towards hydrosystem management: case study of the Loire and Allier rivers. *Geodinamica Acta* **1**: 29-43.
- Gilvear DJ, Cecil J, Parsons H (2000). Channel change and vegetation diversity on a low-angle alluvial fan, River Feshie, Scotland. *Aquatic Conservation: Marine and Freshwater Ecosystems* **10**: 53-71.
- Green DR, Hartley S (2000). Integrating photointerpretation and GIS for vegetation mapping: some issues of error. In: Alexander R, Millington AC (Eds.). *Vegetation Mapping: From Patch to Planet*. John Wiley & Sons Ltd., Chichester. pp. 103-134.
- IGN (1990). *Carte Série bleue Top25 de France. Map no. 26270 (Moulins)*. Institut Géographique National, Paris.
- Kent M, Coker P (1994). *Vegetation Description and Analysis: a practical approach*. Wiley, Chichester.
- Klijn F, Udo de Haes HA (1994). A hierarchical approach to ecosystems and its implications for ecological land classification. *Landscape Ecology* **9**: 89-104.
- Kondolf GM, Piégay H, Landon N (2002). Channel response to increased and decreased bedload supply from land use change: contrasts between two catchments. *Geomorphology* **45**: 35-51.
- Küchler AW, Zonneveld IS (1988). *Vegetation Mapping*. Kluwer Academic Publishers, Dordrecht.
- Lenders HJR (2003). *Environmental rehabilitation of the river landscape in the Netherlands. A blend of five dimensions*. PhD thesis, University of Nijmegen, Nijmegen.
- Lenders HJR, Leuven RSEW, Nienhuis PH, de Nooij RJW, van Rooij SAM (2001). BIO-SAFE: a method for evaluation of biodiversity values on the basis of political and legal criteria. *Landscape and Urban Planning* **55**: 121-137.
- Marston RA, Girel J, Pautou G, Piégay H, Bravard J-P, Arneson C (1995). Channel metamorphosis, floodplain disturbance, and vegetation development: Ain river, France. *Geomorphology* **13**: 121-131.

- McGarigal K, Marks B (1995). *FRAGSTATS: Spatial analysis program for quantifying landscape structure*. Gen Tech. Rep., USDA Forest Service.
- Mendonca-Santos ML, Claramunt C (2001). An integrated landscape and local analysis of land cover evolution in an alluvial zone. *Computers, Environment and Urban Systems* **25**: 557-577.
- Micheli ER, Kirchner JW, Larsen EW (2004). Quantifying the effect of riparian forest versus agricultural vegetation on river meander migration rates, Central Sacramento River, California, USA. *River Research and Applications* **20**: 537-548.
- Millar RG (2005). Theoretical regime equations for mobile gravel-bed rivers with stable banks. *Geomorphology* **64**: 207-220.
- Miller JR, Schulz TT, Hobbs NT, Wilson KR, Schrupp DL, Baker WL (1995). Changes in the landscape structure of a southeastern Wyoming riparian zone following shifts in stream dynamics. *Biological Conservation* **72**: 371-379.
- Mount NJ, Zukowskyj PM, Teeuw RM, Stott TA (2002). Use of aerial photography and digital photogrammetry in the assessment of river channel destabilisation. In: Leuven RSEW, Pourdevigne I, Teeuw RM (Eds.). *Application of Geographic Information Systems and Remote Sensing in River Studies*. Backhuys Publishers, Leiden. pp. 41-62.
- Muller E (1997). Mapping riparian vegetation along rivers: old concepts and new methods. *Aquatic Botany* **58**: 411-437.
- Narumalani S, Deepak RM, Rothwell RG (2004). Change detection and landscape metrics for inferring anthropogenic processes in the greater EFMO area. *Remote Sensing of Environment* **91**: 478-489.
- Nienhuis PH, Buijse AD, Leuven RSEW, Smits AJM, de Nooij RWJ, Samborska EM (2002). Ecological rehabilitation of the lowland basin of the river Rhine (NW Europe). *Hydrobiologia* **478**: 53-72.
- Nienhuis PH, Leuven RSEW (2001). River restoration and flood protection: controversy or synergism. *Hydrobiologia* **444**: 85-99.
- Petts GE, Amoros C (1996). *Fluvial Hydrosystems*. Chapman & Hall, London.
- Photothèque-Nationale (2003). *Aerial images of years 1954, 1960, 1967, 1978, 1985, 1992, and 2000*. Photothèque Nationale, 2/4 avenue Pasteur. Saint-Mandé Cedex.
- Piégay H, Salvador P-G (1997). Contemporary floodplain forest evolution along the middle Ubaye river, Southern Alps, France. *Global Ecology and Biogeography Letter* **6**: 397-406.
- Prach K, Pysek P (2001). Using spontaneous succession for restoration of human-disturbed habitats: Experience from Central Europe. *Ecological Engineering* **17**: 55-62.
- Smits AJM, Havinga H, Marteiijn ECL (2000). New concepts in river and water management in the Rhine river basin: how to live with the unexpected? In: Smits AJM, Nienhuis PH, Leuven RSEW (Eds.). *New approaches to river management*. Backhuys Publishers, Leiden. pp. 267-286.

- Tockner K, Malard F, Ward JV (2000). An extension of the flood pulse concept. *Hydrological Processes* **14**: 2861-2883.
- Van den Berg JH, Balyuk T (2004). *Interaction of vegetation and morphodynamics in pointbars of the Lower Volga (Russia) and the Allier (France)*. Inter-university Centre for Geo-Ecological Research, Utrecht.
- Van der Nat D, Tockner K, Edwards PJ, Ward JV, Gurnell AM (2003). Habitat change in braided floodplains (Tagliamento, NE-Italy). *Freshwater Biology* **48**: 1799-1812.
- Van Stokkom TC, Smits AJM, Leuven RSEW (2005). Flood defense in the Netherlands, a new era, a new approach. *Water International* **30**: 76-87.
- Vulink JT (2001). *Hungry Herds. Management of temperate Lowland Wetlands by Grazing*. PhD thesis. Rijkswaterstaat Directie IJsselmeergebied, Lelystad. Rijksuniversiteit Groningen, Groningen.
- Ward JV, Tockner K, Uehlinger U, Malard F (2001). Understanding natural patterns and processes in river corridors as the basis for effective river restoration. *Regulated Rivers: Research & Management* **17**: 311-323.
- Wilbers AWE (1997). *The Allier, a river with two patterns*. MSc-thesis Utrecht University, Utrecht. (In Dutch).
- Wolfert HP (2001). *Geomorphological Change and River Rehabilitation*. PhD-thesis Wageningen University. Alterra Green World Research, Wageningen.

3 Nature rehabilitation by floodplain excavation: the hydraulic effect of 16 years of sedimentation and vegetation succession along the Waal River, NL.

G.W. Geerling, E. Kater, C. van den Brink, M.J. Baptist, A.M.J. Ragas, A.J.M. Smits

Geomorphology (2008) **99**: 317-328.

3.1 Abstract

The “Ewijkse Plaat” is a floodplain along the Waal River, NL. In 1988, the floodplain was excavated as part of a program for enlargement of the discharge capacity and was assigned a nature rehabilitation area. This paper describes the combined geomorphological and vegetation evolution of the floodplain until 16 years after the initial excavation using elevation data and data on vegetation structure derived from detailed aerial stereographic imagery. The impact of these processes on flow velocity and water surface elevation was evaluated by using a hydraulic model. Within 16 years, the excavated amount of sediment was redeposited in the area. The dominant geomorphological process after excavation was vertical accretion of the floodplain which resulted in the formation of natural levees. The amount of sedimentation was correlated to the across-floodplain flow ($R^2 = 0.89$). In the research period, 41% of the sedimentation took place during two single major flood events. The creation of pioneer stages by excavation promoted softwood forest establishment, which influenced the sedimentation pattern significantly. The landscape evolved toward structure-rich vegetation. Nine years after excavation the initial hydraulic gain was lost by the combined effect of sedimentation and vegetation succession. Implications for river and nature management are discussed.

3.2 Introduction

In highly regulated river systems, landscape patterns are often “frozen in time”. Important habitats may exist but are mostly remnants of a former dynamic system (Ward et al. 2002). As these remnants evolve towards climax vegetation due to succession, the overall riverine landscape diversity will deteriorate unless new habitats are allowed to be created (Petts and Amoros 1996, Ward et al. 2001, Tockner and Stanford 2002, Geerling et al. 2006, Van der Velde 2006). Geomorphological interventions and integration of geomorphological processes in floodplain rehabilitation plans are effective instruments for rehabilitation of regulated systems (Gilvear 1999, Wolfert 2001, Middelkoop et al. 2005, Gregory 2006). An intervention combined with a change in land use, say from agriculture to nature, can restore the ability of processes to act. Processes such as sedimentation, erosion, and ecological succession can lead to a more diverse landscape compared to the nonrehabilitated situation.

Several examples of interventions to restore geomorphological processes and to rehabilitate nature can be found in the literature. In some cases, sedimentation processes are used in combination with intentional levee breaches alongside a sediment-rich stream. These breaches (or crevasses) promote the formation of sand splay complexes in subsiding wetlands in the Mississippi River Delta (Boyer et al. 1997) or upon floodplains formerly in agricultural use in the Lower Cosumnes River basin (Florsheim and Mount 2002). In both cases, sedimentation creates a diverse

floodplain topography and enhances ecological rehabilitation. Along the Danube, floodplains formerly disconnected from the main channel have been reconnected to restore connectivity and acting hydrological and geomorphological processes (Schiemer et al. 1999). Excavation is a possibility in regulated floodplains lacking erosion or other geomorphological disturbance processes. Man-made secondary channels have been dug along the Dutch Rhine River which lacks processes for the formation of side channels (Simons et al. 2001, Buijse et al. 2002). These artificial channels serve as a habitat for riverine species that lack proper habitats in the regulated main channel, such as the more demanding rheophilic species. In systems where dams decrease downstream peak flows and sediment load, floodplain disturbance is also diminished greatly. In some cases, this intervention is reversible and the natural hydraulic regime can be reintroduced when dams are removed (Orr and Stanley 2006). In case dam removal is not possible, downstream channel narrowing occurs and softwood forest regeneration is inhibited from lack of fresh bare substrate formerly provided by floods and channel movement. Along Boulder Creek (Colorado), settlement of seedlings was achieved after removal of the top layer (16 cm) to bare gravel (Friedman et al. 1995).

Rehabilitation by geomorphologic intervention can be successful from the nature rehabilitation point of view. However, in regulated systems other interests are important as well. The high waters in the river Rhine (years 1993, 1995) and the river Oder (year 1997) showed that the capacity of these highly regulated rivers to accommodate high discharges is limited because of the embanked floodplains. Therefore, nature rehabilitation by geomorphologic intervention may conflict with maintaining the discharge capacity of these highly regulated systems (Baptist et al. 2004). Knowledge on the direction and impact of geomorphological as well as ecological processes is important from a river manager's perspective.

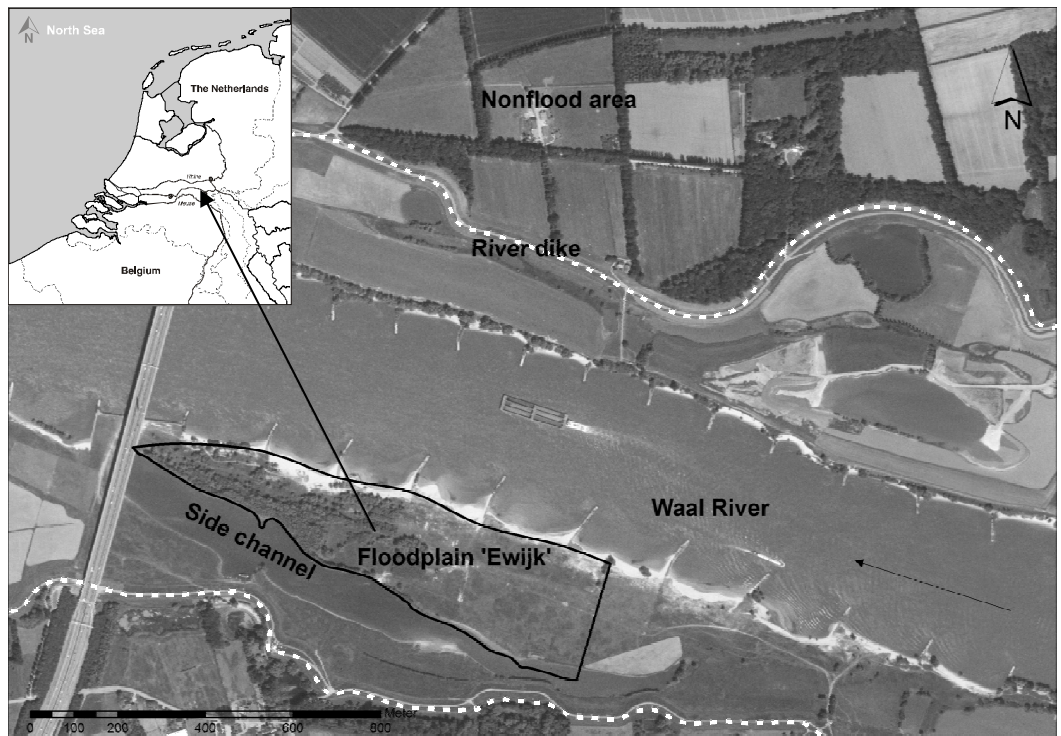
The aims of the present paper are to describe the geomorphological and vegetation evolution and to quantify the hydraulic effects of a floodplain after partial excavation down to 2 metres below the previous floodplain surface level. After excavation, the existing agricultural use ceased and the site was left bare as an ecological pioneer situation; giving ecological and hydromorphological processes freedom to shape the topography. The topography and vegetation structure were monitored between 1986 and 2005. The questions addressed are: (1) How and how fast did sedimentation and erosion processes shape the floodplain topography after excavation? (2) What kind of vegetation structure evolved out of the pioneer situation under the acting hydromorphological regime? (3) What was the impact of the intervention and subsequent evolution on water levels and flow velocities at high discharges?

3.3 Study Area and Methods

Study area

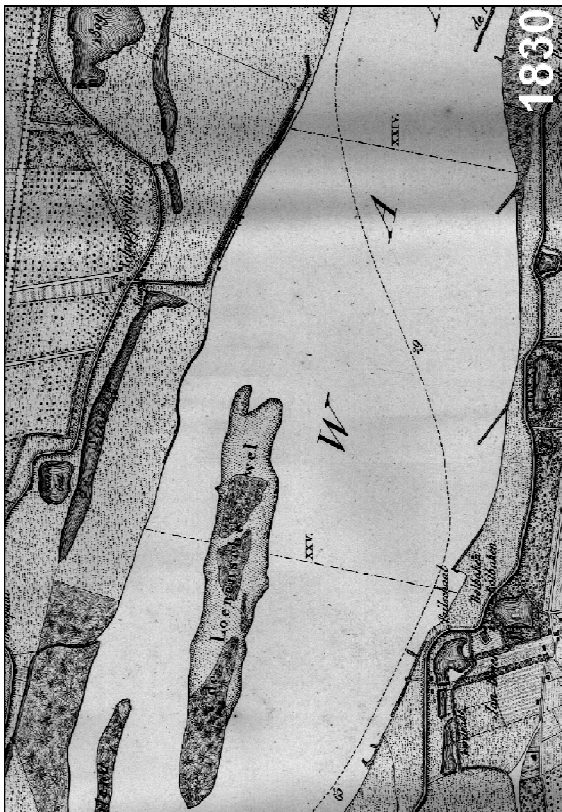
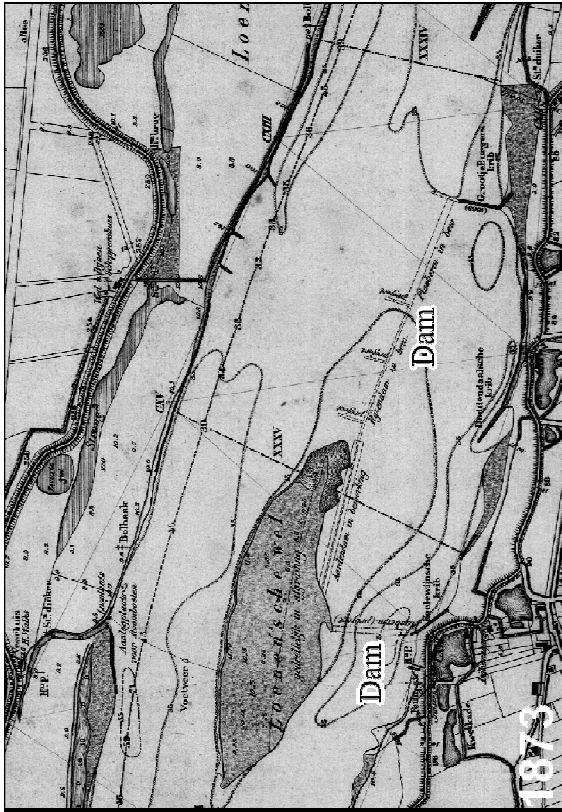
The river Rhine is a strongly regulated European river with a mean discharge of $2300 \text{ m}^3\text{s}^{-1}$ (at Lobith, NL) and a catchment area of $185,000 \text{ km}^2$ (Simons et al. 2001, Wolfert 2001). In 1926, 1993, and 1995, extreme peak discharges of up to $12,600 \text{ m}^3\text{s}^{-1}$ (at Lobith) were measured. The study area “Ewijkse Plaat” is a floodplain along the Waal River, the main branch of the Dutch Rhine (Bosman and Sorber 1997). Figure 3.1 shows the location of the Ewijkse Plaat in The Netherlands. The size of the study area is 21.4 ha , and it is located on the left bank of the Waal River at river kilometre

Figure 3.1
Location of the “Ewijkse Plaat” in the Waal River (NL); the black line indicates the research area. The white dotted lines indicate river dykes that protect the nonflood area against a flood.



893. Initial acting geomorphological processes were restrained by river regulation. Figure 3.2 shows the regulations in the immediate surroundings of the study area during the last two centuries. In the autumn of 1988, the floodplain was excavated as part of a program for enlargement of the discharge capacity and was assigned a nature rehabilitation site. The floodplain became a perfect example of spontaneous nature

Figure 3.2 (next page) A map series illustrate the change in floodplain topography from river regulation works in the period 1830 to 1986. In 1830, the river had been regulated by dykes and an occasional groin, but its morphology was still dynamic enough to produce downstream migrating meanders, point bars, and sand islands in the main stream (Middelkoop et al. 2005). In 1873, the regulation works started at the research site with connecting the island to the shore by building two dams. The purpose was to shift and subsequently confine the course of the main channel to the north. The part of the island still located in the new main channel was excavated. By 1923, this process was completed, and the floodplain Ewijk started to build up by overbank sedimentation of sand; sandy levees formed alongside the river. In the 1960s, the river authorities excavated the floodplain, and it was sown in with grassland. In 1986 it was still in agricultural use.



rehabilitation. The site was left bare and the combination of sandy substrate with a mild grazing regime (0.5 livestock units per hectare during summer) initiated a process of vegetation succession. The process introduced many new pioneer species to the area (Helmer 1990, Helmer et al. 1991, Bosman 1992, 1994, 1995, Bosman and van der Veen 1996, Bosman and Sorber 1997).

Method overview

To reconstruct the evolution of the floodplain, the geomorphological and vegetation changes within a 16-year period were analysed. To realise this, two different data types were gathered and combined in a GIS: elevation data and data on vegetation structure. In addition to this, the elevation and vegetation data were used to compute water surface elevation changes and stream velocity changes with a hydraulic model. The data collection methods and the hydraulic model applied are described in more detail below.

Geomorphology

Different methods were used to gather the elevation data for: (1) the pre-excavation situation (1982), (2) the 1990-2000 period, and (3) the year 2005. All elevation data were referenced to the Amsterdam Ordnance Datum (NAP).

The pre-excavation situation (1982) was reconstructed using a 1:5000 river map containing 110 elevation points and several break lines (Anonymous, 1982). This data was used as a reference and not for volume calculations. The elevation data was originally measured using photogrammetry of 1:5000 aerial images with an approximate error of 0.1 m.

Geomorphological data for the years 1990 to 2000 (except 1998) was gathered by the responsible river authority. Up to 21 transects were laid out perpendicular to the river axis (every 50 m along the 1 km floodplain), ensuring the major elevation gradient was captured. An elevation point was measured at least every 10 m by leveling, but more often when the elevation changed. The approximate elevation error was 0.01 m (Van Hal 1995).

For the 2005 data, the site was revisited by the authors in August 2005 and the elevation and breaklines were recorded using a DGPS-LTK (Ashtech Z-Max). Because the GPS coverage was poor in densely forested parts, these were revisited in winter (February 2006). No flooding occurred between these dates. The horizontal and vertical error of the GPS points was 0.05 m. The floodplain was covered with a maximum point to point distance of 30 m (in every direction) but more frequently when topography varied.

The elevation data was used to create digital elevation models in a GIS. The method of Triangular Irregular Network (TIN) was used to interpolate the point data. TINs were chosen above Inverse Distance Weighting (IDW) and Kriging methods because the latter two produced artifacts such as “tent poles” in the interpolated surface when applied to transect-based elevation data. TIN has the additional advantage that

break lines can be included. The outer border of the research area was marked by the base of the groins in the north (excluding the high dynamic sand beaches from the analysis) and by a side channel in the south. These borders were implemented as hard break lines to ensure consistency within the time series. The root mean square error (RMSE) of the TINs was estimated by splitting the data randomly in a training and a test set, containing 95% and 5% of the data, respectively. The TINs used in the final analyses included all data points.

Floods and sediment

To describe the rate of geomorphologic change, it was assumed that floodplain sedimentation is proportional to the total water flow (m^3) across the floodplain (Middelkoop 1998, Florsheim et al. 2006). Across floodplain flow starts at flood levels of about 9.9 m, i.e., above a discharge of $3435 m^3s^{-1}$. In a major flood, water surface tables at the site can reach to 12.5 m amounting to flood depths of 4.6 m in lower parts to 2.6 m in higher parts. The amount of sedimentation is related to the accumulated flow in the river cross section of water above 9.9 m water surface level which was calculated for each period between two subsequent elevation surveys. This accumulated flow equals the surface area of the flood peaks starting at $3435 m^3s^{-1}$ (Figure 3.3). For the interval $t = 0$ at the start of exceeding $3435 m^3s^{-1}$ to $t = T$ at the end of exceeding $3435 m^3s^{-1}$, each flood event yields a total overbank flow which is given by:

$$I_f = \int_0^T (Q_f - 3435) dt \quad [1]$$

where I_f = total overbank flow (m^3) and Q_f = flood discharge (m^3s^{-1}).

The information on discharges and water surface elevation (vertical datum: Amsterdam Ordinance Datum or NAP) was provided by the Dutch river authority (<http://www.waterbase.nl/>). To calculate the water surface elevation at the research area at a given discharge, linear interpolation (distance on river axis) between an upstream and a downstream gauging station was applied.

Vegetation structure maps

To study the changes in vegetation structure, the research site was mapped using an aerial photograph time series taken on the following dates (dd/mm/yyyy when available): summer 1986, autumn 1989, 19/08/1991, 11/07/1997, 09/06/2000, and 18/08/2005. The scale varied between 1:5000 and 1:10,000, and all photographs are stereographic, except for the images taken in the years 1986 and 1989. The aerial images of 1986 and 1989 were black and white, the 1991 to 1997 images were true colour, and the 2000 and 2005 images were false colour images.

The mapping method used is one of the standard methods of the Survey Department of the Ministry of Transport, Public Works and Water Management for mapping vegetation structure in lowland floodplain areas (Küchler and Zonneveld 1988,

Jansen and Backx 1998, Janssen and Gennip 2000). The map legend is based on a vegetation structure typology designed for hydraulic computations (Table 3.1, Van Velzen et al. 2003, Van de Steeg 2005). Two methods were used to create polygon outlines. For the years 1989 to 2000, the aerial photographs were viewed using a Topcon stereoscope, and vegetation types were outlined upon transparent sheets together with geographical reference points. The sheets were scanned, georeferenced to a 1:5000 base map (xy RMSE < 10 m), and vectorised (Anonymous 1996, Erdas 1999, ESRI 2000). The aerial images of 1986 and 2005 were scanned and georeferenced (xy RMSE < 1 m), and polygon outlines were identified using the software package Ecognition (Definiens 2006). After the polygons were created in GIS by either one of these methods, the polygon's vegetation type was determined using a stereographic view (only the 1986/1989 photos could not be stereographically viewed).

To investigate the vegetation evolution and heterogeneity in time, two landscape indexes were applied. The Shannon Index (SI) was used as a landscape diversity measure. The SI is high when all vegetation types occupy a similar area and decreases when the vegetation type area distribution becomes more uneven. The SI is not sensitive for patch composition and interspersion, for example a landscape of four classes lumped in 4 large patches gives the same SI value as a landscape having the same overall composition but spread over 100 patches. Therefore, to measure the changes in heterogeneity of the landscape, the Contagion Index (CI) was calculated (McGarigal and Marks 1995). A landscape in which patch types are interspersed has a lower CI than a landscape in which patches are lumped. Both the SI and CI were computed using Fragstats (McGarigal and Marks 1995).

Hydraulic computations

The two dimensional (2D) hydraulic model WAQUA was used to calculate the effect of the floodplain excavation and the subsequent vegetation succession on the local flow velocity, flow direction, and water surface elevation (Vollebregt et al. 2003, Anonymous 2004). WAQUA is a grid-based model regularly used by the Dutch river authority to assess flood safety in the Rhine and Meuse rivers (NL), and also in scientific studies (Middelkoop and Van der Perk 1998, Wijngaarden 1999, Anonymous 2001, Van het Hof 2005). In WAQUA, the water flow between grid cells is calculated by numerically solving the Saint-Venant equations of mass balance and of convective and diffusive motion in two dimensions (Van Rijn 1993). In the present case study, an orthogonal curvilinear grid of approximately 30x30 m was applied to fit the geometry of the river; smaller mesh sizes were chosen in dynamic areas. The modeled river segment reached from 8.5 km upstream of the study area to 4.5 km downstream. The downstream water level was predicted for a discharge of 7760 m³s⁻¹ at the upstream boundary, which equals the (stationary) peak level of the 1995 flood wave. Model input consisted of river bed elevation, floodplain surface elevation, hydraulic roughness data for river channel and floodplain surface, and objects that

cause flow turbulence such as dams and groins. The vegetation and elevation parameters in the study area were adjusted for each model run, while the other input parameters were kept stable. The hydraulic resistance of the vegetation was determined using the river authorities' standards on floodplain vegetation (Van Velzen et al. 2003). The model uses Chézy values for submerged and non-submerged vegetation that vary with water depth (Baptist et al. 2007). The Nikuradse approximation for a water depth of 4 m is given in Table 3.1.

Table 3.1 Recorded vegetation structure types, a brief botanical classification and an indication of the hydraulic roughness applied in the hydraulic model calculations (Van Velzen et al. 2003, Van de Steeg 2005).

Structure type	Species indication	roughness indication* (k at 4m water depth)
Dry bank / Sand	-	0.15
Pioneer vegetation	Siberian bugseed (<i>Corispermum intermedium</i>); Red goosefoot (<i>Chenopodium rubrum</i>); Glaucous goosefoot (<i>Chenopodium glaucum</i>); Willow weed (<i>Persicaria lapathifolia</i>); Amaranth (<i>Amaranthus spp.</i>); Goosefoot (<i>Chenopodium spp.</i>); <i>Solanum spp.</i>	0.28
Groin	(no vegetation)	0.30
Production grassland	Grazed, low vegetation height: Perennial ryegrass (<i>Lolium perenne</i>); Meadow grass (<i>Poa trivialis</i>)	0.25
Natural grassland	Open grassland: Bentgrass (<i>Agrostis stolonifera</i>); Couch grass (<i>Elytrigia repens</i>); Creeping cinquefoil (<i>Potentilla reptans</i>); Silver weed (<i>Potentilla anserine</i>); British fleabane (<i>Inula Britannica</i>); Curled dock (<i>Rumex crispus</i>)	0.39
Mixed grassland & herbaceous	Grassland mixed with patches of herbaceous vegetation: Couch grass (<i>Elytrigia repens</i>); Bentgrass (<i>Agrostis stolonifera</i>); Common foxtail (<i>Alopecurus pratensis</i>); Creeping cinquefoil (<i>Potentilla reptans</i>); Cinquefoil (<i>Potentilla anserina</i>); Creeping thistle (<i>Cirsium arvense</i>)	0.73
Herbaceous Levee	Field eryngo (<i>Eryngium campestre</i>); Red fescue (<i>Festuca rubra</i>); Yarrow (<i>Achillea millefolium</i>); Greater plantain (<i>Plantago lanceolata</i>)	1.07
Dry herbaceous vegetation	Jewel weed (<i>Impatiens glandulifera</i>); Stinging nettle (<i>Urtica dioica</i>); Spotted dead-nettle (<i>Lamium maculatum</i>); Creeping thistle (<i>Cirsium arvense</i>); Common tansy (<i>Tanacetum vulgare</i>); Black mustard (<i>Brassica nigra</i>)	1.45
Softwood bush / bush	Osier willow (<i>Salix viminalis</i>);	24.41
Softwood forest	White willow (<i>Salix alba</i>); Crack willow (<i>Salix fragilis</i>); Black poplar (<i>Populus nigra</i>)	12.84

*In the WAQUA model vegetation roughness values vary with flood depth. The reported Nikuradse (k) values are an approximation of the roughness value at 4 m water depth (Van Velzen et al. 2003).

Computations were performed for each year of which vegetation maps were available, i.e. 1986, 1989, 1991, 1997, 2000 and 2005. Of most years elevation data were available from the same year, except for 1986 and 1989. For these years, the 1982 and 1990 elevation data were used, respectively.

3.4 Results

Elevation data and TINs

Table 3.2 summarises the elevation data used for constructing the TINs and the RMSE of the TINs. The 1982 TIN has the largest RMSE (1.0 m), but this TIN was only used as a reference and not for volume calculations. The relatively large RMSE in 2005 (0.57 m) can be attributed to a few critical elevation points which were measured on top of isolated raised parts encountered in the field. The randomly chosen test set incorporated one of these critical points of raised parts. Subsequently, the raised part was not modeled in the training set TIN which increased the RMSE by a factor of 2. It should be realised that the RMSE values represent the estimated error for the prediction of individual point values. The error in average height and sedimentation is only a fraction of this value.

Table 3.2 Year, month, number of elevation points in the study area and the Root Mean Square Error (RMSE) of the elevation models (TINs) generated from field data. To calculate the RMSE, the data was randomly separated in a training (95%) and testing (5%) set.

Year, Month	# elev. points inside Area	RMSE (m)
1982	110	1.00
1990, December	493	0.58
1991, February	523	0.16
1992, January	400	0.23
1993, February	535	0.26
1994, June	425	0.25
1995, June	1254	0.07
1996, November	1497	0.10
1997, November	1014	0.09
1999, September	1110	0.07
2000, October ^A	-	-
2005, August ^B	496	0.57

^A Accuracy could not be tested, 2000 field data was archived by river manager only as gridded (1m) tin.

^B Forested sites were revisited in February 2006

Geomorphological evolution

After excavation in 1989, the floodplain was largely subject to sedimentation as shown in Figure 3.3 (left axis). The amount of sedimentation over the whole research period (1990-2005) returned the area to the 1982 sediment level. Some erosion

occurred between 1991 and 1992. The absolute sediment deposits per period and yearly sedimentation rates are shown in Table 3.3. The overall sedimentation rate was $3.7 \text{ cm m}^{-2}\text{y}^{-1}$ and ranged from slightly negative (meaning erosion) to $12.6 \text{ cm m}^{-2}\text{y}^{-1}$. As shown in Figure 3.3 (right axis), the major changes in sedimentation rates coincided with extreme floods, some of the largest in the last century. In the flood years 1993/1994 and 1995, 41% of the total sediment was deposited. Figure 3.4 shows that the sediment deposition per period correlates strongly with the total accumulated flow ($R^2 = 0.89, p < 0.01$).

Figure 3.5 shows the difference in spatial distribution of sediment between 1982 and 2005. Part of this difference can be attributed to vegetation succession. The mean sedimentation (1990-2005) in the softwood forest patches of 2005 was 0.96 m compared to 0.47 m for all other areas. This difference is significant ($n = 509, p < 0.05$).

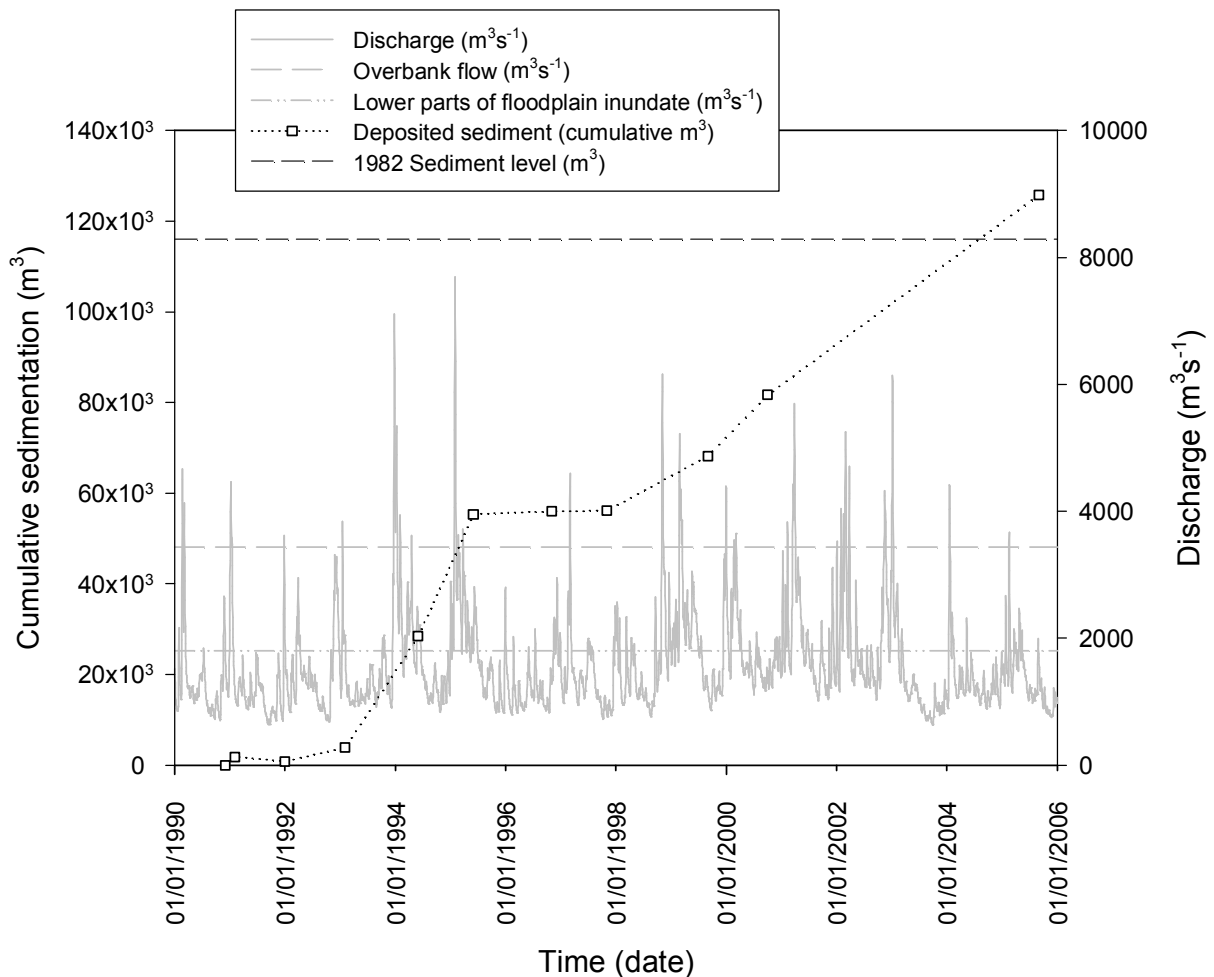


Figure 3.3 Cumulative sedimentation in the study area in the period 1990 to 2005 (left axis; 1990 = 0) and the discharge of Waal River at the floodplain “Ewijkse Plaat” in the same period (right axis). Reference lines are given for the 1982 sediment level, the discharge at which first inundation occurs and the discharge of first overbank flow ($3435 \text{ m}^3\text{s}^{-1}$).

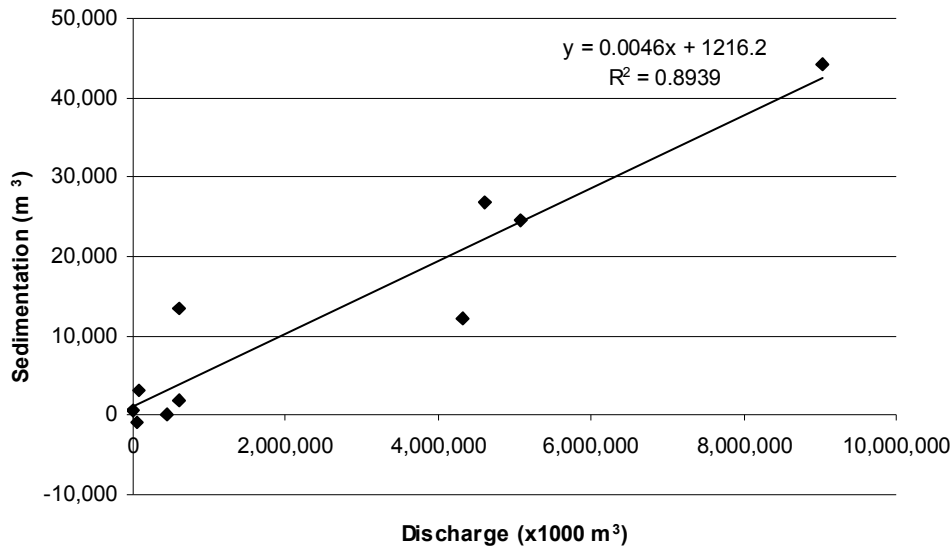


Figure 3.4 Relation between sediment deposition and the accumulated flow above a discharge of $3435 \text{ m}^3 \text{ s}^{-1}$ (water surface elevation of 9.9 m) at which across floodplain flow starts and sedimentation takes place. Accumulated flow is shown on the x-axis in 1000 m^3 . Sedimentation is shown on the y-axis in m^3 . The correlation is significant at $p < 0.01$.

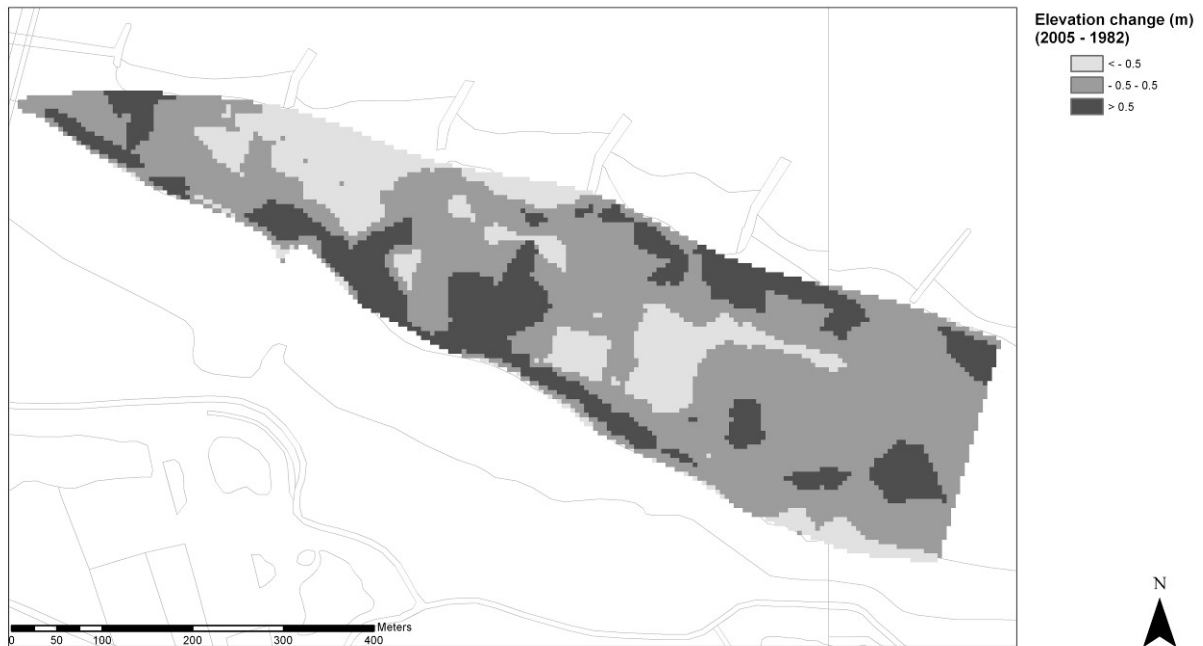


Figure 3.5 The elevation difference between the situation in 1982 (agricultural land) and 2005 (nature rehabilitation area). Lighter areas indicate elevation is more than 0.5 m lower compared to 1982; darker areas indicate that the 2005 elevation is more than 0.5 m higher than in 1982. The darker areas coincide with presence of softwood forest (south side) and natural levee formation (north side) in 2005.

Table 3.3 Yearly absolute sedimentation in 10,000 m³ for the whole study area and sedimentation rates (cm y⁻¹ m⁻²). Shorter intervals between two measurements have been indexed to one full year.

	1990-1991	1991-1992	1992-1993	1993-1994	1994-1995	1995-1996	1996-1997	1997-1999	1999-2000	2000-2005	mean
Sedimentation (10 ³ m ³ y ⁻¹)	10.6	-1.1	2.8	18.6	27.0	0.5	0.1	6.6	12.5	9.1	
Sedimentation rate (cm y ⁻¹ m ⁻²)	5.0	-0.5	1.3	8.7	12.6	0.2	0.1	3.1	5.8	4.3	3.7

Vegetation structure

The vegetation structure distribution in 1986, 1989, 1991, 1997, 2000, and 2005 is shown in Figure 3.6. In 1986, the vegetation was dominated by agricultural use; more than 80% of the surface area was grassland. In 1989, the area was mainly composed of bare soil (> 70%) and natural grassland. In 1991, the area was fully covered with vegetation. After this year, the trend towards structure-rich vegetation is clearly visible. Because of Willow (*Salix alba*) settlement between 1991 and 1997, bush vegetation shows an optimum of about 14 % coverage in 1997 and 2000. In 2005, the proportion of bush declined and forest coverage increased. Please note that young Willows are first classified as bush (5 m or smaller) and subsequently become forest. The surface area of dry herbaceous vegetation increased while natural grassland decreased over the period analysed.

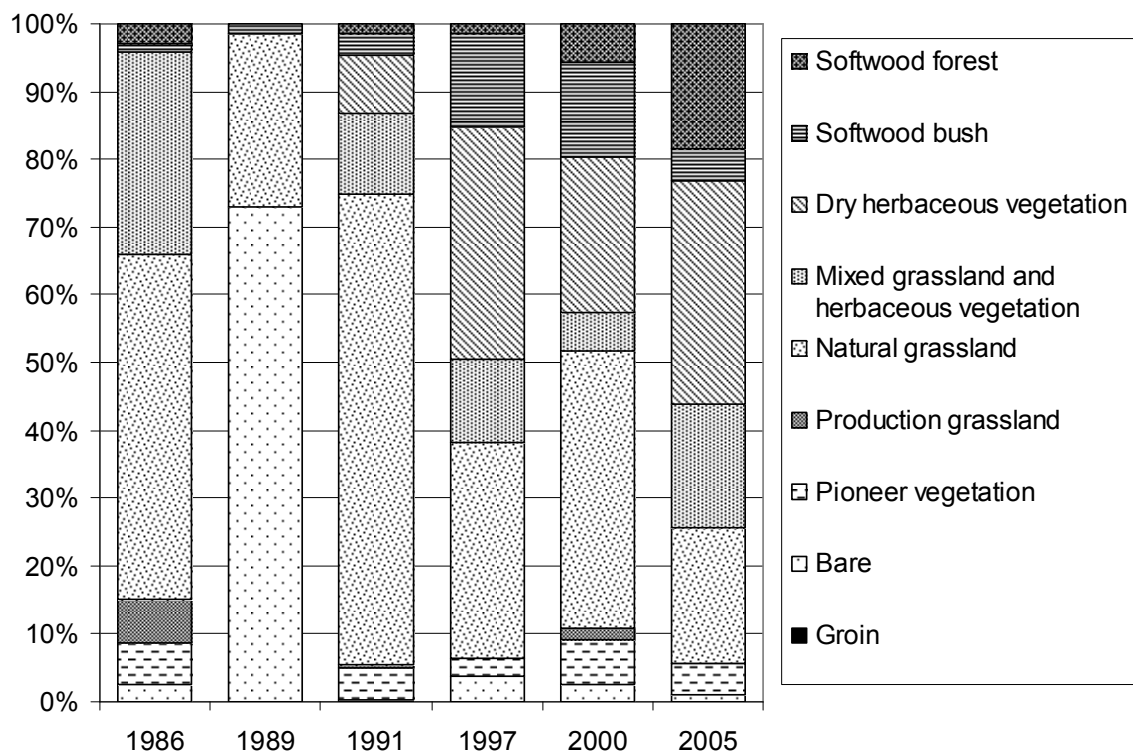
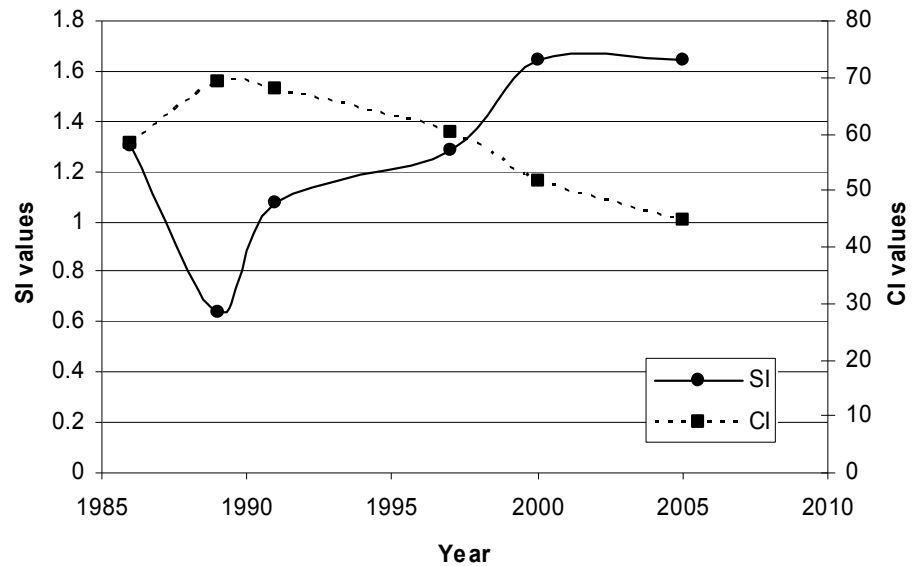


Figure 3.6 Relative vegetation distribution of the years 1986 to 2005.

The graph of the Shannon Index shows that the diversity of the mapped vegetation stabilised in the year 2000 after an initial decrease below starting levels after excavation (Figure 3.7). At the same time, the patch interspersion increased as shown by the gradually lower values of the CI (Figure 3.7), indicating the landscape became less clumped through time. Between 1997 and 2000, the landscape became more diverse (SI) and more interspersed (CI) than before excavation. Interspersion continued to increase after 2000 while diversity stabilised.

Figure 3.7 The Shannon diversity Index (SI) and Contagion Index (CI) are shown for all map years. The SI scale is depicted on the left axis, the CI scale on the right axis. Note that the SI value increases when diversity increases while the CI value decreases when patches become more interspersed (less clumped).



Hydraulic effects

Table 3.4 shows the mean flow velocity, the peak level of the water surface elevation (highest difference on the river axis) and discharge changes in all years analysed. In 1997, the initial drop in water surface elevation and discharge was neutralised by sedimentation and vegetation succession. Although the study area (21 ha) covers only 0.17 percent of the total flood area of the River Waal (11,909 ha), the geomorphological changes decreased the discharge capacity at the 1995 peak level with 0.7 percent ($54 \text{ m}^3\text{s}^{-1}$). Over the whole period, the mean flow velocity across the study area decreased. For all modeled years (1986-2005), a linear correlation was found between the landscape diversity indexes and the mean flow velocity with R^2 values of 0.97 ($p < 0.01$) and 0.72 ($p < 0.05$) for SI and CI, respectively.

Figure 3.8 shows the flow velocity and direction in the study area in 1986 and 2005. The influence of the change in vegetation cover between 1986 and 2005 is evident. In 2005, flow velocities in the “rougher” western part of the study area were much lower than in 1986. The flow direction in the immediate surroundings also differs between 1986 and 2005. In 2005, there is a decreased flow across the floodplain and an increased flow through the side channel around the “rough” part. As shown earlier, the change in flow patterns influenced sedimentation patterns e.g. by an increase in sedimentation in the softwood forests.

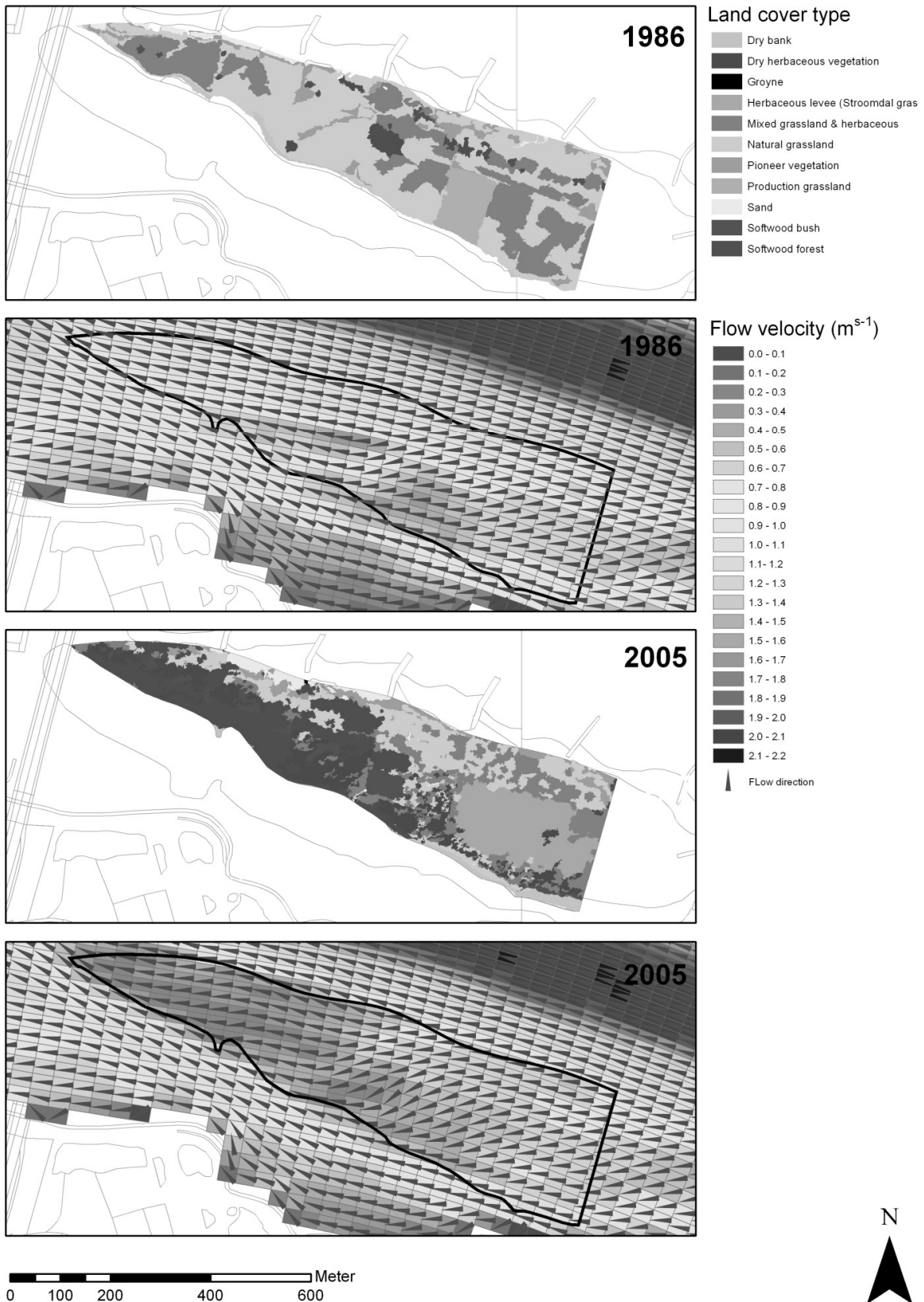


Figure 3.8 (In full colour on page 186) The vegetation maps, flow velocities, and flow direction are shown for the 1986 (pre-excavation) situation and the 2005 situation. The grid cells in the flow velocity and flow direction maps correspond to the grid cells of the hydraulic model.

Table 3.4 Mean flow velocity, the standard deviation and water surface elevation change as computed by the WAQUA model of the study area in the years 1986, 1989, 1991, 1997, 2000 and 2005. Additionally, the discharge capacity changes were computed on the basis of the water surface elevation changes at a flood discharge of $7760 \text{ m}^3\text{s}^{-1}$.

	1986	1989	1991	1997	2000	2005
Mean flow velocity (ms^{-1})	0.58	0.80	0.65	0.55	0.48	0.50
Standard deviation ^{a)}	0.13	0.20	0.17	0.20	0.19	0.17
Water surface elevation change ^{b)} (mm)	0	-15	-4	1	4	5
Change in discharge capacity ^{c)} (m^3s^{-1})	0	+43	+9	+2	-9	-11

^{a)} The difference between the mean flow velocities ($n=213$) is significant (student t test; 95% confidence) for all subsequent years, except the 2000/2005 interval.

^{b)} Maximum change on river axis.

^{c)} Calculated from discharge vs. water surface elevation data.

3.5 Discussion

The present study analysed the geomorphological and vegetation evolution of a floodplain after excavation of the top layer and a subsequent change in land use. The results show that these changes created possibilities for vertical accretion of natural levee, floodplain accretion (see Figure 3.5), and vegetation succession to act and also interact as the major landscape-shaping processes. These processes are discussed in more detail below.

Sedimentation rates and deposition

Vertical accretion or sedimentation is the major geomorphological process in the excavated floodplain. The mean sedimentation rates can be compared to some others found in the same river. The overall mean rate of $3.7 \text{ cm m}^{-2}\text{y}^{-1}$ is much higher than the range of mean rates for Rhine branch floodplains found by Middelkoop (1997), ranging from $0.056 \text{ cm m}^{-2}\text{y}^{-1}$ to $0.219 \text{ cm m}^{-2}\text{y}^{-1}$. These rates apply for larger floodplains, including floodplains with lower flow velocity and silt sedimentation. Baptist et al. (2004) used expert knowledge sedimentation rates for different parts of Rhine branch floodplains in mm/day inundation. Computed for the research period, the rates used are 0.013 cm y^{-1} for silt in less dynamic floodplain parts, 1.23 cm y^{-1} for point bar extensions, and 15 cm y^{-1} for a natural levee. Our mean rate is below the estimated rate for a natural levee and above the rate estimated for point bar extensions.

Although a mean sedimentation rate is convenient, it does not accurately describe the actual sedimentation. Our results show that sedimentation is directly and significantly related to the total across-floodplain flow between elevation measurements. Total across-floodplain flow combines flood duration and magnitude, our data set did not permit a per flood analysis. Asselman and Middelkoop (1998) and Steiger and Gurnell (2003) come to a similar conclusion between sedimentation and flood magnitude for the Rhine River and Garonne River respectively, especially for near river parts of floodplains. The exceptional floods of

1993/1994 and 1995 were responsible for 41% of the total sediment deposition in the study area. Without the extreme floods, the floodplain would have caught sediment at a much lower rate. These results imply that the predicted increase in extreme floods from climate change as reported by Lenderink et al. (2007) may have a substantial impact on sedimentation rates in floodplains.

Vegetation

Excavation of the study area and a change in land use created freedom for spontaneous ecological succession. The grassland-based landscape changed toward a landscape partly containing grasslands, herbaceous vegetation, bush, and softwood forest. The amount of softwood forest steadily increased as the settlements grew via a bush phase toward the forest stage. As found by Friedman et al. (1995) for Cottonwood (*Populus spp.*), spontaneous regeneration of softwood species such as Willow (*Salix spp.*) is possible on man-made pioneer situations. Once the pioneer stage is overgrown, hardly any new settlement of softwood species such as Willow and Black Poplar (*Populus nigra*) is possible (Friedman et al. 1995, van Splunder 1998). Our results confirm these findings. When examining both the SI/CI indexes and the bar graphs, three stages of recolonisation can be recognised: (i) a pioneer situation, unpredictable, low vegetation, high dynamics (1-2 years); (ii) settlement stage of softwood forest species as bush and grassland dominance shifts to herbaceous vegetation dominance (2-5 years after excavation); (iii) growth toward dense softwood forest (5-16 years after excavation) and grasslands become more structure rich by an increase of herbaceous vegetation types. Figure 3.6 shows that the vegetation classes still change in 2005; but relative areas are swapped, resulting in the same SI diversity value. That the landscape is still changing is confirmed by the CI; the patches become more interspersed, i.e., the landscape more heterogeneous, largely because of ongoing succession in the herbaceous grasslands. These findings support the hypothesis that continuous creation of new pioneer stages in regulated river systems contributes to an ecological diversity similar to natural systems (Geerling et al. 2006).

Sedimentation and vegetation

Establishment of vegetation influenced sedimentation in the years 1991-2005. This reduced the overall mean flow velocity as compared to velocities in an agricultural setting (pasture). This probably had a positive effect on the overall sedimentation rate compared to sedimentation rates on less rough agricultural surfaces, also shown by the significantly higher sedimentation in forested areas. The spatial distribution of sediment also changed. The rehabilitated floodplain has a more diverse flow velocity distribution than the pre-excavation situation (Figure 3.8). The vegetation change contributed to a different sedimentation regime and spatial sedimentation pattern (Figure 3.5).

We conclude that the creation of a pioneer situation and freedom for ecological

succession not only gives rise to diverse vegetation, but also influences the spatial pattern of sedimentation processes, also noted by Steiger and Gurnell (2002). On its turn, sedimentation changes the direction of local successions by influencing abiotic parameters like local elevation and soil type. In this way, vegetation succession enhances the diversity in floodplain topography when compared to sites strictly under agricultural management.

Flood pulse and grazing

The exceptional large flood events of 1993 and 1995 acted as powerful flood pulses in the river system (Junk et al. 1989, Tockner et al. 2000). The flood pulse did not dramatically affect the succession sequence of landscape configuration in this regulated system because erosion processes and therewith landscape rejuvenation are suppressed. However, flood pulses do affect vegetation locally by sedimentation and affect the abundance of fauna such as invertebrates and small mammals (Wijnhoven et al. 2006, Schipper et al. 2007).

The mild grazing regime (about 0.5 cattle per hectare) under which the floodplain was placed can influence succession (Bosman and Sorber 1997, Vulink 2001). Cattle and horses for year-round low density grazing (except in case of floods) were introduced after the initial settlement of softwood species had taken place. The results show that grazing did not stop the succession toward structure-rich vegetation nor did it inhibit the growth of already established softwood forest. Additional research is necessary to determine the exact impact of grazing on the settlement of large landscape structures such as bush and forest and on sedimentation patterns (Stallins 2006).

Hydraulic effects

A strong correlation ($R^2 = 0.97$) was found between the SI values and mean velocity. As the landscape becomes more diverse through succession, its impact on hydraulic resistance and stream velocities increases. This is probably a general rule for former cultivated landscapes in unidirectional succession (no rejuvenation), as the succession leads toward a more hydraulically rough stage.

Implications for management

This study shows that floodplain excavation and subsequent landscape evolution influences the conveyance capacity of the river. Embanked regulated rivers have a finite capacity and therefore knowledge of geomorphological and ecological processes has to be incorporated in rehabilitation plans (Gilvear 1999).

The study area was the first nature rehabilitation area along the Waal River (NL) that was allowed to regenerate from bare substrate. It was thought it would take at least 20 years before the flow stage would return to previous levels. The river authority clearly underestimated the impact of sedimentation and vegetation succession. Partly based on this experience, the Dutch re-enforced a legal restriction on the hydraulic

effect as a consequence of changes in floodplains in order to maintain flood protection levels (Anonymous 2001). In current Dutch practice, the hydraulic impact of interventions is assessed by computing the water surface elevation difference on the axis of the river using hydraulic models as shown in table 3.4.

When multiple plans are implemented at the river reach level, the creation of these nature rehabilitation sites should be spread in time to ensure diversity and to avoid a large cumulated impact on flood levels, also noted by Baptist et al. (2004). Once the vegetation cover has been established after excavation, the evolution and hydraulic impact become more or less predictable as shown above and the river manager can anticipate future management activities.

3.6 Conclusions

Excavation of an agricultural floodplain and changing the land use rehabilitates natural levee-forming processes and ecological succession. Excavation leads to settlement and subsequent growth of softwood forest species. Within the research period, the regulated river system did not show signs of rejuvenation, not even during the large flood events. Major floods are the main sources of sediment deposition and the amount of sedimentation is well correlated to the total amount of water flow across the floodplain during a flood.

A hydraulic model study suggests that flood flow velocities decrease and water surface elevations increase as sediment is deposited and vegetation is established on the excavated floodplain. After 16 years of landscape evolution, the flood capacity is lower than in the pre-project situation and mean flow velocities have dropped 14% below the pre-project situation. The rate of change diminishes in time and flow velocity change is strongly correlated to landscape diversity.

Acknowledgements

We thank Leo van Hal, Lisette the Hey, Dian Jansen, Peter Jesse, Henk Koppejan, Simon Mosterd, Sybrant Oosterhof, Bart Peters, Margriet Schoor, Madelein Vreeken-Buijs and Adri Wagener. This project was funded by the Ministry of Transport, Public Works and Water Management, Survey Department, Delft and the BSIK “Leven met Water” program.

References

- Anonymous (1982). *Revised River Map of the Rhine Branches*. Ministry of Transport, Public Works and Water Management, Survey Department, Delft, The Netherlands.
- Anonymous (1996). *Digital Terrain Map of National Rivers*. Ministry of Transport, Public Works and Water Management, Survey Department, Delft, The Netherlands.

- Anonymous (2001). *Hydraulische Randvoorwaarden 2001*. Directorate for Public Works and Water Management, Ministry of Transport, Public Works and Water management, Delft, The Netherlands.
- Anonymous (2004). *WAQUA User's Guide version 10.36*. Ministry of Transport, Public Works and Water Management, Directorate-General for Public Works and Water Management, Rijswijk, The Netherlands.
- Asselman NEM, Middelkoop H (1998). Temporal variability of contemporary floodplain sedimentation in the Rhine-Meuse Delta, The Netherlands. *Earth Surface, Processes and Landforms* **23**: 595-609.
- Baptist MJ, Penning WE, Duel H, Smits AJM, Geerling GW, Van der Lee GEM, Van Alphen JSL (2004). Assessment of the effects of cyclic floodplain rejuvenation on flood levels and biodiversity along the Rhine River. *River Research and Applications* **20**: 285-297.
- Baptist MJ, Babovic V, Rodriguez Uthurburu J, Keijzer M, Uittenbogaard RE, Mynett A, Verwey A (2007). On inducing equations for vegetation resistance. *Journal of Hydraulic Research* **45**: 435-450.
- Bosman W (1992). *Ewijkse Plaat: Jaarverslag 1991*. Stichting Ark, Laag Keppel, The Netherlands.
- Bosman W (1994). *Ewijkse Plaat: Jaarverslag 1992-1993*. Stichting Ark, Laag Keppel, The Netherlands.
- Bosman W (1995). *Ewijkse Plaat: Jaarverslag 1994*. Stichting Ark, Laag Keppel, The Netherlands.
- Bosman W, Sorber A (1997). De Ewijkse Plaat; Natuurontwikkeling in relatie tot overstroming en begrazing. *Landschap* **14**: 131-146.
- Bosman W, Van der Veen J (1996). *Ewijkse Plaat: Jaarverslag 1995*. Stichting Ark, Laag Keppel, The Netherlands.
- Boyer ME, Harris JO, Turner RE (1997). Constructed crevasses and land gain in the Mississippi River Delta. *Restoration Ecology* **5**: 85-92.
- Buijse AD, Coops H, Staras M, Jans LH, Van Geest GJ, Grifts RE, Ibelings BW, Oosterberg W, Roozen CJM (2002). Restoration strategies for river floodplains along large lowland rivers in Europe. *Freshwater Biology* **47**: 889-907.
- Definiens (2006). *Definiens Professional 5 User Guide*. Definiens, München, Germany.
- Erdas Imagine (1999). *Erdas Imagine 8.x Tour Guide*. Erdas Inc., Atlanta, GA.
- ESRI (2000). *ArcGIS 8.x and ArcInfo Workstation*. Environmental Systems Research Institute, Redlands, CA.
- Florsheim JL, Mount NJ (2002). Restoration of floodplain topography by sand-splay complex formation in response to intentional levee breaches, Lower Cosumnes River, California. *Geomorphology* **44**: 67-94.
- Florsheim JL, Mount JF, Constantine CR (2006). A geomorphic monitoring and adaptive assessment framework to assess the effect of lowland floodplain river restoration on channel-floodplain sediment continuity. *River Research and Applications* **22**: 353-375.

- Friedman JM, Scott ML, Lewis WMJ (1995). Restoration of riparian forest using irrigation, artificial disturbance and seedfall. *Environmental Management* **19**: 547-557.
- Geerling GW, Ragas AMJ, Leuven RSEW, van den Berg JH, Breedveld M, Liefhebber D, Smits AMJ (2006). Succession and rejuvenation in floodplains along the river Allier (France). *Hydrobiologia* **565**: 71-86.
- Gilvear DJ (1999). Fluvial geomorphology and river engineering: future roles utilising a fluvial hydrosystems framework. *Geomorphology* **31**: 229-245.
- Gregory KJ (2006). The human role in changing river channels. *Geomorphology* **79**: 172-191.
- Helmer W (1990). *De Ewijkse Plaat: Jaarverslag 1989*. Sichtung Ark, Laag Keppel, The Netherlands.
- Helmer W, Litjens G, Overmars W (1991). *De Ewijkse Plaat: Jaarverslag 1990*. Stichting Ark, Laag Keppel, The Netherlands.
- Jansen BJM, Backx JJGM (1998). *Biologische monitoring zoete rijkswateren. Ecotopenkartering Rijntakken-Oost 1997*. RIZA report 98.054, Ministry of Transport, Public Works and Water Management, Institute for Inland Water Management and Waste Water Treatment (RIZA), Lelystad, The Netherlands.
- Janssen J, Van Gennip B (2000). De oude grenzen methode. *Landschap* **17**: 177-185.
- Junk WJ, Bayley PB, Sparks RE (1989). The Flood Pulse concept in river-floodplain systems. In: Dodge DP (Ed.), *Proceedings of the International Large River Symposium*. *Canadian Special Publication of Fisheries and Aquatic Sciences* **106**: 110-127.
- Küchler AW, Zonneveld IS (1988). *Vegetation Mapping*. Kluwer Academic Publishers, Dordrecht, The Netherlands.
- Lenderink G, Buishand A, Van Deursen W (2007). Estimates of future discharges of the river Rhine using two scenario methodologies: direct versus delta approach. *Hydrology and earth system sciences* **11**: 1143-1159.
- McGarigal K, Marks B (1995). *FRAGSTATS: Spatial Analysis Program for Quantifying Landscape Structure*. General Technical Report PNW-GTR-351, USDA Forest Service, Pacific Northwest Research Station, Portland.
- Middelkoop H (1997). *Embanked floodplains in The Netherlands; geomorphological evolution over various time scales*. PhD Dissertation, University of Utrecht, Utrecht, The Netherlands.
- Middelkoop H, Van der Perk M (1998). Modelling spatial patterns of overbank sedimentation on embanked floodplains. *Geografiska Annaler. Series A, Physical Geography* **80**: 95-109.
- Middelkoop H, Schoor MM, Wolfert HP, Maas GJ, Stouthamer E (2005). Targets for ecological rehabilitation of the lower Rhine and Meuse based on a historic geomorphologic reference. *Archiv für Hydrobiologie - Supplement* **155**: 63-88.

- Orr CH, Stanley EH (2006). Vegetation development and restoration potential of drained reservoirs following dam removal in Wisconsin. *River Research and Applications* **22**: 281-295.
- Petts GE, Amoros C (1996). *Fluvial Hydrosystems*. Chapman & Hall, London.
- Schiemer F, Baumgartner C, Tockner K (1999). Restoration of floodplain rivers: the "Danube Restoration Project". *Regulated Rivers: Research and Management* **15**: 231-244.
- Schipper AM, Wijnhoven S, Leuven RSEW, Ragas AMJ, Hendriks AJ (2007). Spatial distribution and internal metal concentrations of terrestrial arthropods in a moderately contaminated lowland floodplain along the Rhine River. *Environmental Pollution*, in press, doi:10.1016/j.envpol.2007.03.007.
- Simons JHEJ, Bakker C, Schropp MHI, Jans LH, Kok FR, Grift RE (2001). Man-made secondary channels along the river Rhine (The Netherlands); results of post-project monitoring. *Regulated Rivers: Research and Management* **17**: 473-491.
- Stallins JA (2006). Geomorphology and ecology: unifying themes for complex systems in biogeomorphology. *Geomorphology* **77**: 207-216.
- Steiger J, Gurnell AM (2003). Spatial hydrogeomorphological influences on sediment and nutrient deposition in riparian zones: observations from the Garonne River, France. *Geomorphology* **49**: 1-23.
- Tockner K, Malard F, Ward JV (2000). An extension of the flood pulse concept. *Hydrological Processes* **14**: 2861-2883.
- Tockner K, Stanford JA (2002). Riverine floodplains: present state and future trends. *Environmental Conservation* **29**: 308-330.
- Van Rijn LC (1993). *Principles of Sediment Transport in Rivers, Estuaries and Coastal Seas part I*. Aqua Publications, Amsterdam, The Netherlands.
- Van de Steeg H (2005). *Een overzicht van de plantengroei van de Ewijkse Waard*. Internal report. Experimental Plant Ecology, Faculty of Science, Radboud University Nijmegen, The Netherlands.
- Van der Velde G, Leuven RSEW, Ragas AMJ, Smits AJM (2006). Living rivers: trends and challenges in science and management. *Hydrobiologia* **565**: 359-367.
- Van Hal L (1995). *Meetverslag Erosie- en Sediment Metingen 1990-1995 "De Plaat Ewijk"*. Internal Report nr. 95.163X, Ministry of Transport, Public Works and Water Management, Institute for Inland Water Management and Waste Water Treatment (RIZA), Arnhem, The Netherlands.
- Van het Hof B, Vollebregt E (2005). Modelling of wetting and drying of shallow water using artificial porosity. *International Journal for Numerical Methods in Fluids* **48**: 1199-1217.
- Van Splunder I (1998). *Floodplain forest recovery*. PhD. Dissertation, University of Nijmegen, The Netherlands.

- Van Velzen EH, Jesse P, Cornelissen P, Coops H (2003). *Stromingsweerstand Vegetatie In Uiterwaarden. Deel 1 Handboek*. Report nr. 2003.028 or ISBN 9036956420. Ministry of Transport, Public Works and Water Management (RIZA), Arnhem, The Netherlands.
- Vollebregt EAH, Roest MRT, Lander JWM (2003). Large scale computing at Rijkswaterstaat. *Parallel Computing* **29**: 1-20.
- Vulink JT (2001). *Hungry herds: management of temperate lowland wetlands by grazing*. Ph.D. Dissertation, Rijksuniversiteit Groningen, The Netherlands.
- Ward JV, Tockner K, Uehlinger U, Malard F (2001). Understanding natural patterns and processes in river corridors as the basis for effective river restoration. *Regulated Rivers: Research and Management* **17**: 311-323.
- Ward JV, Malard F, Tockner K (2002). Landscape ecology: a framework for integrating pattern and process in river corridors. *Landscape Ecology* **17**: 35-45.
- Wijngaarden M (1999). A two-dimensional model for suspended sediment transport in the southern branch of the Rhine-Meuse estuary, The Netherlands. *Earth Surface, Processes and Landforms* **24**: 1173-1188.
- Wijnhoven S, Van der Velde G, Leuven RSEW, Smits AJM (2006). Modelling recolonisation of heterogeneous river floodplains by small mammals. *Hydrobiologia* **565**: 135-152.
- Wolfert HP (2001). *Geomorphological change and river rehabilitation*. PhD. Dissertation, Alterra Green World Research, Wageningen, The Netherlands.

4 Classification of floodplain vegetation by data-fusion of Spectral (CASI) and LiDAR data

G.W. Geerling, M. Labrador-Garcia, J.G.P.W. Clevers, A.M.J. Ragas, A.J.M. Smits.

International Journal of Remote Sensing (2007) **28**: 4263 – 4284.

4.1 Abstract

To safeguard the goals of flood protection and nature development, a river manager requires detailed and up-to-date information on vegetation structures in floodplains. In this study, remote sensing data on the vegetation of a semi-natural floodplain along the river Waal in the Netherlands was gathered by means of a Compact Airborne Spectrographic Imager (CASI; spectral information) and LiDAR (structural information). This data was used to classify the floodplain vegetation into 8 and 5 different vegetation classes, respectively. The main objective was to fuse the CASI and LiDAR-derived data sets on a pixel level, and to compare the classification results of the fused data set with those of the non-fused data sets. The performance of the classification results was evaluated against vegetation data recorded in the field. The LiDAR data alone provided insufficient information for accurate classification. The overall accuracy amounted to 41% in the 5-class set. Using CASI data only, the overall accuracy was 74% (5-class set). The combination produced the best results, raising the overall accuracy to 81% (5-class set). It is concluded that fusion of CASI and LiDAR data can improve the classification of floodplain vegetation, especially for those vegetation classes which are important to predict hydraulic roughness, i.e. bush and forest. A novel measure, the balance index, is introduced to assess the accuracy of error matrices describing an ordered sequence of classes such as vegetation structure classes that range from bare soil to forest.

4.2 Introduction

Climate change is expected to result into more extreme peak discharges in large Western European rivers, particularly in winter. The floods of the river Rhine in 1993 and 1995 and of the river Oder in 1997 show the limited capacity of these main rivers to accommodate present peak discharges. To increase the discharge capacity, embanked floodplains in use by farmers have been restructured to accommodate higher peak discharges and are at the same time designated as nature rehabilitation site (Smits et al. 2000, Wolfert 2001, Lenders 2003, van der Velde et al. 2006). Due to this management change, the floodplain vegetation will change over time (Bekhuis et al. 1995, Prach and Pysek 2001, Sýkora 2002, Geerling et al. 2006).

Accurate and up-to-date information on this dynamic vegetation is of vital importance to the river manager because the maximum discharge capacity depends on it through its hydraulic resistance. If the discharge capacity becomes too low, special measures are necessary, e.g. removal of bushes and softwood forests. A readily available, labour efficient, reliable and cost effective instrument to monitor the floodplain vegetation for hydraulic and ecological evaluation is needed (Geerling and Van den Berg 2002, Dowling and Accad 2003, Turner et al. 2003, Baptist et al. 2004). This paper explores the possibilities of digital remote sensing techniques to monitor and classify semi-natural floodplain vegetation (Leuven et al. 2002).

Two promising techniques to remotely sense vegetation are imaging spectroscopy (IS) and the Light Detection And Ranging (LiDAR) sensor technology. With IS spectral information (reflected sunlight) in the visible and shortwave Infra Red (IR) range is collected. In the current study we used the Compact Airborne Spectrographic Imager (CASI). This sensor has been used in several studies for high resolution vegetation mapping (Kurnatowska 1998, Shang et al. 1998, Protz et al. 1999, Von Hansen and Sties 2000, Leckie et al. 2005). On the basis of spectral information alone especially bush and forest types were confused (Geerling and Van den Berg 2002). The distinction between these vegetation classes is important because they differ considerably in hydraulic resistance.

LiDAR was originally introduced to facilitate the collection of data for digital elevation models (DEMs, Ackermann 1999, Wehr and Lohr 1999, Lillesand and Kiefer 2000, Charlton et al. 2003). In the process of creating a DEM, only reflections from the ground level are used and reflections from vegetation are considered redundant. Recent studies with LiDAR data have explored the possibilities to use these redundant vegetation reflections to map vertical vegetation structures. The results can be applied in woodland management (tree density, timber volume, tree height) and ecological (habitat) mapping (Protz et al. 1999, Zimble et al. 2003, Hill and Thompson 2005, Suárez et al. 2005, Straatsma and Middelkoop 2006). Studies to map riparian vegetation using LiDAR showed that discrimination of some vegetation types was possible based on vegetation height and density. The vegetation types that were similar in structure (e.g. bare soil and short grassland) were difficult to separate, but discrimination between bushes and trees was high (Asselman 2001, Cobby et al. 2001, Asselman et al. 2002, Dowling and Accad 2003). In this paper LiDAR will be used both for the technique and for the instrument used. Based on the above, the IS and LiDAR data seem complementary. As suggested by Leckie et al. (2005), the use of both data types in one classification could be synergetic. This idea is called data fusion. Pohl and van Genderen (1998) describe three types of data fusion: data-fusion at the decision level, at the feature level and at the pixel level. When data sets are fused at the decision level, they are processed completely separately and only the end results (say maps) are “fused” by combination in a GIS. Ordinary GIS overlays already qualify for this level of data fusion. At the feature level, the data sets are processed individually, resulting in unidentified features. The identification of the features is done by combining feature information of the two data sets. Finally, at the pixel level, the data sets are fused immediately and processed together to produce the end result.

Hill et al. (2002) and Hill and Thompson (2005) used CASI, HyMap and LiDAR data for landscape modelling applying a parcel-based approach in an English field-based landscape configuration. Although the data was pixel compatible after pre-processing, the data fusion took place at the feature level. The parcels were segmented using CASI. The parcel spectral properties were used for identification. LiDAR data were used to calculate additional parcel properties and assisted the

segmented CASI data in identifying different woodland types. This approach worked well in a patchy cultural landscape but seems not applicable for classifying heterogeneous patches of natural vegetation.

Hudak et al. (2002) estimated canopy height at unsampled locations by LiDAR based on the statistical and geostatistical relations between the LiDAR data and a Landsat ETM+ image at sample locations. In this process, the canopy height is extracted from the LiDAR data and is subsequently correlated to the ETM+ image. This is considered a feature level data fusion.

Currently no results have been published combining and processing IS and LiDAR data at the pixel level. Fusing the data from these two sensor types could contribute to vegetation maps with classes separated on vegetation type and vertical structure as required for modern nature and river management. The idea of transforming the raw LiDAR data into one or several data layers, added as extra layer(s) to an IS image, seems a straightforward way to fuse data sets. To extract features, the fused data can be processed by standard classification algorithms, thus making the process readily available and cost effective.

The aim of this paper is to combine IS and LiDAR data by data fusion at the pixel level to improve the classification accuracy of an 8-class and 5-class set of natural vegetation types. The 8-class set represents the vegetation classes relevant for nature and river management, while the 5-class set serves as a minimum set to estimate hydraulic resistance for river management purposes. The classification results of the fused data are compared to classification results of IS only and LiDAR only of the same data set.

4.3 Material and Methods

A case study area was chosen along the Waal River; one of the main branches of the river Rhine in the Netherlands (Figure 4.1). The nature area consists of former fields and grasslands, which have been bought from farmers through time. Between 1990 and 1994 the nature area was formed and ever since the site has been left to develop itself under a regime of natural grazing. The surface area of the research area is 5.8 hectares and it contains mixed patches and ecotones, i.e. the transitions between plant communities, of grass, herbaceous vegetation, some bushes and part of a 40 year old softwood forest (Bekhuis et al. 1995, Sýkora 2002).

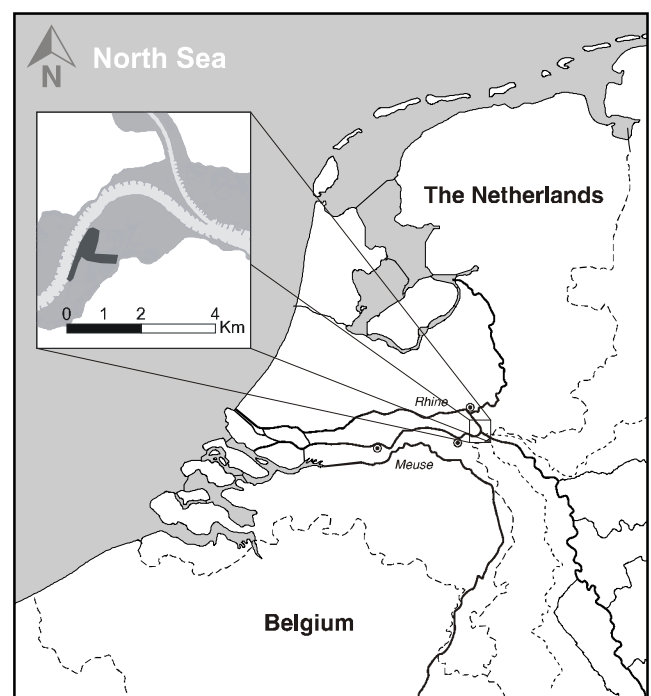


Figure 4.1 The location of the study area in the Netherlands along the Waal River, a Rhine branch.

Table 4.1 lists the characteristics of the CASI data set. To cover the whole study area, two CASI flight lines were mosaiced using the mosaic function in Erdas Imagine (Erdas 2005). The original geo-rectification of the CASI data proved insufficiently accurate (error of about 5 to 8 m or 3 to 4 pixels) and was re-georectified using a standard photogrammetrically generated river map of scale 1:1000 with planimetric error of 0.06 m (Anonymous 2003). To conserve the original DN values, nearest neighbour resampling was applied. The geo-rectification resulted in a root mean square (RMS) error of 2 m in x- and y-direction, i.e. about one pixel.

The LiDAR data set of the study area was flown on 12th of October 2001 using an ALTM 2033 scanner. The first return pulse was recorded. This first return may be the result of a hit of the laser pulse somewhere on a vegetation layer (or even the top) or a hit on the ground if no vegetation is hit. The data set was delivered as an ASCII file containing xyz coordinates. The mean density in the resulting data set is about 1 point per square metre. The approximate elevation error is 0.07 m and the planimetric error less than 0.5 m. The elevation error was determined using standard test surfaces (total 270m²) close to the research area (Brügelmann 2003). The planimetric error was determined using building perimeters from the same standard river map as used in the CASI geo-rectification (Anonymous 2003).

Table 4.1 Specification of the Compact Airborne Spectral Imager (CASI) data used.

Date of Flight	15 august 2001
Flight elevation	1500m
Swath width	1536m
Pixel size ^{*)}	2m
Number of spectral bands	10
Spectral range	437-890 nm

^{*)} The original pixel size was 3 m but resampled to 2 m by the imaging company; the original 3 m data was unavailable for this study

Field data on the floodplain vegetation were collected in August 2002 by botanists as part of a long term monitoring programme. The vegetation differences between the field data collection period (August 2002) and the date of flight (August and October 2001) can be considered negligible (Sýkora 2002). Within the monitoring programme, the plots were classified into 24 plant communities in accordance with the communities described by Schaminée et al. (1995) using TWINSPAN (Hill 1979). Additional bush and forest plots were added bringing the total to 405 plots in 25 classes which were used for classification and accuracy assessment.

The distinction of 25 vegetation classes is unnecessary for river management purposes and large-scale nature management. Furthermore, the number of plots is too low for a statistically sound classification into 25 classes. Therefore, the 25 original vegetation classes were regrouped into two related classification sets based on increasing vertical structure (Table 4.2). The vertical structure of vegetation is most important because it relates to the hydraulic resistance of the vegetation (van

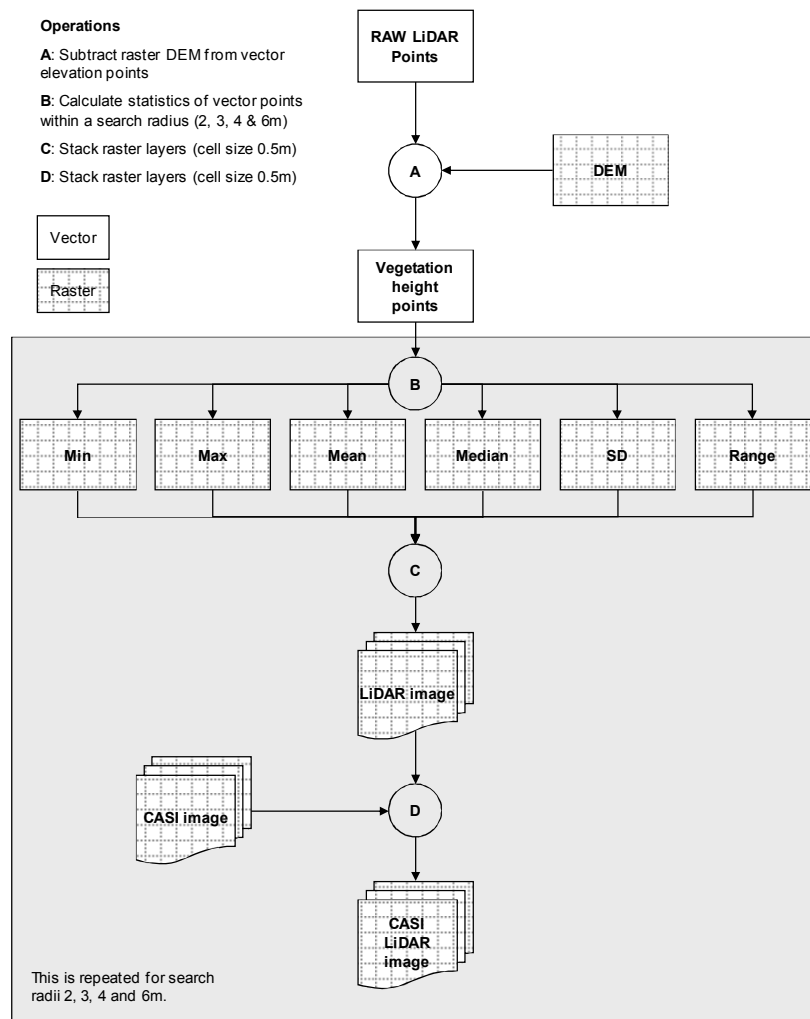
Velzen et al. 2003). The 5-class set (classes A to E) serves as a minimum set to estimate hydraulic resistance for river management purposes. In this set, herbaceous vegetation represents a large group of plant communities and is divided over classes B and C. Class B contains low herbaceous vegetation and class C contains higher herbaceous vegetation. The 8-class set provides more detail in the lower vegetation types and can be considered a minimum set for nature management purposes.

Table 4.2 Classes used for classification. The plant communities are used from Sýkora (2002) and described in Schaminée *et al.* (1995). Some plant communities are preceded by RG which is Romp Gemeenschap (Dutch) meaning “fragmented community”. When plant communities are preceded by RG, this means that the communities found did not always contain all community species, i.e., were not fully saturated, and sometimes consisted of overlapping communities.

5 class set	8 class set	Plant communities
A Bare and pioneer communities	A	Chenopodietum rubri Fragmented Medicagini-Avenetum pubescentis / Fragmented Bromo inermis-Eryngietum campestris Lolio-Potentillion anserinae / Fragmented Bromo inermis-Eryngietum campestris RG of <i>Cirsium arvense</i> en <i>Polygonum amphibium</i> [Artemisietia vulgaris]
		Fragmented Medicagini-Avenetum pubescentis / Bromo inermis-Eryngietum campestris with <i>Cynodon dactylon</i>
B Grasses and herbaceous vegetation	B1	Fragmented Ranunculo-Alopecuretum geniculati with <i>Trifolium repens</i> RG of <i>Cynodon dactylon</i> + <i>Euphorbia esula</i> [Sedo-Cerastion] / Fragmented Bromo inermis-Eryngietum campestris
	B2	Fragmented Arrhenatheretum elatioris Fragmented Medicagini-Avenetum pubescentis / Bromo inermis-Eryngietum campestris with <i>Oenothera erythrosepala</i> and <i>Sedum acre</i> Fragmented Ranunculo-Alopecuretum geniculati
	B3	Bromo inermis-Eryngietum campestris Bromo inermis-Eryngietum campestris / fragmented Medicagini-Avenetum pubescentis Fragmented Medicagini-Avenetum pubescentis / Bromo inermis-Eryngietum campestris with <i>Euphorbia cyparissias</i> and <i>Medicago falcata</i> Rorippo-Oenanthetum aquaticae
C Herbaceous and low woody vegetation	C1	Fragmentair Ranunculo-Alopecuretum geniculati Ranunculo-Alopecuretum geniculati RG of <i>Brassica nigra</i> [Phragmitetea] / Fragmented Ranunculo-Alopecuretum geniculati RG of <i>Calamagrostis epigejos</i> and <i>Epilobium hirsutum</i> [Galio-Urticetea] RG of <i>Mentha aquatica</i> and <i>Lycopus europaeus</i> [Narsturtio-Glycerietalia]
		C2
D Bush	D	RG <i>Sambucus nigra</i> [Galio-Urticetea] RG of <i>Ulmus minor</i> [Galio-Urticetea]
E Forest	E	RG of <i>Urtica dioica</i> [Salicion albae]

The classification procedure consisted of the following steps: (1) pre-processing of the LiDAR data and subsequently the fusion of the CASI and LiDAR data; (2)

Figure 4.2 Flowchart showing the general procedure for pre-processing of the raw LiDAR data and the pixel based fusion of CASI and LiDAR data.



classification of the LiDAR data, the CASI data and of the fused image, and (3) evaluation of the results. These steps are explained in more detail below. Step 1 is illustrated in a flowchart (Figure 4.2).

Pre-processing of LiDAR data and fusion with CASI data

A digital elevation model (DEM) was created and subtracted from the LiDAR data (vector points) to correct for variations in ground level. Per 2x2 m pixel the lowest point in an area of a 10 m search radius was chosen to represent the ground level and used to create the DEM. After subtraction of the DEM, the resulting LiDAR data was assumed to reflect variations in vegetation height only (step A in Figure 4.2; Figure 4.3a). The vegetation's vertical structure was described using the following statistics derived from the vegetation height points: minimum, maximum, mean, median, range and standard deviation (step B in Figure 4.2). These statistics (or 'textural bands') were computed for every 2x2 m cell in the research area (matching the CASI raster cell size), using a 'moving window' operation (Figure 4.3a and 4.3b, Lillesand

and Kiefer 2000, ESRI 2005). This yielded 6 LiDAR based rasters each containing one textural band, these bands were stacked (step C in Figure 4.2).

The number of LiDAR-points in the 'moving window' is defined by the size of the search radius (Figure 4.3b). If the radius is chosen too small, it will result in insufficient data points to calculate the required statistics. If it is chosen too large, it will smoothen the image detail. To test this, four stacked LiDAR raster sets were derived using search radii of 2 m, 3 m, 4 m and 6 m, respectively. The average number of LiDAR points per radius ranged

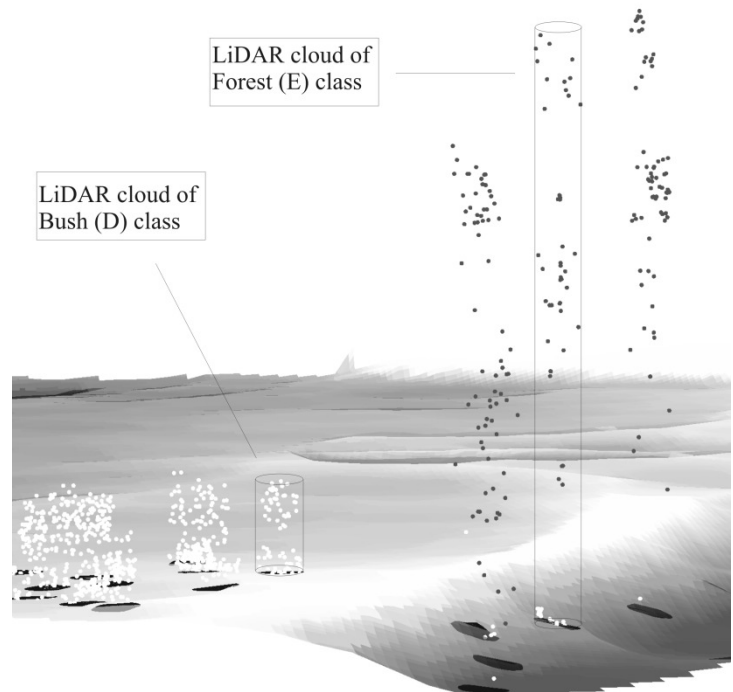
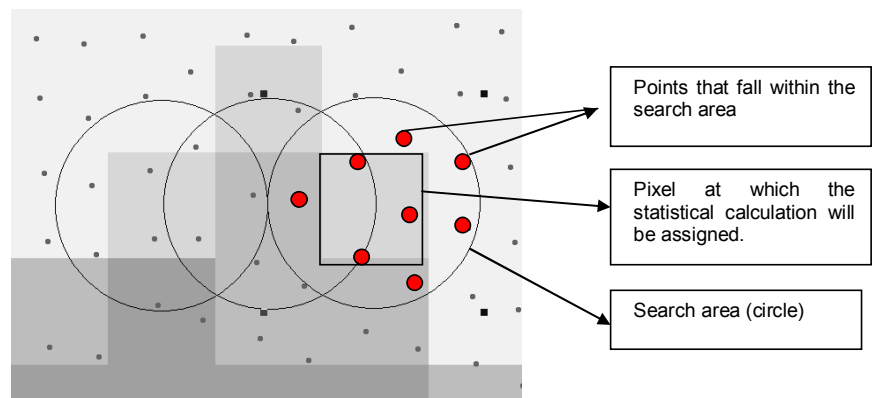


Figure 4.3a Example of LiDAR point clouds of training plots of classes Bush (D) on left and Forest (E) on the right. Points fall into a circular search area which are depicted as black circles overlaid on the DEM.

Figure 4.3b Preparation of LiDAR texture statistics min, max, mean, median, standard deviation and range. The scattered dots represent the LiDAR point cloud from above. The grid is according to the CASI grid and the circles represent the search area.



from 13.8 (± 8.8 SD) for 2 m to 81.3 (± 51.9 SD) for 6 m. The variances in LiDAR point density are relatively high due to high concentration of LiDAR points in small borderlines of the flight paths where points per column range up to 160 for the 2 m search radius.

The data-fused image was created by stacking the layers in Erdas Imagine (Erdas 2005). Before stacking, the grid size of the CASI and pre-processed LiDAR data was reduced to 0.5 m to minimise the potential impact of a grid shift during the stacking procedure. The fused images contained the 10 CASI bands and the 6 LiDAR texture bands and the cell size is 0.5 m. Four final fused-images were tested of which only the LiDAR bands differed: CASI fused with LiDAR bands derived from point statistics in a search area radius of 2 m, 3 m, 4 m and 6 m.

Classification

Maximum likelihood classification (MLC) was chosen to classify the data (Lillesand and Kiefer 2000, Thomas et al. 2003). MLC is a proven and robust method which gives a straightforward approach to classify and compare the different generated images and has been used previously to classify texture, e.g. by Liapis et al. (1997), Maas (1999) and Haack and Bechdol (2000).

All the bands of the fused image were normalised prior to classification by using a standard deviation stretch of 2 times the standard deviation (Mather 2004, Erdas 2005). Figure 4.4 shows an excerpt of the normalised fused image (LiDAR search radius 4 m) with the maximum vegetation height in red, green reflectance values in green and blue reflectance values in blue.

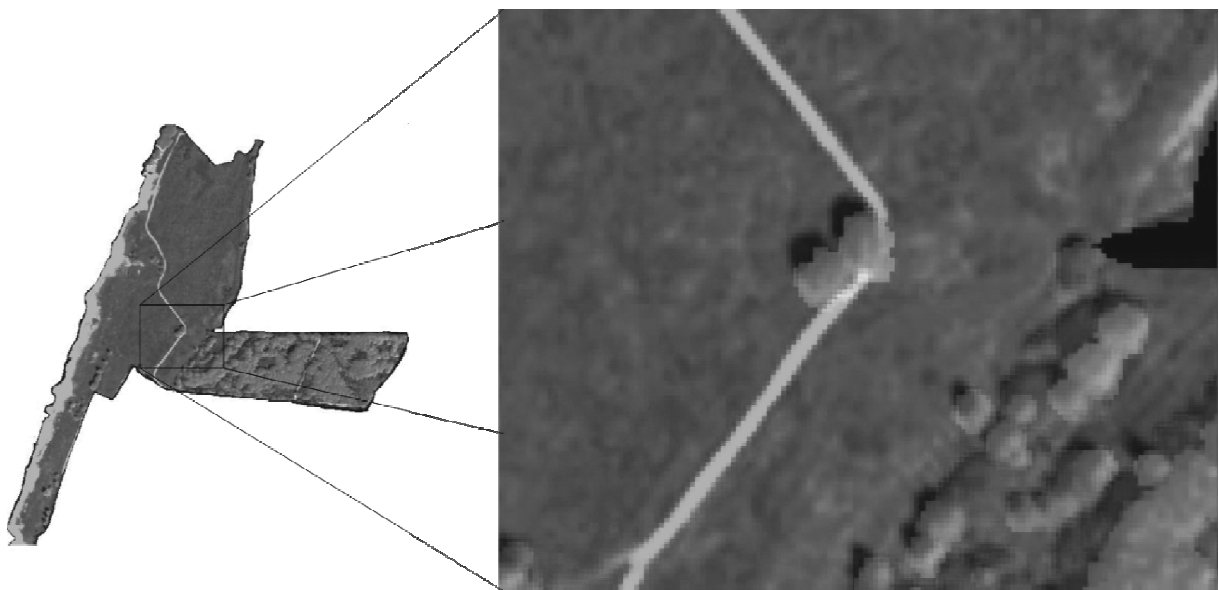


Figure 4.4 (In full colour on page 187) Example of the fused CASI and LiDAR image. Of the 16 band image (10 CASI and 6 LiDAR texture bands) 3 bands are shown, indicating the potential of data-fusion. RGB values correspond to maximum vegetation height, and reflectance of band (549-559 nm) in green and the band (437-447 nm) in blue. The bushes (dark red) and trees (bright red) stand out in this band combination. The light blue-ish line is a sandy path.

The field data were split in two halves by spatially stratified random selection, resulting in separate training and testing sets for the MLC procedure. The training set was used to produce the signature files for MLC. Pixels within 3 m of the centre point of the botanical field plots (3x3 m) were considered representative for the plot. The test set was used to derive error matrices, to calculate overall accuracies (Kappa Average, overall percentage) and to produce maps. MLC was performed in Erdas Imagine (Erdas 2005).

Evaluation

The quality of the classification results was evaluated using conventional indicators

such as error matrices, overall accuracy, Kappa and the Kappa-Z-test (Congalton 1991, Congalton 1999, Mather 2004). Furthermore, a new indicator was used which is referred to as the balance index (BI). The BI accounts for the fact that a misclassification between thematically distant classes (e.g. bare soil and forest) is considered worse than confusion of neighbouring classes (e.g. grass and herbaceous vegetation). The BI is calculated as the product of an error matrix (M) and a balance matrix (V) (Equation 1). If the error matrix is an $n \times n$ matrix, the balance matrix is an $n \times n$ matrix with maximum values (equalling $n-1$) on the top-left to bottom-right diagonal. The balance matrix is used to value the amount of misclassification and its values decrease towards the top-right and bottom-left corners (Equation 1). The product of the error and balance matrices is normalised by the maximum score possible, i.e. $n-1$ times the number of test plots (Equation 2). The result is a value between 0 and 1, where a value of 1 indicates a perfect classification and a value of 0 indicates the worst possible classification from the thematic distance point of view.

$$V = \begin{matrix} n-1 & .. & .. & .. & .. & .. & .. & 0 \\ .. & .. & .. & .. & .. & .. & .. & .. \\ .. & .. & n-1 & n-2 & n-3 & n-4 & .. & .. \\ .. & .. & n-2 & n-1 & n-2 & n-3 & .. & .. \\ .. & .. & n-3 & n-2 & n-1 & n-2 & .. & .. \\ .. & .. & n-4 & n-3 & n-2 & n-1 & .. & .. \\ .. & .. & .. & .. & .. & .. & .. & .. \\ 0 & .. & .. & .. & .. & .. & .. & n-1 \end{matrix} \quad (1)$$

$$BI = \frac{\sum(M \cdot V)}{(n-1) \cdot \sum M} \quad (2)$$

The BI is only applicable when, as in Table 4.2, the vegetation classes are ordered according to their vertical structure: from bare soil and pioneer vegetation (class A) to forest (class E), or any other principle of order. Only then the distance between a misclassified pixel and the diagonal is related to the amount of misclassification. This misclassification is valued by using the balance matrix. Two examples are given. Error matrices A and B both have an overall accuracy of 80 percent, i.e. 40 out of 50 test plots accurately classified, and only differ in the amount of misclassification. $V_{n=5}$ is the Balance matrix for a 5x5 error matrix, it values the classified pixels according to their distance from the diagonal. The Balance Indexes for A and B are computed as shown below; values for BI_A and BI_B are respectively 0.95 and 0.90.

$$\begin{array}{ccccc}
 8 & 2 & 0 & 0 & 0 \\
 1 & 8 & 1 & 0 & 0 \\
 A = 0 & 1 & 8 & 1 & 0 \\
 0 & 0 & 1 & 8 & 1 \\
 0 & 0 & 0 & 2 & 8
 \end{array}
 \quad
 \begin{array}{ccccc}
 8 & 0 & 2 & 0 & 0 \\
 0 & 8 & 0 & 2 & 0 \\
 B = 1 & 0 & 8 & 0 & 1 \\
 0 & 2 & 0 & 8 & 0 \\
 0 & 0 & 2 & 0 & 8
 \end{array}
 \quad
 \begin{array}{ccccc}
 4 & 3 & 2 & 1 & 0 \\
 3 & 4 & 3 & 2 & 1 \\
 V_{n=5} = 2 & 3 & 4 & 3 & 2 \\
 1 & 2 & 3 & 4 & 3 \\
 0 & 1 & 2 & 3 & 4
 \end{array}$$

$$BI_A = \frac{\sum(A \cdot V)}{4 \cdot \sum A} = \frac{(5 \cdot 8 \cdot 4 + 10 \cdot 3)}{4 \cdot 50} = \frac{190}{200} = 0.95$$

$$BI_B = \frac{\sum(B \cdot V)}{4 \cdot \sum B} = \frac{(5 \cdot 8 \cdot 4 + 10 \cdot 2)}{4 \cdot 50} = \frac{180}{200} = 0.90$$

4.4 Results

Tables 4.3, 4.4 and 4.5 show the error matrices for the classification into 8 vegetation classes using only the CASI bands, only the LiDAR bands (of the 4 m search area radius image), and using both CASI and LiDAR bands, respectively. The columns show the distribution of the ground truth plots over the vegetation classes. The rows show the composition of the MLC results. Producers Accuracy and Users Accuracy are indicated as respectively PA and UA. The PA summarises the probability of a vegetation plot being correctly classified. The UA represents the probability of a classified pixel belonging to the class it represents (Congalton 1991). Error matrix results for the images based on 2 m, 3 m and 6 m search area LiDAR statistics are not separately given but their results are summarised in Tables 4.6 and 4.7. Tables 4.6 and 4.7 show the Kappa index per class and the overall indexes Kappa Average, accuracy percentage and balance index for the 8-class and condensed 5-class set, respectively.

Table 4.3 The error matrix of the classification using only the CASI bands of the fused image, based on a separate test set. Producers Accuracy (PA) and Users Accuracy (UA) are shown.

Classified data	Reference data								UA
	A	B1	B2	B3	C1	C2	D	E	
A	11	2	0	2	2	0	0	0	65%
B1	0	8	5	7	4	3	0	0	30%
B2	0	0	7	8	0	2	0	0	41%
B3	3	6	5	31	0	3	0	1	63%
C1	0	2	3	2	12	1	1	0	57%
C2	0	5	7	1	3	13	3	0	41%
D	0	0	1	2	0	2	12	0	71%
E	0	0	0	0	0	0	3	28	90%
PA	79%	35%	25%	58%	57%	54%	63%	97%	

Table 4.4 The error matrix of the classification of only the LiDAR bands (in the fused image with search area 4 m radius for LiDAR points), based on a separate test set. Producers Accuracy (PA) and Users Accuracy (UA) are shown.

Classified data	Reference data								UA
	A	B1	B2	B3	C1	C2	D	E	
A	6	6	4	15	3	1	0	0	17%
B1	0	1	2	0	0	0	0	0	33%
B2	4	2	5	1	0	3	0	0	33%
B3	1	1	5	4	0	2	0	0	31%
C1	3	13	12	33	16	16	0	0	17%
C2	0	0	0	0	2	2	3	0	29%
D	0	0	0	0	0	0	16	1	94%
E	0	0	0	0	0	0	0	28	100%
PA	43%	4%	18%	8%	76%	8%	84%	97%	

Table 4.5 The error matrix of classification of both CASI and LiDAR bands (in the fused image with search area 4 m radius for LiDAR points), based on a separate test set. The Producers Accuracy (PA) and Users Accuracy (UA) are shown.

Classified data	Reference data								UA
	A	B1	B2	B3	C1	C2	D	E	
A	11	2	0	2	2	0	0	0	65%
B1	0	6	1	0	1	0	0	0	75%
B2	0	1	15	7	0	4	0	0	56%
B3	3	10	5	40	3	2	0	0	63%
C1	0	3	5	4	13	13	0	0	34%
C2	0	1	2	0	2	4	3	0	33%
D	0	0	0	0	0	1	16	0	94%
E	0	0	0	0	0	0	0	29	100%
PA	79%	26%	54%	75%	62%	17%	84%	100%	

The overall CASI results were average (8-class set) to good (5-class set) with overall accuracies of 57.8% and 74% (Tables 4.6 & 4.7). CASI classification results were average to good for classes A, D and E (Tables 4.3 & 4.6). PA was low for classes B1 and B2; their plots were distributed over classes B1 to C2. UA was lowest for class B1. Overall LiDAR results of the 8-class set and the 5-class set were poor (Tables 4.4 & 4.6). The confusion between the classes with smaller vegetation structure (A to C2) was large, clearly represented in the low class-specific Kappa values (Table 4.6) and the LiDAR (4 m) UA of class A (17%) and C1 (17%; Table 4.4). Structurally well-defined classes like bush (D) and forest (E) show good results.

For some classes all test plots are misclassified, i.e. zero on the diagonal in the corresponding error-matrices, this results in the negative class-specific Kappa values found in Table 4.5.

When comparing the results for the different LiDAR sets, the overall accuracy and

Kappa index show a downward trend with an increasing search radius. The class-specific Kappa indexes show different trends per class: classes B1 and B2 have their optimum in the 3 m set, B3 and C2 have their optimum in the 2 m set and C2 and D in the 4 m set. The balance index is highest for the 3 m set.

Table 4.6 The per-class accuracies (Kappa index) and overall accuracy indexes (Kappa Average, Percentage and Balance) for all 8-class classifications. The distance value between brackets (2, 3, 4 and 6 m) refers to the search area radii used to compute the LiDAR statistics from the LiDAR points.

	CASI	LiDAR (2m)	Fused (2m)	LiDAR (3m)	Fused (3m)	LiDAR (4m)	Fused (4m)	LiDAR (6m)	Fused (6m)
Class	Accuracy (Kappa)								
A	0.62	0.13	0.62	0.11	0.62	0.11	0.62	0.11	0.62
B1	0.21	0.00	-0.12	0.44	0.44	0.25	0.72	-0.12	0.25
B2	0.32	0.00	0.62	0.26	0.40	0.23	0.49	0.23	0.40
B3	0.51	0.27	0.41	0.25	0.49	0.08	0.51	-0.34	0.58
C1	0.52	0.22	0.23	0.10	0.27	0.08	0.27	0.04	0.24
C2	0.33	0.00	0.44	-0.13	0.36	0.19	0.25	0.06	0.25
D	0.68	0.84	0.84	0.93	0.88	0.94	0.94	0.68	0.79
E	0.89	0.96	1.00	1.00	1.00	1.00	1.00	1.00	1.00
Overall indexes									
Kappa Average	0.51	0.36	0.52	0.33	0.55	0.29	0.57	0.23	0.53
Accuracy %	57.8	44.6	59.7	42.2	61.6	37.0	63.5	31.3	59.7
Balance	0.871	0.835	0.905	0.852	0.907	0.836	0.910	0.821	0.886

The overall results of the fused CASI and LiDAR data are average for the 8-class set (highest overall accuracy 63.5%) to good (81%) for the 5-class set. In all cases, the fused image had higher Kappa and overall accuracies than the CASI, but these differences were not significant at $p < 0.01$ (Kappa Z-test). For the 8-class (4m) and 5-class set, the differences were significant at $p < 0.26$ and $p < 0.19$ respectively. The fused image always performed significantly better than LiDAR ($p < 0.01$).

Generally, the results in the fused CASI and LiDAR error matrices were more balanced when compared to the error matrices of LiDAR and CASI alone, i.e.,

Table 4.7 The per-class accuracy (Kappa index) and overall accuracy (Kappa Average, Percentage and Balance) for the CASI, LiDAR (4 m) and Fused CASI LiDAR (4 m) 5-class classification. The distance value between brackets (4 m) refers to the search area radius used to compute the LiDAR statistics from the LiDAR points.

	CASI	LiDAR (4m)	Fused (4m)
Class	Accuracy (Kappa)		
A	0.62	0.03	0.62
B	0.69	0.04	0.64
C	0.44	0.39	0.57
D	0.52	0.87	0.88
E	0.89	1.00	1.00
Overall Indexes			
Kappa Average	0.63	0.28	0.71
Accuracy %	74.4	41.2	80.6
Balance	0.929	0.835	0.948

the confusion with distant classes decreased as shown in the balance index (Tables 4.6 & 4.7). The final maps for the 8-class set are shown in Figure 4.5. The heterogeneity of the area can be clearly recognised in these maps. Figure 4.6 illustrates the performance in shadows. When using CASI only, the shadows are classified as Forest or Bush. In the fused image result, the shadows are classified as lower vegetation.

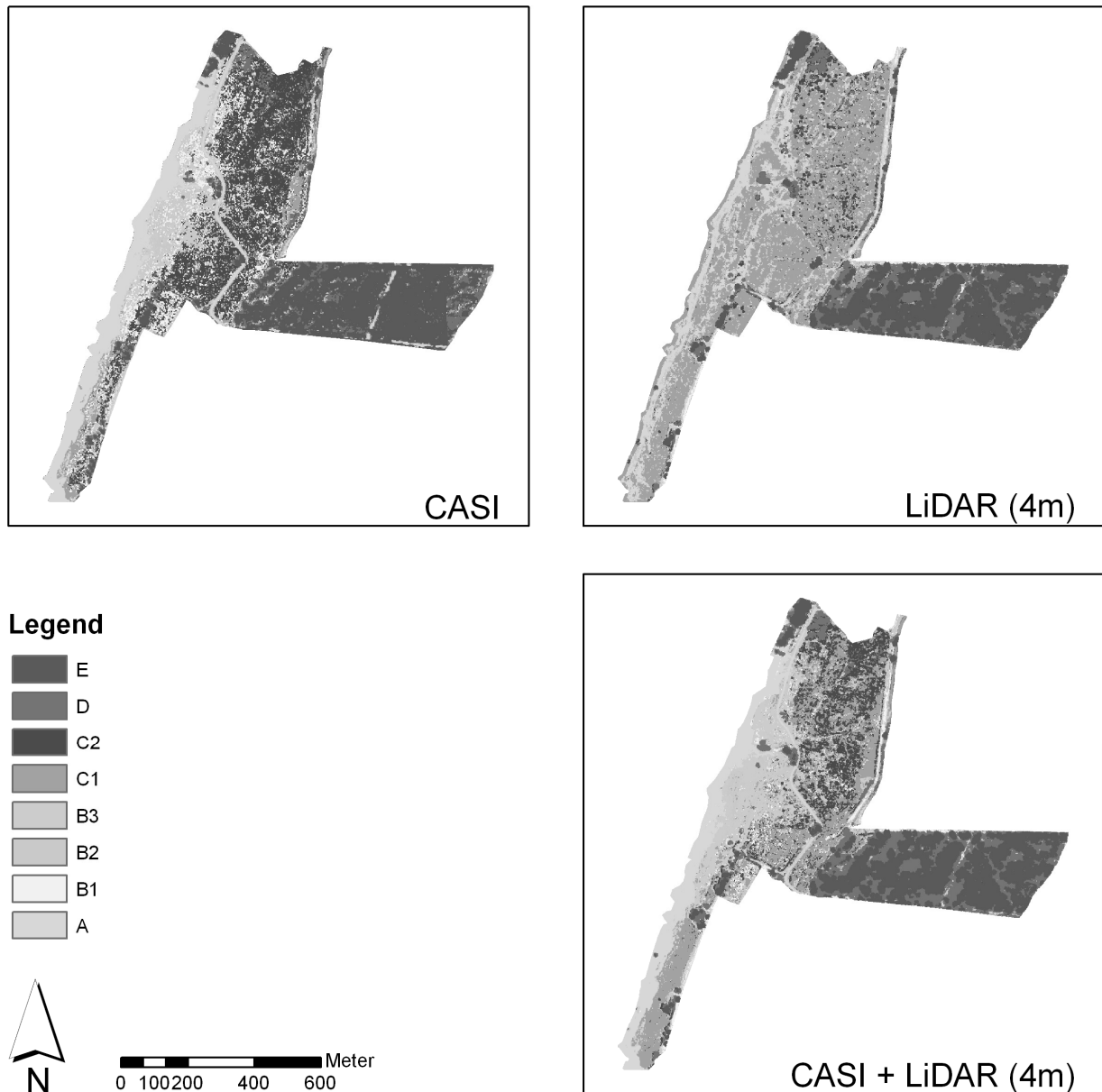


Figure 4.5 (In full colour on page 188) Maps of classification results LiDAR (4m), CASI, and Fused CASI LiDAR (4m).

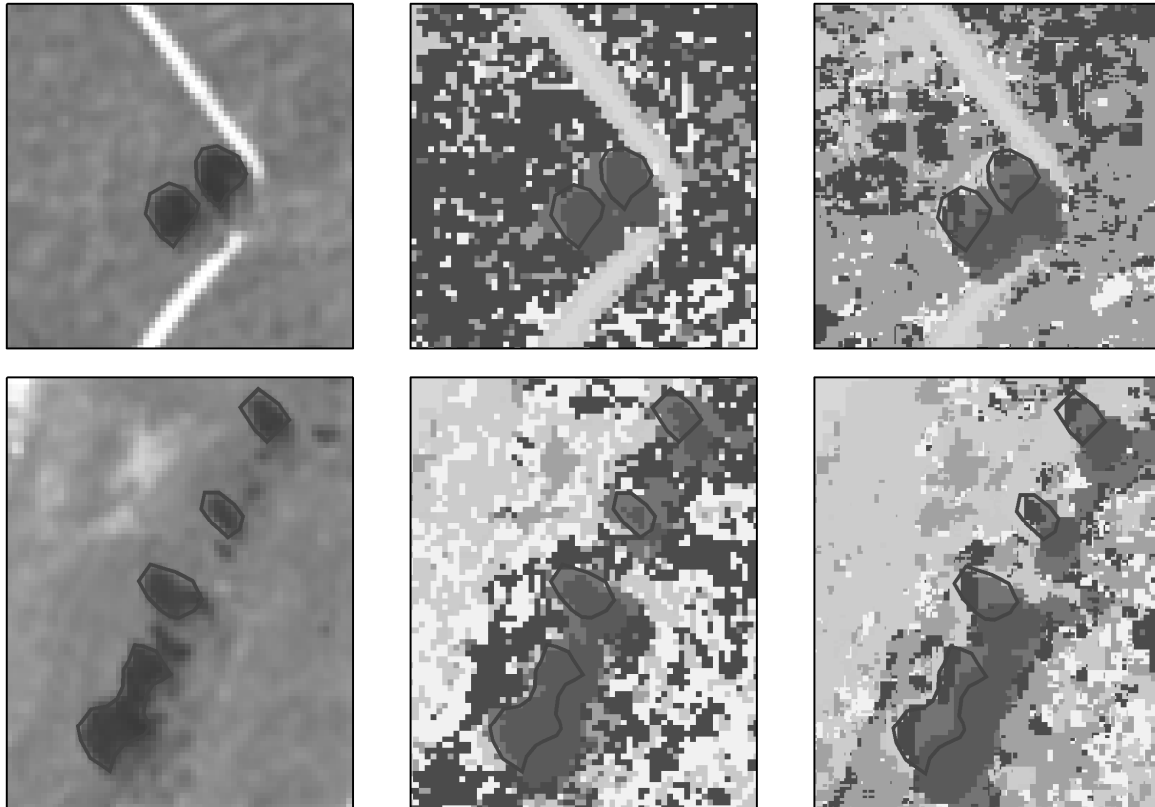
Classification of shadow

Legend

Shadow	C2	B2
E	C1	B1
D	B3	A



Meter 0 10 20 40 60



CASI (true colour)

CASI classification

CASI + LiDAR (4m)

Figure 4.6 (In full colour on page 187) Two examples of classification of shadows. On the left, a true colour image (CASI bands 615-625 nm (red), 549-559 nm (green) and 437-447 nm (blue)) on which the shadows are outlined in red. The middle image shows shadows mainly classified as trees in the CASI classification. On the right, shadows classified using the fused CASI LiDAR data appear partly as tree (covered in shadow) and partly as surrounding lower vegetation.

4.5 Discussion

In this study, LiDAR and CASI data were combined using a pixel-based method. The principle of pixel-based fusion worked well for this CASI and LiDAR data set.

Although the approach can be refined, the transformation of the LiDAR data into a layered grid containing LiDAR point statistics proved to be useful. The LiDAR data became an integral part of the image (Figure 4.4) and were easily used in existing

classification algorithms and GIS applications, making it a readily available, labour efficient, reliable and cost effective method.

The LiDAR only approach used in this study performs well as a 3-class instrument: bare soil, grasses and herbaceous vegetation (A to C2) as one class, and bush (D) and forest (E) as another two classes. Confusion is high between classes with a relatively low vegetation structure. Asselman (2001) and Asselman et al. (2002) reached a similar conclusion for grassland vegetation.

The LiDAR results in Table 4.6 show that an increase of the search radius leads to a decrease of the overall accuracy. This can be explained by the smoothing effect that occurs at larger search radii. The accuracy of the classification of the individual vegetation classes, indicated by the class-specific Kappa index, does not always decrease with an increasing search radius. The vegetation classes have an optimum that seems related to the spatial variability within the class. The length of the search radius has little influence for bare soil & pioneer vegetation (A) which is relatively homogeneous over large areas. Vegetation that is variable on a small scale level is classified best using a 2 or 3 m radius (e.g. classes B1-C1: grassland and herbaceous vegetation), but vegetation that forms bigger homogeneous patches performs best using a 4 m radius (e.g. C2-D: herbaceous & low woody vegetation and bush). Forest patches have lowest kappa for the 2 m search radius and perform best at larger search radii.

The CASI data produced much better results than the LiDAR data. The classification accuracies obtained in this study (57.8 % for the 8-class set and 74 % for the 5-class set) are comparable to previous studies (60 to 80% overall accuracy for classification into 6 to 9 vegetation classes, Green et al. 1998, Thomas et al. 2003, Leckie et al. 2005). However, it should be noted that other studies deal with relatively homogeneous vegetation structures (i.e., patchy fields) when compared to the heterogeneous floodplain vegetation used in the study at hand. For the classes bush and forest, the CASI data produced less accurate results than the LiDAR data. To estimate the hydraulic resistance for river management, the discrimination of bush and forest is of major importance. Geerling and Van den Berg (2002) also showed that spectral discrimination of bush and forest with CASI can be difficult, probably because both classes mainly consist of Willow (*Salix* spp).

From the LiDAR perspective, adding spectral data to the LiDAR data improved the results by more than 25% in the 8-class set to a 40% improvement in the 5-class set. Especially discrimination of low vegetation such as grasses and bare soil improved. The higher balance index indicates that confusion with distant classes diminished. From the CASI perspective, adding LiDAR data to CASI data improved the overall classification accuracy up to 7 percent. Especially the classes with a well-defined structure, such as bush and forest, were classified more accurately when compared to CASI only. These are classes with a high hydraulic resistance and, as such, very important for the river manager. The results of our study are in line with Mundt et al.

(2006) who found an improvement of 14% accuracy in the classification of sagebrush (*Artimisia tridentate Spp. wyomingensis*) after adding LiDAR to spectral data.

A common problem encountered in the classification of spectral data is misclassification due to shadows (Leckie et al. 2005). Figure 4.6 illustrates that this misclassification is reduced after fusion of the CASI and LiDAR data. It can be concluded that the classification of shady areas in the fused image is dominated by the added height information contained in the LiDAR texture bands, instead of the spectral information contained in the CASI bands.

The 2 m LiDAR set resulted in the highest overall accuracy and Kappa indexes of all LiDAR sets (Table 4.6). Remarkably, the results of its fusion with the CASI data were lowest. The 4 m LiDAR set produced the best results after fusion. These findings indicate that the classification of a fused image is not simply the sum of the separate CASI and LiDAR classifications. The MLC calculates the class probabilities for each pixel using the multivariate normal distribution fitted over the training set, with the values of the CASI and/or LiDAR bands as input values. The addition of extra bands to a pixel can influence the classification in different ways. If the extra bands have a low distinctive power, the calculated class probabilities will more or less remain unchanged. If the extra bands have a high distinctive power, the calculated class probabilities will increase for the pixel values falling within the range of high probability density, but will decrease for pixel values outside this range. However, a decrease or increase in class probability does not automatically imply that a pixel will be classified in a different class. This also depends on the change in probability for the other classes because a pixel is classified in the class with the highest probability. Addition of extra bands will only result in a different class if the new probability calculated for the original class is exceeded by that of another. This combination of changing (absolute) class probabilities and classification according to relative probabilities makes it particularly difficult to predict the classification results of the fused image based on the results of the separate CASI and LiDAR images.

Nonetheless, some tendencies can be observed. The results in Table 4.6 indicate that the LiDAR bands have a large distinctive power for high vegetation classes, i.e. classes D and E. The CASI bands have a relatively large distinctive power for classes A, B3 and C1. Classes B1, B2 and C2 performed relatively poor in the CASI set and produced variable results in the 2, 3, 4 and 6 m LiDAR set. These varying LiDAR results seem to provide an explanation for the fact that the fused 2 m LiDAR image performed worse than the fused 4 m LiDAR image. In the 2 and 6 m LiDAR sets, classes B1, B2 and C2 performed worst; the kappa indexes of zero or lower indicate that the average class probability of the pixels for their true class is lower than for the other classes. The 3 m LiDAR image performs well for classes B1 and B2, but this is counterbalanced by a bad performance for class C2. The 4 m LiDAR performs relatively well in all three classes, which may explain why the fused image with the 4 m LiDAR has the highest overall classification accuracy. Remarkably, classes B1 and B2 perform best in the 3 m LiDAR image before fusion, but after fusion they perform

best in the fused image with the 4 m LiDAR. This illustrates that the performance of the fused image cannot easily be predicted based on the performance of the separate CASI and LiDAR images.

Classifier

In this study, a maximum likelihood classifier was used, but there are several other options available. A test with the same data set using neural network and CART decision tree classifiers produced similar results (Psomas 2003). Using another part of the same CASI flight line, promising results were generated while developing new unsupervised classification algorithms, but these results were not tested against ground data (Tran et al. 2003). Another option is segmentation (Hill et al. 2002, Hill and Thompson 2005). This approach is suitable for classification of large-scale patchy landscapes, but it seems less suitable for small-scale heterogeneous vegetation as found in the case study area. The 'soft borders' or transitions between plant communities encountered within semi-natural vegetation are difficult to segment. Therefore, a pixel-based approach seems more appropriate.

Input data

The LiDAR only results were relatively poor in the lower vegetation types. Firstly, a higher LiDAR point density could improve the classification because a better discrimination in classes with similar height is expected as the 3D structure is better recorded. In addition, when using higher density data, the search area (Figure 4.3) can be optimised for different vegetation types because the number of LiDAR points in smaller search areas will be sufficient for reliable statistics. However, the collection of high density LiDAR data may be constrained by the footprint size, which currently equals 25 to 40 cm for a small footprint (Reutebuch 2003).

Secondly, LiDAR signals are often reflected multiple times because of its footprint. The last return pulse is the reflection of that part of the beam which has travelled the longest distance, hence is more likely to be a ground level point. The LiDAR data set used in this study contained only first return pulse values and was used for DEM and vegetation classification. The combined use of first and last return pulses can be expected to improve the quality of the DEM and the classification results. Especially for the detection of smaller objects, the accuracy of the DEM becomes more important. The generation of accurate DEMs out of LiDAR data sets is subject of extensive study (Cobby et al. 2001, Reutebuch et al. 2003).

Before classification a 2 times the standard deviation stretch normalisation was applied to the CASI and LiDAR fused images due to the difference in range of digital number between the CASI and LiDAR data. The visualisation of the images improved after this. Upon classifying a none normalised data set with MLC, the results were identical. The MLC method is insensitive to differences in ranges as it calculates the class probabilities for each pixel using the multivariate normal distribution fitted over the training set. When using other classification algorithms,

normalisation can influence the results. An example is classification with neural networks; the bands are normalised by pre-processing functions before the neural model is trained (Psomas 2003).

As mentioned in the Materials and Methods, the CASI data used consists of data from two flight lines. The use of multiple flight lines can have effects on the classification results due to differences of atmospheric condition, imaging condition and illumination geometry between these flight lines. Cross flight line radiometric normalisation can improve the results. In this research, one of the two CASI flight lines covers about 95% of the research area and contains 403 of the 405 plots used for training and testing. Effects on the results are considered minimal.

Differentiation of input

Classification of vegetation was realised in one step, but a natural landscape consists of elements of different scale. In the case study area, forest typically is of large scale and natural grasslands are of small scale because they contain heterogeneous patches of grasses and herbs. The area needed for representative sampling varies accordingly: the plot size needed for a representative area of forest typically is 10-30 metre, while the plot size of grassland typically is 2-5 m. As shown, the ML classifier classifies the major differences between forest, bush, and small-scale vegetation when using the LiDAR data only, i.e. the LiDAR image results in 3 broad classes. More subtle differences might be too small for a single classification step. Based on the above, the landscape could be divided into large-scale and small-scale elements, and these elements could be treated separately in ML classification. This could improve the discrimination between smaller differences. This approach of separating the landscape in different scale levels and subsequently the use of ML classification is in fact a mix of a decision tree and ML classification.

Geometric accuracy

Geometric accuracy is of major importance when two independently acquired data sources are fused (Hill and Thompson 2005, Mundt et al. 2006). In this study the planimetric accuracy of the LiDAR data was higher than of the CASI data, which is a general problem when combining high resolution spectral and LiDAR data. For accurate results the use of combined sensors, acquiring multi sensor data at the same time, and so minimising co-registration errors, is highly favoured.

Another aspect favouring combined sensors is resampling of input data. While preparing and fusing the two different data sets, the CASI data was resampled during geo-rectification and stacking. Nearest neighbour resampling was chosen, so the original DN values of the CASI remained unaltered and because of its straightforwardness. Other resampling methods such as bilinear interpolation and cubic convolution, compute a DN value out of neighbouring pixels and so change the measured DN values but yield a visually smoother image (Mather 2004). As there are drawbacks to every resampling method, the number of times an image is resampled

should be minimised to preserve image detail and reduce possible negative effects on the image classification results. Recording images the same time eliminates at least one of the resampling steps.

Reliability of botanic field data

The remote sensing community often regards botanic field data as hard facts. However, there are two sources of subjectivity enclosed in the botanic field data: The botanic classification of plant species into 25 different plant classes was originally developed for plant science purposes and is subsequently used in nature conservation and management. It is inevitably based on arbitrary borders between classes. This botanic classification might not be the optimum for remote sensing purposes (Thomas et al. 2003). The relation between botanic classification of plant species and classification of remotely sensed vegetation is topic of ongoing research. The botanic field data used in the present study originates from field plots. The plots were classified (Hill 1979) on the basis of the plot's plant composition until they could be assigned to a botanic class described in Schaminée et al. (1995). Obviously, the assignment of classes to field plots involves some level of expert judgement by the botanist. Especially when a plot contains a mixture of different vegetation types, the assigned class will not always accurately reflect the heterogeneous nature of the vegetation within a plot.

Data collection

Collecting LiDAR data for vegetation purposes solely is expensive. However, lower density LiDAR is already systematically being used for the creation of DEMs. Combination of these purposes will make application of LiDAR for vegetation studies more feasible. For CASI images, a similar argument counts. If future digital scanners combine high resolution and Infra Red data, these images can be used as a substitute for aerial photographs (which are applied in plan processes of the river manager) and at the same time provide data for vegetation classification.

4.6 Conclusions

Fusion of CASI and LiDAR data can improve the classification of floodplain vegetation. Firstly, the overall accuracy is higher and the classification of shadows has improved. Secondly, the fused data set classification shows diminished confusion with distant classes, i.e. the results become more balanced. This reduces errors in overall vegetation roughness when the maps are used as input in hydrological models. The best classification results of the fused data do not necessarily follow from the combination of separate sets with highest overall accuracy. They depend on the per-class added value of the probability distribution. It is expected that the classification results can be further improved by (1) using higher density LiDAR data, (2) the combined use of first and last return pulses, (3) the

division of the landscape into large-scale and small-scale elements and subsequent classification and (4) optimising the botanic clustering of plant communities. The balance index proved to be a useful indicator for classification quality which takes into account the distance between classes.

Acknowledgements

Thanks to Division East and Survey Department of the Ministry of Transport, Public Works and Water Management for kind permission to use the CASI and LiDAR data. Many thanks to Prof. Dr. Karle Sýkora of Wageningen University for contributing his field data and advice. Thanks to Regine Brügelmann and Madelein Vreeken-Buijs, the project leaders of Ministry of Public Works and Transport, Survey Department, Delft. Also thanks to Achilleas Psomas for his discussions and valuable input. This project was funded by the Ministry of Public Works and Transport, Survey Department, Delft.

References

- Ackermann F (1999). Airborne laser scanning - present status and future expectations. *ISPRS Journal of Photogrammetry and Remote Sensing* **54**: 64-67.
- Anonymous (2003). Digitaal Topgrafisch Bestand – Nat. Ministry of Transport, Public Works and Water Management. Directorate-General of Public Works and Water Management. Survey Department (AGI), Delft.
- Asselman NEM (2001). *Laser altimetry and hydraulic roughness of vegetation*. WL | Delft hydraulics, Delft.
- Asselman NEM, Middelkoop H, Ritzen, MR, Straatsma MW (2002). Assessment of the hydraulic roughness of river floodplains using laser altimetry. In: Dyer FJ, Thoms MC, Olley JM (Eds.). *The structure, function and management implications of fluvial sedimentary systems*. *IHAS Publication* **276**: 381-388.
- Baptist MJ, Penning WE, Duel H, Smits AJM, Geerling GW, van der Lee GEM, van Alphen JSL (2004). Assessment of the effects of Cyclic Floodplain Rejuvenation on flood levels and biodiversity along the Rhine river. *River Research & Applications* **20**: 285-297.
- Bekhuis J, Bosman W, Woesthuis H (1995). *Millingerwaard, Development report of years 1993-1994, In Dutch*. Ark Foundation, Laag Keppel.
- Brügelmann R (2003). *Quality test of the LiDAR data set*. Internal document. Personal Communication. Ministry of Transport, Public Works and Water Management. Directorate-General of Public Works and Water Management. Survey Department (AGI), Delft.
- Charlton ME, Large ARG, Fuller IC (2003). Application of Airborne lidar in river environments: the River Coquet, Northumberland, UK. *Earth Surface Processes and Landforms* **28**: 299-306.

- Cobby DM, Mason DC, Davenport IJ (2001). Image processing of airborne scanning laser altimetry data for improved river flood modelling. *ISPRS Journal of Photogrammetry and Remote Sensing* **56**:121-138.
- Congalton RG (1991). A review of assessing the accuracy of classifications of remotely sensed data. *Remote Sensing of Environment* **37**: 35-46.
- Congalton RG, Green K (1999). *Assessing the Accuracy of Remotely Sensed Data: Principles and Practices*. Lewis Publishers, Boca Raton, Florida, US.
- Dowling R, Accad A (2003) Vegetation classification of the riparian zone along the Brisbane river, Queensland, Australia, using light detection and ranging (lidar) data and forward looking video. *Canadian Journal of remote sensing* **29**: 556-563.
- ERDAS (2005). *Erdas Imagine 8.7. Tour Guide*. Erdas Inc., Atlanta, Georgia.
- ESRI (2005). *ArcGIS 9.1 and ArcInfo workstation*. Environmental Systems Research Institute, Redlands.
- Geerling GW, Van den Berg GJ (2002). *Monitoring and Dynamic River Management*. In Dutch Department of Environmental studies, section nature management of river corridors, University of Nijmegen, Nijmegen. Ministry of Transport, Public Works and Water Management, Directorate-General of Public Works and Water Management, Survey Department (AGI), Delft.
- Geerling GW, Ragas AMJ, Leuven RSEW, van den Berg JH, Breedveld M, Liefhebber D, Smits AJM (2006). Succession and rejuvenation in floodplains along the River Allier (France). *Hydrobiologia* **565**: 71-86.
- Green EP, Mumby PJ, Edwards AJ, Clark CD, Ellis AC (1998). The assessment of mangrove areas using high resolution multispectral airborne imagery. *Journal of Coastal Research* **14**: 433-443.
- Haack B, Bechdol M (2000). Integrating multisensor data and RADAR texture measures for land cover mapping. *Computers & Geosciences* **26**: 411-421.
- Hill MO (1979). *TWINSPAN - A FORTRAN program for arranging multivariate data in an ordered two-way table by classification of individuals and attributes*. Cornell University, Ithaca, N.Y.
- Hill RA, Smith GS, Fuller RM, Veitch N (2002). Landscape modelling using airborne multispectral and laserscanning data. *International journal of remote sensing* **23**: 2327-2334.
- Hill RA, Thompson AG (2005). Mapping woodland species composition and structure using airborne spectral and LiDAR data. *International Journal of Remote Sensing* **26**: 3763-3779.
- Hudak AT, Lefsky MA, Cohen WB, Berterretche M (2002). Integration of lidar and Landsat ETM+ data for estimating and mapping forest canopy height. *Remote sensing of Environment* **82**: 397-416.

- Kurnatowska AM (1998). Large-scale vegetation mapping in mountain environments using remote sensing and plant physiology methods. In: Nieuwenhuis GJA, Vaughan RA, Molenaar M (Eds.) *Operational Remote Sensing for Sustainable Development*. Balkema, Lisse. pp.61-65.
- Leckie DG, Cloney E, Jay C, Paradine D (2005). Automated mapping of stream features with high resolution multispectral imagery: an example of the capabilities. *Photogrammetric Engineering & Remote Sensing* **71**: 145-155.
- Lenders HJR (2003). *Environmental rehabilitation of the river landscape in the Netherlands. A blend of five dimensions*. PhD thesis, University of Nijmegen, Nijmegen.
- Leuven RSEW, Pourdevigne I, Teeuw RM (2002). Remote sensing and Geographic Information Systems as emerging tools for riverine habitat and landscape evaluation: from concepts to models. In: Leuven RSEW, Pourdevigne I, Teeuw RM (Eds.) *Application of Geographic Information Systems and Remote Sensing in River Studies*. Backhuys Publishers, Leiden.
- Liapis S, Alvertos N, Tziritas G (1997). Maximum likelihood texture classification and Bayesian texture segmentation using discrete wavelet frames. In: *International Conference on Digital Signal Processing, 2-4 July 1997, Santorini, Greece* (<http://ieeexplore.ieee.org>). pp. 1107-1110.
- Lillesand TM, Kiefer RW (2000). Remote sensing and image interpretation. John Wiley & Sons, Inc., New York.
- Maas GH (1999). The potential of height texture measures for the segmentation of airborne laser scanner data. In: *Fourth International Airborne Remote Sensing conference and Exhibition / 21st Canadian symposium on Remote Sensing, 21-24 June 1999, Ottawa, Ontario, Canada*.
- Mather PM (2004). Computer processing of remotely sensed images, an introduction. John Wiley & Sons Ltd., Chichester, West Sussex, England.
- Mundt JT, Streutker DR, Glenn NF (2006). Mapping sagebrush distribution using fusion of hyperspectral and lidar classifications. *Photogrammetric Engineering & Remote Sensing* **72**: 47-54.
- Pohl C, van Genderen JL (1998). Multisensor image fusion in remote sensing: concepts, methods and applications. *International journal of remote sensing* **19**: 823-854.
- Prach K, Pysek P (2001). Using spontaneous succession for restoration of human-disturbed habitats: Experience from Central Europe. *Ecological Engineering* **17**: 55-62.
- Protz R, van den Bygaart AJ, Wood MD, Hulshof BGA (1999). *Evaluation of high resolution airborne imagery and global positioning systems for monitoring changes in agro ecosystems*. RES/MON-012/97, COESA.
- PSOMAS A (2003). *Vegetation mapping of floodplain areas by means of Artificial Neural Networks*. MSc thesis report GIRS-2003-18. Centre for Geo-Information, Wageningen University and Research, Wageningen.

- Reutebuch SE, McGaughey RJ, Andersen HE, Carson WW (2003). Accuracy of high resolution lidar terrain model under a conifer forest canopy. *Canadian Journal of Remote Sensing* **29**: 527-535.
- Schaminée JHJ, Stortelder AHF, Westhoff V (1995). The vegetation of the Netherlands. *Introduction to plantsociology: basics, methods and applications (In dutch)*. Opulus Press, Upsala and Leiden.
- Shang J, Jollineau MY, Howarth PJ, Wang J (1998). A comparison of spatial- and spectral-mode CASI imagery for coastal wetland mapping in the Lake St. Clair delta: preliminary results. In: *The 20th Canadian Symposium on Remote Sensing*, 10-13 May, Calgary, Canada. pp. 215-218.
- Smits AJM, Nienhuis PH, Leuven RSEW (2000). *New Approaches to River Management*. Backhuys Publishers, Leiden.
- Straatsma MW, Middelkoop H (2006). Airborne laser scanning as a tool for lowland floodplain vegetation monitoring. *Hydrobiologia* **565**: 87-103.
- Suarez JC, Ontiveros C, Smith S, Snape S (2005). Use of airborne LiDAR and aerial photography in the estimation of individual tree heights in forestry. *Computers and Geosciences* **31**: 253-262.
- Sýkora K (2002). *On vegetation surveys and succession in the floodplain Millingerwaard, Waal river, the Netherlands. Research data. Personal Communication*. Wageningen University, Nature Conservation and Plant Ecology Group, Chair: Ecological Construction and Management of Infrastructure, Wageningen.
- Thomas V, Treitz P, Jelinski D, Miller J, Lafleur P, McCaughey JH (2003). Image classification of a northern peatland complex using spectral and plant community data. *Remote Sensing of Environment* **84**: 83-99.
- Tran TN, Wehrens R, Buydens LMC (2003). SpaRef: a clustering algorithm for multispectral images. *Analytica Chimica Acta* **490**: 303-312.
- Turner W, Spector S, Gardiner N, Fladeland M, Sterling E, Steininger M (2003). Remote sensing for biodiversity science and conservation. *Trends in Ecology and Evolution* **18**: 306-314.
- Van der Velde G, Leuven RSEW, Ragas AMJ, Smits AJM (2006). Living rivers: trends and challenges in science en management. *Hydrobiologia* **565**: 359-367
- van Velzen E, Jesse P, Cornelissen P, Coops H (2003). Hydraulic resistance of floodplain vegetation (in Dutch), parts 1 and 2. Ministry of Transport, Public Works and Water Management, Directorate-General of Public Works and Water Management, Institute for Inland Water Management and Waste Water Treatment (RIZA), Arnhem.
- Von Hansen W, Sties M (2000). On the capabilities of digital high resolution multispectral remote sensing techniques to serve nature conservation requirements. *International archives of Photogrammetry and Remote Sensing XXXIII(Part B7)*.
- Wehr A, Lohr U (1999). Airborne laser scanning - an introduction and overview. *ISPRS Journal of Photogrammetry and Remote Sensing* **54**: 68-82.

Wolfert HP (2001). *Geomorphological Change and River Rehabilitation*. PhD thesis, Alterra Green World Research, Wageningen.

Zimble DA, Evans DL, Carlson GC, Parker RC, Grado SC, Gerard PD (2003). Characterizing vertical forest structure using small-footprint airborne LiDAR. *Remote Sensing of the Environment* **87**: 1-182.

5 Mapping floodplain plant communities: clustering and ordination techniques adopted in remote sensing

J. Verrelst, G.W. Geerling, K.V. Sýkora, J.G.P.W. Clevers

Submitted to International Journal of Applied Earth Observation and Geoinformation.

5.1 Abstract

Various approaches are used in vegetation science to cluster species abundance data into plant communities. Remote sensing offers the potential to map and monitor plant communities based on their characteristic reflectance. The problem is however, that narrowly defined plant communities i.e. plant communities at a low hierarchical level of classification in the Braun-Blanquet system, often cannot be linked directly to remote sensing methods for vegetation mapping. We studied whether and how an ecological data set can be classified into a few major discrete, mappable classes without substantial loss of ecological meaning. Botanical field data and airborne data (CASI and LiDAR) were collected for a floodplain along the river Waal in the Netherlands. The results show that floodplain vegetation mapping by remote sensing yields results with higher accuracy if combined clustering and ordination techniques are applied to discriminate environmentally linked floristic assemblages, mainly determined by the related parameters elevation and soil moisture.

5.2 Introduction

Mapping is one of the most efficient methods to visualise trends of plant community patterns in space and time. The problem is that, although in most cases plant communities can clearly be recognised in the field, the detection of borders between different vegetation types is not always easy. Vegetation units are abstractions of reality and boundaries between them are not always sharp (Whittaker 1973). Between two adjacent plant communities there is a transition, which may be long or short (Sykora 1984a, 1984b). According to Barkman (1990) real boundaries may be absent (local continua) or very sharp (usually man made) but both cases are rare and in general real boundaries are fairly sharp. Glavac et al. (1992) state that in nature that has not been uninfluenced by humans, transitions between plant communities may be continuous or discontinuous, but usually the “non-linear but continuous” model (Scott 1974) holds. In this spatial model, areas in which species composition changes very slowly are alternated by areas with quick species turn-over. To enable vegetation mapping, the core emphasis is on how to simplify vegetation gradients into discrete units while a maximal ecological meaning is preserved. Remotely sensed reflectance data offer capabilities to map vegetation but require spectral signatures of pre-identified vegetation classes. Plant communities need to be defined prior to mapping. Since these plant communities should be mapped in discrete units, probabilistic classifiers are needed yielding classes with crisp boundaries that are mutually exclusive (Fisher 1999). For a long time plant ecologists have already been developing methods to identify species assemblages (Hill 1979), though a match of these methodologies with remote sensing (RS) techniques has only been recently tackled (Nilsen et al. 1999, Thomas et al. 2003, Schmidlein and Sassini 2004). In this respect the use of ordination techniques and ancillary abiotic field data

is suggested to organise plant community data along environmental gradients across space. Such organisation asks for the use of multispectral data of high spatial resolution to spectrally delineate such classes. Yet spectral discrimination of vegetation classes with similar species composition or environmental conditions remains subject to inaccuracies (Thomas et al. 2003, Lawrence et al. 2006).

In a previous study, Geerling et al. (2007) gathered remote sensing data on the vegetation of a semi-natural floodplain along the river Waal in the Netherlands by means of the Compact Airborne Spectrographic Imager (CASI) for spectral information and Light Detection And Ranging sensor technology (LiDAR) for structural information. They concluded that the fusion of CASI and LiDAR data can improve the classification of floodplain vegetation, particularly vegetation classes differentiated by their vertical structure. These classes are important to predict the hydraulic roughness of a floodplain, but were almost exclusively based on structure and not on species composition. As such they miss syntaxonomic relevance.

In this work we used the Braun-Blanquet method for data collection and vegetation analysis (Westhoff and Van der Maarel 1978). The described plant communities were grouped together into broader vegetation classes that can be discriminated through remotely sensed data and at the same time maintain ecological and syntaxonomical significance. Adopting plant community data can speed up the classification process not only due to its potential use as ground truth data, indispensable for mapping, but also by analysing its inherent informative value for improving classification quality. The objectives of this study are (1) to explore the adequacy of field data using clustering techniques, and (2) to optimise the class delineation procedure by incorporating ancillary abiotic variables and ordination techniques in the mapping process. The same study area and data sets are used as in the study of Sykora 2002. First, the usual methods for classification and ordination of plant communities and then the remote sensing way of plant community detection are briefly described.

Classification and ordination of plant communities.

In vegetation science plant communities (discrete plant assemblages) are distinguished by grouping species abundance data through cluster analysis and ordination (Austin and Smith 1989, Fortin et al. 2000). Cluster analysis in botanic studies essentially seeks to group floristic abundance data into classes or groups in such a way that within-group similarity is maximised and between-group similarity is minimised according to some objective criteria (Jongman et al. 1995). Basically, cluster analysis techniques divide plot samples of species (relevés) into a hierarchy of statistically similar clusters and then examine their dissimilarity. Amongst the most widely employed techniques by field ecologists are: Two Way Indicator Species Analysis (TWINSPAN) (Hill 1979, Gauch and Whittaker 1981) and cluster analysis by dendrogram method (McCune and Mefford 1999). TWINSPAN is a polythetic, hierarchical clustering technique, involving the joint clustering of samples and species by successive partitions of ordination axes generated at each step by

reciprocal averaging. At each step the algorithm weights the estimated species abundance, thus giving emphasis to particularly useful diagnostic species. While a dendrogram is a treelike plot that depicts the agglomeration sequence in cluster analysis, in which entities are enumerated along one axis and the dissimilarity level at which each fusion of clusters occurs on the other axis. Both methods show the hierarchy of clustering respectively as a vegetation table showing all plots (TWINSPAN) and as a graphical representation (dendrogram). Due to differences in algorithm, the clusters made by TWINSPAN and dendrogram do not fully correspond. TWINSPAN classifies the plots in a divisive way, dividing the clusters using ordination space partitioning, whereas dendrogram groups the plots together based on a cluster distance measure in an agglomerative way. Nevertheless, as vegetation units are abstractions of reality and boundaries between them are not always sharp, in vegetation science, classification and ordination are nowadays both used as complementary methods.

Ordination analysis, as a kind of gradient analysis, seeks to detect a set of factors that accounts for the major patterns across all the original variables without a substantial loss of information. Generally a few major gradients will explain most of the variability in the total data set. Detrended Correspondence Analysis (DCA, Hill and Gauch 1980) is an 'unconstrained' ordination technique which means that it refers to plot based species data without considering any explanatory variables. A correspondence analysis (CA) is a form of weighted averaging which constructs theoretical environmental variables that best explain the species data (Jongman et al. 1995). This is done by maximising the dispersion of the species scores along an ordination axis and the correlation between species and sites. The first axis symbolises the 'longest' gradient in species composition; the second one describes the 'longest' gradient in the remaining floristic variation and so on. Multiple axes can be constructed, with the constraint that they are uncorrelated with the previous axes. With a DCA two additional steps, detrending and rescaling are added to remove two major faults: the arch effect and axis compression (McGarigal et al. 2000). Special problems arise with ordination in that it is subject to a number of assumptions about joint relationships of variables (Gauch 1982).

In fact, despite case specific shortcomings, ordination and cluster analysis may be seen as complementary, and when applied together they may provide useful information about the relationships among species (e.g. Thomas et al. 2003). In practice more than one solution is possible for defining plant communities. For instance, multiple plant assemblages can be defined, depending on the required level of detail, applied method, skills of the user and expert knowledge.

Plant community detection by airborne remote sensing

Detection of plant assemblages through optical remote sensing data concerns the spectral differentiation of a group of species, rather than the specific spectral response of one species. Species assemblages have distinct spectral characteristics

when compared to single plants. The spectral influence of the non-vegetation elements, the multiple scattering between different plants and the structural layering of the vegetation can be seen as characteristic of a plant community (Schmidt and Skidmore 2003). The success of mapping these communities by remote sensing data depends therefore mainly on the type of remotely sensed data and the botanical classes used for the classification. Concerning the type of data, there are numerous examples of studies where high spatial resolution airborne hyperspectral data were applied to derive thematic maps of floristic composition (e.g. Treitz and Howarth 2000, Schmidlein and Sassini 2004). Previous studies of river dynamics using multispectral and hyperspectral sensors include Winterbottom and Gilvear (1997), Malthus and George (1997) and Schmidt and Skidmore (2003). Also LiDAR has significant potential for generating a high resolution digital terrain map of complex river channel environments and vegetation characteristics (e.g. see review Straatsma and Middelkoop 2006). For instance, Cobby et al. (2001) and Mason et al. (2003) employed laser altimetry for the assessment of floodplain vegetation height. The direct LiDAR observations of vegetation structure can thus present an independent information source complementing the spectral information content for a comprehensive floodplain characterisation (Gillespie et al. 2004, Hill and Thomson 2005, Geerling et al. 2007). However, regardless of the type of remotely sensed data and the applied method, the botanical assignment of the ground truth data that precedes the classification step is usually taken for granted by cartographers. Given that various botanical assignments are possible from the same floristic data, it is this 'grey zone' of identification and, thus, the possibilities for improvement of the mapping that will be further exploited. The aforementioned methods of vegetation sampling, classification and ordination, will be used to optimise characterisation of plant community classes that can be discriminated through reflection and altimetry data. In the material and methods section we will present a botanical data set of a nature area that will be used for testing the map-ability of vegetation clusters.

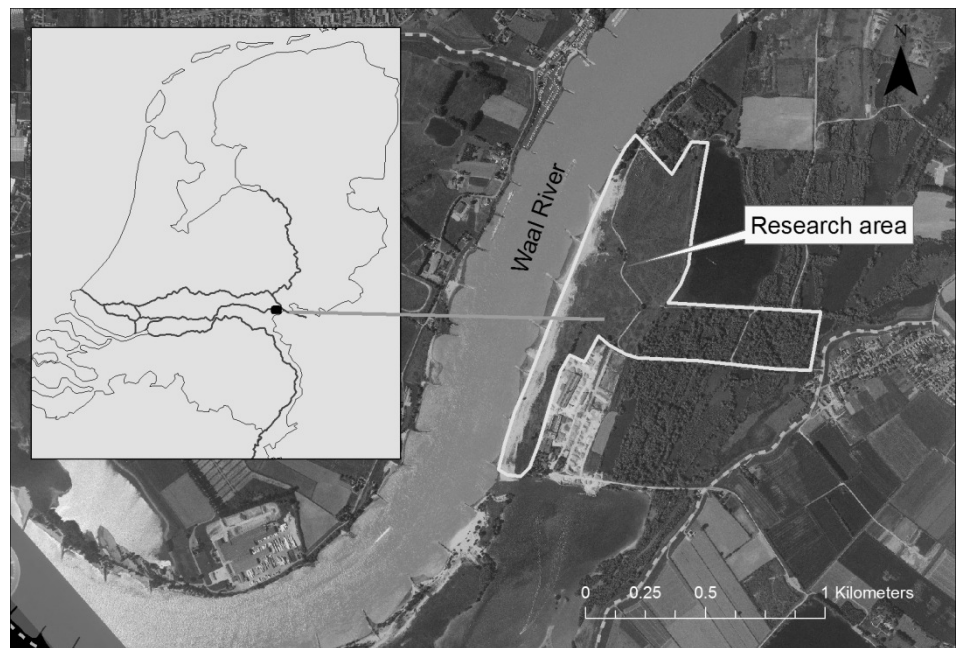
5.3 Material and Methods

Study area

Abiotic and floristic field data have been collected in August 2002 in the nature area "Millingerwaard" (51.5° N and 5° E) by the third author and his co-workers as part of a long term monitoring programme. The Millingerwaard is a floodplain along the river Waal, one of the main branches of the river Rhine in the Netherlands (Figure 5.1). The size of the study area is 58 hectares with sand dunes, low vegetation, bushes and forest included within its boundaries. In 1989, the nature area was formed and has been left to develop itself. In the following years, cattle, horses and beavers were introduced to stimulate spontaneous development of riverine woods, open water, a living river dune, marshes and grassland. The erratic dynamics of the river play a very important role by creating mixed patches of different stages of vegetation

succession. Vegetation varies from riverbank pioneer vegetation, dry open grasslands, ruderal grasslands, tall forb communities (roughage) to softwood and hardwood forests.

Figure 5.1 The Location of the study area in the Netherlands along the river Waal, a branch of the river Rhine. The area is part of the nature area “Millingerwaard” (coordinates: 51.5° N and 5° E).



Ground truth data

The field component of this study involved quadrant sampling (each 3 x 3 m²) of 317 plots randomly distributed over the study site (Van Geloof and De Ronde 2002). Within each plot the species composition (vascular plants), abundance in terms of percentage cover and the abiotic variables were recorded. Abiotic variables were: moisture, elevation, organic matter, soil type, light, nitrogen, mowing, pH and vegetation structure height. The abundance data were converted into 9 percentage classes to allow further analysis following the classification system of Braun-Blanquet (Westhoff and Van der Maarel 1978). Field sampling catalogued over 266 vascular plant species in the floodplain. We removed one plot that exclusively consisted of a shrub species (*Sambucus nigra*). This would have resulted in a single plant community and cause an extreme outlying position in the ordination space. Shrubs and tree classes (single species) will later again be added in the mapping process. In order to clarify the floristic similarity among the 317 plots, 23 plant communities were initially distinguished with TWINSpan (Table 5.1) and, based on the presence of characteristic and differential species, described according to the overview of Dutch plant communities (Schaminée et al. 1995-99). The Braun-Blanquet system describes plant assemblages at different hierarchical levels: class, order, alliance and association. Ideally, vegetation types are described at the level of associations. This, however, is not always possible due to a lack of characteristic species from the lower levels of classification. In this case ‘fragmentary communities’ (FC, see Table 5.1) are distinguished. For some purposes associations have to be generalised into broader vegetation types. The benefit of the used phytosociology is that plant assemblages

are quite well studied, particularly the synecology: the environmental conditions of communities. For most of the syntaxonomical classes, environmental factors are fairly well understood; so, by interpreting the synecology, additional information about the habitat is gained.

Table 5.1 Plant communities used for classification. The plant communities are distinguished by Sýkora (2002) and named according to Schaminée et al. (1995-99). “/” means transition between two mentioned communities. Major structure types are: P: Pioneer vegetation, G: Grassland, R: Ruderal vegetation, S: Swamp vegetation.

Cluster number	Plant communities	Structure type
1	Fragmented Medicagini-Avenetum pubescentis / Fragmented Bromo inermis-Eryngietum campestris	(G, P)
2	Lolio-Potentillion anserinae / Fragmented Bromo inermis-Eryngietum campestris	(G,P)
3	RG of <i>Cynodon dactylon</i> + <i>Euphorbia esula</i> [Sedo-Cerastion] / Fragmented Bromo inermis-Eryngietum campestris	(G,P)
4	Fragmented Medicagini-Avenetum pubescentis / Bromo inermis-Eryngietum campestris with <i>Cynodon dactylon</i>	(G,P)
5	Bromo inermis-Eryngietum campestris	(P)
6	Fragmented Medicagini-Avenetum pubescentis / Bromo inermis-Eryngietum campestris with <i>Oenothera erythrosepala</i> and <i>Sedum acre</i>	(G,P)
7	Bromo inermis-Eryngietum campestris / fragmented Medicagini-Avenetum pubescentis	(P, G)
8	Fragmented Medicagini-Avenetum pubescentis / Bromo inermis-Eryngietum campestris with <i>Euphorbia cyparissias</i> and <i>Medicago falcata</i>	(G,P)
9	Fragmented Arrhenatheretum elatioris	G
10	Fragmented Ranunculo-Alopecuretum geniculati with <i>Trifolium repens</i>	G
11	Fragmented Ranunculo-Alopecuretum geniculati	G
12	Chenopodietum rubri	P
13	FC of <i>Cirsium arvense</i> en <i>Polygonum amphibium</i> [Artemisietia vulgaris]	P
14	FC of <i>Urtica dioica</i> [Galio-Urticetea]	R
15	FC of <i>Rubus caesius</i> [Galio-Urticetea]	R
16	FC of <i>Calamagrostis epigejos</i> and <i>Epilobium hirsutum</i> [Galio-Urticetea]	R
17	FC <i>Sambucus nigra</i> [Galio-Urticetea]	R
18	Fragmented Ranunculo-Alopecuretum geniculati / FC of <i>Rubus caesius</i> [Phragmitetea]	(G,R,S)
19	FC of <i>Brassica nigra</i> [Phragmitetea] / Fragmented Ranunculo-Alopecuretum geniculati	(S,G)
20	Fragmentair Ranunculo-Alopecuretum geniculati	G
21	Ranunculo-Alopecuretum geniculati	G
22	FC of <i>Mentha aquatica</i> and <i>Lycopus europaeus</i> [Narsturtio-Glycerietalia]	S
23	Rorippo-Oenanthetum aquaticae	S

Airborne remote sensing data

The remote sensing data set used in this study is based on a previous study done by Geerling et al. (2007) in the same study area. It was shown that a fusion of CASI (spectral information) and LiDAR (structural information) improved numeric vegetation classification of a floodplain compared to using solely their single data sets (Geerling et al. 2007).

CASI is a visible/ near-infrared pushbroom imaging spectrometer ranging from 437 to 890 nm. The spectral bands measured and the bandwidths used are all programmable to meet the user's specifications and requirements. The spatial resolution of the geo-rectified images used was 2x2 m and they contained 10 bands

(Table 5.2). The geo-rectification accuracy resulted in a root mean square error of 2 m, i.e. about one pixel (Geerling et al. 2007). No multi-image analysis was performed, so atmospheric correction was not necessary. An ALTM 2033 scanner was used to collect the LiDAR data set. Flight altitude was about 800 m, the repetition rate of the laser pulse was 33 kHz, the scan frequency of the mirror was 30 Hz and the scan angle was 19°. Based on standard test surfaces covering 270 m² of the scanned area the approximate elevation precision was within 0.15 m and the planimetric precision was within 0.5 m (Anonymous 2003, Brügelmann 2003). The LiDAR data set consisted of almost 800,000 height measurements covering the entire study area with a point density of about 1.3 point per square metre. Height here refers to the feature hit by the laser pulse, which can be the soil surface but also vegetation elements. A digital elevation model was created from the surface hits and then subtracted from the LiDAR data to correct for elevation differences. Standard descriptive vegetation height parameters were generated: Maximum; Mean; Median; Minimum; Range and Standard deviation (Table 5.2).

Table 5.2 Wavelengths of the 10 CASI bands and the calculated LiDAR parameters which are added as extra bands (11 to 16). All these bands are used in the classification of the PCs.

CASI Bands	Waveband (nm)	Range
1	437-447	Blue
2	549-559	Green
3	615-625	Red
4	671-680	Red
5	681-689	Red
6	695-705	Red
7	729-739	NIR
8	757-767	NIR
9	860-867	NIR
10	880-890	NIR
LiDAR Bands	Value	Explanation
11	MAX	The maximum z value
12	MEAN	The mean z value
13	MEDIAN	The median z value
14	MIN	The minimum z value
15	RANGE	The range of z values (MAX - MIN)
16	STD	The standard deviation of the z values

The data sets of CASI and LiDAR were fused at pixel level. The main advantage of this approach is the rapid calculation and the simplicity of the procedure (Geerling et al. 2007). The fusion of the CASI and LiDAR data sets was procured by means of the rasterisation of the LiDAR image as described in Geerling et al. (2007). The vegetation differences between the field data collection period (August 2002) and the date of flight (CASI: 15 August 2001; LiDAR: 12 October 2001) can be considered negligible (Sykora 2002).

Classification of vegetation data

The raw vegetation data were clustered in 23 plant communities through TWINSpan (Figure 5.2, operation A). For the aggregation of the 23 plant communities (PC) into the final map classes several methods were tested. By means of multivariate statistics the similarity between PCs was evaluated so that PC's or clusters can be grouped based on the original classification information in a syntaxonomically meaningful way. The approach aims to relate the remotely sensed data to cluster and ordination methods in order to map the dominant vegetation classes, as outlined in Figure 5.2. Two grouping approaches were pursued: (1) cluster analysis and, (2) analysing trends from the DCA ordination plots. The aggregations with highest mapping accuracy were linked to known vegetation types following Schaminée et al. (1995-99) (Figure 5.2, operation B and C). The two approaches are described below.

Clustering: dendrogram based approach

Species signatures of corresponding PCs were sorted into vegetation classes following the logic of dendrogram relationships. With a dendrogram the clustering of PCs is purely based on their floristic similarity. For construction of the dendrogram we used the group average method with Sørensen Distance measure (weighed by the used 9 ordinal classes). First the data were simplified up to (TWINSpan-derived) PC level (Figure 5.2, operation B). Due to the contrasting divisive versus agglomerative nature of TWINSpan and dendrogram respectively, it appeared that some branches of the simplified dendrogram were shared by more than one PC and some PCs were scattered over several branches. PCs that were exclusively found within one branch were firstly grouped. The following groupings comprised of those PCs that were scattered across a group of branches. Once no more disparity occurred, higher up in the dendrogram tree, PC grouping was determined by the remaining dendrogram structure.

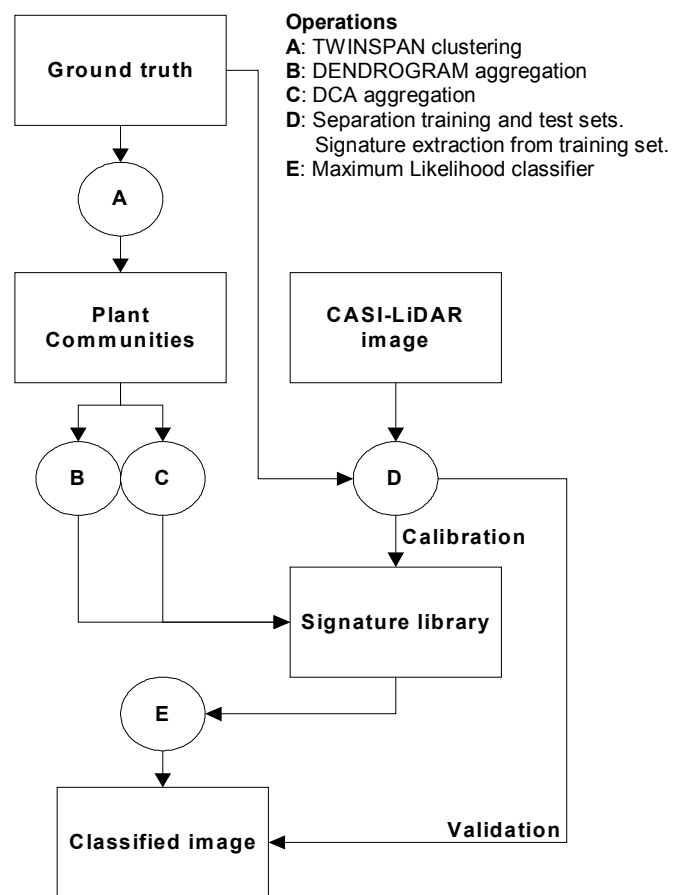


Figure 5.2 Flowchart of the used approach. Capital letters (A, B, ..) indicate operations.

Ordination: DCA-based aggregation

Solely referring to species abundance data and ignoring the influence of additional abiotic factors may lead to unrealistic maps. To overcome this discrepancy, the potential of recorded environmental data and ordination techniques was explored to achieve eco-botanic vegetation classes (syntaxonomical defined vegetation classes with respect to their environment). Additionally recorded environmental data may well include important variables that not only structure and determine the spatial distribution of the plant communities but these variables may also be associated with other ground cover elements (e.g. soil). Consequently, PCs that are linked to one or more of these ground cover-related variables may lead to superior mapping. A DCA was used to reveal gradients in species composition change. The relation between the main variation in the vegetation composition (axis 1 and 2) and environmental factors is expressed as arrows. These arrows point in the direction of maximum change of the given environmental factor. The length of the arrow is proportional to the degree of change in the direction indicated. Long arrows are correlated more strongly with the species data than shorter arrows. The arrow is a vector that shows to what extent the given environmental factor is correlated with the first and second axis. As DCA is an indirect ordination method i.e. the axes are constructed independently from the environmental variables and external variables are entered into the ordination after the extraction of the DCA axes. All ordinations were conducted in CANOCO (Ter Braak and Smilauer 1998). Based on the dendrogram and DCA outcomes were examined to gain insight in how to aggregate the 23 classes into a few major vegetation classes while preserving their eco-botanical value.

Classification of remote sensing data

Numeric vegetation classification is usually done at pixel level by performing a supervised classification. In case of the fused image, a signature of a specific PC consists not only of spectral properties but also of structural properties (Geerling et al. 2007). Ideally, each PC can be represented by a unique signature composed of spectral and height information. Mapping of grouped PCs rests then on the premise that merging of the PC-specific signatures will result in a unique generalised signature that sufficiently covers the range of spectral and structural features of all participating PCs. To achieve a plot-based mapping, randomly selected training plots were standardised into circles with radii of 3 m from where signatures were extracted. Per class signatures were merged and from the merged signatures a signature library was generated (Figure 5.2, operation D). This signature library provided the inputs to generate generalised signatures depending on the PC grouping. For each set of generalised signatures the fused image was subsequently mapped by means of the conventional Maximum Likelihood classifier (Richards 1999) (Figure 5.2, operation E). Finally, error matrices and kappa coefficients were calculated. Considering the classification accuracy, the most appropriate (i.e.,

minimum) sample size for a valid error assessment was calculated using (Rosenfield and Melley 1980, Fitzpatrick-Lins 1981, Rosenfield et al. 1982):

$$N = Z^2 \cdot p \cdot q / E^2 \tag{1}$$

where: N is total number of points to be sampled, Z is 2 (generalised from the standard normal deviate of 1.96 for the 95% two-sided confidence level), p is expected percent accuracy, q is $(100 - p)$ and E is the allowable error (standard deviation from the mean: 5%). An overall accuracy of about 75% was considered as acceptable which requires a minimum of 300 samples. Additional bush and forest plots were added bringing the total to 405 plots in 25 classes which were used for classification and as accuracy assessment points. Subsequently, 310 centre points (=76%) of the total field samples were left apart as testing points whereas 24% was used for training. When aggregating the 25 classes iteratively into fewer main classes, an increasing amount of training and testing data per class should in principle result in an improved distribution of training and testing data amongst classes.

5.4 Results

Image classification using dendrogram-based aggregation

In total 6 steps of the dendrogram-based grouping were carried out. The first two steps took place at a level of >80% similarity (Figure 5.3). Some plots of the TWINSPAN-based PCs were divided over one group of branches while other branches incorporated plots of more than one TWINSPAN-based PC. This spread

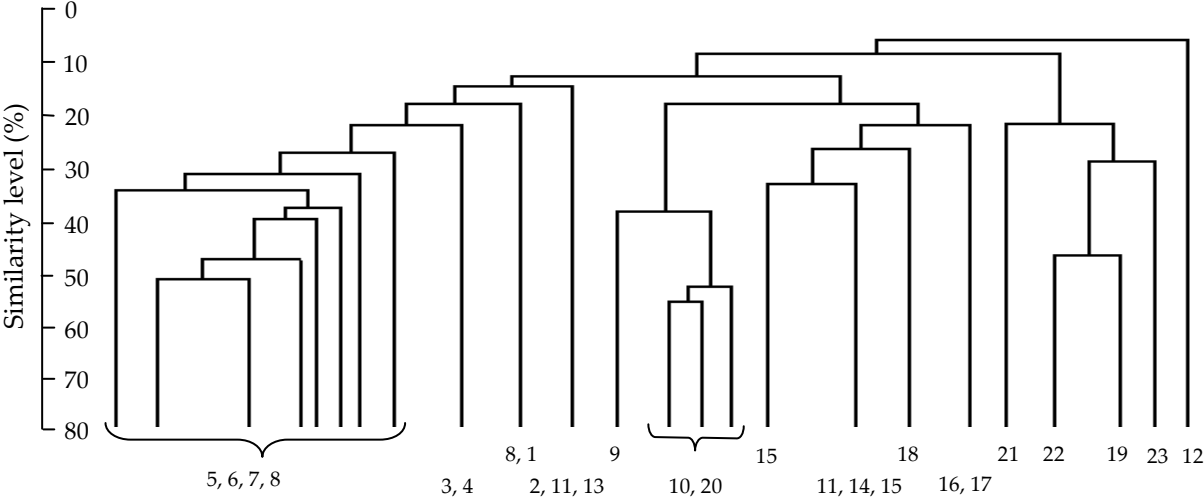


Figure 5.3 Simplified dendrogram (shown for the 23 PCs). The numbers refer to the plant communities (PCs). The initial dendrogram was calculated on the raw species-plot matrix. Data were then simplified up to PC level in TWINSPAN.

facilitated PC aggregation because it can reasonably be assumed that PCs mixed up in one branch, or a dense group of branches, are closely interrelated. Hence such mixed up PCs were first grouped. Signatures of the newly grouped vegetation classes were used to classify the RS data. The following steps consisted of grouping PCs along the dendrogram branches using a lower level of information resemblance. Overall classification accuracies were obtained from the generated maps when grouping more PCs (Table 5.3). The final 8-class grouping (6 groups of PCs plus a shrub and tree class) resulted in an overall accuracy of 68.4%.

Table 5.3 Steps of dendrogram grouping and their overall classification accuracies (%) and Kappa. Plant communities (PC) are indicated by their cluster number; PC descriptions and numbers are given in Table 5.1. The grey and white cell shades in every row indicate the grouping of plant communities (PC).

Group composition																							Overall Accuracy	Kappa		
1	3	4	5	6	7	8	2	13	9	10	20	11	14	15	16	17	18	12	19	22	21	23	S	T	45%	0.40
1	34	5	6	7	8	213	9	10	20	11	14	15	1617	18	12	19	22	21	23	S	T	38%	0.33			
1	34	5678	213	9	10	20	11	14	15	1617	18	12	19	22	21	23	S	T	55%	0.46						
1	34	5678	213	91020	11	14	15	1617	18	12	1922	21	23	S	T	58%	0.49									
1	34	5678	213	91020	11	14	15	1617	18	12	1921	22	23	S	T	61%	0.53									
1	34	5678	213	91020	111415	161718	12	19212223	S	T	61%	0.53														
	1345678	213	91020	111415161718	12	19212223	S	T	68%	0.60																

Image classification using DCA-based aggregation

The DCA-ordination diagram (Figure 5.4a) shows that the spread of plant communities was particularly stretched along the x-axis with the exception of the true pioneer communities 12 and 13, which are located on the river sandbanks. Some PC points tended to be clumped, indicating that those PC points were equally influenced by environmental gradients. Explanatory variables of the first axis (x-axis) are: moisture and elevation (negatively correlated) and to a lesser extent organic matter and soil type. The R² values of the abiotic variables are shown in Table 5.4. The arrows in Figure 5.4b graphically

Table 5.4 Coefficient of determination (R²) of abiotic variables of the DCA, indicating the explanatory variables of the 2 axes. The columns 1st axis and 2nd axis represent the 2D view of the DCA-CCA shown in figures 4a and 4b. The first axis represents the main variation in the vegetation composition and the second axis the second main variation.

Abiotic variable	1 st axis	2 nd axis
Moisture	97.4	0.4
Elevation	91.6	0.7
Organic matter	67.0	9.0
Soil type	58.5	26.1
Light	46.9	10.3
Nitrogen	28.5	15.3
Structure 0.60-1.0 m	30.6	10.6
Structure 0 m	0.8	61.3
Mowing	16.3	11.0
pH	7.6	9.9
Structure 0.15-0.30 m	2.3	9.8
Structure 0.30-0.60 m	7.4	5.2
Structure >1.0 m	0.3	1.3
Structure 0-0.15 m	15.2	0.6

display the interrelationships.

Neighbouring PC points consist of plots (relevés) with a high similarity in species composition. As the similarity reflects a similar relation to environmental factors our grouping although based on species composition inherently also expresses environmental conditions (Figure 5.4a). For instance, the pioneer communities 12 and 13 located in the lower part of the DCA diagram at some distance of the other PC plots were grouped. Their location at the end of the structure 0 m arrow indicates that they are strongly related to bare soil (Figure 5.4b). Located on the riverbank, these two pioneer PCs are characterised by spots of bare soil.

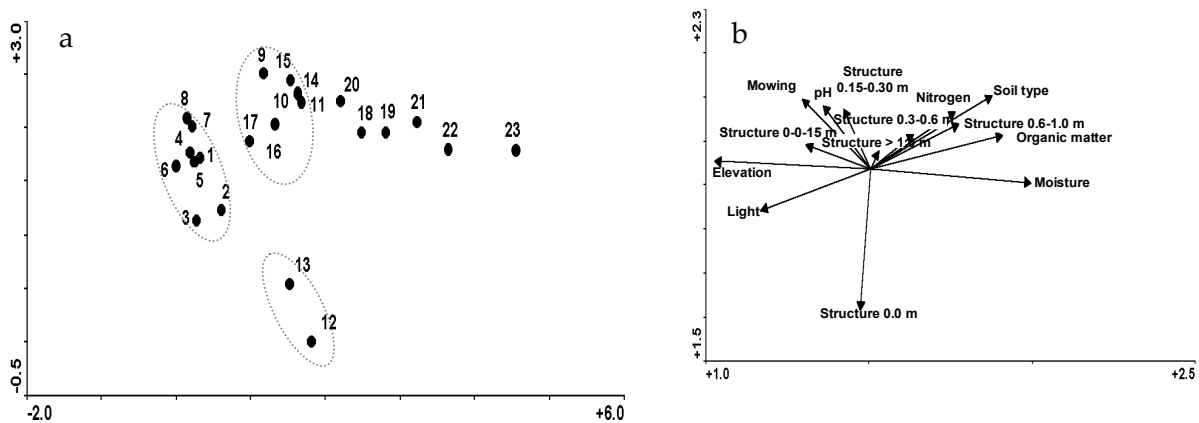


Figure 5.4 DCA ordination diagram of the 23 plant communities (a), and the ordination diagram of the environmental variables based on the DCA (b). The coefficients of determination of the external variables are given in table 4.

The DCA-ordination of Figure 5.4b shows that the main variation in the species composition of the PCs (axis 1) is negatively related to ‘elevation’ (R^2 : 91.6) and ‘light’ (R^2 : 46.9), and positively to ‘organic matter’ (R^2 : 67.0) and ‘moisture’ (R^2 : 97.4). Canopy and PC structure, shadow interactions and soil type typically control the optical scattering behaviour and thus optical reflectance values, while the additional LiDAR bands are influenced by PC structure. Therefore, in turn, accurate mapping results are expected when PC grouping is organised along these gradients. Amongst the most notable group of PCs was the extremely left cloud of PCs (1 to 8), consisting of grassland and pioneer vegetation. In the middle of the x-axis a second cloud of PC points could be discerned: 9, 10, 11, 14, 15, 16 and 17. These PCs are influenced by a set of environmental vectors (e.g. pH, nitrogen, mowing) and are members of grassland and ruderal vegetation. The leftovers (PCs 18-23), mainly members of reed vegetation (*Phragmitetea*), were generally positioned along gradients of organic matter and moisture content. For those remaining PC points no clumping could be observed, pertaining 11 vegetation classes (9 PC groups plus shrubs and forest). Overall accuracy of the 11-class based classified fused image was 71% (Table 5.5, Kappa coefficient=0.61).

Optimised image classification using 'combined' dendrogram-DCA-based aggregation

Further grouping of the PC 18 to 23 was not possible on DCA data only (Figure 5.5a). In the dendrogram PCs 18 and 20 are both more distinct from PCs 19, 21, 22 and 23 (Figure 5.5b). Thus, PC 18 was grouped with PC 20 and PC 19 was grouped with PCs 21 and 22. Because plant community 23 (swamp vegetation: *Rorippo-Oenanthetum aquatica*) is found at the extreme end of the moisture gradient (Figure 5.4b), it was left as an independent class. In total, by keeping PC 23 isolated eight vegetation classes were discriminated: 6 grouped plant communities and a shrub and tree class. The accuracy of the classified image with eight classes did not really improve as compared to the 11-class, but the detection of the reed class 19-21-22 improved. Overall accuracy was calculated as 71% (Table 5.5, Kappa coefficient=0.62).

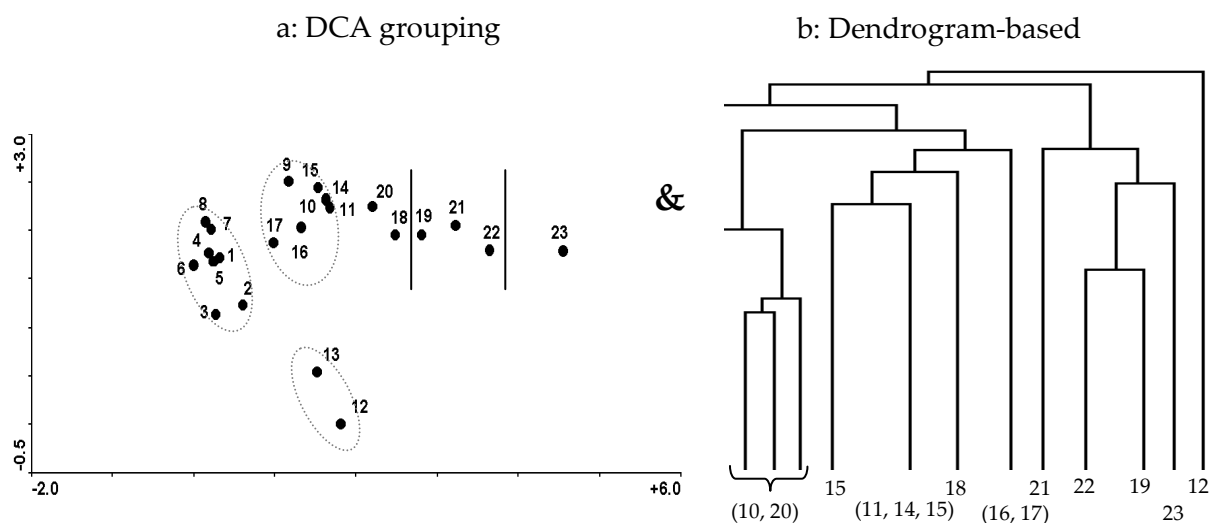


Figure 5.5 The first two axes of a DCA ordination diagram of the 23 vegetation communities (a), and the righter part of the simplified dendrogram of figure 1 (b). PCs 1 to 17 and 23 are grouped into three separate groups based on ordination space partitioning in the DCA output, for PCs 18 to 22 the dendrogram logic was used.

A final 6-class grouping followed further the logic of the dendrogram (Figure 5.5b). PCs 18 and 20 were joined with the group of PCs 9, 10, 11, 14, 15, 16 and 17, and PC 23 was grouped with the PCs 19, 21 and 22. The resulting classes of the final aggregation were: (i) a grassland vegetation of sandy levees (PCs 1-8), clearly influenced by elevation and light; (ii) a nitrophilous pioneer community on riverbanks (PCs 12, 13); (iii) nitrophilous short grazed inundation grasslands and tall-herb communities influenced by grazing intensity (PCs 9-11, 14-18, 20); (iv) reed vegetation and temporarily inundated fertile pastures (PCs 19, 21-23), particularly influenced by moisture and organic matter; (v) a shrub and (vi) a tree class. Maximum likelihood classification of the final set of classes resulted in an overall accuracy of 74% (Table 5.5, 6, overall Kappa coefficient=0.66). All classes have been

reasonably mapped; with class Kappa values ranging from 0.26 to 0.97. The final classification result is shown in Figure 5.6, the plant communities are syntaxonomically described in Table 5.6.

Table 5.5 Steps of DCA-dendrogram grouping, overall classification accuracies (%) and Kappa. Plant communities (PCs) are indicated by their cluster number; PC descriptions and numbers are given in Table 5.1. The grey and white cell shades in every row indicate the grouping of plant communities (PC).

Group composition														Overall Accuracy	Kappa											
1	2	3	4	5	6	7	8	12	13	9	10	11	14	15	16	17	18	19	20	21	22	23	S	T	71%	0.61
1	2	3	4	5	6	7	8	12	13	9	10	11	14	15	16	17	18	20	19	21	22	23	S	T	71%	0.62
1	2	3	4	5	6	7	8	12	13	9	10	11	14	15	16	17	18	20	19	21	22	23	S	T	74%	0.66

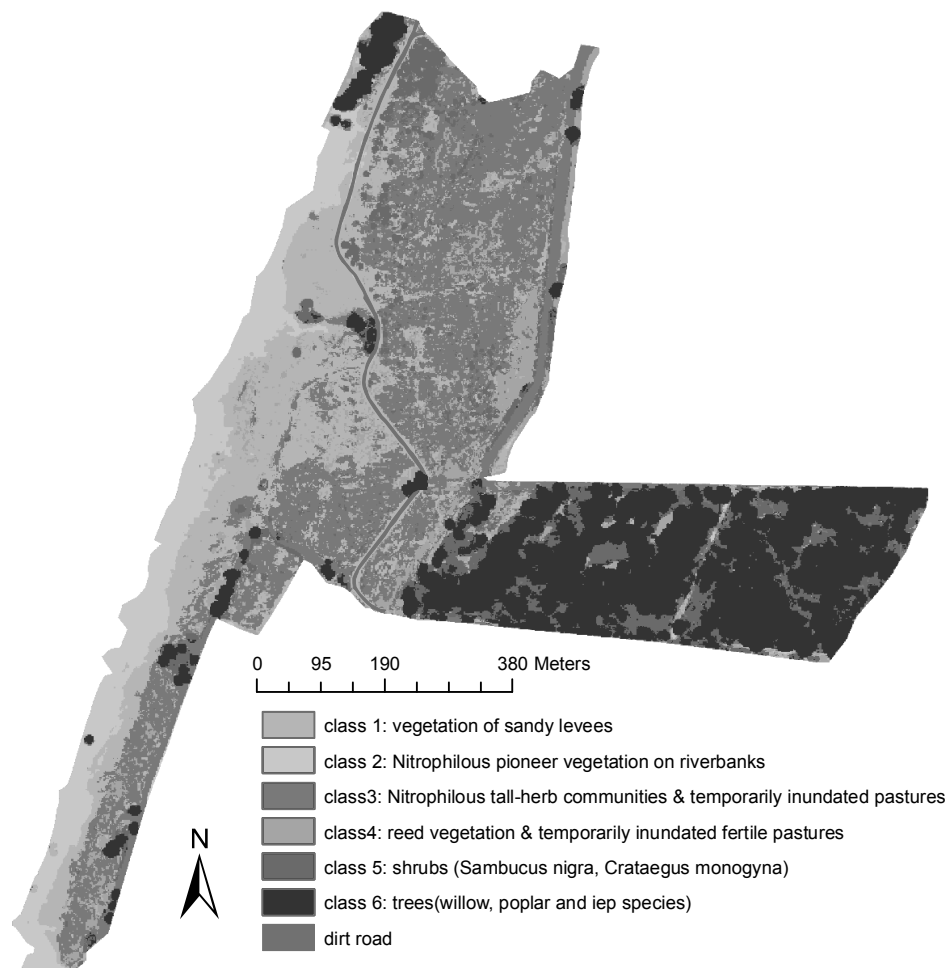


Figure 5.6 (In full colour on page 189) Classified image with 6 vegetation classes according to DCA-Dendro grouping. The added dirt road was taken from topographic data.

Table 5.6 Ecological description of the final 6 classes.

Class	Ecological description
1	This group consists of a vegetation transitional between the <i>Medicagini-Avenetum pubescentis</i> and the <i>Bromo inermis-Eryngietum campestris</i> . Only PC 5 can be considered to be a pure <i>Bromo inermis-Eryngietum campestris</i> . The <i>Medicagini-Avenetum pubescentis</i> has a high nature conservation value and is characteristic of high river banks and sandy dyke slopes. It grows on sunny, dry, unfertilised or lightly fertilised, variably calcareous, somewhat humic sand and light silt loam. It is either grazed or cut for hay. Base content is maintained by river water or blown-in sand. The <i>Bromo inermis-Eryngietum</i> has a more open pioneer character and occurs under the same conditions around the high water mark on levees and if the soil is more disturbed or if there is considerable sand deposition.
2	This group consists of two different PCs, one belonging to the <i>Chenopodietum rubri</i> and one to the <i>Artemisietea</i> . The <i>Chenopodietum rubri</i> grows in a pioneer environment that arises from sedimentation, grazing, or excavation. In summer the base-rich soil dries out. The <i>Artemisietea</i> community is dominated by <i>Cirsium arvense</i> and grows on a thick layer of organic matter deposited as flood mark.
3	From a syntaxonomic and ecological point of view this group is heterogeneous as it comprises two different groups of PCs. Mainly two distinct vegetation types are combined in class 3, i.e. short intensively grazed nutrient rich grasslands of the <i>Ranunculo-Alopecuretum geniculati</i> and tall nitrophilous communities of the <i>Galio-Urticetea</i> (roughage). The ecological difference is almost exclusively a difference in succession stage and structure due to differences in grazing intensity. The <i>Ranunculo-Alopecuretum</i> occurs on hydromorphic, basic, nitrogen-rich soils, varying from sand to heavy clay, that are submerged for a long time outside the growing season. It is grazed, mostly by cows or horses; in winter also grazed by geese and swans.
4	This group consists of a mixture of short intensively grazed nutrient rich grasslands of the <i>Ranunculo-Alopecuretum geniculati</i> and reed vegetation of the <i>Phragmitetea</i> . Again two different structural types are combined, the short grazed <i>Ranunculo-Alopecuretum geniculati</i> and the tall reed vegetation. In comparison to class 3 the PCs of class 4 probably have a longer inundation period in common. The <i>Narsturtio-Glycerietalia (Phragmitetea)</i> grows in shallow flowing or vertically moving water that may dry up in summer. It is optimal on banks of eutrophic lowland streams, in little-disturbed nutrient-rich seepage ditches, old river channels & along regularly cleaned drainage canals. The <i>Rorippo-Oenantheum aquaticae</i> occurs in shallow, nutrient-rich, greatly fluctuating water, where the substrate is temporarily exposed, i.e. in abandoned meanders, clay pits and eutrophying ditches that are frequently dredged.
5	This group consists of scrub vegetation mainly consisting of the nitrophylous European elder (<i>Sambucus nigra</i>) and to a lesser extent also of hawthorn (<i>Crataegus monogyna</i>) which is strongly increasing recently.
6	This group comprises the forest adjacent to the floodplain flats which belongs to the <i>Salicion albae</i> , characterised by willow species like <i>Salix alba</i> , <i>S. fragilis</i> , <i>S. viminalis</i> , <i>S. triandra</i> . The <i>Salicion albae</i> is characteristic of long inundated riverine environments with strongly fluctuating water levels and a mineral soil. <i>Populus nigra</i> and <i>P. x Canadensis</i> are also found in the area. Single trees on the floodplain are willow and poplar.

5.5 Discussion

We evaluated vegetation sampling, classification and description according to the Braun-Blanquet method and by means of TWINSpan and dendrogram clustering for their potential to be incorporated in a remote sensing mapping scheme. Use of dendrogram-based grouping as input into remote sensing schemes rests on the assumption that similar plant communities encompass similar spectral and height properties. DCA-based grouping (ordination space partitioning) rests on the premise that, as species composition is strongly related to environmental conditions, plant communities located adjacently along an environmental gradient show similar spectral and height properties. Ordination and cluster analysis may be seen as complementary, when applied together they offer useful information about the relationships among species and their distribution across sites. Geerling et al. (2007) obtained a classification accuracy of 63.5% dividing the same data set as used in this study in 8 classes solely based on structural properties. This study showed that when relying on dendrogram-based groupings the accuracy of an 8-class set improved with 4.9% (to 68.4%). Moreover, when relying on combined species resemblance and abiotic variables through DCA-dendrogram grouping, the 8-class set improved with 6.5% (to 71.0%). Figure 5.7 shows that the improved accuracy of the DCA-dendrogram was not a coincidence. This figure shows that the combined DCA-dendrogram method exhibits a superior trend in comparison to the dendrogram method alone. These findings are consistent with literature where higher classification accuracies were achieved when combining ecological information obtained from a suite of analysis techniques (e.g. Lewis 1998, Nilsen et al. 1999, Thomas et al. 2003, Schmidtlein and Sassini 2004).

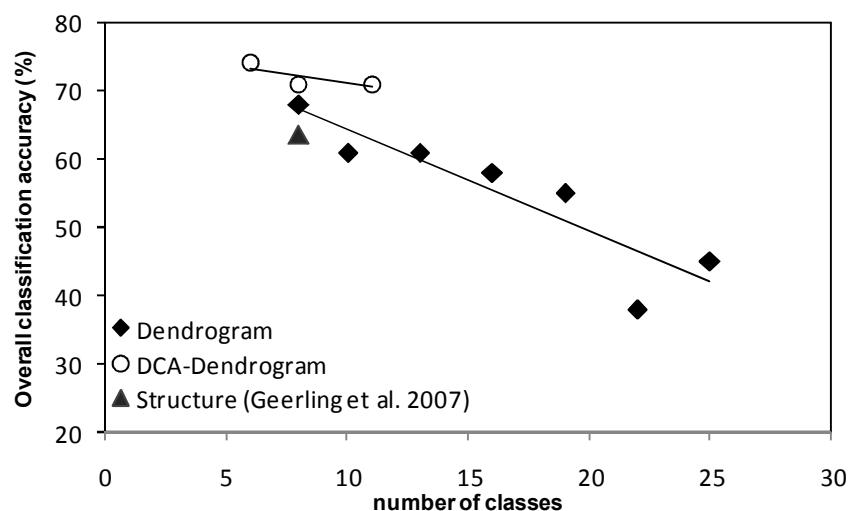


Figure 5.7 Overall accuracies of the Structure Approach (Geerling et al. 2007), Dendrogram approach and DCA-dendrogram approach.

Environmental factors

Results from the DCA demonstrated that the predominant underlying environmental gradients were (1) elevation, (2) moisture and (3) organic matter content, whereby the latter two are negatively correlated to elevation. Apart from the Millingerwaard floodplain, also other floodplain vegetation studies showed that elevation (Schickhoff et al. 2002, Fernández-Aláez et al. 2005) or hydraulic gradients (Sykora 1984a, 1984b, Grevilliot et al. 1998, Sykora et al. 1988, Grevilliot and Muller 2002) shape floodplain plant assemblages. Although the plant assemblages follow environmental gradients, it proves not to be sufficient to match RS data solely to plant assemblages as basis for land cover classes. Using both environmental data and botanical data to aggregate land cover classes from PCs improved the classification accuracy compared to classes based on botanical data only. As the spectral RS data contain reflectance values of the earth surface, it records not only the vegetation, but it is also influenced by soil properties. Especially moisture is a well known factor influencing reflectance (Lillesand and Kiefer 2000) that negatively correlates with elevation in the floodplain plant communities. Based on the DCA, most of the grouping occurred along the main variation in species composition (the first axis), strongly related to the moisture-elevation gradient. Nevertheless, from a syntaxonomical point of view, some grouped plant communities were not homogeneous. They still differed in structure and species composition. For instance, class 3 consisted of 2 distinct vegetation types, i.e. *short intensively grazed* nutrient rich grasslands (PC 9-11,20) and *tall not or hardly grazed* nitrophilous ruderal vegetation (PC 14-17). From the 2D ordination diagram these vegetation types were not noticeably distinguishable along the moisture-elevation gradient. This does not mean that they are not distinguishable at all. The ordination diagram is merely a multidimensional space where discrimination can occur along other dimensions, e.g. axis 3, expressing less important variation in species composition. This axis might be related to other variables like differences in vegetation structure due to differences in grazing intensity, as is the case in this data set. To achieve a more detailed mapping, a 2D ordination-based grouping might be insufficient. In the multi-dimensional space other environmental gradients might gain importance and it might be necessary to consider more ordination axes in the PC grouping analysis. However, the question arises whether such environmental gradients are having sufficient influence on the spectral or altimetry domain to be detected with the current remote sensing techniques. For instance, Geerling et al. 2007 showed that subtle variations in vegetation structure cannot be detected by this altimetry data set, limiting detection of PCs grouped using the structure dimensions.

Another important factor is the vegetation cover of a plot (in this study depicted as 'structure 0 m'); this is the vector driving the grouping of PC 12 and 13 in the DCA aggregation. In case plant species cover an insignificant fraction of the total area (e.g., the pioneer communities 12 and 13), the additional value of species composition

information for remote sensing is small. Especially in harsh or dynamic environments like riparian areas, sand dunes or coastal land and water interfaces the degree of vegetation cover in relation to the exposure of the soil can be the predominant factor for distinguishing classes as also proved by Thomson et al. (2004) for salt marshes.

Botanic data

Multivariate techniques such as clustering and ordination are widely used methods designed to classify vegetation data. We evaluated whether these techniques can be adopted into a remote sensing scheme for improved vegetation mapping. In order to implement multivariate techniques in an operational way for RS classification purposes the current study revealed that there is room for improvement on the following points:

As a result of the random sampling scheme and since plant communities are not always immediately visible in the field - they might reveal only after phytosociology analysis - ground truth plots per PC were not equally distributed and, thus, might be undersampled. This skewed distribution tends to introduce biases into the error matrix, which results in over- or underestimations of accuracy. Revisiting the site after establishing the initial PCs to equalise the sampling distribution is necessary.

A dissimilar species composition does not necessarily lead to dissimilar spectral or structural properties of the signature of the vegetation. For instance, PC differentiation through phytosociology analysis often occurs through the appearance of less abundant indicator species with small coverage or species below a dominant canopy. These species remain undetectable by remote sensing instruments. Likewise, in botanic methods no information is included about the physiology and phenology of a plant species; factors which significantly influence the spectral response. A first step to resolve the latter problems would be to extract additional information from the field plots (when gathered using the Braun-Blanquet or similar methods) on the fractional cover of the dominant species. Typically this would be the species that is responsible for the greatest contribution to the reflectance signal. A second step would be to include key environmental variables in the botanical survey so these can be incorporated in the classification scheme. An appealing, more advanced, alternative would be to incorporate field spectroradiometric measurements. Use of field spectroscopy possesses capabilities to bridge the gap from the botany domain towards the spectral domain. Although this way of joint data collection is by botanists still in an embryonic stage, good mapping results were achieved when collecting floristic data parallel to field spectroradiometric data (e.g. Schmid et al. 2005, Rosso et al. 2005, Schaepman et al. 2007).

5.6 Conclusions

In natural vegetation borders between vegetation units are not always sharp, a condition required for mapping. We demonstrated that it is possible to organise the natural vegetation of a floodplain into a few major discrete classes while keeping syntaxonomical and ecological significance. Yet, given the way conventional methods in vegetation science are currently applied, care is required when implementing these methods in remote sensing techniques for vegetation mapping. If lessons could be learned for floodplain mapping, we suggest that plant community mapping by remote sensing can be considerably improved when fulfilling the following conditions: (1) to combine elevation and moisture variables with botanical data collection and define the vegetation classes along the elevation-moisture gradient as this gradient tend to be captured through remote sensing techniques; and (2) to adopt a combination of clustering and ordination techniques when aggregating botanical data higher up in the hierarchy of the Braun-Blanquet system. We showed from ordination on the collected floristic data that elevation was a major driver shaping the floristic variability. Given that plant communities embody next to spectral properties also elevation-specific properties, it becomes beyond question that LiDAR measurements owe a great potential in floodplain mapping. This suggests that fused imagery of a spectral and altimetry source capitalises the full potential for floodplain vegetation monitoring.

Acknowledgements

The authors want to thank Isabel van Geloof and Iris de Ronde within their Msc-thesis work collected and analysed the ecological data under supervision of the third author.

References

- Anonymous (2003). *Digitaal Topgrafisch Bestand – Nat.* Ministry of Transport, Public Works and Water Management. Directorate-General of Public Works and Water Management. Survey Department (AGI), Delft.
- Austin MP, Smith TM (1989). A new model for the continuum concept. *Vegetatio* **83**: 35-47.
- Barkman JJ (1990). Controversies and perspectives in plant ecology and vegetation science. *Phytocoenologia* **18**: 565-589.
- Brügelmann R (2003). *Quality test of the LiDAR data set.* Internal document. Personal Communication. Ministry of Transport, Public Works and Water Management. Directorate-General of Public Works and Water Management. Survey Department (AGI), Delft.

- Cobby DM, Mason DC, Davenport IJ (2001). Image processing of airborne scanning laser altimetry data for improved river flood modelling. *ISPRS Journal of Photogrammetry and Remote Sensing* **56**: 121-138.
- Fernández-Aláez C, Fernández-Aláez M, Garcia-Criado F (2005). Spatial distribution pattern of the riparian vegetation in a basin in the NW Spain. *Plant Ecology* **179**: 31-42.
- Fisher PF (1999). Models of uncertainty in spatial data. In: Longley PA, Goodchild MF, Maguire DJ, Rhind DW (Eds). *Geographical Information Systems, Vol. 1*. John Wiley and Sons, New York.
- Fortin MJ, Olson RJ, Ferson S, Iverson L, Hunsaker C, Edwards G, Levine D, Butera K, Klemas V (2000). Issues related to the detection of boundaries. *Journal of Ecology* **69**: 135-152.
- Fitspatrick-Lins K (1981). Comparison of sampling procedures and data analysis for a land-use and landcover map. *Photogrammetric Engineering and Remote Sensing* **47**: 343–351.
- Gauch HG (1982). *Multivariate analysis in community ecology*. Cambridge University Press, Cambridge.
- Gauch HG, Whittaker RH (1981). Hierarchical classification of community data. *Journal of Ecology* **69**: 135-152.
- Geerling GW, Labrador-Garcia M, Clevers JGPW, Ragas AMJ, Smits AJM (2007). Classification of floodplain vegetation by data-fusion of Spectral (CASI) and LiDAR data. *International Journal of Remote Sensing* **28**: 4263- 4284.
- Gillespie TW, Brock J, Wright CW (2004). Prospects for quantifying structure, floristic composition and species richness of tropical forests. *International Journal of Remote Sensing* **25**: 707-715.
- Glavac V, Grillenberger C, Hakes W, Ziezold H (1992). On the nature of vegetation boundaries, undisturbed flood plain forest communities as an example — a contribution to the continuum/discontinuum controversy. *Vegetatio* **101**: 123-144.
- Grevilliot F, Muller S (2002). Grassland ecotopes of the upper Meuse as references for habitats and biodiversity restoration: A synthesis. *Landscape Ecology* **17**: 19-33.
- Grevilliot F, Broyer J, Muller S (1998). Phytogeographical and phenological comparison of the Meuse and the Saone valley meadows (France). *Journal of Biogeography* **25**: 339-360.
- Hill MO (1979). *TWINSPAN - A FORTRAN program for arranging multivariate data in an ordered two-way table by classification of individuals and attributes*. Cornell University, Ithaca, N.Y.
- Hill MO, Gauch HG (1980). Detrended correspondence analysis: an improved ordination technique. *Vegetatio* **42**: 47–58.
- Hill RA, Thomson AG (2005). Mapping woodland species composition and structure using airborne spectral and LiDAR data. *International Journal of Remote Sensing* **26**: 3763-3779.

- Jongman RHG, Ter Braak CJF, Van Tongeren OFR (1995). *Data analysis in community and landscape ecology*. Cambridge University Press, Cambridge.
- Lawrence RL, Wood SD, Sheley RL (2006). Mapping invasive plants using hyperspectral imagery and Breiman Cutler classifications (randomForest). *Remote Sensing of Environment* **100**: 356-362.
- Lillesand T, Kiefer R (2000). *Remote sensing and image interpretation*. John Wiley and sons, Inc., New York.
- Lewis MM (1998). Numeric classification as an aid to spectral mapping of vegetation communities. *Plant Ecology* **136**: 133-149.
- Malthus TJ, George DG (1997). Airborne remote sensing of macrophytes in Cefni Reservoir, Anglesey, UK. *Aquatic Botany* **58**: 317-332.
- Mason DC, Cobby DM, Horritt MS, BATES PD (2003). Floodplain friction parameterization in two-dimensional river flood models using vegetation heights derived from airborne scanning laser altimetry. *Hydrological Processes* **17**: 1711-1732.
- McCune B, Mefford MJ (1999) *Multivariate Analysis of Ecological Data, Version 4*. MjM Software Design, Gleneden Beach, Oregon.
- McGarigal K, Cushman S, Stafford S (2000). *Multivariate statistics for wildlife and ecology research*. Springer, New York.
- Nilsen L, Elvebakk A, Brossard T, Joly D (1999). Mapping and analysing arctic vegetation: Evaluating a method coupling numerical classification of vegetation data with SPOT satellite data in a probability model. *International Journal of Remote Sensing* **20**: 2947-2977.
- Richards JA (1999). *Remote sensing digital image analysis*. Springer, Berlin.
- Rosenfield GH, Melley ML (1980). Applications of statistics to thematic mapping. *Photogrammetric Engineering and Remote Sensing* **46**: 1287-1294.
- Rosenfield GH, Fitzpatrick-Lins K, Ling HS (1982). Sampling for thematic map accuracy testing. *Photogrammetric Engineering and Remote Sensing* **48**: 131-137.
- Rosso PH, Ustin SL, Hastings A (2005). Mapping marshland vegetation of San Francisco Bay, California, using hyperspectral data. *International Journal of Remote Sensing* **26**: 5169-5191.
- Schaepman ME, Wamelink GWW, Van Dobben HF, Gloor M, Schaepman-Strub G, Kooistra L, Clevers JGPW, Schmidt A, Berendse F (2007). River floodplain vegetation scenario development using imaging spectroscopy derived products as input variables in a dynamic vegetation model. *Photogrammetric Engineering and Remote Sensing*. **73**: 1179-1188.
- Schaminée JHJ, Hommel PWF, Stortelder AHF et al. 1995-1999. *The vegetation of the Netherlands Vol. 1-5 (in Dutch)*. Opulus Press, Uppsala and Leiden.
- Schickhoff U, Walker MD, Walker DA (2002). Riparian willow communities on the Arctic Slope of Alaska and their environmental relationships: A classification and ordination analysis. *Phytocoenologia* **32**: 145-204.

- Schmid T, Koch M, Gumuzzio J (2005). Multisensor approach to determine changes of wetland characteristics in semiarid environments (Central Spain). *IEEE Transactions on Geoscience and Remote Sensing* **43**: 2516-2525.
- Schmidt KS, Skidmore AK (2003). Spectral discrimination of vegetation types in a coastal wetland. *Remote Sensing of Environment* **85**: 92-108.
- Schmidtlein S, Sassan J (2004). Mapping of continuous floristic gradients in grasslands using hyperspectral imagery. *Remote Sensing of Environment* **92**: 126-138.
- Scott JT (1974). Correlation of vegetation with environment: A test of the continuum and community-type hypotheses. In: B. R. and Billings, W. D (Eds.) *Vegetation and Environment. Handbook of Vegetation Science Strain*. Junk, The Hague. pp. 89-109.
- Straatsma MW, Middelkoop H (2006). Airborne laser scanning as a tool for lowland floodplain vegetation monitoring. *Hydrobiologia* **565**: 87-103.
- Sýkora KV (1984a). A synecological study of the Lolio-Potentillion anserinae Tx. 1947 by means of permanent transects. I: Brackish stenosalutic habitats. *Proceedings of the Koninklijke Nederlandse Akademie van Wetenschappen. Series C, Biological and Medical Sciences* **86**: 525-566.
- Sýkora KV (1984b). A synecological study of the Lolio-Potentillion anserinae Tuexen 1947 by means of permanent transects. II: Riverine eurysalutic habitats. *Proceedings of the Koninklijke Nederlandse Akademie van Wetenschappen. Series C, Biological and Medical Sciences* **87**: 181-230.
- Sýkora KV, Scheper E, Van Der Zee F (1988). Inundation and the distribution of plant communities on Dutch river dykes. *Acta Botanica Neerlandica* **37**: 279-290.
- Sýkora KV (2002). Nature development in the Millingerwaard. In: Grootjans A, van Diggelin R (Eds.) *Selected Restoration Objects in The Netherlands and NW Germany: A Field Guide*. 2nd ed., University of Groningen, Groningen.
- Ter Braak CJF, Smilauer P (1998). *CANOCO reference manual and user's guide to Canoco for windows: software for canonical community ordination (version 4)*. Microcomputer Power, Ithaca, N.Y.
- Thomas V, Treitz P, Jelinski D, Miller J, Lafleur P, McCaughey JH (2003). Image classification of a northern peatland complex using spectral and plant community data. *Remote Sensing of Environment* **84**: 83-99.
- Thomson AG, Huikes A, Cox R, Wadsworth RA, Boorman LA (2004). Short-term vegetation succession and erosion identified by airborne remote sensing of Westerschelde salt marshes, The Netherlands. *International Journal of Remote Sensing* **25**: 4151-4176.
- Treits P, Howarth P (2000). High spatial resolution remote sensing data for forest ecosystem classification: An examination of spatial scale. *Remote Sensing of Environment* **72**: 268-289.

- Van Geloof I, De Ronde I (2002). *The vegetation of the Millingerwaard after 10 years of "nature development" (in Dutch)*. Msc-thesis, Wageningen University, Wageningen.
- Westhoff V, Van Der Maarel E (1978). The Braun-Blanquet approach. In: Whittaker RH (Ed.) *Classification of plant communities*. Junk, Boston.
- Whittaker RH (1973) *Ordination and classification of plant communities*. Junk, The Hague.
- Winterbottom SJ, Gilvear DJ (1997). Quantification of channel bed morphology in gravel-bed rivers using airborne multispectral imagery and aerial photography. *Regulated Rivers: Research and Management* **13**: 489-499.

6 Mapping river floodplain ecotopes by segmentation of spectral (CASI) and structural (LiDAR) remote sensing data

G.W. Geerling, M.J. Vreeken-Buijs, P. Jesse, A.M.J. Ragas, A.J.M. Smits.

River Research and Applications, accepted with revisions.

6.1 Abstract

Floodplain land cover maps are important tools for river management and ecological assessment. These maps have to be revised regularly due to the dynamic nature of floodplains. Automation of the mapping process cuts the map processing time and can increase overall accuracy. Manual delineation and classification of vegetation is based on colour, contrasts (texture) and often stereoscopic view of aerial images. In this study, this is mimicked by the simultaneous use of both structural (LiDAR) and spectral (CASI) remote sensing data in an image segmentation routine (FNEA). The segmentation results are tested against manually delineated ecotopes. Ecotope delineation improves when LiDAR and CASI are used simultaneously; the combination significantly lowers the number of segmented objects needed to accurately map ecotopes. Overall map accuracy of the LiDAR and CASI combination is 8 to 19 percent higher than single CASI and LiDAR respectively.

6.2 Introduction

Spatial information on floodplains plays an important role in river management. Information on the vegetation and land cover of floodplains is of vital importance to the river manager because the maximum discharge capacity depends on it through its hydraulic resistance (Straatsma 2006, Geerling et al. 2008). Furthermore, this type of information also provides relevant insights for nature management, i.e. about landscape diversity and dynamics. The floodplain maps used by most river authorities are produced by means of manual digitisation of aerial photographs and stored in a Geographic Information System (GIS). However, manual digitisation is a time-consuming and costly approach. Automation increases the speed of the mapping process, reduces the amount of untraceable human errors, and the information content of the river maps can be enhanced by applying state of the art remote sensing data sources (Mertes 2002, Pietroniro and Leconte 2005). An example is the use of laser altimetry in floodplain management data providing information on elevation and vegetation structure (Portman 1997, Mason et al. 2003, Pietroniro and Leconte 2005, Geerling et al. 2007, Straatsma and Middelkoop 2007). Automated techniques to classify remotely sensed data into vegetation and land cover maps can be roughly divided into pixel and segmentation oriented approaches. They mainly differ in the moment of classification: either per pixel or per group of pixels (Blaschke et al. 2004). Pixel oriented methods generate accurate maps but they may suffer from the “salt and pepper effect”, i.e. individual pixels that are classified differently from surrounding pixels, resulting in areas of mixed composition. This result is not compatible with traditional polygon maps where larger spatial units are generally classified into one specific land cover class, ignoring potential variations within the spatial unit. The only way to smooth the image is to use filters, which however work without considering the original information. Segmentation oriented

approaches do not suffer from this “salt and pepper effect” and do not need filter operations (Blaschke et al. 2000). Homogeneous regions (or image objects) are built up first using contextual information found in the image and then these homogeneous regions are classified into land cover classes based on the object’s properties. This process is more similar to the identification of homogeneous units by a human interpreter. Several segmentation algorithms have been developed over recent years, all with their own strong and weak points. The reader is referred to Baatz & Schäpe (2000) and Blaschke et al. (2004) for an overview; the studies of Van der Sande et al. (2003) and Straatsma (2006) are examples of the application of image segmentation in floodplains.

Different types of remote sensing data can be used as input for the development of vegetation and land cover maps based on segmentation. Two common data sources are imaging spectroscopy (IS) and light detection and ranging (LiDAR) sensor technology. With IS, spectral information (reflected sunlight) in the visible and shortwave infrared (IR) range is collected. Distinction between vegetation and land cover classes based on IS images generally works well, but it can be difficult to distinguish between the classes bush and forest. LiDAR images provide information on the height of objects. Studies to map riparian vegetation using LiDAR showed that discrimination of some vegetation types was possible based on vegetation height and density. The vegetation types that were similar in structure (e.g. bare soil and short grassland) were difficult to separate, but discrimination between bushes and trees was high (Asselman 2001, Cobby et al. 2001, Asselman et al. 2002, Dowling and Accad 2003). Several studies have shown that a combined analysis of IS data gathered by the Compact Airborne Spectral Imager (CASI) and LiDAR images can improve classification results significantly (Blackburn 2002, Sault et al. 2005, Geerling et al. 2007). However, studies where CASI and LiDAR data are combined and subsequently segmented are scarce (Lennon et al. 2006, Straatsma 2006, Walker et al. 2007).

The aim of the present paper is to test the performance of an automated segmentation technique for the classification of vegetation and land cover in a river floodplain along the River Waal in the Netherlands using a combination of CASI and LiDAR images as input. The vegetation and land cover classes distinguished here are based on the Dutch riparian ecotope system (Rademakers and Wolfert 1994, Jansen and Backx 1998, Houkes 2007). Ecotopes are landscape units used for stratifying landscapes into ecologically relevant units, e.g. for the measurement and mapping of landscape structure, function and change. They can be defined as spatial units of a certain extent (up to about 1.5 Ha) that are relatively homogeneous in vegetation structure, succession stage and the main abiotic site factors that are relevant for plant growth (Klijn and De Haes 1994). Ecotope maps have for example been used in wildlife studies, hydraulic modelling and floodplain reconstruction plans (De Nooij et al. 2004, Ellis et al. 2006, Wijnhoven et al. 2006, Schipper et al. 2008).

The high resolution spectral data (CASI) and elevation data (LiDAR) used in this

study are evaluated on their separate and combined segmentation and classification potential. The study compares the results of automated image segmentation and classification to an existing manually digitised ecotope map. The research questions are: (1) How do manually drawn and automatically derived ecotope objects compare when using IS data, LiDAR data and both? (2) How does identification of ecotopes compare when using IS data, LiDAR data and a combination of both? Additionally, the implications for implementation will be discussed.

6.3 Material and Methods

Study area

A case study area called the Millinger- and Klompenwaard (N 51° 52', E 5° 44') was chosen along the Waal River. The Waal River is one of the main branches of the river Rhine in the Netherlands (Figure 6.1). The whole area is a nature rehabilitation site and consists of a mixture of natural and agricultural land cover. The land cover

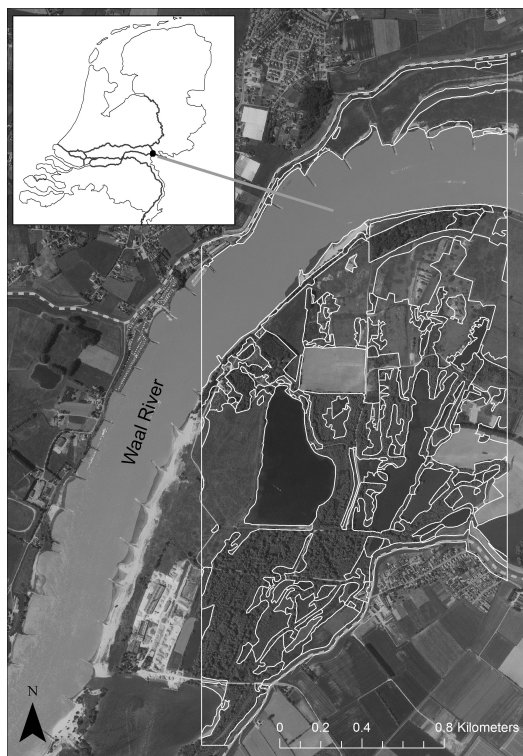


Figure 6.1 An aerial image overlaid with the ecotope map with the extent of the research area. The north and south borders are defined by the floodplain extent. The east and south borders are the slightly trimmed edges of the CASI flight line.

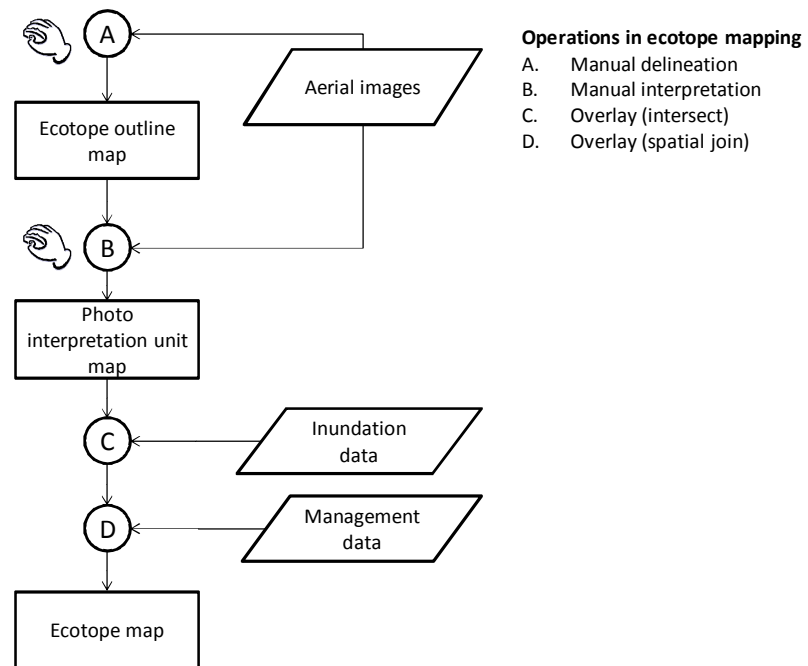
consists of pastures, fields, patches of sand, grass, herbaceous vegetation, bushes and softwood forest patches in different age categories between 15 and 40 years (Bekhuis et al. 1995).

Present method of mapping ecotopes

The present day mapping routine applied by Dutch river managers follows an 8 year renewal cycle. The ecotope maps are based on floodplain vegetation cover and abiotic factors such as inundation frequency and management style, i.e. intense agriculture or self steering nature (Rademakers and Wolfert 1994, Jansen and Backx 1998, Lorenz 2001, Molen et al. 2003, Willems et al. 2007). The maps are prepared in four steps (Figure 6.2). The first two steps consist of manual delineation and interpretation using aerial images. It results in a map with photo-interpretation (PI) units, generally referred to as the photo-interpretation map. The images used are analogue stereographic 1:10,000 true colour (1998) and false colour (2005) photographs taken in the growing season. In the third step, the photo-interpretation map is

overlaid with an inundation map. The inundation map contains information on the number of days an area is flooded per year, based on statistics since the early 1900s. The result is an almost complete ecotope map, but some grasslands are further refined in a fourth step using information on land use such as agriculture, intense grazing or low density grazing. The final map contains over 30 ecotope types (Jansen and Backx 1998, Houkes 2007).

Figure 6.2 Flowchart of the operational manual ecotope mapping procedure. Manual operations A and B are automated and tested in this study.



The first two steps, i.e. ecotope delineation and interpretation, are the most important and labour intensive steps because here the spatial extent and the initial classification are manually interpreted from the aerial imagery. The segmentation and classification routines applied in this paper are tested against the results of these two steps, i.e. the photo-interpretation map. Table 6.1 shows the photo-interpretation (PI) classes distinguished on the PI map and the associated ecotopes.

Remote sensing data used

The data used in this study consists of spectral data collected by the Compact Airborne Spectrographic Imager (CASI) and elevation data collected by Light Detection and Ranging (LiDAR); the latter is also called Airborne Laser Scanning (ALS). Table 6.2 lists the characteristics of both data sets. Spatial compatibility is important when combining data sets from two different sources. The original georectification of the CASI data proved to be inaccurate (error of 5 to 8 m) and the data was re-georectified using a standard photogrammetrically generated river map of scale 1:1000 with planimetric error of 0.06 m (Anonymous 2000). This re-georectification (32 geo-reference points) resulted in a root mean square (RMS) error of 2.6 m in x and 1.0 m in y-direction, i.e. about one pixel.

Table 6.1 Photo interpretation units (PI) used by the Dutch river manager for the freshwater river system. Final ecotope types (not shown) are directly derived from PI units and divide each PI unit in sub-units based on local inundation and land management data from hydraulic models and agricultural statistics, see also Figure 6.2. The classes of River system and Bare shores are aggregated in this paper, see the last column. Classes indicated with a “-” sign are absent in the research area.

Main class	Photo-interpretation unit (PI)	PI-code	Used classes
River system	Summer bed	r1	Water
	Side channel	r2	Water
	Artificial or oxbow lake	r3	Water
	Pioneer vegetation	p	-
Bare shores	Gravel	k1	-
	Natural shell bank	k2	-
	Hard clay or peat bank	k3	-
	Beach or shelf	k4	bare
	Bare shore levee	k5	-
	Rest (often temporarily bare soil)	k6	bare
hard substrate	Build up / hardened	a	a
Grass and herbaceous vegetation	Production grassland	g1	g1
	Structure rich grassland	g2	g2
	Agricultural Field	g3	g3
	Bulrush	g4	g4
	Reed and other helophytes	g5	g5
	Herbaceous vegetation	g6	g6
Forest and bushes (Woody)	Natural forest	b1	b1
	Production forest	b2	-
	Tidal forest	b3	-
	Bush	b4	b4

Resampling of the re-georectified image was done with the nearest neighbour approach to conserve originally recorded data (Mather 2004). Reported LiDAR errors are 0.15 m elevation and less than 0.5 m planimetric error (Brugelmann 2003, Geerling et al. 2007).

General workflow

The general workflow is as follows: (1) Pre-processing of raw LiDAR data to create a raster of vegetation height data which can be used as input for segmentation; (2) Segmentation of the CASI and vegetation height data in series

Table 6.2 Specification of the Compact Airborne Spectral Imager (CASI) data used.

CASI	Date of flight	15 August 2001
	Flight elevation	1500m
	Swath width	1536m
	Pixel size ¹⁾	2m
	Number of spectral bands	10
	Spectral range	437-890 nm
ALTM2033	Date of flight	12 October 2001
	Flight elevation ²⁾	1500m
	Scan angle	19°
	Laser pulse	33 kHz
	Mirror	30 Hz
	Mean density	1.3 hits m ⁻²
	Recorded	First return

¹⁾The original pixel size was 3 m, but this was resampled to 2 m by the imaging company; the original 3 m data were unavailable for this study.

²⁾ Approximate, derived from scan angle and swath width.

running from small objects to large objects and testing of segmentation results against ecotope outlines; (3) Classification of the best segmentation results in PI classes and testing of the classification results against a test set derived from the PI map. The workflow is described in more detail below.

Pre-processing of LiDAR data

The raw LiDAR data contains both information on the elevation of the ground surface and the objects on top, e.g. vegetation cover. As a first step, the variations in ground level were separated from variations in vegetation height by subtracting a Digital Elevation Model (DEM) from the elevations recorded in the unfiltered LiDAR set. In the second step, the vegetation height data were used to create grid data sets that can be applied in the segmentation procedure.

The DEM was created in two iterative steps. First an initial DEM was produced by application of the kriging interpolation technique to the lowest points in 10x10 m squares. Subsequently, all points below this initial DEM were added to the DEM point data set. In total about 9 percent of the LiDAR points was used to interpolate the final DEM. The point data used for construction of the DEM were excluded from further LiDAR processing steps. This relatively simple procedure provides a sufficiently accurate DEM because the study area has little height variation. After subtracting the DEM from the non-DEM LiDAR points, the remaining data was assumed to reflect variations in vegetation height only. Extreme outliers deviating more than four times the standard deviation from the mean were filtered out, amounting to 0.13 percent of the total amount of LiDAR points. These outliers have an elevation of more than 100 metres above the surface and are probably caused by false reflections above water or on birds.

The vertical structure of the vegetation was described using the mean, median, range and standard deviation derived from the vegetation height points within a 4 m search radius. These statistics (or 'textural bands') were computed for each 2x2 m cell in the study area using a 'moving window' operation similar to Geerling et al. (2007). The 2x2 m grid cells corresponded to the CASI grid cell size. This procedure yielded 4 LiDAR based grids, each containing one textural band. Figure 6.3 illustrates the additional information given by data on vegetation structure.

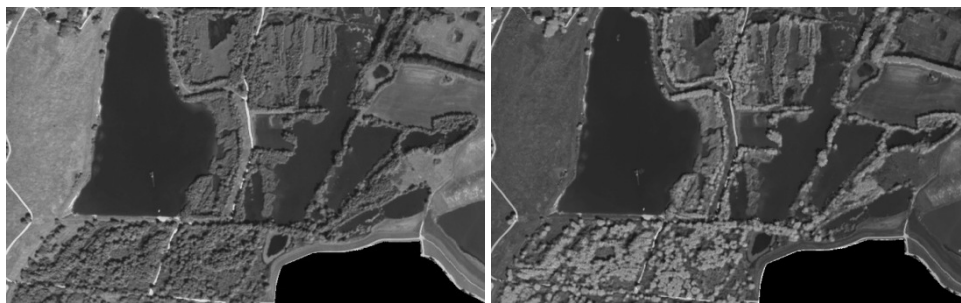


Figure 6.3 (In full colour on page 190) The left image shows a false colour excerpt of the CASI image (bands 2, 3, 7). The right image shows the same view but band 7 is replaced by vegetation elevation. Trees appear brighter on the right image because of their greater height and bushes appear darker red because of their lower height.

Segmentation algorithm and segmentation evaluation

Three sets of data were individually segmented: CASI data only, LiDAR data only and a combined data set of CASI and LiDAR data. The segmentation method used is the multi-resolution segmentation as implemented in Definiens Professional 5.0 (Baatz and Schäpe 2000, Definiens 2006). It uses the Fractal Net Evolution Approach (FNEA) based on step by step growing of regions while minimising region heterogeneity, i.e. favouring the merge of similar regions. Below, the algorithm is described based on Baatz and Schäpe (2000), Hay et al. (2003) and Benz et al. (2004).

Minimisation of heterogeneity is achieved by evaluating the degree of heterogeneity between neighbouring regions (called objects from now on). The human eye uses colour and shape to distinguish objects on aerial images. Therefore, the similarity between two neighbouring objects is evaluated in terms of colour and shape. Within the context of this study, the term “colour” should not be taken literally; it refers to the bands of both the CASI and LiDAR images.

Formula 1 gives the overall change in heterogeneity when 2 objects are merged, the relative weight of spectral and shape heterogeneity changes is given by w . It should be noted, that no segmentation is possible without colour and colour generally determines the segmentation result far more than shape does.

$$f = w \cdot \Delta h_{spectral} + (1 - w) \cdot \Delta h_{shape} \quad (1)$$

Definitions for spectral heterogeneity for a single object ($h_{spectral}$) are the variance of spectral mean values or the standard deviation of spectral mean values of for example remotely sensed properties (Baatz and Schäpe 2000). Benz et al. (2004) give formula 2 for computation of $\Delta h_{spectral}$ as applied in Definiens software based on standard deviations of values spectral bands (called channels). The number of pixels (n) is used to weigh the standard deviation (σ) for merged and unmerged objects 1 and 2 for each band (or channel) c . Specific weights can be assigned to each band (w_c) prior to segmentation.

$$\Delta h_{spectral} = \sum_c w_c (n_{merge} \cdot \sigma_{c_merge} - (n_1 \cdot \sigma_{c,1} + n_2 \cdot \sigma_{c,2})) \quad (2)$$

The shape heterogeneity of an object (h_{shape}) consists of a compactness parameter and a smoothness parameter. Compactness reflects the deviation from the ideal compact form (an $n \times n$ pixel square) and is calculated based on the edge length l of the object (Equation 3). Smoothness reflects the deviation of the shortest possible edge length of the object given by a rectangle around the object, i.e. length b (Equation 4). Changes in heterogeneity when merging 2 objects are computed using equations 5 and 6, again weighted by the number of pixels of the merged and unmerged (1 and 2) objects. Both parameters can be combined into one final shape parameter using a user-defined weight w_{comp} (Equation 7). Effectively the shape criterion poses a barrier

for merging objects with different shapes, such as thin and long roads and patches of forest.

$$h_{comp} = \frac{l}{\sqrt{n}} \quad (3)$$

$$h_{smooth} = \frac{l}{b} \quad (4)$$

$$\Delta h_{comp} = n_{merge} \cdot \frac{l_{merge}}{\sqrt{n_{merge}}} - \left(n_1 \cdot \frac{l_1}{\sqrt{n_1}} + n_2 \cdot \frac{l_2}{\sqrt{n_2}} \right) \quad (5)$$

$$\Delta h_{smooth} = n_{merge} \cdot \frac{l_{merge}}{b_{merge}} - \left(n_1 \cdot \frac{l_1}{b_1} + n_2 \cdot \frac{l_2}{b_2} \right) \quad (6)$$

$$\Delta h_{shape} = w_{comp} \cdot \Delta h_{comp} + (1 - w_{comp}) \cdot \Delta h_{smooth} \quad (7)$$

Overall, FNEA segmentation process is a region-growing procedure starting at each point in the image with one pixel objects and merging these image objects into bigger ones. The merger of two neighbours having the lowest change in heterogeneity (f in formula 1) is chosen but is only allowed when it does not exceed a given value called the ‘scale parameter’. The scale parameter effectively limits the spatial growth of objects, hence the word ‘scale’ in its name. The higher the scale parameter is set, the more merges are allowed. A small scale parameter can lead to over segmentation, i.e. features of interest are divided in more objects, a larger scale parameter can lead to under segmentation, i.e. features of interest are merged with neighbouring features. A special procedure ensures an even growth of objects over the whole image in each step to produce image objects of comparable scale for a single scale parameter setting, details can be found in Baatz and Schäpe (2000).

In the present study, the scale parameter was varied to identify the value that produced optimal segmentation results for floodplain ecotopes. Scale parameter values used were 10, 20, 40, 60, 80, 100, 200, 300, 400, 500, and 600. The corresponding segmentation results ranged from over-segmentation (i.e. many small objects) to correct or under-segmentation (i.e. few large objects). To determine the segmentation quality, each result was compared to the existing PI map. To this purpose, 8 ecotope outlines of the PI map were selected based on their difference in PI class or size and expected segmentation difficulties because of low spectral or structural contrast to their surroundings. The study area consisted of a mixture of rectangular cultivated and irregular natural areas; the shape criterion was used to discourage the merger of these different types. The influence of the shape criterion (h_{shape}) proved to be marginal compared to change of sensor data, and was therefore kept constant in this study. After some testing, the colour / shape ratio (w , Equation 1) was set at 0.5 and

more emphasis was given to compactness than to smoothness (i.e. $w_{comp} = 0.8$; Equation 7).

The quality of the segmentation results was tested using a method based on Möller et al. (2007) in which the surface areas of segmentation objects and manually digitised ecotope outlines are being compared. Segmentation accuracy was computed by calculating 2 index values (Figure 6.4). The ecotope coverage index (E-cov) is the proportion of the common area (C) inside the area of the ecotope (A+C) of the PI map, resulting in $C/(A+C)$. The object coverage index (Ob-cov) is the proportion of the common area (C) inside the area of the segmented object (B+C), resulting in $C/(B+C)$. Mostly, segmented objects were smaller than the ecotope, especially in the lower range of the scale parameter series. If this was the case, the total object surface area (B+C) was calculated as the total area of all segmentation objects which had their centre point inside the ecotope area.

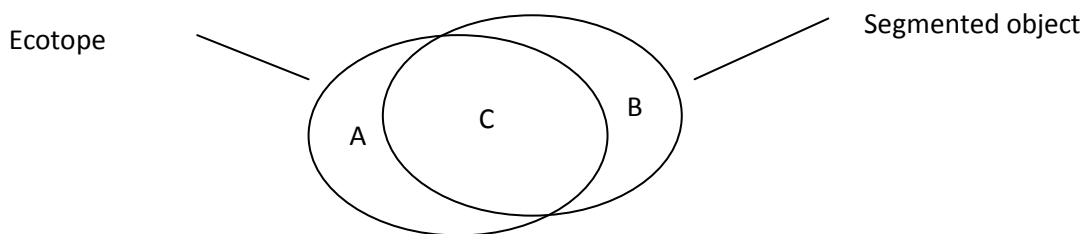


Figure 6.4 Segmentation accuracy was computed by calculating 2 index values. The first index is the proportion of the common area (C) in the area of the ecotope (A+C), resulting in $C/(A+C)$. The second index is the common area (C) proportion in the area of segmented object (B+C), resulting in $C/(B+C)$. In case the two objects are perfectly aligned, both the indexes approach 1. Note, mostly more than one segmented object falls inside the ecotope. Then, the total object surface area (B+C) consists of all objects with their centre point inside the ecotope area.

When one segmentation object exactly matches a PI ecotope outline, the segmentation is successful. Therefore, a successful segmentation is defined as having index values approaching 1 (good fit) and consisting of as few segmentation objects as possible. It was tested whether the mean amount of segments differed significantly between the sensor types, i.e. CASI, LiDAR and the combination of CASI and LiDAR.

Classification and evaluation

The segmented data sets were classified using a supervised classification approach in which the nearest neighbour classification of all classes is applied on the basis of a training set (Definiens 2006). In nearest neighbour classification, the properties of the object to be classified are compared to a training set. The object is assigned to the class with the nearest match between class and object properties. Classification did not improve when using more than 8 bands for each class, but band combinations varied per class. Band means performed best and were used as object properties for

classification, for example the mean green reflectance (digital number) of an object. The per-class training set consisted of 3 to 5 randomly selected training objects at segmentation level 20. Class selection was based on classes being present in the study area and is indicated in Table 6.1. Not all segmentation results were classified but classification was limited to data sets producing optimal segmentation results and data sets one level below and above the optimum. Although it is possible to optimise scaling for different classes, it was considered unnecessary for this comparative study and therefore not pursued. A test set consisting of 348 randomly chosen test points was used for evaluation of the classifications. The test set was based on the 2005 ecotope map and the class of each test point was additionally verified by manual interpretation of the CASI and LiDAR images, the false and true colour aerial photographs taken in 2003 and 2005, and expert knowledge of the area. Error matrices were computed for all results. Test results are reported as per class KIA values (also known as Kappa index), overall KIA and percentage overall accuracy. The KIA is a measure for the difference between the change agreement and actual agreement in the error matrix (Mather 2004). Possible KIA scores are weak agreement (<0.4), moderate to good agreement (0.4 to 0.8), and strong agreement (>0.8). The significance of the differences between the highest scoring error matrices of each input data set (i.e. CASI, LiDAR and the combination) were tested by computing the Kappa Z statistic (Congalton 1983, Congalton 1999).

6.4 Results

Segmentation

Table 6.3 shows the most successful segmentation results for the three different data sets and each of the 8 examined ecotope outlines. In effect, a successful segmentation is a trade-off between high ecotope / object coverage index values and a low number of objects covering an ecotope.

Table 6.3 Optimal segmentation results for the eight investigated ecotope outlines per data set. The ecotopes are characterised as PI-types, see also Table 6.1. Given are the segmentation scale (SCL), the number of objects with centre point in ecotope (NO), ecotope coverage index (E-cov), object coverage index (Ob-cov).

Name (PI type)	Area (ha)	SCL	NO	CASI		LiDAR		CASI+LiDAR					
				E-cov	Ob-cov	SCL	NO	E-cov	Ob-cov	SCL	NO	E-cov	Ob-cov
Natural forest (b1)	4.83	400	5	0.90	0.73	200	9	0.91	0.71	300	4	0.88	0.89
Agricultural field (g3)	6.89	600	1	1.00	0.95	400	1	0.93	0.99	600	1	0.97	0.98
Herbaceous veg. (g6-a)	20.45	500	13	0.94	0.73	200	7	0.96	0.84	600	7	0.94	0.74
Structure rich grassland (g2)	7.6	600	1	0.87	0.94	80	6	0.88	0.98	600	1	0.94	0.99
Bare soil (k4)	1.5	100	29	0.84	0.89	20	44	0.82	0.84	600	2	0.81	0.72
Structure rich grassland (g6b)	1.2	200	2	0.80	0.79	100	3	0.71	0.91	600	1	0.88	0.77
Water, Lake (r3)	1.32	600	2	0.87	0.71	80	2	0.79	0.93	600	1	0.89	0.82
Bush (b4)	0.63	60	20	0.84	0.93	100	2	0.89	0.81	100	1	0.77	0.88

Visual inspection showed that successful ecotope delineation was possible when both ecotope and object coverage indexes were above 0.7. In all cases, the segmentation results became meaningless when one or both indexes went below 0.7. As can be seen in Table 6.3, the amount of objects needed for proper delineation of herbaceous vegetation (g6a), bush (b4) for CASI and bare soil (k4) for both LiDAR and CASI is high, indicating that these cannot be accurately delineated using the respective data sets. The amount of objects needed to outline the ecotopes is clearly the lowest for the CASI+LiDAR combination. An example is given in Figure 6.5, depicting over-, optimal and under-segmentation for all 3 data sets. The differences between the mean number of objects needed as shown in Table 6.3 are significant at $p < 0.1$ for CASI vs. CASI+LiDAR and $p = 0.05$ for LiDAR vs. CASI+LiDAR (Mann-Whitney U test). No conclusion can be drawn from a direct comparison of the

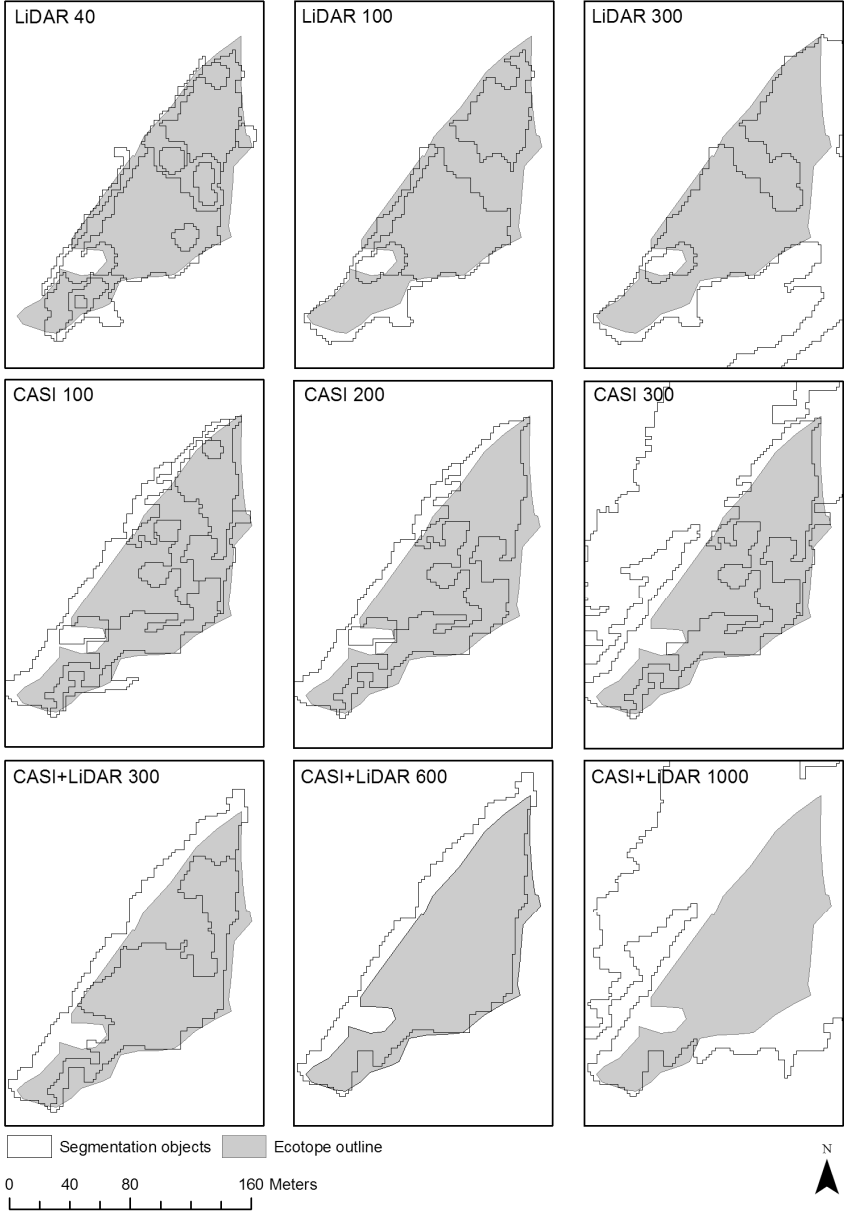


Figure 6.5 Illustration of over-segmentation (too many objects, left column), optimal-segmentation (middle column) and under-segmentation (too few objects, right column) for each data set. The ecotope outline depicted in grey is herbaceous vegetation, also shown as g6b in Table 3 and Figure 4. The optimal segmentation levels are taken from Table 3. The objects shown here have their centre point inside the ecotope except for the under-segmented examples (selection based on intersect). LiDAR and CASI single segmentation results need more objects to cover the ecotope than CASI+LiDAR.

optimal scale parameters for the different data sets. The number of remote sensing bands vary per set (CASI 10, LiDAR 4, CASI+LiDAR 14). The same scale parameter will lead to different results when the input data changes. An increase of the number of input bands mostly leads to higher degree of heterogeneity changes resulting in smaller objects at the same segmentation level.

Figure 6.6 gives an overview of the segmentation results underlying Table 6.3 by showing the number of segmented objects (x-axis, logarithmic scale) versus the ecotope-coverage and object-coverage indexes (y-axis). The first data point at the left of every graph is generated at scale parameter 10. Although both the coverage indexes were always high at this level, this is not a successful segmentation because of the high number of objects involved. By changing the scale parameter setting, the number of generated objects lowered and the coverage indexes changed. The relationship between the coverage index and 'number of objects' is data set and ecotope specific. In the LiDAR segmentation results, sudden decreases of object and ecotope coverage are observed when the number of objects is approaching 1.0, most notably in ecotope outlines with low vegetation height such as herbaceous vegetation (g6a and g6b), bare soil (k4), floodplain lake (r3). CASI results are more stable, except for herbaceous vegetation (g6b) and bush (b4). In the CASI+LiDAR segmentation series, only the bush (b4) performed slightly erratic, including an extra centre point at the highest segmentation level. The coverage index / no. of objects behaviour is elaborated further in the discussion section.

Table 6.4 Error matrix for CASI+LiDAR classification (scale factor = 80) showing per class classification and misclassification results, number of reference plots and producer / user accuracies. Plots classified correctly are shown in bold. The Producers Accuracy summarises the probability of a vegetation plot being correctly classified. The Users Accuracy represents the probability of a classified pixel belonging to the class it represents (Congalton 1991).

User \ Ref. Class	b4	b1	a	g1	g2	g3	g5	g6	bare	water	User Acc.
b4	24	5	0	1	2	0	2	2	0	0	0.67
b1	6	47	1	0	0	0	0	0	0	3	0.82
a	1	0	14	0	0	0	0	0	1	0	0.88
g1	1	2	0	13	13	0	0	11	0	0	0.33
g2	0	0	0	11	7	0	0	2	0	0	0.35
g3	0	0	0	4	1	13	0	1	0	0	0.68
g5	3	0	0	0	0	1	12	1	0	1	0.67
g6	0	0	0	2	7	0	0	43	0	0	0.83
bare	0	0	3	0	0	0	0	0	39	1	0.91
water	0	0	0	0	0	0	0	0	0	47	1.00
Producer Acc.	69	87	78	42	23	93	86	72	98	90	
No. reference plots	35	54	18	31	30	14	14	60	40	52	

Classification

From Table 6.3 the objects generated at scale setting values of herbaceous vegetation (g6b) for CASI, water (r3) for LiDAR and bush (b4) for CASI+LiDAR were used for

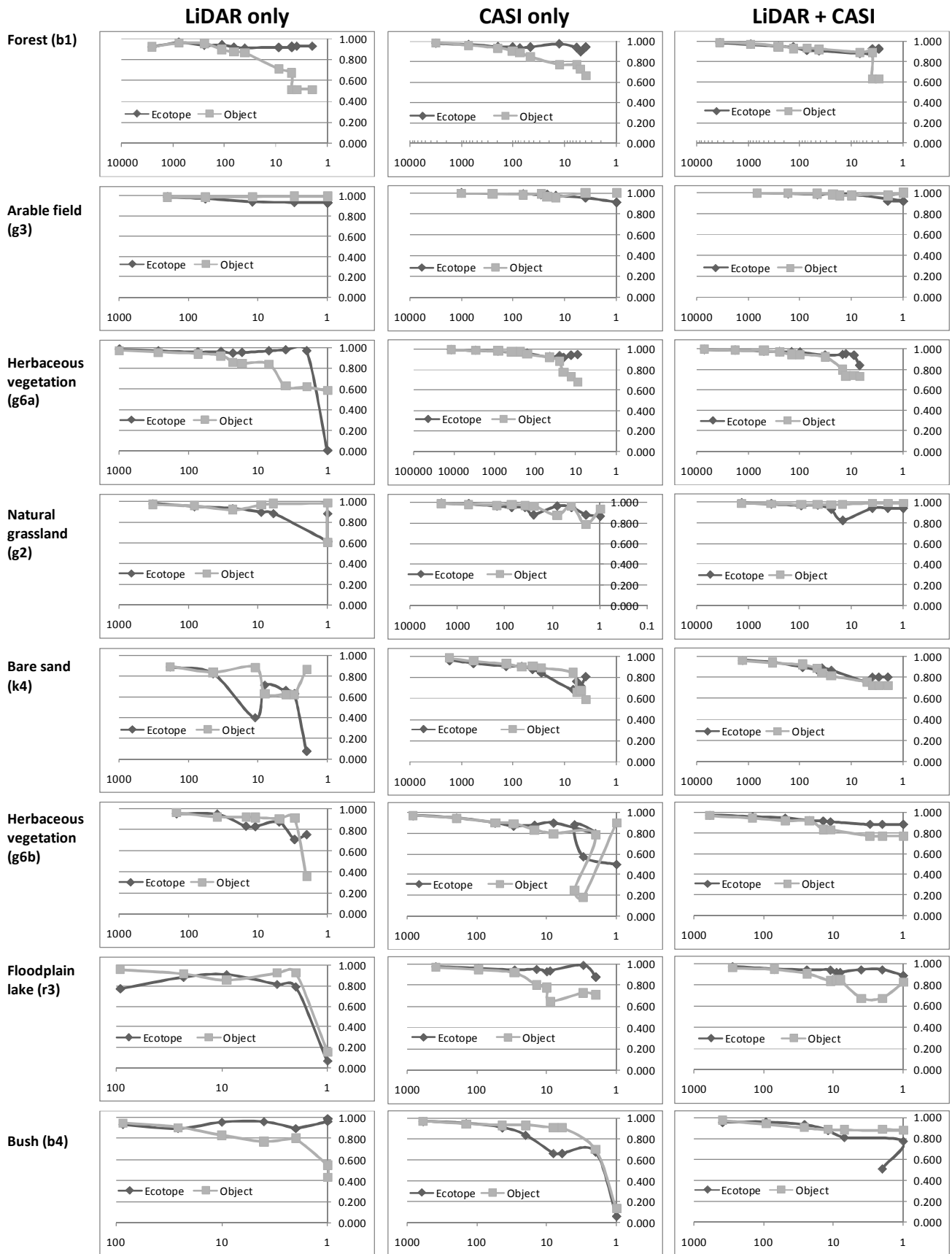


Figure 6.6 Figures showing for selected ecotope outlines (PI-type indicated in left column) the number of segmentation objects with centre inside the ecotope (x-axis) set against the ecotope coverage (dark line with rhombuses) and object coverage indexes (light grey line with squares) on the y-axis.

classification. Although these scale parameter settings lead to over-segmentation for other ecotopes, choosing the lowest scale parameter from Table 6.3 made sure that the smaller ecotopes could be classified as separate objects. The corresponding scale parameter settings were 200 (CASI), 80 (LiDAR) and 100 (CASI+LiDAR), as reported in Table 6.3. For all classifications, error matrices were produced. Table 6.4 shows the matrix for CASI+LiDAR (level 80) results. As the classes artificial (a), field (g3) and reed (g5) were relatively scarce in the study area, these have a lower number of reference plots. Table 6.5 shows the results for all classifications. Classification accuracy of the vegetation height data into 10 classes was 55% and very poor in classes of low vegetation. It significantly improved when adding spectral data, i.e. to 74% overall accuracy. Classification of CASI data in the same classes improved from 66% to 74% by adding the vegetation height data. The error matrices of the three input data sets differed significantly based on the Kappa-Z statistic: CASI vs. LiDAR ($p = 0.05$), CASI+LiDAR vs. CASI ($p = 0.1$) and CASI+LiDAR vs. LiDAR ($p < 0.05$). All data sets have a tendency to lower accuracy when segmentation levels increase, although the trend for CASI+LiDAR segmentation is weak. Confusion between production grassland (g1) and structure rich grassland (g2) is common in all error matrices, also reflected in the low per class KIA values in all classifications. Furthermore, herbaceous vegetation (g6) is commonly confused with g1 and g2, although not as prominent as the confusion between production (g1) and structure rich (g2) grasslands. A Map of the LiDAR+CASI result is shown in Figure 6.7.

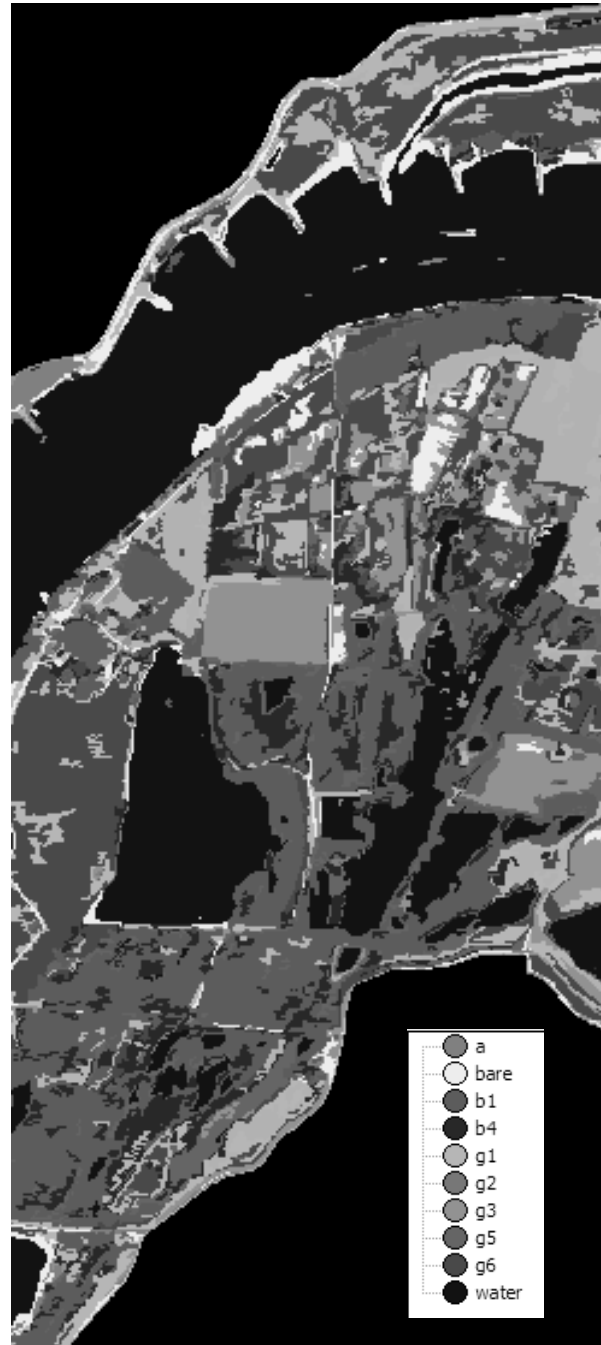


Figure 6.7 (In full colour on page 190)
Classified PI unit map based on the
LiDAR+CASI data set.

6.5 Discussion

Method

Pre-processing of the LiDAR data set was the most labour intensive part of the procedure. Especially creating the DEM from the raw LiDAR set was time and computer intensive. Once the grid had been created, application gave no problems. The CASI data as delivered by the supplier proved to be poorly geo-referenced. Its original accuracy was about 5 to 8 metres. By re-geo-referencing it was improved to about 2 m (the approximate pixel level) and could be used together with the LiDAR grids. However, collecting the multi-source data in one flight is preferable because it limits co-registration errors and the amount of resampling needed for geo-correction. A laser beam aimed from high altitude can have a footprint of up to 0.5 m. Reflected beams seldom return as one pulse but are reflected by objects they encounter, such as various levels in the vegetation layer. The recorded LiDAR set contained first return pulses, giving the elevation of the first encountered object. Additional recording of the last or the whole reflected signal increases the possibilities to differentiate between vegetation and soil and could increase the accuracy of the procedure (Blair et al. 1999, Wehr and Lohr 1999, Straatsma and Middelkoop 2007).

The segmentation test method of Möller et al. (2007) was simplified. In addition to the overlap coefficients, they also computed the error of centre point locations. This worked well on the field based agricultural landscapes they studied, but did not have additional value here. Calculation of the ecotope overlap and object overlap provided sufficient information to identify the optimal segmentation values.

Segmentation stability

When looking at Figure 6.5, several distinct cases appear: (1) completely stable object coverage over the whole range of number of objects, for example g3 in Figure 6.6; (2) stable high ecotope- and object coverage, but a slight drop when the number of objects decreases below 10, for example b1 and g6a in Figure 6.6; (3) semi stable but drop towards index 0 well before 1 object is reached, for example LiDAR r3 and CASI b4 in Figure 6.6; (4) erroneous behaviour of index values, for example LiDAR k4 and CASI g6b in Figure 6.6. Type 1 fulfils the criteria for good segmentation results, i.e. high overlap indexes and a low number of segmentation objects. Type 2 can give good segmentation results when indexes are not too low (0.7 is used in Table 6.3). It mostly results from a slight but stable mismatch between ecotope delineation and object delineation causing either of the indexes to be lower depending on the type of mismatch (Figure 6.5). Type 3 and 4 indicate segmentation problems. When the scale parameter increases, the object areas get bigger. Therefore, when RS data lacks distinct features for delineation, objects merge with neighbouring objects that have similar properties. In type 3, the poorly delineated objects will become larger than the ecotope itself and a drop in coverage values will occur when the object centre points shift out of the ecotope. When object sizes are increasing even

more, a loss of centre points laying in the ecotope causes the ecotope coverage to approach zero. Additionally, in type 4, false object centres are taken into account belonging to irregularly shaped neighbouring objects that causes their object centre to be inside the ecotope area (and often outside the object of origin, like in U-shaped objects). This causes an increase in the number of objects when a decrease is expected, such as in Figure 6.6 (CASI g6b; CASI+LiDAR b4). Although, this is partly caused by the chosen centre-point method, it still only occurred in areas with segmentation problems.

Segmentation of the data sets

It was possible to segment the rasterised LiDAR data into useful objects, i.e. objects with distinct structural properties. Asselman et al. (2001) reaches the same conclusion for border detection of floodplain objects using geo-statistical techniques and a LiDAR data set of lower point density.

The amount of objects generated was high in forested parts as these have a relatively high heterogeneity in LiDAR data (Figure 6.6; b1). The differences in number of objects in areas with high and low heterogeneity is also noted by Baatz and Schäpe (2000) and inherent to the procedure. The use of textured vegetation structure data increased the 'change in heterogeneity' for a merge with neighbouring objects. It requires a higher scale parameter setting. Small, single trees or bush, were kept as separate objects and did not merge readily into a surrounding homogenous area when compared to spectral segmentation. Compare bush (b4) of LiDAR and CASI results in Figure 6.6 (note the difference in x-axis units).

Grasslands and fields were readily segmented into few objects. This can lead to under-segmentation because the low vegetation height and variance caused a 'high degree of fit', i.e. type 3 behaviour (see herbaceous vegetation (g6b) and structure rich grassland (g2)). Delineation of flat areas without clear contrasting surrounding objects is difficult. For example, the bare sand (k4) bordering to water showed erratic behaviour (type 4). The arable field was delineated correctly (Figure 6.4) because of its contrast with surrounding objects.

CASI results were mostly of type 1 and 2, except herbaceous vegetation (g6b) and bush (b4; type 4 and 3, respectively). Different from LiDAR segmentation, the shadows recorded by the scanner generated extra objects in forested areas.

Furthermore, it was expected that bare soil (k4) would have been better delineated by CASI, as water and sand have contrasting spectral properties. Upon visual investigation, the shallow slope of the sandy beach produced a gradient of mixed water and sand values, complicating delineation.

The incorporation of both RS sources into the segmentation algorithm increased the possibilities to detect contrasts in neighbouring objects. CASI+LiDAR performed best. All tested delineations are of type 1 or 2, leading to few objects with high overlap indexes. Even the excess delineation of smaller objects decreased (Figure 6.5) was diminished by the inclusion of spectral data.

Classification

Of the 3 data sets tested, the combination of CASI with LiDAR performed best and the combination proved to be synergetic in some classes (Tables 6.4 and 6.5). This synergy was also found in other studies combining different data sources (Polh and Van Genderen 1998, Töyrä et al. 2002, Leckie et al. 2003, Geerling et al. 2007).

Landscape objects manifest themselves at different scale levels (Forman and Godron 1986). Therefore, the segmentation scale used for classification in this study was calibrated on the smallest stable segmentation level. The overall results show that an increasing scale parameter decreases the accuracy, especially in the single sensor data sets. In general, the larger polygons of a heterogeneous nature, such as structure rich grassland and herbaceous vegetation, represent the underlying surface on which the test set is based less accurately. Additionally, mistakes in delineation manifest themselves at higher scales and lead to inaccurate classification. To overcome this, multiscale or contextual approaches that apply knowledge on landscape constitution in classification seem promising (Hay et al. 2003, Sluiter et al. 2004).

When discussing the per class results, agricultural field stands out as a tricky class. Depending on crop type and harvest state, they represent a multitude of different structural and spectral values (Lillesand and Kiefer 2000). When fields are harvested, even bare soil is classified upon fields. Fields containing heavy and wet clay will sometimes appear as artificial cover. Seen from a classification point of view, it would be best to weed the fields out in a separate GIS step on the basis of cadastral or management information.

The confusion between different grasslands and herbaceous vegetation is prominent in both the CASI and LiDAR data sets. In the classification results, patches of different grassland types are dispersed in herbaceous vegetation and vice versa. Confusion is inherent to these classes as production grassland, rough grassland and herbaceous vegetation are part of a continuum. Especially in nature rehabilitation sites such as the study area, grasslands in ecological succession will change from one stage to another over time in a patchy way (Geerling et al. 2007). A continuous classification approach can be more applicable and accurate, e.g. fuzzy classification in a range between production grassland and herbage (Schmidtlein et al. 2007; Benz et al. 2004). Additionally, higher optical resolution and extra bands can provide better results. For LiDAR, a higher point density and a more detailed LiDAR 3D-segmentation algorithm could provide the information needed to more accurately classify these classes (Straatsma 2006, Straatsma and Middelkoop 2007).

To keep methods and results transparent and comparable, the classification was based on the remote sensing data band means, using segmentation only as a pre-classification step. To further optimise classification, the object's neighbourhood could be taken into account as advocated by Blaschke et al. (2004). For example, bare sand would become sandy beach when the object is located next to water, water would be defined as a lake when completely surrounded by land, and a small but long object surrounded by water is likely to be a boat (and therefore eliminated). In

this way, classification can be refined to produce a topographic meaningful result.

6.6 Conclusions

When combining data on vegetation height (LiDAR) and spectral data (CASI) in a segmentation algorithm, outlining of ecotopes is better than compared to outlines based on spectral data alone. The amount of objects needed to cover the ecotope is lower and ecotope-object overlap is stable across more segmentation scales. Adding LiDAR improves delineation of structure rich ecotopes, while spectral data improved delineation of grasslands and herbage.

Classification accuracy of the vegetation height data into 10 classes was 55% and very poor in classes of low vegetation, it significantly improved when adding spectral data to 74% overall accuracy. Classification of CASI data in the same classes improved from 66% to 74% by adding the vegetation height data. The method can be a good method to automatically segment to the floodplain ecotope level.

Acknowledgements

The authors would like to thank Johan Bekhuis, Bart Beekers, Emiel Kater, Bart Peters and Mariëlle van Riel. This project was funded by the Ministry of Transport, Public Works and Water Management, Survey Department (AGI) in Delft, the Netherlands.

References

- Anonymous (2000). *Digital Terrain Map of National Rivers*. Ministry of Transport, Public Works and Water Management, Survey department, Delft.
- Asselman NEM (2001). *Laser Altimetry and Hydraulic Roughness of Vegetation*. WL | delft hydraulics, Delft.
- Asselman NEM, Middelkoop H, Ritzen MR, Straatsma MW (2002). *Assesment of the Hydraulic Roughness of River Floodplains using Laser Altimetry*. In: Dyer FJ, Thoms MC, Olley JM (Eds). *The Structure, Function and Management Implications of Fluvial Sedimentary Systems*. IHAS publication 276: 381-388.
- Baatz M, Schäpe A (2000). *Multiresolution Segmentation — an Optimization Approach for High Quality Multi-Scale Image Segmentation*. In: Strobl J, Blaschke T, Griesebner (Eds). *Angewandte Geographische Informationsverarbeitung, vol. XII*. Wichmann, Heidelberg. pp. 12–23.
- Bekhuis J, Bosman W, Woesthuis H (1995). *Millingerwaard. Jaarverslagen 1993-1994*. Ark Foundation, Laag Keppel.
- Benz UC, Hofmann P, Willhauck G, Lingenfelder I, Heynen M (2004). Multi-resolution, object-oriented fuzzy analysis of remote sensing data for GIS-ready information. *ISPRS Journal of Photogrammetry & Remote Sensing* 58: 239–258.

- Blair JB, Rabine DL, Hofton MA (1999). The Laser Vegetation Imaging Sensor: a medium-altitude, digitisation-only, airborne laser altimeter for mapping vegetation and topography. *ISPRS Journal of Photogrammetry & Remote Sensing* **54**: 115–122.
- Blackburn GA (2002). Remote sensing of forest pigments using airborne imaging spectrometer and LIDAR imagery. *Remote Sensing of the Environment* **82**: 311-321.
- Blaschke T, Lang S, Lorup E, Stroble J, Zeil P (2000). *Object-Oriented Image Processing in an Integrated GIS/Remote Sensing Environment and Perspectives for Environmental Applications*. In: Cremers AB, Greve K. (Eds.). *Computer Science for Environmental Protection '00*. Volume II, Marburg. pp. 555-570.
- Blaschke T, Burnett C, Pekkarinen A (2004). *Image Segmentation Methods for Object-based Analysis and Classification*. In: de Jong SM, van der Meer FD. (Eds.). *Remote sensing image analysis: including the spatial domain*. Kluwer Academic Publishers, Dordrecht. pp. 211-236.
- Brügelmann R (2003). *Quality Test of the LiDAR Data set*. Internal document. Ministry of Transport, Public Works and Water Management, Survey department, Delft.
- Cobby DM, Mason DC, Davenport IJ (2001). Image processing of airborne scanning laser altimetry data for improved river flood modelling. *ISPRS Journal of Photogrammetry and Remote Sensing* **56**: 121-138.
- Congalton, RG (1991). A review of assessing the accuracy of classifications of remotely sensed data. *Remote Sensing of Environment* **37**: 35-46.
- Congalton RG, Green K (1999). *Assessing the Accuracy of Remotely Sensed Data: Principles and Practices*. Lewis Publishers, CRC Press Inc., New York, N.Y.
- Congalton RG, Oderwald RG, Mead RA (1983). Assessing Landsat Classification Accuracy Using Discrete Multivariate Analysis Statistical Techniques. *PERS* **49**: 1671-1678.
- De Nooij RJW, Lenders HJR, Leuven RSEW, De Blust G, Geilen N, Goldschmidt B, Muller S, Poudevigne I, Nienhuis PH (2004). BIO-SAFE: assessing the impact of physical reconstruction on protected and endangered species. *River Research and Applications* **20**: 299-313.
- Definiens (2006). *Definiens Professional 5 User Guide*. Definiens, München.
- Dowling R, Accad A (2003). Vegetation classification of the riparian zone along the Brisbane River, Queensland, Australia, using light detection and ranging (lidar) data and forward looking digital video. *Canadian Journal of Remote Sensing* **29**: 556-563.
- Ellis EC, Wang H, Xiao HS, Peng K, Liu XP, Li SC, Ouyang H, Cheng X, Yang LZ (2006). Measuring long-term ecological changes in densely populated landscapes using current and historical high resolution imagery. *Remote Sensing of Environment* **100**: 457 – 473.
- Forman RTT, Godron M (1986). *Landscape Ecology*. John Wiley and Sons, New York.

- Geerling GW, Kater E, Van den Brink C, Baptist MJ, Ragas AMJ, Smits AJM (2008). Nature rehabilitation by floodplain excavation: the hydraulic effect of 16 years of sedimentation and vegetation succession along the Waal River, NL. *Geomorphology*, doi:10.1016/j.geomorph.2007.11.011
- Geerling GW, Labrador-Garcia M, Clevers JPGW, Ragas AMJ, Smits AJM (2007). Classification of floodplain vegetation by data-fusion of Spectral (CASI) and LiDAR data. *International journal of remote sensing* **28**: 4263 – 4284.
- Hay GJ, Blaschke T, Marceau DJ, Bouchard A (2003). A comparison of three image-object methods for the multiscale analysis of landscape structure. *ISPRS Journal of Photogrammetry and Remote Sensing* **57**: 327-345.
- Houkes G (2007). *Ecotopenkartering Rijntakken-Oost 2005, Biologische Monitoring Zoete Rijkswateren*. Ministry of Transport, Public Works and Water Management, Survey department, Delft.
- Jansen BJM, Backx JJGM (1998). *Biologische Monitoring Zoete Rijkswateren. Ecotopenkartering Rijntakken-Oost 1997*. RIZA rapport 98.054 (ISBN 9036952085), Ministry of Transport, Public Works and Water Management, Institute for Inland Water Management and Waste Water Treatment (RIZA), Lelystad.
- Klijn F, Udo de Haes HA (1994). A hierarchical approach to ecosystems and its implications for ecological land classification. *Landscape Ecology* **9**: 89-104.
- Leckie D, Gougeon F, Hill D, Quinn R, Armstrong L, Shreenan R (2003). Combined high-density lidar and multispectral imagery for individual tree crown analysis. *Canadian Journal of Remote Sensing* **29**: 633–649.
- Lennon M, Babichenko S, Thomas N, Mariette V, Mercier G, Lisin A (2006). Detection and mapping of oil slicks in the sea by combined use of hyperspectral imagery and laser-induced fluorescence. *EARSeL eProceedings* **5**: 120-128.
- Lillesand TM, Kiefer RW (2000). *Remote Sensing and Image Interpretation*. John Wiley & Sons, Inc., New York.
- Lorenz CM (2001). *Rijkswateren-Ecotopen-Stelsels Oevers*. Witteveen en Bos. Rw993.1. Ministry of Transport, Public Works and Water Management, Institute for Inland Water Management and Waste Water Treatment (RIZA) & Survey department, Delft.
- Mason DC, Cobby DM, Horritt MS, Bates PD (2003). Floodplain friction parameterization in two-dimensional river flood models using vegetation heights derived from airborne scanning laser altimetry. *Hydrological processes* **17**: 1711-1732.
- Mather PM (2004). *Computer Processing of Remotely-Sensed Images; An Introduction*. John Wiley & Sons Ltd., Chichester, England.
- Mertes LAK (2002). Remote sensing of riverine landscapes. *Freshwater Biology* **47**: 799–816.

- Möller M, Lymburner L, Volk M (2007). The comparison index: A tool for assessing the accuracy of image segmentation. *International Journal of Applied Earth Observation and Geoinformation* **9**: 311–321.
- Pietroniro A, Leconte R (2005). A review of Canadian remote sensing and hydrology 1999-2003. *Hydrological processes* **19**: 285-301.
- Pohl C, Van Genderen JL (1998). Multisensor image fusion in remote sensing: concepts, methods and applications. *International Journal of Remote Sensing* **19**: 823-854.
- Portmann FT (1997). Hydrological runoff modelling by the use of remote sensing data with reference to the 1993-1994 and 1995 floods in the River Rhine Catchment. *Hydrological processes* **11**: 1377-1392.
- Rademakers JGM, Wolfert HP (1994). *Het Rivier-Ecotopen-Stelsel; Een Indeling van Ecologisch Relevante Ruimtelijke Eenheden ten behoeve van Ontwerp- en Beleidsstudies in het Buitendijkse Rivoierengebied (in Dutch with English summary)*. Ministry of Transport, Public Works and Water Management, Institute for Inland Water Management and Waste Water Treatment (RIZA), Lelystad.
- Sault M, Parrish C, White S, Sellars J, Woolard J (2005). A sensor fusion approach to coastal mapping. *Proceedings of the 14th Biennial Coastal Zone Conference*. July 17-21, New Orleans, Louisiana.
- Schipper AM, Loos M, Ragas AMJ, Lopes JPC, Nolte B, Wijnhoven S, Leuven RSEW (2008). Modeling the influence of environmental heterogeneity on heavy metal exposure concentrations for terrestrial vertebrates in river floodplains. *Environmental Toxicology and Chemistry* (accepted).
- Schmidlein S, Zimmermann P, Schüpferling R, Weiß C (2007). Mapping the floristic continuum: Ordination space position estimated from imaging spectroscopy. *Journal of Vegetation Science* **18**: 131-140.
- Sluiter R, de Jong SM, van der Kwast H, Walstra J (2004). *A Contextual Approach to Classify Mediterranean Heterogeneous Vegetation using the Spatial Reclassification Kernel (SPARK) and DAIS7915 Imagery*. In: *Remote Sensing Image Analysis: Including the Spatial Domain*. de Jong SM, van der Meer FD. (Eds.). Kluwer Academic Publishers, Dordrecht. pp. 291-310.
- Straatsma M (2006). *Floodplain Roughness Mapping Synergy: LiDAR and Spectral Remote Sensing*. ISPRS Commission VII Mid-term Symposium "Remote Sensing: From Pixels to Processes", Enschede, the Netherlands, 8-11 May 2006.
- Straatsma M, Middelkoop H (2007). Extracting structural characteristics of herbaceous floodplain vegetation under leaf-off conditions using airborne laser scanner data. *International Journal of Remote Sensing* **28**: 2447-2467.
- Töyrä J, Pietroniro A, Martz LW, Prowse TD (2002). A multi-sensor approach to wetland flood monitoring. *Hydrological Processes* **16**: 1569–1581.

- Van der Molen DT, Geilen N, Backx JJGM, Jansen BJM, Wolfert HP (2003). Water Ecotope Classification for integrated water management in the Netherlands. European Water Management Online. *Official Publication of the European Water Association (EWA)*.
- Van der Sande CJ, de Jong SM, de Rooc APJ (2003). A segmentation and classification approach of IKONOS-2 imagery for land cover mapping to assist flood risk and flood damage assessment. *International Journal of Applied Earth Observation and Geoinformation* **4**: 217–229
- Walker WS, Kellndorfer JM, LaPoint E, Hoppus M, Westfall J (2007). An empirical InSAR-optical fusion approach to mapping vegetation canopy height. *Remote Sensing of the Environment* **109**: 482-499.
- Wehr A, Lohr U (1999). Airborne laser scanning— an introduction and overview. *ISPRS Journal of Photogrammetry & Remote Sensing* **54**: 68–82.
- Wijnhoven S, Thonon I, Van der Velde G, Leuven R, Zorn M, Eijsackers H, Smits T (2006). The impact of bioturbation by small mammals on heavy metal redistribution in an embanked floodplain. *Water, Air, and Soil Pollution* **177**: 183-210.
- Willems D, Bergwerf J, Geilen N (2007). *Rijkswateren-Ecotopen-Stelsels Terrestrisch. Actualisatie Ecotopen Overstromingsvrije Zone Rijkswateren*. Ministry of Transport, Public Works and Water Management, RWS-RIZA, Lelystad.

7 Synthesis

7.1 Scope of this study

Nature restoration (or rehabilitation¹) of regulated rivers is an ongoing effort, with several projects finished and many more in the planning stage (Buijse et al. 2002). The development and application of remote sensing techniques can support these restoration projects in various ways. For example, nature restoration along regulated rivers requires knowledge about the processes that act in natural reference rivers and the potential to reintroduce these processes in regulated rivers. The ecotope dynamics of a river stretch in a non-regulated meandering river was studied to serve as a process example for river restoration (Chapter 2). Furthermore, the hydromorphological evolution of a nature restoration site along a regulated river was analysed and the hydraulic impact of this evolution process was quantified (Chapter 3). Another application of remote sensing techniques in nature restoration projects consists of monitoring restored floodplains in terms of vegetation type and structure. Within this context, the combined use of LiDAR and spectral data in floodplains was studied in Chapters 4, 5 and 6. This concluding chapter discusses Cyclic Floodplain Rejuvenation as a restoration strategy within the context of the results of these studies. Furthermore, the potential of the combined use of LiDAR and spectral data for monitoring vegetation and floodplain dynamics is discussed. Overall, the preceding chapters contribute to different planning phases of floodplain management, as illustrated in Figure 7.1.

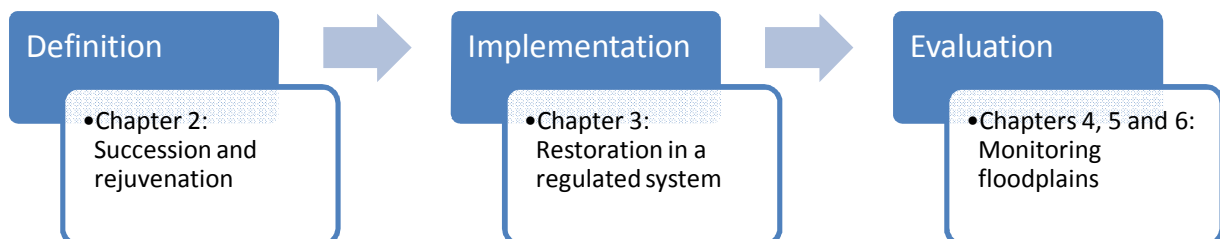


Figure 7.1 Relation between planning phases and research topics of the various chapters.

7.2 Rejuvenation and succession in riverine landscapes: the Allier River

Nature thrives by disturbance. In most systems, disturbance and subsequent succession are an integral part of the system. For example in forests, when a fire has cleared the landscape, the altered landscape creates opportunities for new species (Keeley 1987, Dixon et al. 1995). A regular disturbance by burning ensures the forest

¹ Restoration and rehabilitation are often used interchangeable; the internationally more accepted term of restoration is applied throughout this synthesis.

system is rejuvenated and succession can start anew, supporting an overall species-rich system. Another example is the coastal dune system, where aeolian processes disturb the landscape configuration on a regular basis. Here, sand is redistributed by wind, which gives the dune its characteristic shape (Strahler and Strahler 2003). The eolian rejuvenation ensures that pioneer stages such as bare sand are continuously present and can be colonised by pioneer species like the sand lizard (Wouters et al. in prep). The dynamics of the river system is also based on rejuvenation and succession, which are mostly triggered by changing river discharges and sediment loads (Junk et al. 1989, Amoros and Wade 1996, Ward 1998, Tockner et al. 2000). How do rejuvenation and succession shape the landscape along a near-natural river? Rejuvenation and the resulting spatial and temporal diversity of the riverine landscape of the freely meandering Allier River were analysed in Chapter 2. The Allier served as a reference river for the Dutch / Belgian stretch of the Meuse (the so-called Border-Meuse) and can serve as a process example for meandering rivers in general. The overall rejuvenation rate, ecotope transition rate, floodplain age and steady state were established. In this section, the implications of these results for river restoration are discussed.

The study on the Allier (F) showed that, in this meandering system, the floodplains were rejuvenated at a rate of about 33.5 ha per 5 years for the 7 km stretch, amounting to 0.97 ha km⁻¹

year⁻¹ (river length was measured along the axis of the river). Direct comparison with other studies is difficult as most studies on meandering river dynamics follow changes after human disturbance, do not analyse land cover changes spatially, do not cover a historical time span or express channel movement in m year⁻¹ (Miller et al. 1995, Hupp 1996, Large and Petts 1996, Gurnell 1997,

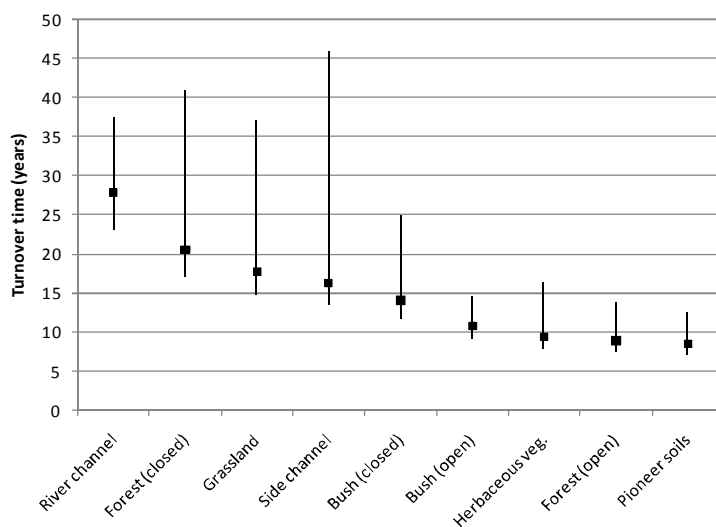


Figure 7.2 Mean and standard deviation of turnover time (years) of Allier ecotopes, based on Table 2.5 in Geerling et al. (2006).

Johnson 1997, Maekawa and Nakagoshi 1997, Yin 1998, Bryant and Gilvear 1999, Merrit and Cooper 2000, Marston et al. 2001, Rumby et al. 2001, Parsons and Gilvear 2002, Freeman et al. 2003, Uribe Larrea 2003, Hooke 2004, Latterell 2006). Greco et al. (2007) found a rejuvenation rate for the Sacramento River (USA) that is comparable to the rate reported in this study, i.e. 141.7 ha yr⁻¹ for 155.95 km or 0.9 ha km⁻¹ yr⁻¹. Although the Sacramento River has a higher discharge and lower mean sinuosity

than the Allier River, and parts of the Sacramento floodplains are covered by riprap, the net rejuvenation rates of both rivers are comparable.

Ecotope transition rates vary per ecotope, depending on both rejuvenation and succession. Along the Allier these rates varied between 18 and 59 percent per 5 years. Figure 7.2 shows the arithmetic mean and standard deviation of ecotope turnover time for the Allier ecotopes (Table 2.5, Geerling et al. 2006). These turnover values provide a quantitative estimate of the spatio-temporal processes identified by Tockner and Stanford (2002) as illustrated in Figure 7.3. The Allier results reach up to the primary and secondary floodplain succession stages, and the area studied is located in the 1 to 100 year flood event. As a consequence of the rejuvenation, half the landscape was younger than 15 years while 24% was older than 46 years.

Data on historical dynamics and floodplain age of reference rivers, such as the Allier in France, can provide a guideline for the reintroduction of natural dynamics in regulated rivers (Middelkoop et al. 2005, Greco 2007). Rejuvenation rates of reference rivers cannot be copied directly to regulated rivers. As a result of

hydromorphological processes, the landscape composition is highly dependent on river scale (Hughes 1997, Richards 2002). Small, dynamic braided systems like the Tagliamento River in Italy exhibit high turnover rates compared to larger rivers like the Allier or Sacramento (Van der Nat 2003, Geerling et al. 2006, Greco et al. 2007). If we assume that the rate of succession in temperate rivers is more or less comparable, than landscape composition mainly depends on rejuvenation. Systems with very high or very low dynamics have relatively low landscape diversity because the majority of the landscape consists of young or mature succession stages, respectively (Richards 2002). Meandering sections of larger rivers, like

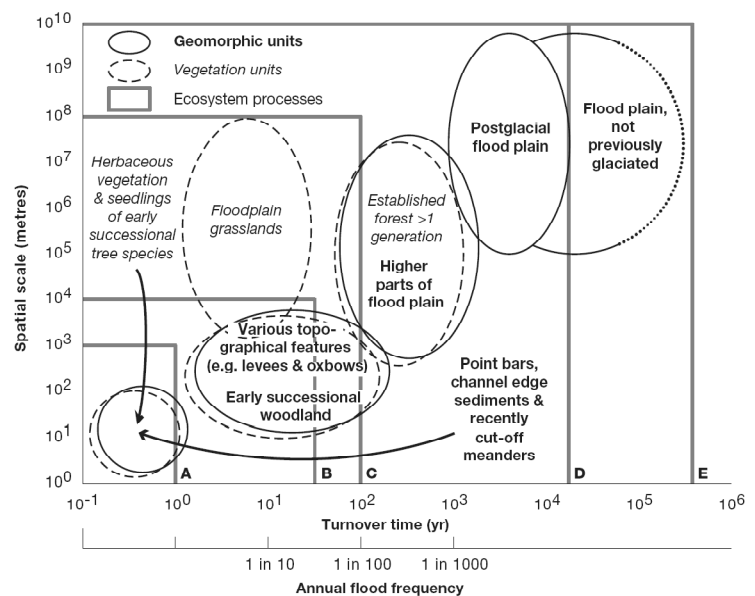


Figure 7.3 The spatiotemporal hierarchy of floodplain components and processes (after Hughes 1997): (A) the primary succession of herbaceous vegetation and early successional woody species, associated with annual floods; (B) primary and secondary floodplain succession, associated with medium-magnitude/frequency floods; (C) long-term floodplain succession, widespread erosion and reworking of sediment, associated with high magnitude/low-frequency floods; (D) species migration upstream/downstream, local species extinction, long-term succession on terraces, and life-history strategies, associated with climate and base-level change, and the influence of postglacial relaxation phenomena on hydrological and sediment inputs to floodplains; and (E) species evolution, and changes in biogeographical range, associated with tectonic change, eustatic uplift and climate change (adapted from Tockner and Stanford 2002).

the Rhine or Meuse, can be assumed to meander more slowly than the Allier and therefore should contain older succession stages. For these systems, the landscape age distribution of the Allier can serve as a maximum for pioneer sites and as a minimum for old floodplain parts. Regarding the types of ecotopes found on young and older parts, the results on the Allier River show that approximately 80% of the pioneer sites was 15 years or younger, whereas substantial parts of the floodplain forest (50%) were 40 years or older. Again, the latter figure could be considered a minimum target for less dynamic systems.

Some authors propose the steady state or meta-climax concept and state that, although a system may be continually disturbed and in succession, it is in balance at an overall (higher) spatial scale level (Amoros and Wade 1996, Merritt 2000, Laterell 2006). This means that, although the ecotope configuration is dynamic at the ecotope level, the overall composition is stable on the river stretch level. Our study showed that within the 50 years of change studied, the steady state or meta-climax concept could be applicable in this system on the scale of about 1.5 to 2 meanders. However, it should be noted that long term trends seem of influence, as the “steady state unit” decreased stepwise from about 2 meanders in the 1950s to about 1.5 in 2000. This decrease was caused by a change towards a more closed and structure rich heterogeneous landscape. A “steady state unit” could be applied as basic management unit for which uniform policies, management practices, monitoring and evaluation methods apply. In Paragraph 7.4 further implications for river restoration are discussed.

7.3 Restoration of regulated rivers

The Dutch Rhine Branches have been extensively regulated (see Chapter 1). Reasoning from a near natural river perspective, hardly anything resembles the landscape pattern and the processes associated with a natural dynamic river (Ward et al. 2001). It is often unfeasible to restore a regulated river to its pristine conditions. However, it may be partly restored by the partial reintroduction of natural dynamic processes (Buijse et al. 2002, Van der Velde et al. 2006). Studies on the landscape evolution of rejuvenated nature restoration sites in a regulated river are scarce. Available studies are mostly based on expert knowledge, like the modelling study undertaken by Baptist et al. (2004). The case study on the Ewijk floodplain (Chapter 3) represents a restoration attempt within the present context of the river environment. The floodplain was artificially rejuvenated by setting back sedimentation (excavation) and by creating pioneer soils. The landuse reverted from agriculture to no-interference, or, as defined in Dutch policy documents, to “process nature” (Peters et al. 2006).

Our study showed that excavation of an agricultural floodplain and changing the landuse rehabilitated natural levee-forming processes and ecological succession. Excavation led to settlement and subsequent growth of softwood forest species. In

the first 7 years, the development of bare soil to softwood bush and softwood forest was clearly visible. Within 10 years, the overall landscape diversity and patch heterogeneity increased to a level higher than before excavation. Many species returned to the area (Helmer 1990, Helmer et al. 1991, Bosman 1992, Bosman 1994, Bosman 1995, Bosman and van der Veen 1996, Bosman and Sorber 1997). Although not directly examined in this study, the diversity of habitats is correlated to species diversity and lower channel migration is correlated with lower species diversity (Nilsson et al. 1991, Cordes et al. 1997, Hughes 2001, Hupp et al. 2007). In free flowing rivers, biodiversity varies along the river course and is generally high in middle reaches and especially in meandering sections (Nilsson 1989, Nilsson and Svedmark 2002). Therefore, landscape diversity could be an indicator for biodiversity in formerly meandering regulated middle reaches.

The succession scheme as shown in Chapter 2 for the Allier floodplains is applicable; pioneer stages are replaced by herbaceous and grassland vegetation and bush by forest. Even the spatial pattern of softwood forest settlement on the (rejuvenated) less dynamic shoreline of the old side channel resembles settlement patterns along the Allier. In the research period, succession to stages A and B as shown in Figure 7.3 were reached. However, the excavated system did not show signs of large-scale rejuvenation, not even during two extremely large flooding events.

The amount of sediment deposited returned the sediment level to the pre-excavation level of 1982. The rate of sedimentation was directly related to over bank flow; 40 percent of the total sediment was deposited in two extreme discharge events (i.e., in the years 1993 and 1995). The floodplain's topography developed differently than it did when under agricultural management (i.e. the pre-excavation period). The influence of vegetation, and especially forest, on the local flow velocity and flow direction changed the sedimentation patterns. Levee formation seemed stronger than under previous agrarian management (Figure 3.5, Chapter 3).

A hydraulic model study suggests that flood flow velocities decreased and water surface elevations increased as sediment deposited and vegetation established on the excavated floodplain. After 16 years of landscape evolution, the flood capacity was lower than in the pre-project situation and mean flow velocities dropped 14% below the pre-project situation. The rate of change diminished in time and flow velocity change was strongly correlated to landscape diversity.

The Ewijk case study showed that: (1) natural succession out of an artificially created pioneer situation is possible and results in a diverse landscape, (2) sedimentation patterns vary due to changing vegetation patterns, and (3) the combined succession and sedimentation affects the local discharge capacity. Therefore, if applied on a large scale, floodplain restoration in embanked systems may threaten flood safety, especially if the existing embankments are dimensioned to accommodate floods over low hydraulic resistance agrarian floodplains such as the embankments that evolved along the Rhine in the past 500 years (Van der Ven 2003). Continuous management is required, of which the intensity depends on the restoration targets defined, rates of

floodplain change and the storage space between the embankments for accommodating floods. The next paragraph discusses the findings of the first two studies and proposes a 'temporal discontinuity' hypothesis for regulated rivers.

7.4 Temporal discontinuity and restoration in regulated rivers

A natural dynamic system depends on the balance of processes that determine landscape change. In a simplified manner, it can be considered a balance between succession and rejuvenation. In the following, it is assumed that the Allier case is an ideal case of steady state dynamics, regardless of long-term changes such as geological, climate change or shifts in landuse. The river dynamics continuously removes older succession stages and establishes pioneer soils where succession starts over, resulting in a mosaic landscape of succession stages of various ages, analogous to Figure 3.7 of Chapter 3. Based on the results of the Allier study, the distribution of floodplain age in the active river corridor can be conceptualised as in Figure 7.4. Here, floodplain age is defined as the time in years since the last rejuvenation event. The relative area of older succession stages depends on the floodplain boundary; in this example a hypothetical flood area with a flood frequency of historical timescale (<100 years) is chosen, similar to the area of the Allier study.

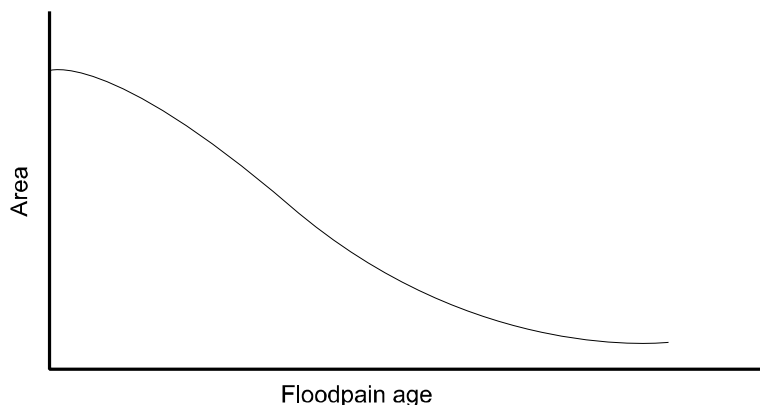


Figure 7.4 Conceptual graph of a hypothetical area versus age distribution in the active corridor of a meandering river.

Suppose the river is regulated and dynamics are strongly inhibited, as shown in Figure 3.2 of Chapter 3. Rejuvenation ceases while succession continues, and thus the overall landscape age increases. The landscape composition changes dramatically in favour of species typical for less dynamic habitats, as was shown and discussed in several studies (Petts and Amoros 1996, Johnson 1997, Hughes 2001, Marston et al. 2001, Tockner and Stanford 2002). It takes some time for effects to become visible in the landscape. An observed high biodiversity is often a relict of former conditions that will develop towards a lower diversity and a shift in landscape composition (Bravard et al. 1986, Tockner and Stanford 2002). In such a setting, floodplain age

distribution can develop as shown in Figure 7.5.

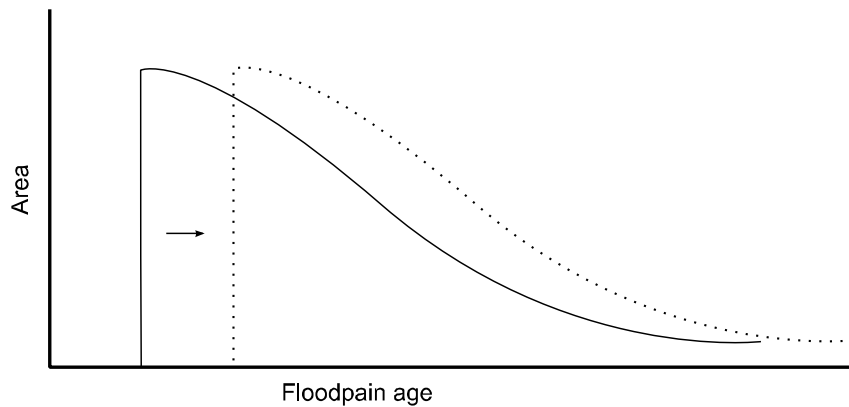


Figure 7.5 Conceptual graph of a hypothetical area versus age distribution of natural ecotopes of a regulated river without rejuvenation. Existing ecotopes continue their succession, while pioneer sites are disappearing.

In addition to rejuvenation, succession will also cease if landuse in the floodplains is (partially) changed towards agriculture, as is the case along most rivers in populated areas. Some ecotopes will be converted to pastures or fields, others will remain nature. The latter will become relic ecotopes that stay in ecological succession, e.g. relic disconnected side channels. Such a landscape has ‘gaps’ in its age distribution; it is a *temporal discontinuous landscape* (Figure 7.6). Although not indicated in the figure the ecotopes move towards older succession stages, similar to developments in Figure 7.5.

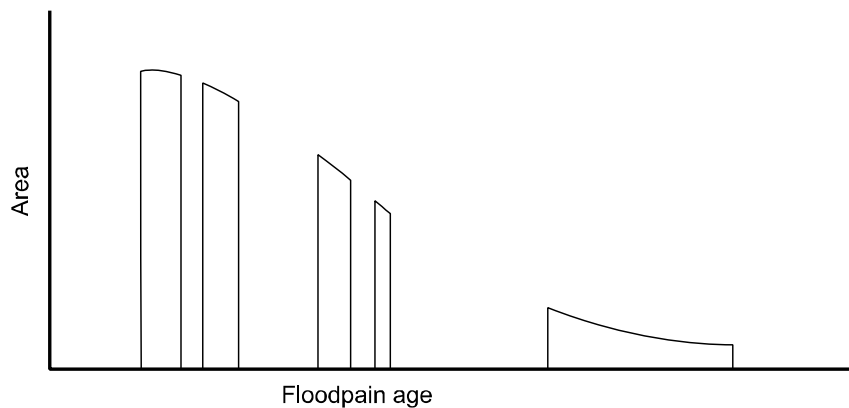


Figure 7.6 Conceptual graph of a hypothetical area versus age distribution of natural ecotopes in regulated river floodplains without rejuvenation and with landuse changed to agriculture.

Restoration of a temporal fragmented landscape depends foremost on the constraints that apply to the floodplain use. The concept in restoration practise is to ‘let the river do the work’; in this case, to activate rejuvenation processes (Stanford et al. 1996). Generally, three degrees of restoration are recognised (FISRWG 1998):

- “Non-intervention and undisturbed recovery: where the stream corridor is recovering rapidly and active restoration is unnecessary and even detrimental.”

- “Partial intervention for assisted recovery: where a stream corridor is attempting to recover, but is doing so slowly or uncertainly. In such a case, action may facilitate natural processes already occurring.”
- “Substantial intervention for managed recovery: where recovery of desired functions is beyond the repair capacity of the ecosystem and active restoration measures are needed.”

In highly regulated systems, probably not all processes can be restored. Therefore, “substantial intervention for managed recovery” is needed (Amoros et al. 1987, Geerling et al. 2008). If socio-economic possibilities exist to revert landuse from agriculture to no-intervention zones, at least some processes can be restored (Geerling et al. 2008). To sustain a presence of pioneer situations and create a temporal continuous and diverse landscape, artificial rejuvenation may be applied as a management strategy. In time, depending on how discontinuous the landscape initially was, a cascade of pioneer sites, set off at different years, will contribute to a temporally more continuous river stretch with all succession stages present, and landscape diversity will increase. This strategy is called Cyclic Floodplain Rejuvenation (CFR, Smits et al. 2000, Duel et al. 2001, Baptist et al. 2004). CFR can be regarded as a special case of restoration management, applied in river stretches that do not allow full restoration of rejuvenation processes. Some prerequisites for successful implementation of CFR are:

- To consider the riverine landscape as a system that is in dynamic equilibrium (Petts and Amoros 1996). On small spatial and time scales, change is prominent. On larger spatial (river stretch) and time (10-100 years) scales, a quasi-equilibrium can be possible (Petts and Amoros 1996, Geerling et al. 2006).
- Manage river stretches of similar nature as a whole. If possible, define a “steady state unit” as the basic management unit for which uniform policies, management practices, monitoring and evaluation methods apply (see Section 7.2).

Suppose CFR has to be implemented in a highly regulated river, what should be done? Define the management actions needed based on a comparison of the present state of the system with the restoration targets set. To assess the present state, identify floodplain age and types of ecotopes. Incorporate present relic natural ecotopes and age, but also include the age, i.e. time since implementation, of existing restoration actions in newly established nature areas. Set restoration targets in terms of floodplain age distribution and a distribution between aquatic and terrestrial habitats in floodplains. Targets can be based on landscape age derived from the river migration pattern from historical maps, see for example Figure 3.2 in Chapter 3 (Middelkoop et al. 2005., Geerling et al. 2006). If these are not present, floodplain age could be derived from reference rivers, such as the Allier River. Although a reference river is never exactly the same, it can provide upper and lower boundaries for floodplain age and ecotope distribution. For example, along the Allier half the floodplain is 15 years or younger, in systems with lower dynamics this figure would

be an upper boundary. Figures showing the per ecotope age distribution of for example floodplain forest are useful for setting restoration targets for ecotopes with longer cycles. Yet, studies that can serve this purpose are scarce (Geerling et al. 2006, Greco et al. 2007). Furthermore, it is assumed that succession from a pioneer situation in a regulated system is similar compared to succession in a natural system, but this is not necessarily true (Bravard et al. 1986, Leyer 2005). Studies similar to the one presented in Chapter 3, but on a larger scale are needed to gather empirical data on landscape evolution in a regulated setting. Until then, CFR seems a perfect case for the Adaptive Management strategy, managing and evaluating in cycles while increasing system knowledge step by step (Walters 1997). A lot of river restoration projects have been carried out without prior knowledge but have greatly contributed to our present understanding of river systems (Buisse et al. 2002).

What kinds of management actions are applicable? Some guidelines can be derived from Chapters 2 and 3. An important rejuvenation process in naturally meandering rivers is the formation of pointbars on convex (inner) bends, which subsequently develop by succession and sedimentation. The excavation of a regulated floodplain as shown in Chapter 3 creates similar starting conditions. In freely meandering rivers, water bodies can follow different succession paths according to their different degrees of connection to the main channel (Large et al. 1996, Amoros and Wade 1996). Connection degrees vary, e.g. permanently connected side channels, channels cut off at the upstream part, channels semi-connected at higher flood levels, and abandoned side channels (oxbow-lake, Greenwood and Richardot-Coulet 1996, Hooke 2004). Figures 2.4 and 2.5 in Chapter 2 show the formation and development of an oxbow lake and semi-connected floodplain depressions, respectively. These gradients of hydrological connectivity are typical for riparian landscapes and important for biodiversity (Large et al. 1996, Tockner et al. 1999). For example, water table fluctuations in water bodies are correlated with macrophyte richness, but water table amplitude diminishes in older water bodies. This may over time lead to a decline in hydrologically dynamic lakes (Van Geest et al. 2005). Digging lakes and side channels in various stages of connectivity alongside regulated rivers, either new or by following old topography, is a way to create these aquatic ecotopes and conserve their successional sequence (Simons 2001, Buijse et al. 2002, Van Geest et al. 2005, Peters et al. 2006).

Nature restoration is only served when temporal landscape diversity is ensured and repeated management actions, i.e. rejuvenation, are heterogeneously distributed in space. In a fixed system, the choice for a restoration site might not be that straightforward. Site selection is difficult and is subject of ongoing study. Firstly, based on restoration targets set (age, distribution), the spatial distribution of the rejuvenation problem may be simplified to target ecotopes that need to be rejuvenated or, in contrast, need to be preserved (no-rejuvenation areas). Secondly, some broad guidelines derived from the functioning of natural rivers can be applied. For example, older riparian areas are generally located on concave (outer) banks and

in less hydrodynamic areas whereas younger areas are located on convex (inner) banks experiencing higher hydro-dynamics (Steiger and Gurnell 2003, Knighton 1997). The fixed river channel also spatially confines some processes, such as sedimentation of coarse material that is deposited directly adjacent to the main channel (Knighton 1997). It can be reasoned that in a fixed channel, management cycles close to the river are faster than farther away. Additionally, other practical reasons may guide to a specific location as well. Chapter 3 showed that impacts on discharge could be expected within a timeframe of 7 to 16 years. Therefore, in cases where space to accommodate floods is limited due to artificial or natural embankments, the hydraulic effects of floodplain restoration can be unacceptable for society. To enhance the discharge capacity, the rejuvenation site, the kind, and magnitude of the management action can be adapted. A model study by Baptist et al. (2004) showed that CFR could be of benefit to both flood protection and nature restoration.

A practical guidebook to cyclic management of floodplains has been published as part of this research project in which examples of CFR and its policy implications are elaborated for the Dutch situation based on the theory above (Peters et al. 2006). The book is based on scientific insights and expert knowledge from various actors, i.e. the Dutch river authority (Rijkswaterstaat), the State Forestry Service (Staatsbosbeheer) and the Ark Foundation. The guidebook is intended to serve as a starting point for implementation of CFR in practice, and hopefully will be further improved and scientifically underpinned in the near future. The guidebook can be downloaded from www.cyclischbeheer.nl.

7.5 Monitoring of floodplain vegetation

Maps are often used to monitor the ecological status of river floodplains, e.g. within the context of flood safety and nature management (De Nooij et al. 2004, 2006). Because floodplains are dynamic by nature, maps that provide information on these areas are quickly outdated, see maps in Chapters 2 and 3. In regulated systems, the floodplain location may not change, but the unmanaged vegetation cover may change due to succession. Restoration practices, such as Cyclic Floodplain Rejuvenation (CFR), require periodical monitoring of the floodplain cover in order to check whether the hydraulic resistance of the vegetation does not impair flood safety, and whether the nature management targets are realised. The hydraulic impact of floodplain cover is calculated using models in which the vegetation structure is an important aspect (Baptist et al. 2004, 2007). Therefore, accurate and up to date information about floodplain cover is a necessity for river research and management. Traditionally and in the ecotope mapping process presently used by the Dutch river authority, vegetation is manually delineated and characterised by its colour, texture, tone, shape and 3D structure using stereographic analogue aerial images (Jansen and Backx 1998, De Jong et al. 2004). The processing time and the amount of untraceable

human errors can be reduced by automatic classification of data from digital sensors (Mertes 2002, Pietroniro and Leconte 2005). The usage of these sensors became more feasible because the sensors became more sensitive to light over the last 3 decades, which facilitated a reduction in recorded pixel size and the registration of smaller sections (bands) of the electromagnetic spectrum. Furthermore, newly developed sensors such as Light Detection And Ranging (LiDAR) sense additional physical properties of objects. Therefore, it was reasoned that to match human interpretation of stereographic images, the RS data used for floodplain classification in this study should consist of both spectral data and data on vegetation structure. The sensors applied were the Compact Airborne Spectrographic Imager (CASI) and airborne (LiDAR) or Airborne Laser Scanning (ALS). Chapter 4 gives more information on CASI and LiDAR applications. The use of both data types in one classification could be synergetic (Gilvear et al. 2004, Leckie et al. 2005).

The combined use of two or more digital images is generally called data fusion. Three types of data fusion can be distinguished: the pixel level, the feature level and the decision level (Figure 7.7, Pohl and van Genderen 1998).

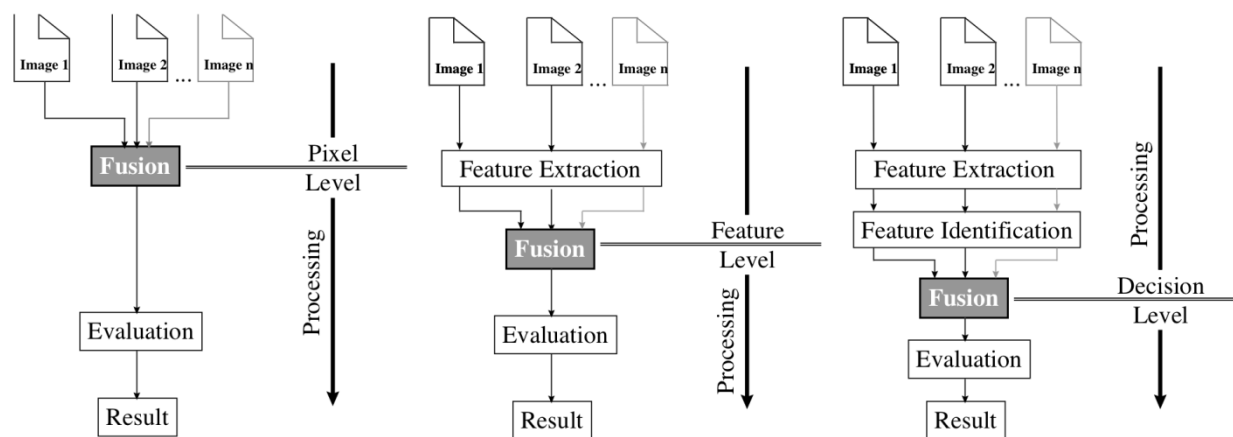


Figure 7.7 Schematic illustration of three different levels of data fusion for digital RS images: the pixel level (left), the feature level (middle) and the decision level (right). Taken from Pohl and van Genderen (1998)

Theoretically, all three methods could be applied to combine LiDAR and CASI data. An example of fusion at the decision level is a combination of a vegetation map based on CASI with a vegetation height map based on LiDAR. The resulting map could contain classes like woodland higher than 5 metres and woodland lower than 5 metres, etc. Fusion at the feature level takes place when features are extracted from the two data sources separately, and the properties of these features, such as mean colour or height, are used to statistically classify the (intersected) features. Often, when fusing spectral and LiDAR data, only the spectral features are used to extract image objects and the object's LiDAR statistics are added separately (Hill et al. 2002, Wulder and Seemann 2003). In the pixel level approach the combined data is used straight from the first step in the process. Although all fusion approaches are valid, fusion at the pixel level is the most straightforward and the resulting image can be

applied directly to classify image pixels or extract and classify image objects (Gilvear et al. 2004, Straatsma 2006, Geerling 2007).

Three chapters in this thesis reported on classification results of fused LiDAR and CASI data. The classifications are pixel and object based. Whereas class composition was optimised for the pixel-based classifications, the classes applied in object-based classification were fixed. Table 7.1 shows the overall best results of the various classification attempts.

Table 7.1 Summary of best classification results of LiDAR, CASI and fused LiDAR+CASI data sets as reported in Chapters 4, 5 and 6. “Pixel” refers to pixel-based classification. “Objects” refers to object-based classification.

	Pixel (8 class)	Pixel (5 class)	Pixel (8 class, optimised)	Pixel (7 class, optimised)	Objects (10 class)
LiDAR data	37%	41%	-	-	55%
CASI data	58%	74%	-	-	66%
LiDAR+CASI data	64%	81%	71%	74%	74%

The fused image consistently gave higher classification results than the single CASI or LiDAR images in both pixel and object based classification. Results of fused images were 6 to 8 percent higher compared to the CASI image, and 20 to 40 percent higher compared to the LiDAR image. Other studies that fuse spectral and LiDAR data report increases of 8 to 14% compared to the original spectral image (Gamba and Houshmand 2002, Mundt et al. 2006, Waske et al. 2007). Further advantages of using both spectral and LiDAR data were improved classification of shadows and the superior ecotope delineation when used in object segmentation. Therefore, combination of spectral and LiDAR data for vegetation mapping is advisable for both pixel and object segmentation approaches, especially in areas rich in vegetation structure. Three topics that influence results are discussed: the size of LiDAR data samples and segmented objects, optimisation of class composition and pixel-based versus object-based classification.

In Chapter 4, the neighbourhood in which laser points were collected for statistical transformation in a raster based map proved to influence classification results. An overall optimum was found at 4 m radii around CASI pixels. A basic constraint is the density of recorded LiDAR points. Higher LiDAR densities can provide more data on the sensed objects, although the footprint of LiDAR beams, 0.1-0.3 m for small footprint systems, ultimately limits this (Baltavistas 1999). The prediction of vegetation structure for herbaceous vegetation did not improve using point densities greater than 30 points m⁻² (Straatsma 2007). However, in this study, the optimal radius varied per vegetation class. This relation between appropriate and inappropriate sample sizes and descriptive statistics is recognised as the Modifiable Area Unit Problem (MAUP), of which remote sensing is a special case (Hay et al. 2003, Hay and Marceau 2004). Digital remote sensing images consist of landscape

properties captured in a rectangular grid (similar to a photographic image) or in this case a radius of certain size, real life objects can be larger or smaller than this fixed grid. Properties of pixels or RS objects that inappropriately sample real life objects may lead to suboptimal classification results. The sampling size used to derive LiDAR statistics could be differentiated to optimise classification of different kinds of floodplain vegetation.

Also in the object-based classification results, object size influenced classification results: larger objects led to lower overall accuracy but single class accuracies behaved differently (Chapter 6, see also p.95 in Geerling 2007). Differentiation of object scale by class type could improve classification robustness, as objects are classified at their appropriate scale. Furthermore, many surveying disciplines recognise that landscapes are multi-scale by nature and use hierarchical classification systems for mapping (Hay et al. 2003, De Jong et al. 2004, Benz et al. 2004). For example, grasslands in various stages of succession vary in their content of non-grassland patches; often these are patches of herbaceous vegetation. Incorporating these sub-ecotopes into the ecotope classification scheme could improve ecotope classification. This can be especially beneficial in landscapes that transform from agriculture to heterogeneous restored nature.

A major factor influencing classification results consists of the actual classes applied in classification (Mather 2004, Chapter 4). As shown in Chapter 4, the overall accuracy increases with a decreasing number of classes. The classes used in Chapter 4 were selected on the basis of vegetation structure, but other classification schemes are possible. However, a classification scheme set based on superior classification results only can be useless if the ontology of the classes is not clear (Comber et al. 2005). Class composition was altered based on clustering and ordination techniques using data on plant species, abundance and environmental factors that can influence the spectral signature of the vegetation class. Class composition could be optimised while maintaining ecological and syntaxonomical significance.

Whether to use pixel based or object based classification is related to the issue of MAUP. Often, segmentation results (i.e. object based classification) are preferred because they relate to human interpretation of aerial images, result in a vector map and can be applied in hierarchical classification schemes (Benz 2004, Blaschke et al. 2004). Furthermore, in contrast to pixels, the segmented objects have properties based on its emergent shape that could improve classification (Hay 2003, Blaschke et al. 2004). However, if maps are used in (hydraulic) model studies, there is no argument to reject a grid-based classification as most hydraulic models use a computational grid. The grid cells in Figure 3.8 in Chapter 3 are about 30x30 m, and larger than small patches of vegetation. Vegetation maps are abstracted to values per grid cell; in effect, the grid size of (hydraulic) models introduces an extra MAUP. Basically, what map to choose depends on the use. Detailed grid maps such as shown in Chapter 4 are useful in determining gradients within ecotopes or vegetation structures (see for example Schmidlein et al. 2007). Ecotope maps, such as produced

in Chapter 6, are useful in planning and management on the floodplain and river stretch scale because they visually simplify the landscape.

7.6 General conclusions and recommendations

The Allier case study provided results that are in line with the steady state or meta-climax concept. It was shown that the dynamic system of the Allier is in a steady state at a spatial scale level of approximately 1.5 to 2.0 meanders. This spatial scale level seems a suitable unit to manage floodplains in accordance with the concept of Cyclic Floodplain Rejuvenation. It is advised that similar case studies are performed for other (semi) natural rivers in order to reveal systematic patterns of floodplain age and ecotope distribution that relate to general river parameters like discharge capacity and sinuosity.

The Ewijk Restoration case study dealt with floodplain rejuvenation along a regulated river. A hydraulic model study showed that flow velocities decreased and water table increased as sediment deposited and vegetation established on the excavated floodplain. After 16 years, the discharge capacity was lower than in the pre-excavation situation and the mean flow velocities dropped by 14%. If not managed adequately, these spontaneous processes may threaten flood safety. Based on the Ewijk Floodplain and Allier case studies, it can be concluded that Cyclic Floodplain Rejuvenation is a process that needs to be carefully planned in space (i.e. taking the steady state level into consideration) and in time (i.e. the periodicity depends on factors such as sedimentation rate, flood safety objectives and nature restoration targets). As more data is required on the appropriate spatial and temporal dimensions of Cyclic Floodplain Rejuvenation, the implementation of Adaptive Management is advised to ensure that management actions taken are used as case studies on the spontaneous development of rejuvenated sites. Furthermore, response of flora and fauna (or biodiversity) to various artificial rejuvenation methods should be monitored.

The spontaneous processes involved Cyclic Floodplain Rejuvenation (i.e. sedimentation and succession) require regular monitoring in order to check compliance with flood safety and nature targets. It was shown that current monitoring techniques based on analogue stereographic images can be substantially improved using new remote sensing and data fusion techniques, e.g. the fusion of CASI and LiDAR images on the pixel level and the subsequent application of pixel-based or object-based classification algorithms. Furthermore, optimising vegetation class composition with environmental parameters and applying a hierarchical classification system can improve classification accuracy and robustness. It is advised that river authorities apply these state-of-the-art monitoring techniques on a regular basis in order to support the implementation of Cyclic Floodplain Rejuvenation projects.

References

- Acreman MC, Riddington R., Booker DJ (2003). Hydrological impacts of floodplain restoration: a case study of the River Cherwell, UK. *Hydrology and Earth System Sciences* **7**: 75-85.
- Amoros C, Rostan J-C, Pautou G, Bravard J-P (1987). The reversible process concept applied to the environmental management of large river systems. *Environmental Management* **11**: 607-617.
- Amoros C, Wade PM (1996). Ecological successions. In: Petts GE, Amoros C (1996). *Fluvial Hydrosystems*. London, Chapman & Hall. pp. 211-241.
- Baltsavias EP (1999). Airborne laser scanning: existing systems and firms and other resources. *ISPRS Journal of Photogrammetry & Remote Sensing* **54**: 164-198.
- Baptist MJ, Babovic V, Rodriguez Uthurburu J, Keijzer M, Uittenbogaard RE, Mynett A, Verwey, A (2007). On inducing equations for vegetation resistance. *Journal of Hydraulic Research* **45**: 435-450
- Baptist MJ, Penning WE, Duel H, Smits AJM, Geerling GW, van der Lee GEM, van Alphen JSL (2004). Assessment of the effects of Cyclic Floodplain Rejuvenation on flood levels and biodiversity along the Rhine River. *River Research & Applications* **20**: 285-297.
- Benz UC, Hofmann P, Willhauck G, Lingenfelder I, Heynen M (2004). Multi-resolution, object-oriented fuzzy analysis of remote sensing data for GIS-ready information. *ISPRS Journal of Photogrammetry & Remote Sensing* **58**: 239-258.
- Blaschke T, Burnett C, Pekkarinen A (2004). Image Segmentation Methods for Object-based Analysis and Classification. In: De Jong SM, Van der Meer FD (Eds.), *Remote sensing image analysis: including the spatial domain*. Kluwer Academic Publishers, Dordrecht, pp. 211-236.
- Bosman W (1992). *Ewijkse plaat. Jaarverslag 1991*. Laag Keppel, Stichting Ark.
- Bosman W (1994). *Ewijkse plaat. Jaarverslag 1992-1993*. Laag Keppel, Stichting Ark.
- Bosman W (1995). *Ewijkse plaat. Jaarverslag 1994*. Laag Keppel, Stichting Ark.
- Bosman W, Sorber A (1997). De Ewijkse Plaat; Natuurontwikkeling in relatie tot overstroming en begrazing. *Landschap*. **14**: 131-146.
- Bosman W, van der Veen J, (1996). *Ewijkse plaat. Jaarverslag 1995*. Laag Keppel, Stichting Ark.
- Bravard J-P, Amoros C, Pautou G (1986). Impact of civil engineering works on the successions of communities in a fluvial system. *Oikos* **47**: 92-111.
- Bryant RG, Gilvear DJ (1999). Quantifying geomorphic and riparian land cover changes either side of a large flood event using airborne remote sensing: River Tay, Scotland. *Geomorphology* **29**: 307-321.
- Buijse AD, Coops H, Staras M, Jans LH, van Geest GJ, Grifts RE, Ibelings BW, Oosterberg W, Roozen CJM (2002). Restoration strategies for river floodplains along large lowland rivers in Europe. *Freshwater Biology* **47**: 889-907.

- Comber A, Fisher P, Wadsworth R (2005). You know what land cover is but does anyone else?...an investigation into semantic and ontological confusion. *International Journal of Remote Sensing* **26**: 223-228.
- Cordes L, Hughes FMR, Getty M (1997). Factors affecting the regeneration and distribution of riparian woodlands along a northern prairie river: the Red Deer River, Alberta, Canada. *Journal of Biogeography* **24**: 675–695.
- De Jong SM, Pebesma EJ, van der Meer FD (2004). Spatial variability, mapping methods, Image analysis and pixels. In: De Jong SM, van der Meer FD (Eds.) (2004). *Remote Sensing Image Analysis: Including the spatial domain*. Pg. 17-35.
- De Nooij RJW, Verberk WCEP, Lenders HJR, Leuven RSEW, Nienhuis PH (2006). The importance of hydrodynamics for protected and endangered biodiversity of lowland rivers. *Hydrobiologia* **565**: 153–162.
- De Nooij RJW, Lenders HJR, Leuven RSEW, de Blust G, Geilen N, Goldschmidt B, Muller S, Poudevigne I, Nienhuis PH (2004). BIO-SAFE: Assessing the impact of physical reconstruction on protected and endangered species. *River Research and Applications* **20**: 299–313.
- Duel H, Baptist MJ, Penning WE (2001). *Cyclic Floodplain Rejuvenation. A new strategy based on floodplain measures for both flood risk management and enhancement of the biodiversity of the river Rhine*. Duel H, Baptist MJ, Penning WE. Delft, Netherlands Centre for River Studies. Publication 14-2001.
- Dixon KW, Roche S, Pate JS (1995). The promotive effect of smoke derived from burnt native vegetation on seed germination of Western Australian plants. *Oecologia* **110**: 185-192.
- FISRWG (1998). *Stream Corridor Restoration: Principles, Processes, and Practices*. By Interagency Stream Restoration Working Group. (FISRWG). GPO Item No. 0120-A; SuDocs No. A 57.6/2:EN3/PT.653. ISBN-0-934213-59-3.
- Gamba P, Houshmand B (2002). Joint analysis of SAR, LIDAR and aerial imagery for simultaneous extraction of land cover, DTM and 3D shape of buildings. *International Journal of Remote Sensing* **23**: 4439 –4450.
- Geerling GW, Van den Berg GJ (2002). *Monitoring and Dynamic River Management*. Department of Environmental studies, section nature management of river corridors. University of Nijmegen. Ministry of Public Works and Transport, Survey Department, Delft. (In Dutch).
- Geerling GW, Ragas AMJ, Leuven RSEW, van den Berg JH, Breedveld M, Liefhebber D, Smits AJM (2006). Succession and rejuvenation in floodplains along the river Allier (France). *Hydrobiologia* **565**: 71-86.
- Geerling GW (2007). *Nature rehabilitation in regulated rivers. Management and monitoring of floodplain vegetation*. Report no. AGI-2007-GAB-2007b005. Centre for sustainable Management of resources, Radboud University, Nijmegen Adviesdienst Geo-informatie en ICT (AGI), Delft

- Geerling GW, Kater E, van den Brink C, Baptist MJ, Ragas AMJ, Smits AJM (2008). Nature rehabilitation by floodplain excavation: The hydraulic effect of 16 years of sedimentation and vegetation succession along the Waal River, NL. *Geomorphology* **99**: 317-328.
- Gilvear D, Tyler A, Davids C (2004). Estuarine, Detection of estuarine and tidal river hydromorphology using hyper-spectral and LiDAR data: Forth estuary, Scotland. *Coastal and Shelf Science* **61**: 379–392.
- Hay GJ, Blaschke T, Marceau DJ, Bouchard A (2003). A comparison of three image-object methods for the multiscale analysis of landscape structure. *ISPRS Journal of Photogrammetry & Remote Sensing* **57**: 327 – 345.
- Hay GJ, Marceau DJ (2004). Multiscale object-specific analysis (MOSA): An integrative approach for multiscale landscape analysis. In: De Jong SM, van der Meer FD (Eds., 2004). *Remote Sensing Image Analysis: Including the spatial domain*. Pg. 71-92
- Helmer W (1990). *De Ewijkse Plaat: Jaarverslag 1989*. Laag Keppel, Sichting ARK.
- Helmer W, Litjens G, Overmars W (1991). *De Ewijkse Plaat. Jaarverslag 1990*. Laag Keppel, Stichting ARK.
- Hill RA, Smith GM, Fuller RM, Veitch N (2002). Landscape modelling using integrated airborne multi-spectral and laser scanning data. *International Journal of Remote Sensing* **23**: 2327 –2334.
- Hooke JM (2004). Cutoffs galore!: occurrence and causes of multiple cutoffs on a meandering river. *Geomorphology* **61**: 225-238
- Hughes FMR, Adams WM, Muller E, Nilsson C, Richards KS, Barsoum N, Decamps H, Foussadier R, Girel J, Guillois H, Hayes A, Johansson M, Lambs L, Pautou G, Péiry J-L, Perrow M, Vautier F, Winfield M (2001). The importance of different scale processes for the restoration of floodplain woodlands. *Regulated Rivers: Research & Management* **17**: 325-345.
- Hupp CR, Rinaldi M (2007). Riparian Vegetation Patterns in Relation to Fluvial Landforms and Channel Evolution Along Selected Rivers of Tuscany (Central Italy). *Annals of the Association of American Geographers* **97**: 12–30.
doi:10.1111/j.1467-8306.2007.00521.x
- Jansen BJM, Backx JJGM (1998). *Biologische monitoring zoete rijkswateren. Ecotopenkartering Rijntakken-Oost 1997*. Report No. RIZA rapport 98.054 (ISBN 9036952085). Ministry of Transport, Public Works and Water Management. Institute for Inland Water Management and Waste Water Treatment (RIZA), Lelystad.
- Johnson WC (1997). Equilibrium response of riparian vegetation to flow regulation in the platte river, nebraska. *Regulated rivers: Research & Management* **13**: 403-415.
- Junk WJ, Bayley PB, Sparks RE (1989). The flood pulse concept in river-floodplain system. *Canadian special publications of fisheries and aquatic sciences*.
- Large ARG, Petts GE (1996a). Historical channel-floodplain dynamics along the River Trent. *Applied Geography* **16**:191-209.

- Large ARG, Pautou G, Amoros C (1996b). Primary production and primary producers. In: Petts GE, Amoros C (1996). *Fluvial Hydrosystems*. London, Chapman & Hall: 117-136.
- Leuven RSEW, Pourdevigne I, Teeuw RM (2002). Remote sensing and Geographic Information Systems as emerging tools for riverine habitat and landscape evaluation: from concepts to models. In: Leuven RSEW, Pourdevigne I, Teeuw RM (Eds.). *Application of Geographic Information Systems and Remote Sensing in River Studies*. Backhuys Publishers, Leiden.
- Maekawa M-a, Nakagoshi N (1997). Riparian landscape changes over a period of 46 years, on the Azusa River in Central Japan. *Landscape and Urban Planning* **37**:37-43.
- Marston RA, Girel J, Pautou G, Piegay H, Bravard, J-P, Arneson C (1995). Channel metamorphosis, floodplain disturbance, and vegetation development: Ain river, France. *Geomorphology* **13** :121-131.
- Mather PM (2004). *Computer processing of remotely sensed images, an introduction*. Chichester, West Sussex, England, John Wiley & Sons Ltd.
- Middelkoop H, Schoor MM, Wolfert HP, Maas GJ, Stouthamer E (2005). Targets for ecological rehabilitation of the lower Rhine and Meuse based on a historic geomorphologic reference. *Archiv für Hydrobiologie - Supplement* **155**: 63-88.
- Mertes LAK, Daniel DL, Melack JM, Nelson B, Martinelli LA, Forsberg BR (1995). Spatial patterns of hydrology, geomorphology, and vegetation on the floodplain of the Amazon River in Brazil from a remote sensing perspective. *Geomorphology* **13**: 215-232.
- Mertes LAK (2002) Remote sensing of freshwater riverine landscapes: an update. *Freshwater biology* **47**: 799-816.
- Kooistra L, Wehrens R, Leuven RSEW, Buydens LMC (2001). Possibilities of visible-near-infrared spectroscopy for the assessment of soil contamination in river floodplains. *Analytica Chimica Acta* **446**:97-105.
- Leyer I (2005). Predicting plant species responses to river regulation: the role of water level fluctuations. *Journal of Applied Ecology* **42**: 239–250.
- Nilsson C, Grelsson G, Dynesius M, Johansson M, Sperens U (1991). Small rivers behave like large rivers: effects of post-glacial history on plant species richness along riverbanks. *Journal of Biogeography* **18**: 533–541.
- Parsons H, Gilvear D (2002). Valley floor landscape change following almost 100 years of flood embankment abandonment on a wandering gravel-bed river. *River research and applications* **18**: 461-47.
- Peters BWE, Kater E, Geerling GW (2006). *Cyclisch beheer in uiterwaarden, natuur en veiligheid in de praktijk*. Gezamenlijke uitgave van het Centrum voor Water en Samenleving, Radboud universiteit Nijmegen; Staatsbosbeheer; Stichting Ark en Rijkswaterstaat. ISBN13 978 90 810586 1 2. 206 pages.

- Piégay H, Salvador P-G (1997). Contemporary floodplain forest evolution along the middle Ubaye river, Southern Alps, France. *Global Ecology and Biogeography Letters* **6**: 397-406.
- Pohl C, van Genderen JL (1998). Multisensor image fusion in remote sensing: concepts, methods and applications. *International Journal of Remote Sensing* **19**: 823-854.
- Schmidtlein S, Zimmermann P, Schüpferling R, Weiß C (2007). Mapping the floristic continuum: Ordination space position estimated from imaging spectroscopy. *Journal of Vegetation Science* **18**: 131-140.
- Smits AJM, Havinga H, Marteijs ECL (2000). New concepts in river and water management in the Rhine river basin: how to live with the unexpected? In: Smits AJM, Nienhuis, PH, Leuven RSEW (Eds., 2000). *New approaches to river management*. Backhuys Publishers, Leiden. pp. 267-286.
- Steiger J, Gurnell AM (2002). Spatial hydrogeomorphological influences on sediment and nutrient deposition in riparian zones: observations from the Garonne River, France. *Geomorphology* **49**: 1 – 23.
- Straatsma MW, Middelkoop H (2006). Airborne laser scanning as a tool for lowland floodplain vegetation monitoring. *Hydrobiologia* **565**: 87-103.
- Straatsma MW (2007). *Hydrodynamic roughness of floodplain vegetation: Airborne parameterization and field validation*. PhD thesis, Utrecht University, Utrecht.
- Strahler AN, Strahler A (2003). *Introducing physical geography*. John Wiley and Sons, inc., New York.
- Keeley JE (1987). Role of Fire in Seed Germination of Woody Taxa in California Chaparral. *Ecology* **68**: 434-443.
- Tockner K, Malard F, Ward JV (2000). An extension of the flood pulse concept. *Hydrological Processes* **14**: 2861-2883.
- Tockner K, Stanford JA (2002). Riverine floodplains: present state and future trends. *Environmental Conservation* **29**: 308-330.
- Tockner K, Schiemer F, Baumgartner C, Kum G, Weigang E, Zweimueller I, Ward JV (1999). The Danube restoration project: species diversity patterns across connectivity gradients in the floodplain system. *Regulated Rivers: Research and Management* **15**: 245 – 258.
- Uribe-larrea D, Perez-Gonzalez A, Benito G (2003) Channel changes in the Jarama and Tagus rivers (central Spain) over the past 500 years. *Quaternary Science Reviews* **22**: 2209-2221.
- Van Geest GJ, Wolters H, Roozen FCJM, Coops H, Roijackers RMM, Buijse AD, Scheffer M (2005). Water-level fluctuations affect macrophyte richness in floodplain lakes. *Hydrobiologia* **539**: 239-248. Doi: 10.1007/s10750-004-4879-y
- Van der Nat D, Tockner K, Edwards PJ, Ward JV, Gurnell AM (2003). Habitat change in braided floodplains (Tagliamento, NE-Italy). *Freshwater Biology* **48**: 1799-1812.

- Van der Velde G, Leuven RSEW, Ragas AMJ, Smits AJM (2006). Living rivers: trends and challenges in science and management. *Hydrobiologia* **565**: 359-367.
- Van de Ven GP (2004). *Man-made lowlands. History of water management and land reclamation in the Netherlands*. Stichting Matrijs, Utrecht.
- Walters C (1997). Challenges in adaptive management of riparian and coastal ecosystems. *Conservation Ecology* [online] **1**:1. Available from the Internet. <http://www.consecol.org/vol1/iss2/art1/>
- Ward JV (1998). Riverine landscapes: biodiversity patterns, disturbance regimes, and aquatic conservation. *Biological Conservation* **83**: 269-278.
- Ward JV, Malard F, Tockner K (2002). Landscape ecology: a framework for integrating pattern and process in river corridors. *Landscape Ecology* **17**: 35-45.
- Ward JV, Tockner K, Uehlinger U, Malard F (2001). Understanding natural patterns and processes in river corridors as the basis for effective river restoration. *Regulated Rivers: Research & Management* **17**: 311-323.
- Waske B, Menz G, Benediktsson JA (2007). Fusion of support vector machines for classifying SAR and multispectral imagery from agricultural areas. *Proceedings IEEE Geoscience and Remote Sensing Symposium*, 2006, Barcelona, Spain.
- Wouters B, Nijssen M, Geerling GW, van Kleef HH, Verberk WCEP, Esselink H (in prep.) Temporal changes in vegetation composition and patch size distribution: Effects of grazing management on sand lizards (*Lacerta agilis*) habitats in Dutch dunes.
- Wulder MA, Seemann D (2003). Forest inventory height update through the integration of lidar data with segmented Landsat imagery. *Canadian Journal of Remote Sensing* **29**: 536-543.

Summary

In natural rivers, channel movement and sedimentation rejuvenate ecological succession stages allowing pioneer stages to co-exist with old floodplain forest. In most regulated rivers, these processes are influenced by regulation measures such as groins and levees that prevent lateral channel movement and confine the sedimentation area. Moreover, the floodplain landscape is largely used for agriculture; natural elements present are mostly remnants of the past. In the 1980s, nature restoration plans were presented for Dutch Rhine floodplains that promoted the reintroduction of natural processes replacing (scanty) agriculture uses. However, as rejuvenation processes are hampered by the regulation measures, succession will eventually lead to a less diverse landscape. Furthermore, the ability to accommodate large floods is an important function of regulated rivers and can be compromised by a changing floodplain cover. The main aim is to support the understanding and management of natural and regulated rivers using GIS and remote sensing tools, two components are: (1) to contribute new data and insights on floodplain and vegetation dynamics of natural and regulated river systems; (2) to develop and test new data fusion techniques and to demonstrate their value for monitoring floodplain and vegetation development along regulated rivers.

The study on the Allier River showed that in meandering systems processes can be categorized as succession or rejuvenation. Riverine nature was constantly rejuvenated by erosive hydro-morphological processes at a rate of about 8 percent of the total area studied per 5 years. The resulting landscape was a mosaic of ecotopes, half the area was 15 years or younger and a quarter 46 years or older. The balance between succession and rejuvenation led to diversity in time and space. While local dynamics had a strong impact on local diversity, e.g. a meander shift destroying part of a forest, the diversity on a scale of 1.5 to 2 meanders seemed to be stable. For example, an emerging forest on a neighbouring location replaces a rejuvenated forest.

Strong erosive rejuvenation processes have disappeared in regulated systems and artificial rejuvenation could be a management strategy to reintroduce pioneer stages. One way of rejuvenation is excavating the top layer of sediment, which was done for the "Ewijkse plaat" (Rhine, the Netherlands). Eleven years after the artificial rejuvenation, the landscape composition was more diverse compared to the previous agricultural situation. After sixteen years, softwood forest and herbaceous vegetation dominated the floodplain cover and the amount of sediment deposited equalled the excavated amount. The sedimentation speed was directly related to the amount of over-bank flow during flood events and significantly higher in forested areas. The resulting floodplain topography differed from the pre-project topography, probably because of the different vegetation composition that influenced local stream velocity. Within the sixteen year research period, 40% of the sediment was deposited during two single high water events (1993/1994 and 1995). Computations using the WAQUA hydraulic model showed that the initial lowering effect on the water table during a

flood was neutralised within seven years after excavation. Post project mean flow velocities have dropped 14 percent below the pre-project situation. No signs of rejuvenation were found during the research period.

The Allier case clearly shows that a natural functioning riverine landscape is based on a balance between succession and rejuvenation on a river stretch scale; i.e. a continuous distribution of floodplain age and ecological succession stages. In this regard, landscape composition in regulated rivers is fragmented (or discontinuous). Data from the “Ewijkse plaat” showed that artificial rejuvenation contributed to nature restoration by creating a diverse semi-natural landscape, but the landscape developments also contributed to a water table rise during floods. Rejuvenation of floodplains can be a viable management strategy to restore continuity of succession stages. Although rejuvenation is a spatially distributed continuous process, it implies constant management on the river stretch scale. Management choices made should be based on accurate and up to date floodplain cover data. For gathering large quantities of spatial data on a frequent and systematic basis, digital remote sensing is the most promising option because of its automatic processing capabilities.

To monitor floodplain vegetation, this study tested the combination of a spectral sensor and airborne LiDAR sensor. The spectral sensor categorises vegetation types on the basis of their colour. The airborne LiDAR sensor categorises vegetation on the basis of their 3D structure. The signals of these sensors were fused by transforming the raw LiDAR data, basically x,y,z points, in an image-like format compatible to the spectral image. The LiDAR density used was about 1.5 elevation measurements per square metre. The LiDAR based image layers were applied successfully as additional bands to the spectral bands in the classification of a semi-natural floodplain (Milingerwaard, River Waal, NL).

Classification was performed at the pixel level and on image objects after initial image segmentation. Classification results at the pixel level showed higher accuracies for the fused image (accuracy of 64% in eight classes and 81% in five classes), raising the spectral result by 6% and the LiDAR result by almost 40%. Especially classification of important hydraulically rough vegetation types improved by using fused data instead of spectral data only. An additional advantage of combining spectral and LiDAR data was information on the structure of vegetation hidden in shadows cast by trees or bushes.

An image segmentation technique was used to test the automated delineation and classification of ecotopes. Results showed that ecotope delineation of the fused image was superior compared to delineations based on LiDAR or spectral data alone.

Classification accuracy of image objects using fused data was 74% for ten classes, 8 to 19% higher than accuracies of the single sensor classifications.

The classes used in the classification determine the classification results. Therefore, to optimise class composition without losing the semantic relation to vegetation, classes were varied based on clustering and ordination techniques that use plant species and abundance data. Results showed that class composition could be optimised on the

basis of botanical data to increase discrimination by their remote sensing properties. In addition to vegetation type and structure, the recorded reflection of sunlight could be influenced by soil type, moist content, etc. The incorporation of these environmental factors in class composition further improved the classification result for floodplain vegetation.

The application of fused CASI and LiDAR data is useful as an instrument for monitoring floodplains and facilitates their active management. Further results of this study show that rejuvenation in meandering rivers leads to continuity in landscape succession stages and steady state conditions on 1.5 to 2 meander lengths. In discontinuous regulated rivers, floodplain vegetation diversity increased after artificial rejuvenation. However, the initially lowered water table also rose. Therefore, cyclic rejuvenation in regulated river stretches appears to be a promising management strategy that can balance nature restoration and flood protection.

Samenvatting

Natuurlijke rivieren verjongen zichzelf doordat meanders zich verleggen als gevolg van erosie- en sedimentatieprocessen. Hierdoor kunnen nieuwe pionierstadia naast oud ooibos ontstaan. In gereguleerde rivieren belemmeren de kades en kribben deze processen, wat leidt tot een verminderde laterale (zijwaardse) erosie en een vastgelegd erosie –en sedimentatiepatroon. In een gereguleerd systeem stopt de aanwas van jonge natuur en verdwijnen pioniersoorten uit het ecosysteem.

In de jaren 80 werd een aantal natuurontwikkelingsplannen voor de grote rivieren in Nederland gelanceerd met als doel het herstel van natuur en natuurlijke processen in de tot dusver agrarisch beheerde uiterwaarden. Dit beleid heeft tot grote arealen “uiterwaardennatuur” geleid waarbij de ontwikkeling van struwelen en zachthoutooibos weer een kans kreeg. Dat was goed voor de natuur maar diezelfde vegetatie zorgde er ook voor dat de waterafvoercapaciteit van de rivieren verminderde. Het natuur-veiligheidsdilemma was geboren.

Het doel van dit proefschrift is om de kennis met betrekking tot de processen en het beheer van natuurlijke en gereguleerde rivieren te bevorderen, met als componenten: (1) het verkrijgen en onderbouwen van inzicht in uiterwaarddynamiek door het bestuderen van (semi-)natuurlijke en gereguleerde riviersystemen; (2) het ontwikkelen en testen van nieuwe datafusie technieken om uiterwaardvegetatie van intensief beheerde rivieren automatisch te kunnen karteren.

De eerste studie uit dit proefschrift richt zich op een semi-natuurlijke rivier in Frankrijk: de Allier. De analyse van een tijdserie luchtfoto's van de Allier laat zien dat dynamische processen in meanderende systemen uiteindelijk bestaan uit verjonging en successie van verschillende vegetatietypen (ecotopen).

Hydromorfologische processen in de Allier “verjongen” de natuur in het studiegebied met ongeveer 8% per vijf jaar. Daardoor ontstaat er een mozaïek aan ecotopen in het landschap; de helft van het bestudeerde areaal was 15 jaar of jonger en een kwart 46 jaar of ouder. De balans tussen successie en verjonging leidde tot een ecotoopdiversiteit in tijd en ruimte. De landschapsdynamiek had een sterke invloed op lokale ecotoopdiversiteit, zoals erosie van een stuk bos op een hoge uiterwaard. Op een riviertraject waarvan 1.5 tot 2 meanders onderdeel van uitmaken is de ecotoopdiversiteit in balans; zo wordt bijvoorbeeld de afbraak van een ouder bos elders gecompenseerd door het opgroeien van een jong bos.

In gereguleerde systemen zijn verjongingsprocessen verdwenen of sterk gereduceerd. Daardoor kan artificiële verjonging een managementstrategie zijn om pionierstadia te behouden. Eén van de verjongingsmogelijkheden is het afgraven van de uiterwaard tot op de zand- of grindlaag. Dit is uitgevoerd op de ‘Ewijkse Plaat’, een uiterwaard langs de rivier de Waal. In het kader van dit proefschrift is de landschappelijke ontwikkeling van de Ewijkse Plaat na afgraving in kaart gebracht op basis van een tijdserie luchtopnamen en hoogtegegevens. Hieruit blijkt dat vanaf elf jaar na het afgraven, de ecotoopdiversiteit hoger was dan in de voorafgaande situatie die gedomineerd werd door agrarisch beheer. Na 16 jaar bestond de

uiterwaardvegetatie vooral uit ooibos en kruidenrijke ruigten. Sedimentatie had de verlagings vrijwel geheel teniet gedaan. De sedimentatiesnelheid was direct gerelateerd aan de hoeveelheid water die bij hoge rivierafvoeren over de uiterwaard stroomde, en was significant hoger in beboste delen. De uiteindelijke topografie verschilde met de uitgangssituatie (i.e. voor afgraving), vegetatiesuccessie leidde tot een ander stroomsnelheidspatroon over de uiterwaard wat het sedimentatiepatroon beïnvloedde. In de 16 jaar lange onderzoeksperiode was 40% van het sediment gedurende twee extreme hoogwaterperiodes afgezet (in 1993/1994 en 1995). Waterstromingsberekeningen met het model WAQUA lieten zien dat het verlagende waterstandseffect van de afgraving na zeven jaar was geneutraliseerd. Tijdens de onderzoeksperiode traden geen erosie processen op die de verjonging van de bestaande ecotopen konden bewerkstelligen.

Eén van de belangrijkste verschillen tussen een natuurlijke en gereguleerde rivier is het patroon in landschapsouderdom en de daarmee samenhangende ecotoopdiversiteit. In natuurlijke of bijna-natuurlijk functionerende rivierlandschappen, zoals de Allier, is er een balans tussen successie en verjonging van de vegetatie op de schaal van riviertrajecten zodat op een riviertraject vrijwel alle ecologische successiestadia voorhanden zijn. Vergeleken hiermee, is de landschapsdiversiteit van gereguleerde rivieren beperkt. De onderzoeksresultaten met betrekking tot de 'Ewijkse Plaat' geven aan dat kunstmatige verjonging (door een laag af te graven wordt erosie geïmiteerd) de ecotoopdiversiteit sterk laat toenemen. Een afgeleide conclusie uit deze deelstudie is dan ook dat een gereguleerde verjonging van uiterwaarden een goede strategie kan zijn om de diversiteit van successiestadia te herstellen.

Verjonging in natuurlijke riviersystemen is een continu proces verdeeld over tijd en ruimte. Dit impliceert dat constante, ook wel cyclische, verjonging noodzakelijk is om continuïteit van successiestadia te behouden.

Om keuzen in het cyclisch beheer van riviertrajecten te kunnen onderbouwen, is accurate en up-to-date informatie over de uiterwaardvegetatie nodig. Dit vraagt om een techniek waarmee regelmatig en systematisch grote hoeveelheden vegetatiedata kunnen worden verzameld en geanalyseerd. Digitale remote sensing lijkt hiertoe een goede optie vanwege de automatische dataverwerkingsmogelijkheden. In deze studie is een combinatie van een spectrale sensor en de Light Detection and Ranging (LiDAR) sensor technologie onderzocht. De spectrale sensor, de Compact Airborne Spectrographic Imager (CASI), meet de lichtreflectie van vegetatie. Met LiDAR data kan de 3D structuur van vegetatie worden geclassificeerd. Door de ruwe LiDAR data, bestaande uit x-y-z punten, om te vormen naar een CASI compatibel beeldformaat zijn de signalen van deze sensors gefuseerd. De gebruikte LiDAR punt dichtheid is ongeveer 1.5 punt per m². De LiDAR informatie is in de vorm van extra informatielagen aan spectrale informatielagen toegevoegd en succesvol toegepast in de classificatie van een semi-natuurlijke uiterwaard (Millingerwaard, Rijn/Waal, NL).

De classificatie is uitgevoerd op pixelniveau. De classificatienauwkeurigheden van het gefuseerde beeld op pixelniveau lagen 6% tot 40% hoger (64% in acht klassen, 81% in vijf klassen) dan van het afzonderlijke CASI en LiDAR beeld. De classificatie van hydraulisch belangrijke klassen (ooibos, struweel) verbeterde met het gebruik van de gefuseerde data. Daarbij was de vegetatiestructuur in de schaduw van bomen of struweel in het gefuseerde beeld herkenbaar.

Om ecotopen automatisch te kunnen omlijnen en classificeren is een beeldsegmentatietechniek toegepast op de gefuseerde en afzonderlijke data sets. De ecotoopomlijningsresultaten van de gefuseerde data set waren superieur aan die van de data sets afzonderlijk. De classificatienauwkeurigheid van beeldobjecten op basis van gefuseerde data bedroeg 74% (10 klassen), dat wil zeggen 8 tot 19 procentpunten hoger dan van de ongefuseerde data.

In het algemeen worden classificatieresultaten deels bepaald door de gebruikte klassenindeling. Voor deze studie zijn 25 plantengemeenschappen ingedeeld in verschillende klassenindelingen. Om de klassenindeling te optimaliseren zonder het verlies van de relatie met plantengemeenschappen, zijn de plantengemeenschappen gegroepeerd met cluster- en ordinatietechnieken die het aantal en de plantensoort als invoer gebruiken. Op basis van botanische data kon de klassenindeling worden geoptimaliseerd voor onderscheiding met remote sensing (RS). De in RS de opgenomen lichtreflectie kan naast vegetatietype en -structuur ook worden beïnvloed door milieufactoren zoals bodemtype en -vocht. Door de klassen deels op basis van deze informatie in te delen, konden de classificatieresultaten verder worden verbeterd.

De toepassing van gefuseerde CASI en LiDAR data is bruikbaar als monitoringsinstrument en kan een belangrijke bijdrage leveren bij het modern uiterwaardenbeheer dat streeft naar een betere balans tussen natuur- en veiligheidsbelangen.

Dankwoord

San Jose, Antique, Philippines,

Dertig graden en het regenseizoen is begonnen. Als het in de Alpen ook zo gaat regenen, hoef je in Nederland je borst niet nat te maken, dat gebeurt dan vanzelf wel. Het is bijna af, bijna, 't belangrijkste rest nog: familie, vrienden en collega's. Nu ik meer dan een jaar niet meer in Nederland ben geweest, merk ik dat de makkelijke dagelijkse contacten die zo gewoon leken, bijzonder zijn. Bijzonder. Eigenlijk zijn er zoveel mensen die iets betekenen in je leven, van je beste vrienden tot de kaasboer met die overheerlijk extra belegen kaas.

Toen ik in 2000 op de uni ging werken, zeg maar in den beginne, waren daar Toine Smits, Sander Wijnhoven, Bart Peters en ik. Als clubje waren we ingebed in (of in bed met) de Afdeling Milieukunde. Onder parttime leiding van de onuitputtelijk enthousiaste Toine probeerden Bart en ik onderzoek op de zetten, discussieerden we, kochten we computers, plozen de projectfinanciën na en gingen het veld in. Toine, vaak druk en vaak weg, maar toch altijd tijd voor een praatje. Dank voor je vertrouwen, optimisme en de altijd positieve sfeer. Jij geeft mensen het gevoel dat iets kan, dat is mooi. Bart "genius of the place" Peters, dank voor je onafgebroken waardevolle output van feiten, meningen en boutte uitspraken. Je bent nooit te moe voor een fikse discussie. Café Jos houden we erin! Dr. Sander, dank voor al die jaren als collega, je was er gewoon altijd. En, weet je wel hoe gaaf het duiken is in de Filippijnen? ;-)

In de serie tijdelijke contracten was dat van NCR IRMA SPONGE Cyclisch Beheer het eerste, een mooi project in samenwerking met onder andere enthousiaste WL | Delftenaren als Martin Baptist, Harm Duel en Guda van der Lee. Martin, we begonnen beide met onderzoek aan de rivier, verhuisden naar de zee en wonen op een eiland. Met dit boekje is de cirkel verder rond. Ik ben benieuwd welke volgende stap we gaan maken.

Ik ontmoette Janrik van den Berg en Antoine Wilbers al peddelend en discussierend in een gevaarlijk diep liggende kano. We voeren over de Grensmaas, waar zij enthousiast over de rivier Allier spraken. "Natuurlijke Cyclische Verjonging, dat moet je zien!". En zo geschiedde, samen met Allier freak nummer drie: Jurgen de Kramer. Dank heren! Ik heb genoten van onze zomers "au bord d'Allier", de kookkunsten van Janrik en het gezelschap van alle studenten uit Delft en Utrecht. Zeker met Lara heb ik heel wat Franse uiterwaarden afgestruind.

Nummer twee uit de serie contracten met RU was een remote sensing opdracht voor RWS Meetkundige dienst samen met Ger van den Berg, onder leiding van Henk Kloosterman. Dank je Henk voor je vertrouwen in een student zonder GIS of RS opleiding. Veel dank ook voor de mensen van de oude afdelingen GAR en GAE van de toenmalige meetkundige dienst. Jullie hebben in de loop der tijd veel bijgedragen door alle suggesties en de hulp bij analoge foto-interpretatie.

Na een kort strategisch intermezzo bij Stichting Ark volgde het laatste en langste contract in de serie, met als doelstelling een heus proefschrift. Projectleiders Regine Brügelmann en later Madelein Vreeken-Buijs van het RWS Centrum voor Data en ICT (ook wel bekend als Meetkundige dienst of AGI), dank voor al jullie sturing en waardevolle adviezen. Ik heb heel prettig met jullie samengewerkt. In de lange samenwerking met RWS heb ik veel mensen ontmoet die op een of andere manier hebben bijgedragen aan het werk. Teveel mensen om op te noemen, maar ik ben hen allemaal dank verschuldigd, bij deze. Juist de koppeling van mijn onderzoek met de praktijk was een van de leuke dingen in dit werk. Het schrijven van het Handboek Cyclisch Beheer met Bart en Emiel was daarom een geweldige ervaring. Niet alleen om de verhitte discussies “in huis”, ook het werken met de groep van wijze mannen was super: Johan “de rust zelve” Bekhuis (ARK), Hendrik “op een sigarenkistje” Havinga (RWS), Wouter “met visie” Helmer (ARK), Joep “blauwe en groene koeien” Mannaerts (RWS), onder de bezielende leiding (echt!) van Theo Meeuwissen (Staatsbosbeheer). Ik heb genoten.

Via het Gipsy project, een project van de universiteiten Nijmegen, Wageningen en Amsterdam, kwam ik in contact met de GIS en Remote Sensing afdeling van de WUR. Ik was en ben onder de indruk van de kennis daar. Samen met Jan Clevers heb ik een aantal goede studenten begeleid: Mauritio, Achileas, Monica en Jochem. Bedankt Jan en Thanks Guys! Natuurlijk wil ik ook graag de “Nijmeegse” studenten bedanken voor hun goede werk en gezelschap: Sanne, Lisette, Daan, Maarten, Erika, en Bart.

The international expeditions ventured by prof. Toine brought me some foreign friends whom I really wish not to lose in this wide world. Gao Jing en Wang Ling, I enjoyed your company a lot. Gao Jing, thanks for being my Chinese mother during my short visit in China. The dear Polish ladies Marta and Agnieszka, who made me understand why Dutch men are ugly ;-), I wish you well and hope to see you again. During the last stages of my thesis, Mariëlle and I moved to live and work in another culture. I am writing these acknowledgements, not in the cold cold Netherlands, but far away on the Philippine Isles. I would like to thank our new and dear friends as without them we could not have settled and felt at home at our new place. Thank you Mayor Rony Molina, Adoy and Terry Petinglay! Salamat gid, Manang Dolly, Akay Fe, Gina, Jomag, Bibot, Jesse, Flo, Kune, Boy, June and Lorena, John, Guilly and everybody not mentioned for all the good times we had and those that are still to come.

De hechte band met Milieukunde bleef. Gina, Nellemiek, Marlie, Rob Lenders, Mark, Lammert (die later weer opdook in Wageningen), Reinier, Marieke, Piet en nu Jan, alle AIOs daar en in het bijzonder Mara, Aafke, Arie, Tjisse en ex-kamergenoot Stan. Vond het fijn om met jullie allen te mogen werken. Rob Leuven, je stimuleerde me te schrijven en ik hoor vaak je stem nog als ik met de punten en de komma's van een manuscript bezig ben... Ad, zonder jou was ik niet zover gekomen. Onvermoeibaar

en consequent bleef je commentaar geven en poogde je me op het rechte redentatie pad te houden. Op het laatst zelfs vanuit Kenia. Mooi dat je er bij kan zijn. Toine's groep op de RU veranderde de afgelopen jaren. We gingen samen met de groep van Paul van de Heuvel verder als CSMR, en er kwamen alleen maar mensen bij. Ik wil en kan er geen apart noemen, jullie zijn allemaal stuk voor stuk geweldige collega's. Het is erg leuk werken op zo'n jonge afdeling! Arthur, als kamergenoot hadden we veel lol en damn, wat kan je lekker gitaar spelen. Je vertrok naar de Filippijnen, en warempel, nu zitten wij er ook. Bedankt, voor je gezelligheid, je luisterend oor en tot gauw in Davao. Tja, Emiel, als ik hier in de Filippijnen iets mis, dan is het met jou af en toe een biertje doen na werk. Daar kregen we de beste ideeën, allemaal vastgelegd op viltjes. Ik heb ooit een volgende dag tien genummerde bierviltjes overgetypt in Word. Dank je voor alles, en zeker voor het nog snel napluizen van het manuscript op foutjes. Je bent meteen de link naar al onze vrienden in en buiten Nijmegen, ik hoop jullie allen de rest van mijn leven te blijven zien. Fijn dat jullie er waren, nog fijner dat jullie er zijn! Katja, laat even weten naar welke landen je nog op vakantie wil, da's handig met werk zoeken ☺. Pap, Mam, Frans, ik besef steeds vaker dat ik een hele goede jeugd heb gehad. Jullie stimuleerden altijd met wat ik wilde doen, en ik kon en kan altijd bij jullie terecht, dank je wel. Mijn nieuwe familie heeft nog maar kort van ons kunnen genieten. Maar Jan, Ria, Dorien, Pieter en kleine Sjoerd, zet de BBQ maar vast klaar want we komen eraan!

Lieve Mariëlle. Het ging bliksemsnel, maar ik heb geen seconde spijt. Gelukkig zijn er nog veel seconden samen.

Gertjan

Curriculum vitae

Op 5 september 1972 werd ik geboren in Laren (N.H.) en groeide op in Zevenaar. Nadat ik in 1990 aan het Liemers College mijn VWO diploma behaalde, begon ik de studie Scheikunde aan de Katholieke Universiteit Nijmegen (tegenwoordig de Radboud Universiteit). Na 3 jaar scheikunde stroomde ik door naar Milieukunde, dat mij aansprak vanwege de maatschappelijke problematiek. Voor mijn afstudeeronderzoek woonde ik zes maanden in Galway (Ierland) en onderzocht de indirecte effecten van EU landbouwsubsidies op het gevoelige veenlandschap in Connemara (University of Ireland, College Galway). Hier deed ik mijn eerste ervaringen op met het instrument GIS en liep in het veld met grote accu's en een GPS. In 1997 studeerde ik af als natuurwetenschappelijk (chemisch) milieukundige. Na het afronden van de studie werkte ik als tijdelijk medewerker communicatie bij de afdeling milieukunde en ben aansluitend begonnen aan de 1 jarige opleiding Ruimtelijke Ordening en Infrastructuur (Larenstein), waarvan het laatste halfjaar bij Rijkswaterstaat Oost-Nederland. Vervolgens werkte ik parttime als GIS-adviseur bij Geodan BV en organiseerde daarnaast als freelancer het symposium "Delfstoffenwinning als motor voor rivierverruiming (februari 2000)" in opdracht van Rijkswaterstaat, Provincie Gelderland en de Gezamenlijke Baksteen Fabrikanten. Uiteindelijk won de inhoud het van de techniek en ben ik in de zomer van 2000 begonnen bij het Centrum voor Water en Samenleving aan de Radboud Universiteit, onder leiding van prof. dr. A.J.M. Smits. Als wetenschappelijk onderzoeker ben ik betrokken geweest bij de volgende projecten: Cyclic Floodplain Management (EU, NCR IRMA-SPONGE, WL | Delft, Alterra, RWS), Monitoring en Dynamisch Rivierbeheer (RWS-AGI), GIPSY, GIS in onderwijs (EU, RU, UvA en WUR), Cyclisch beheer in de praktijk (EU, Provincie Gelderland) en tenslotte Nature rehabilitation in regulated rivers, Management and monitoring of floodplainvegetation (RWS). Het laatste project leidde tot dit proefschrift. Het mooie aan deze projecten en de groeiende afdeling is dat je een verscheidenheid aan kennis kunt ontwikkelen: onderwijs (Rivieren en beheer, GIS), veel presentaties voor opdrachtgevers en projectpartners, (financiële) organisatie van projecten, onderzoek en rapportage. Aangezien ik graag nog buitenlandervaring in de tropen op wilde doen en de kans zich voordeed om in 2007 samen met mijn vrouw voor 2 jaar naar de Filippijnen te vertrekken, heb ik die kans genomen. In de Filippijnen heb ik mijn proefschrift afgemaakt en onderzoek voor de RU een rivierstroomgebied en de kustzone. Verder help ik de lokale overheid met rivierbeleid en -beheer.

I was born on the 5th of September 1972 in the city of Laren (N.H.) and spend my youth in the city of Zevenaar. Here, I graduated from high school and started studying Chemistry at the University of Nijmegen (nowadays Radboud University). As my master I chose Environmental science, because of the links to society's problems. For my master thesis I lived for 6 months in Galway (Ireland) and

researched the indirect effects of EU agricultural subsidies on the sensitive blanket bogs (peat) of the Connemara region. I graduated as Environmental Scientist with speciality in Chemistry in 1997. I worked briefly at the Department for Environmental Science (Radboud University) as communication assistant and subsequently started a one-year training in Spatial Planning and Infrastructure of which the last 6 months were spend at the Eastern Division of the Dutch river manager (Ministry of Transport, Public Works and Water Management, Directorate Water Management). Afterwards I worked for Geodan BV as GIS consultant and organised as freelancer a conference for Rijkswaterstaat, Province of Gelderland, and the clay & sand mining industry.

In summer 2000 a research position on a project base became available at the Radboud University. I participated in the following projects concerning Rivers and River Management: Cyclic Floodplain Management (EU sponsored, partners were WL|Delft, Alterra, University of Karlsruhe, ILN and Rijkswaterstaat), Monitoring and Dynamic River Management (sponsored by Survey Department, Ministry of Transport, Public Works and Water Management or RWS), GIS in education, GIPSY (EU sponsored, partners were University of Amsterdam and Wageningen University), Cyclic Management in Practise (sponsored by EU and Province of Gelderland, partners were State forestry Service, Ark Foundation, Rijkswaterstaat), and finally, Nature rehabilitation in regulated rivers, Management and Monitoring of Floodplain Vegetation (RWS). This last project is the basis for the PhD thesis. Long-term experience in a tropical country was missing, therefore my wife and me took the chance to live and work in the Philippines for 2 years. Here, I finished my PhD thesis and research a tropical catchment area and the near-coastal zone. We cooperate with local government units to apply this knowledge in making policies and management.

Publications

Peer reviewed papers

- Geerling GW, van Gestel CBL, Sheehy Skeffington M, Schouten MGC, Nienhuis PH, Leuven RSEW (2002). Blanket bog degradation in the river catchments in the West of Ireland. In: Leuven RSEW, Poudevigne I, Teeuw RM (Eds.) *Application of Geographic Information Systems and Remote Sensing in River Studies*. Backhuys Publishers, Leiden. pp. 25-40.
- Leuven RSEW, Gerig Y, Poudevigne I, Geerling GW, Kooistra L, Aarts, BGW (2002). Cumulative impact assessment of ecological rehabilitation and infrastructure facilities in the middle reach of the river Waal. In: Leuven RSEW, Poudevigne I, Teeuw RM (Eds.). *Application of geographic information systems and remote sensing in river studies*. Backhuys Publishers, Leiden, the Netherlands. pp. 201-216.
- Baptist MJ, Penning WE, Duel H, Smits AJM, Geerling GW, van der Lee GEM, van Alphen JSL (2004). Assessment of the effects of Cyclic Floodplain Rejuvenation on flood levels and biodiversity along the Rhine River. *River Research & Applications* **20**: 285-297.
- Geerling GW, Ragas AMJ, Leuven RSEW, van den Berg JH, Breedveld M, Liefhebber D, Smits AJM (2006). Succession and rejuvenation in floodplains along the River Allier (France). *Hydrobiologia* **365**: 71-86.
- Geerling GW, Labrador-Garcia M, Clevers JGPW, Ragas AMJ, Smits AJM (2007). Classification of floodplain vegetation by data fusion of spectral (CASI) and LiDAR data. *International Journal of Remote Sensing* **28**: 4263 – 4284.
- Van der Heide T, Nes EH, Geerling GW, Smolders AJP, Bouma TJ, Katwijk MM (2007). Positive Feedbacks in Seagrass Ecosystems: Implications for Success in Conservation and Restoration. *Ecosystems* **10**: 1311 – 1322.
- Geerling GW, Kater E, van den Brink C, Baptist MJ, Ragas AMJ, Smits AJM (2008). Nature rehabilitation by floodplain excavation: the hydraulic effect of 16 years of sedimentation and vegetation succession along the Waal River, NL. *Geomorphology* **99**: 317-328.
- Geerling GW, Vreeken-Buijs MJ, Jesse P, Ragas AMJ, Smits AJM (accepted with revisions). Mapping river floodplain ecotopes by segmentation of spectral (CASI) and structural (LiDAR) remote sensing data. *River research & Applications*.
- Wozniak M, Leuven RSEW, Lenders HJR, Chmielewski T, Geerling GW, Smits AJM (submitted). Landscape change and biodiversity values of the Vistula river valley in Poland. Submitted to *Landscape and Urban Planning*.

Verrelst J, Geerling GW, Sýkora KV, Clevers JGPW (submitted). Mapping floodplain plant communities: clustering and ordination techniques adopted in remote sensing. Submitted to International Journal of Applied Earth Observation and Geoinformation.

Other professional publications

- Geerling GW, Smits AJM (Eds., 2000). *Delfstoffenwinning als motor voor rivieroerruiming; kansen en bedreigingen?* Rapport Nederlands Centrum voor Rivierkunde (NCR), Delft. 64 p.
- Geerling GW, Peters B, Smits AJM (2001). Cyclische verjonging in het rivierengebied. In: Wolters, A.F., C.J. Sloff & E.C.L. Marteiijn. NCR-dagen 2000: Het begin van een nieuwe reeks. NCR-publicatie 03-2001. Netherlands Centre for River Studies (NCR), Delft, the Netherlands. pp. 14-15.
- Peters B, Dittrich A, Stoesser T, Smits AJM, Geerling G (2001). *The RestRhine; new opportunities for nature rehabilitation and flood prevention*. IRMA-SPONGE background report. NCR, Delft.
- Geerling GW, van den Berg GJ (2002). *Rivierbeheer en ruimtelijke informatie. Onderzoek naar de mogelijkheden van remote sensing t.b.v. dynamisch uiterwaardenbeheer. Rapport deel 1 en 2*. Meetkundige Dienst, RWS, Delft. Leerstoel Natuurbeheer stroomgebieden, KUN, Nijmegen. 84 p.
- Geerling GW, Smits AJM (2003). Monitoring floodplain vegetation dynamics using remote sensing in the context of cyclic floodplain rejuvenation. In: Leuven, R.S.E.W., A.G. van Os & P.H. Nienhuis (Eds.). *Proceedings NCR-days 2002. Current themes in Dutch river research*. NCR-publication 20-2003. Netherlands Centre for River Studies, Delft, the Netherlands. p. 92-95.
- Geerling GW, Ragas AMJ, Smits AJM (2004). Vegetation dynamics of a meandering river (Allier, France). In: Douben, N. & A.G. van Os (Eds.). *Dealing with floods within constraints*. Proceedings NCR-days 2003 (Roermond, 6-8 November 2003). NCR-publication 24-2004. Netherlands Centre for River Studies, Delft. p. 59-61.
- Leuven RSEW, Geerling GW, Gerrits S, Lenders HJR, De Nooij RJW (2005). Cumulative effect assessment of physical reconstruction and land use changes on riverine biodiversity. In: Maskake A, Wolfert HP, Van Os AG, editors. *NCR-publication 26-2005; 2004*; Wageningen, the Netherlands. NCR. p 87-89.
- Peters B, Kater E, Geerling GW (2006). *Cyclisch beheer in uiterwaarden. Natuur en veiligheid in de praktijk*. Centrum voor Water en Samenleving. Radboud Universiteit. Nijmegen. ISBN 978 90 810586 12. Nijmegen. 206 p.

- Van Katwijk MM, Geerling GW, Rašín R, Van 't Veer R, Bos AR, Hermus DCR, Van Wieringen M, Jager Z, Groeneweg AH, Erfstemeijer PLA, Van der Heide T, De Jong DJ (2006). Macrophytes in the western Wadden Sea: monitoring, invasion, transplantations, dynamics and European policy. In: Laursen K (Ed.). *Monitoring and Assessment in the Wadden Sea*. Proceedings from the 11th International Scientific Wadden Sea Symposium, 4-8 April 2005, Esbjerg, Denmark. Denmark National Environmental Research Institute, Ministry of the Environment; NERI Technical Report no. 573 (142 p). p. 89-98.
- Van der Heide T, Van Katwijk MM, Geerling GW (2006). *Een verkenning van de groeimogelijkheden van ondergedoken Groot zeegrass (Zostera marina) in de Nederlandse waddenzee*. Radboud Universiteit Nijmegen. 39 p.
- Geerling GW (2007). Nature rehabilitation in regulated rivers; Management and monitoring of floodplain vegetation. Centre for Sustainable Management of Resources, Radboud University Nijmegen, Nijmegen. Adviesdienst Geoinformatie en ICT (AGI), Delft. 117 p.
- Peters BWE, Geerling, GW, Kater E (2008). Cyclische verjonging, samengaan van natuur- en hoogwaterbescherming. *De Levende Natuur* **209** (januari 2008).

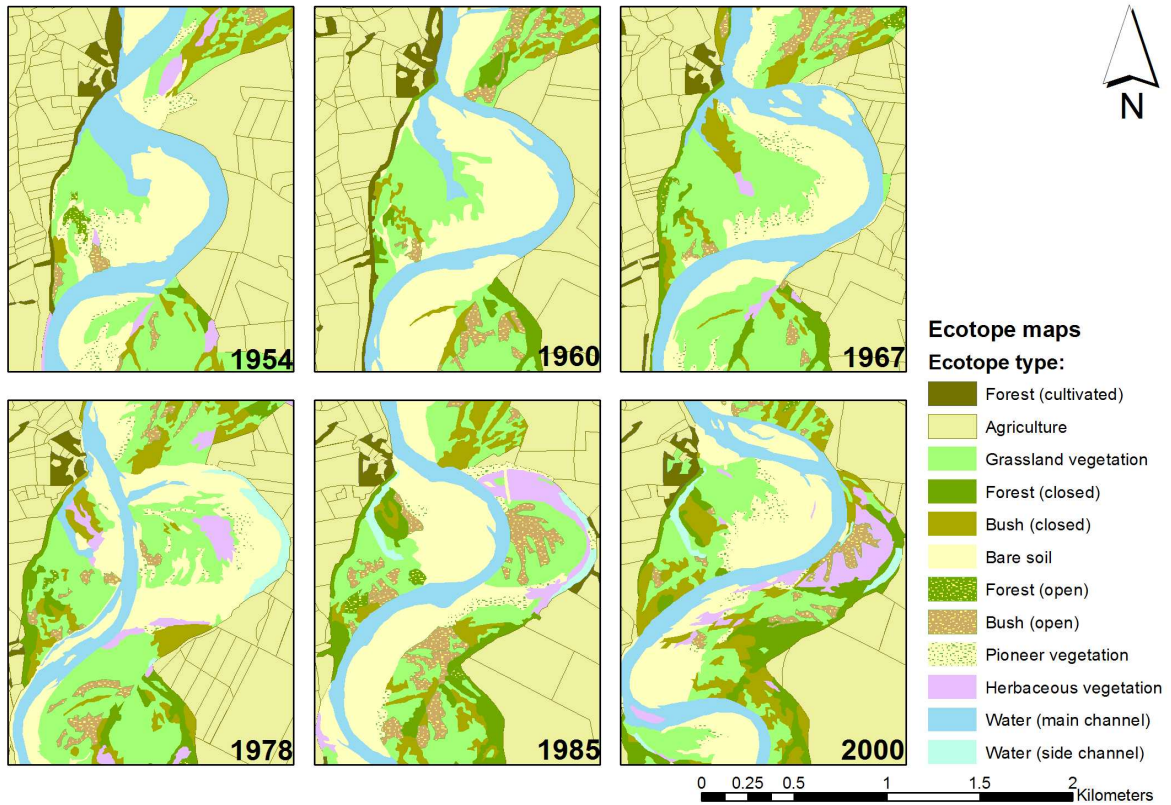
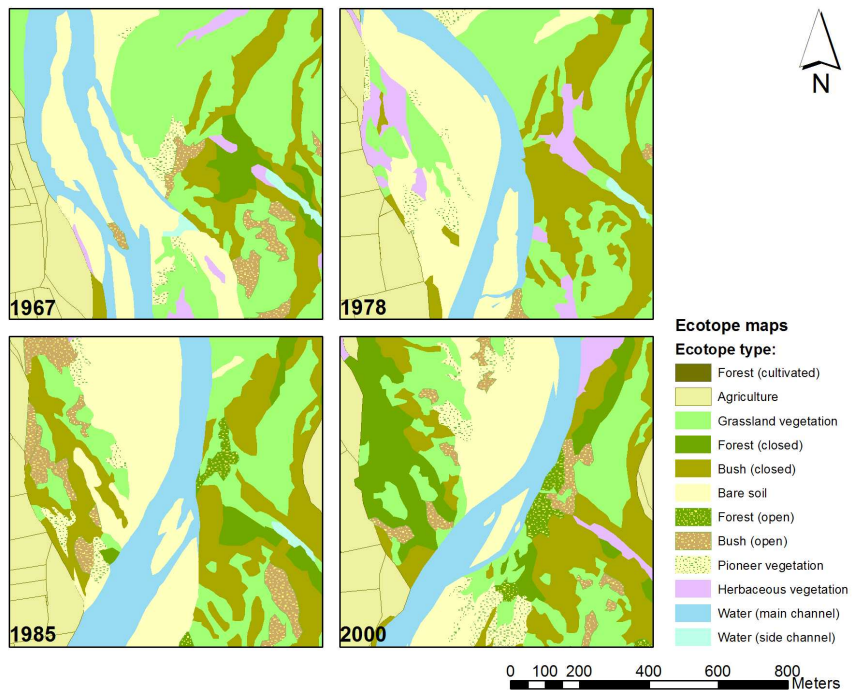


Figure 2.4 Meander progression in a part of the research area over the period 1954 to 2000. The river flows from South to North. From 1954 to 1967 a meander progression is visible. In the period 1967 to 1978 the meander was cut-off. The meandering process is restored in 1985 and 2000.

Figure 2.5 Meander shift rejuvenates ecotopes and creates niches for forest development over the period 1967-2000. The 1967-1978 shift rejuvenates ecotopes and creates niches for forest settlement in the former channels. In 1985 these channels are colonized by bush that grow to forest in the 1985-2000 period.



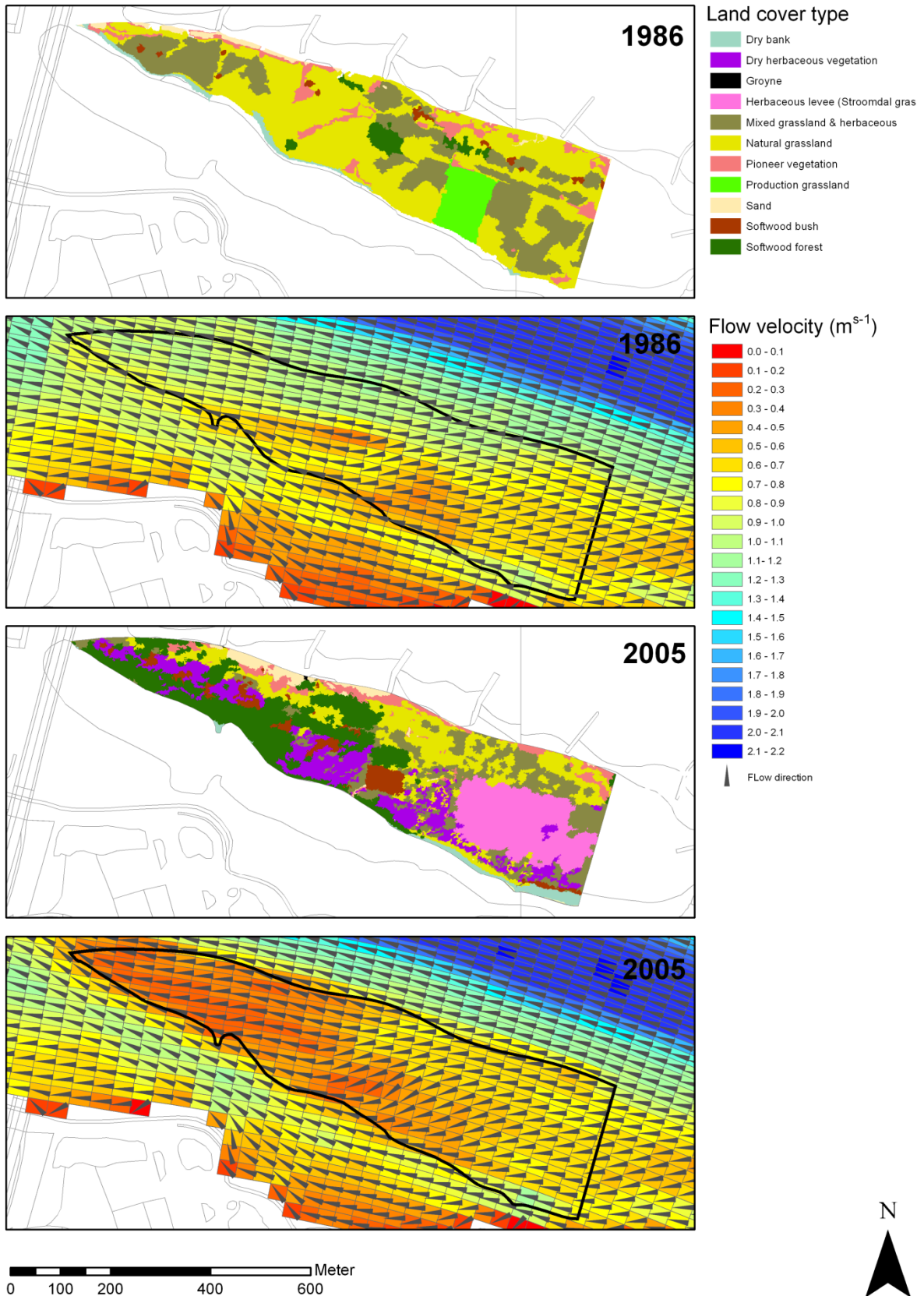


Figure 3.8 The vegetation maps, flow velocities, and flow direction are shown for the 1986 (pre-excavation) situation and the 2005 situation. The grid cells in the flow velocity and flow direction maps correspond to the grid cells of the hydraulic model.

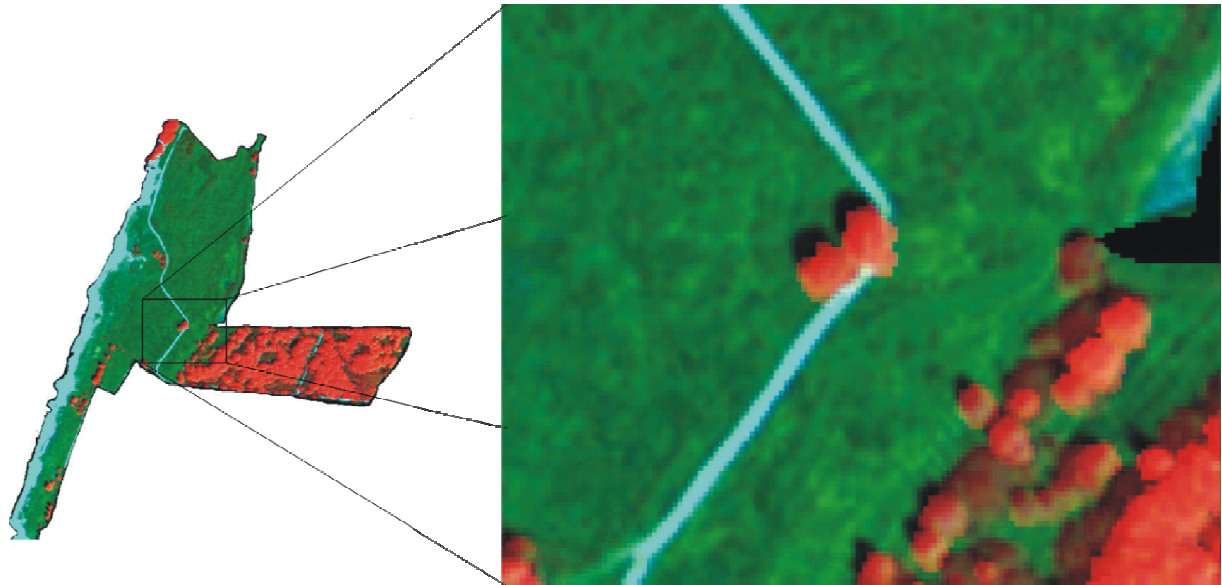


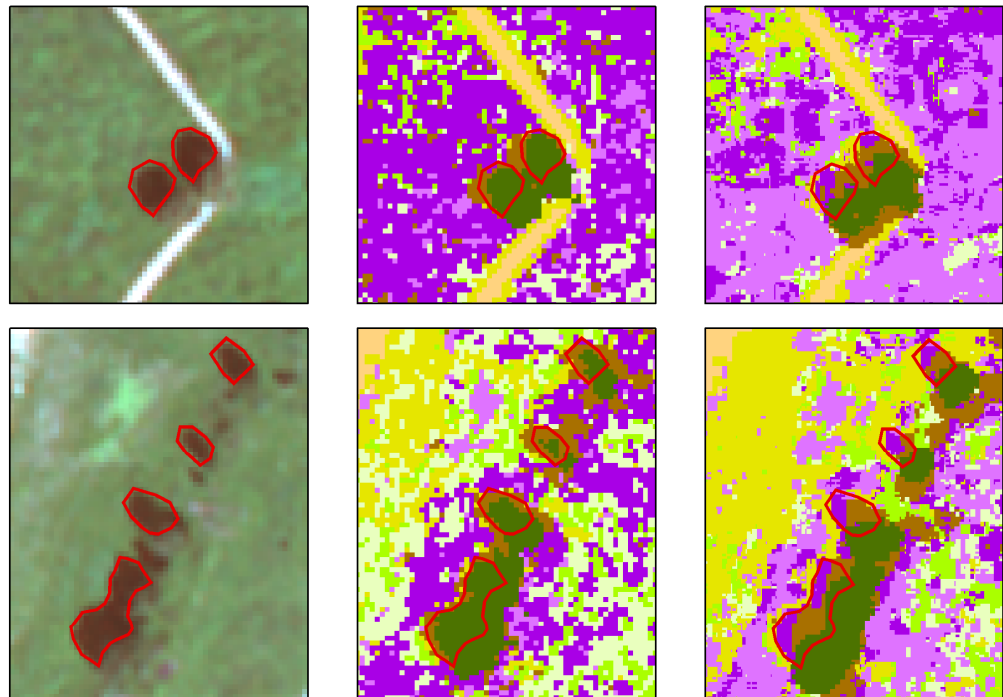
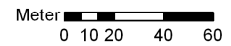
Figure 4.4 Example of the fused CASI and LiDAR image. Of the 16 band image (10 CASI and 6 LiDAR texture bands) 3 bands are shown, indicating the potential of data-fusion. RGB values correspond to maximum vegetation height, and reflectance of band (549-559 nm) in green and the band (437-447 nm) in blue. The bushes (dark red) and trees (bright red) stand out in this band combination. The light blue-ish line is a sandy path.

Figure 4.6 Two examples of classification of shadows. On the left, a true colour image (CASI bands 615-625 nm (red), 549-559 nm (green) and 437-447 nm (blue)) on which the shadows are outlined in red. The middle image shows shadows mainly classified as trees in the CASI classification. On the right, shadows classified using the fused CASI LiDAR data appear partly as tree (covered in shadow) and partly as surrounding lower vegetation.

Classification of shadow

Legend

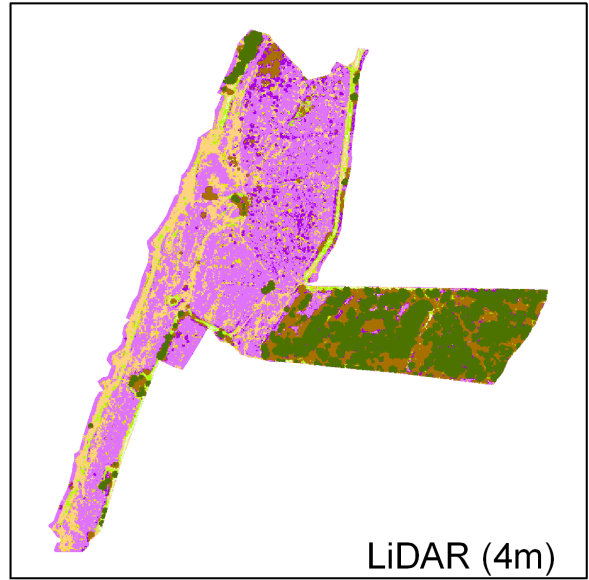
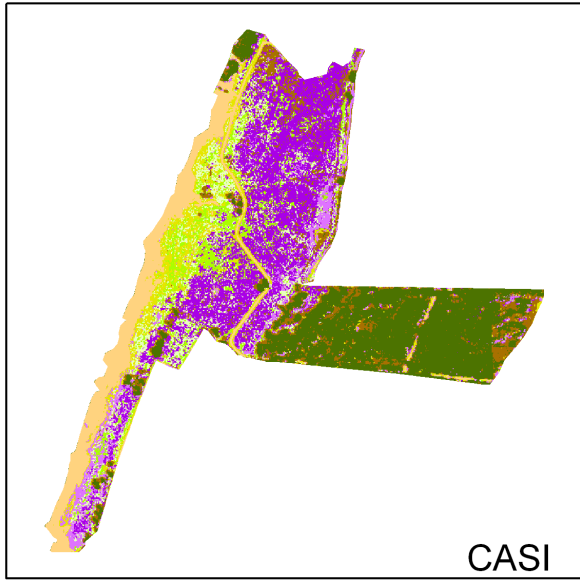
 Shadow	 C2	 B2
 E	 C1	 B1
 D	 B3	 A



CASI (true colour)

CASI classification

CASI + LiDAR (4m)



Legend

- E
- D
- C2
- C1
- B3
- B2
- B1
- A

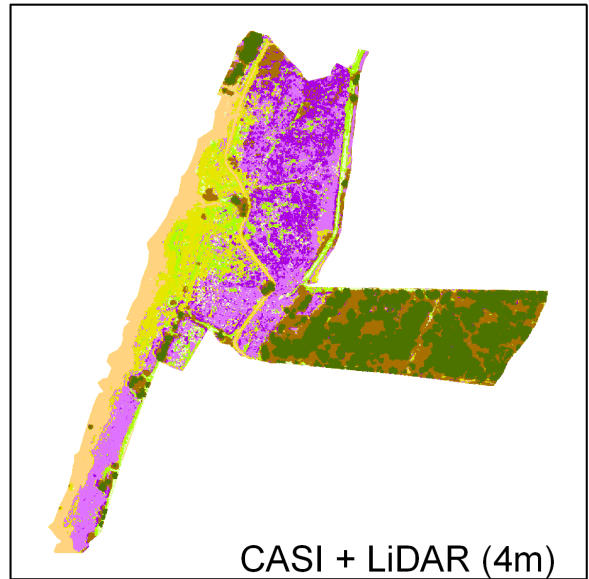
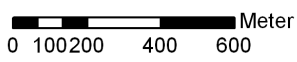


Figure 4.5 Maps of classification results LiDAR (4m), CASI, and Fused CASI LiDAR (4m).

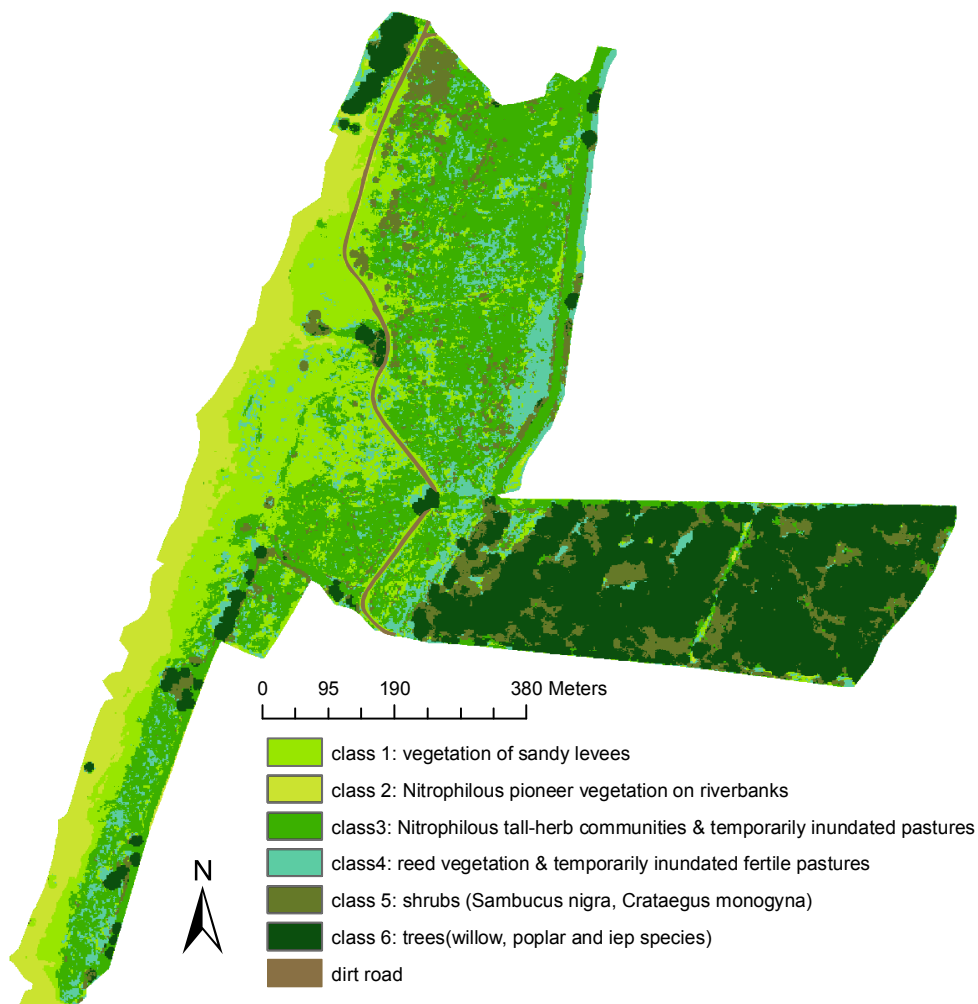


Figure 5.6 Classified image with 6 vegetation classes according to DCA-Dendro grouping. The added dirt road was taken from topographic data.

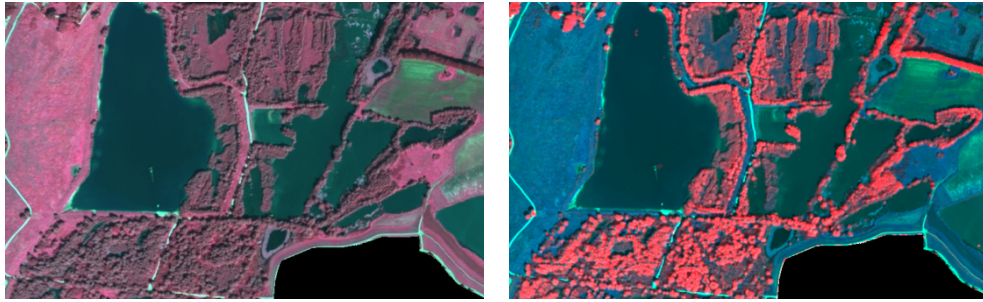


Figure 6.3 The left image shows a false colour excerpt of the CASI image (bands 2, 3, 7). The right image shows the same view but band 7 is replaced by vegetation elevation. Trees appear brighter on the right image because of their greater height and bushes appear darker red because of their lower height.

Figure 6.7 Classified PI unit map based on the LIDAR+CASI data set.

